Identification and characterisation of gallic acid decarboxylase (Agdc1p) and catechol-1,2-dioxygenase (Acdo1p) and their role in the degradation of Tannic Acid in the Yeast *Blastobotrys (Arxula) adeninivorans*.

I n a u g u r a l d i s s e r t a t i o n

zur

Erlangung des akademischen Grades eines

Doktors der Naturwissenschaften (Dr. rer. nat.)

der

Mathematisch-Naturwissenschaftlichen Fakultät

der

Universität Greifswald

vorgelegt von

Anna Karolina Meier, geb. Malak

geboren am 21.06.1989

in Pleszew, Polen

Greifswald, 02.12.2019

Dekan: **Prof. Dr. Werner Weitschies**

1. Gutachter: Prof. Dr. Hans-Joachim Schüller
2. Gutachter: Prof. Dr. Paola Branduardi

Tag der Promotion: 02.12.2019

Table of Contents

Summary 7

Zusammenfassung 9

List of abbreviations 11

1 Introduction 12

1.1 Diversity of the plant secondary metabolites 12

1.2 Properties and industrial applications of phenolic compounds 15

1.3 Persistence of phenolic compounds 17

1.4 Microbial strategies for biodegradation of aromatic compounds 18

1.5 Yeast *Arxula adeninivorans* and its ability to degrade tannin compounds 22

1.5.1 Gallic acid decarboxylase 25

1.5.2 Catechol-1,2-dioxygenase 27

2 Aim of the project 31

3 Materials and methods 32

3.1 Materials 32

3.1.1 Chemicals 32

3.1.2 Software 34

3.1.3 Immunolabeling 34

3.1.4 Kits and enzymes 35

3.1.5 Plasmids and vectors 35

3.2 Biological materials 36

3.2.1 Bacterial strains 36

3.2.2 Yeast strains 36

3.3 Composition of cultivation media 36

3.3.1 Bacterial media 36

3.3.2 Yeast media 37

3.4 Methods 38

3.4.1 Cultivation conditions 38
3.4.1.1 Cultivation of bacterial cells 38
3.4.1.2 Cultivation of yeast cells 38
3.4.2 Techniques used for manipulation of genetic material 38
3.4.2.1 Agarose gel electrophoresis 38
3.4.2.2 DNA extraction from agarose gel 39
3.4.2.3 DNA restriction 39
3.4.2.4 Dephosphorylation of DNA fragments 39
3.4.2.5 DNA ligation 39
3.4.2.6 Mini preparation of plasmid DNA 40
3.4.2.7 Phenol/chloroform extraction of yeast genomic DNA 40
3.4.3 Construction of transgenic strains 41
3.4.3.1 Preparation of chemical competent *E. coli* cells 41
3.4.3.2 Transformation of chemical competent *E. coli* cells 41
3.4.3.3 Preparation of competent *A. adeninivorans* cells 42
3.4.3.4 Transformation of competent *A. adeninivorans* cells 42
3.4.3.5 Stabilization of insert in the yeast genomic DNA 43
3.4.3.6 Transformation of competent *S. cerevisiae* cells 43
3.4.3.7 Construction of knock-out mutant strain of *A. adeninivorans* 43
3.4.4 Techniques used for work with RNA 44
3.4.4.1 RNA isolation from yeast cells, quantification and synthesis of cDNA 44
3.4.4.2 Nested quantitative Real-time PCR 44
3.4.4.3 Gene expression analysis using microarray 44
3.4.5 Yeast cells microscopy 45
3.4.5.1 Digital Microscope and Emission Scanning Electron Microscopes (FE-SEM) 45
3.4.5.2 Confocal leaser scanning microscopy 45

3.4.6 Methods used for work with proteins 46
3.4.6.1 Determination of protein concentration 46
3.4.6.2 Protein electrophoresis on polyacrylamide gel (SDS-PAGE) 46
3.4.6.3 Gel staining for total protein content 46
3.4.6.4 Western blotting (immunoblotting) 47
3.4.6.5 Protein-antibody hybridization 47
3.4.6.6 Cell wall disruption 47
3.4.6.7 Protein purification by immobilized metal ion affinity chromatography (IMAC) 48
3.4.6.8 Desalting of protein eluates 48
3.4.6.9 Size exclusion chromatography 48
3.4.7 Cell growth monitoring 49
3.4.7.1 OD_{600nm} culture measurement 49
3.4.7.2 Determination of dry cell weight (dcw) 49
3.4.8 Enzymatic assays 49
3.4.8.1 Gallic acid decarboxylase 49
3.4.8.2 Catechol-1,2-dioxygenase 50
3.4.9 Metabolite analysis by gas chromatography – mass spectrometry (GC-MS) 50
3.4.9.1 Sample collection, extraction and derivatization procedure 50
3.4.9.2 GC-MS measurement 51
4 Results 52
4.1 Gallic acid tolerance by *A. adeninivorans* 52
4.2 *Arxula* gallic acid decarboxylase 1, Agdc1p 53
4.2.1 Identification of the *A. adeninivorans AGDC1* gene encoding gallic acid decarboxylase (Agdc1p) 53
4.2.2 Generation of an Agdc1-6hp producing yeast strain 56
4.2.3 Generation of Δ*agdc1* gene disruption mutant strain 58
4.2.4 Phenotypic analysis of *AGDC1* wild type and Δ*agdc1* deletion strains 61

4.2.5 Generation of Agdc1-eGFP producing yeast strain 62
4.2.6 Cellular localisation of Agdc1-eGFP 62
4.2.7 Purification of the recombinant Agdc1-6hp 63
4.2.8 Native molecular mass determination of the recombinant gallic acid decarboxylase (Agdc1-6hp) 65
4.2.9 Properties of the recombinant gallic acid decarboxylase 66
4.2.9.1 Determination of the optimal pH 66
4.2.9.2 Optimal temperature and thermostability of Agdc1-6hp 67
4.2.9.3 Kinetic study 69
4.2.9.4 Effect of different additives on Agdc1-6hp activity 70
4.2.9.5 Substrate spectrum of Agdc1-6hp 71
4.2.9.6 Expression of *AGDC1* in dependence of carbon sources 72
4.2.10 Influence of gallic acid on gene expression in *A. adeninivorans* by microarray expression analysis 73
4.2.11 Role of Agdc1p in *A. adeninivorans* on metabolizing gallic acid 77
4.2.12 Role of Agdc1p in *A. adeninivorans* on metabolizing hydroxylated aromatic acids 80
4.2.13 Metabolic conversion of gallic acid and protocatechuic acid by *A. adeninivorans* 81
4.3 *Arxula* catechol-1,2-dioxygenase 1, Acdo1p 83
4.3.1 Identification of an *A. adeninivorans ACDO1* gene encoding for catechol-1,2-dioxygenase (Acdo1p) 83
4.3.2 Generation of an Acdo1-6hp producing yeast strain 86
4.3.3 Generation of Acdo1-eGFP producing yeast strain 88
4.3.4 Cellular localisation of Acdo1-eGFP 88
4.3.5 Generation of Δ*acdo1* gene disruption mutant strain 89
4.3.6 Colony phenotype analysis of control strain (G1212/YRC102) and mutant strain G1235 [Δ*acdo1*] 92
4.3.7 Purification of the recombinant Acdo1-6hp 92

4.3.8 Native molecular mass of recombinant catechol-1,2-dioxygenase (Acdo1-6hp) 94

4.3.9 Properties of recombinant catechol-1,2-dioxygenase 95

4.3.9.1 Determination of the optimal pH 95

4.3.9.2 Determination of optimal temperature and thermostability of Acdo1-6hp 96

4.3.9.3 Effect of different additives on Acdo1-6hp activity 98

4.3.9.4 Kinetic study 99

4.3.9.5 Substrate spectrum of Acdo1-6hp 99

4.3.10 Expression analysis of *ACDO1* on various carbon sources 100

4.3.11 Influence of protocatechuic acid on gene expression in *A. adeninivorans* by microarray expression analysis 102

4.3.12 Role of Acdo1p in metabolism of protocatechuic acid in *A. adeninivorans* 107

4.3.13 Metabolite analysis during degradation of gallic acid and protocatechuic acid by *A. adeninivorans* 110

4.4 Expression of gallic acid decarboxylase (Agdc1p) and catechol-1,2-dioxygenase (Acdo1p) in *Saccharomyces cerevisiae* 114

4.4.1 Cellular localization of Acdo1-eGFP and Acdo1-eGFP in *S. cerevisiae* 114

4.4.2 Screening of transgenic *S. cerevisiae* strains as potential producer for recombinant *Arxula* catechol-1,2-dioxygenase 116

4.4.3 Purification of recombinant Acdo1-6hp and Agdc1-6hp from *S. cerevisiae* 117

5 Discussion 118

5.1 Morphology of *A. adeninivorans* deletion mutants 119

5.2 Gallic acid decarboxylase 120

5.3 Catechol-1,2-dioxygenase 122

5.4 Expression of *AGDC1* and *ACDO1* in *A. adeninivorans* 125

5.5 The role of Agdc1p in *Arxula* tannic acid degradation pathway 127

5.6 The role of Acdo1p in the *Arxula* tannic acid degradation pathway 128

5.7 Microarray data analysis 133

5.8 Expression of *AGDC1* and *ACDO1* in *S. cerevisiae* 134

5.9 Conclusions 135

6 List of Figures and Tables 137

6.1 Figures 137

6.2 Tables 142

7 References 144

8 Appendix 158

9 Declaration of originality 163

10 Curriculum Vitae 164

11 Acknowledgements 168

Summary

Phenolics and its derivatives are aromatic compounds with a wide range of industrial applications. Gallic acid, protocatechuic acid, catechol or pyrogallol are only a few examples of industrially relevant aromatics. The production of bulk fine chemicals primarily for chemical and pharmaceutical industry has put a strong emphasis on optimizing manufacturing conditions. Commercial production of many chemicals is still based on organic chemical synthesis using petroleum derivatives as starting material. Since these processes are considered environmentally unfriendly and posing an irresponsible strain on limited fossil resources, much attention is paid to the development of new microbial factories for the bioproduction of industrially relevant chemicals using renewable sources or organic pollutants as starting material.

Arxula adeninivoras is a non-conventional yeast possessing attractive properties for industrial application such as thermo- and osmotolerance. Another major advantage of this organism is its broad substrate spectrum with tannin at the forefront. The present project is dedicated to the study of the tannic acid degradation pathway in *A. adeninivorans*.

Two genes encoding enzymes annotated as gallic acid decarboxylase (*AGDC1*) and catechol-1,2-dioxygenase (*ACDO1*) have been selected and investigated. Both enzymes were characterized and their function in tannin catabolism analyzed. Agdc1p is a monomeric protein with higher affinity for gallic acid (3,4,5-trihydroxybenzoic acid) (Km - 0.7 $\pm$ 0.2 mM, k_{cat} - 42.0 $\pm$ 8.2 s^{-1}) than for protocatechuic acid (3,4-dihydroxybenzoic acid) (Km - 3.2 $\pm$ 0.2 mM, k_{cat} - 44.0 $\pm$ 3.2 s^{-1}). Other hydroxylated benzoic acids were not recognized as Agdc1p substrates. The second enzyme, Acdo1p, is a dimeric protein with higher affinity for catechol (Km - 0.004 ± 0.001 mM, k_{cat} - 15.6 ± 0.4 s^{-1}) than for pyrogallol (Km - 0.1 ± 0.02 mM, k_{cat} - 10.6 ± 0.4 s^{-1}). Acdo1p is an intradiol dioxygenase and the reaction product formed during the conversion of catechol is *cis,cis*-muconic acid. When grown in minimal medium with nitrate as nitrogen source and 2% glucose as carbon source, *A. adeninivorans* G1212/YRC102-AYNI1-AGDC1-6H achieved a maximum gallic acid decarboxylase activity of 1064.4 U/l and 97.5 U/g of dry cell weight. Under similar conditions but with 1.5% glucose as a carbon source, *A. adeninivorans* G1212/YIC102-AYNI1-ACDO1-6H achieved a maximum catechol-1,2-dioxygenase activity of 280.6 U/L and 26.9 U/g of dry cell weight. Gallic acid decarboxylase and catechol-1,2-dioxygenase activities were not detected for the control strains G1212/YRC102 with *AGDC1* expression and G1212/YIC102 with *ACDO1* expression under the regulation of their respective endogenous promoters. Gene expression

analysis showed that *AGDC1* and *ACDO1* are induced by gallic acid and protocatechuic acid.

In contrast to G1212/YRC102-AYNI1-AGDC1 and G1212/YRC102, *A. adeninivorans* G1234 [*Δagdc1*] is not able to grow on medium with gallic acid as a carbon source but can grow in the presence of protocatechuic acid. Catabolism of protocatechuic acid via Agdc1p to catechol is not the only degradation pathway. This proves that Agdc1p plays an essential role in the tannic acid catabolism and could be useful in the production of catechol and *cis,cis*-muconic acid, which is the precursor for the production of adipic acid (one of the 50 top bulk chemicals).

Combining the microarray analysis of the *A. adeninivorans* genome sequencing data with a metabolite analysis allowed us to create a map of the tannic acid degradation pathway in *A. adeninivorans*. The present project thus contributed to a better understanding of the construction and regulation of the tannic acid degradation pathway in *A. adeninivorans*. These data confirm that this imperfect yeast is a promising new target for diverse strategies of metabolic engineering for the “green” production of aromatic chemicals and their derivatives.

Zusammenfassung

Phenole und deren Derivate sind aromatische Verbindungen mit einem großen Spektrum industrieller Applikationen. Die durch den weltweiten Markt geförderte Bulk-Produktion von Feinchemikalien für die chemische und pharmazeutische Industrie geht einher mit großen Herausforderungen auf dem Gebiet der Synthese und Verarbeitung. Gallussäure, Protocatechusäure, Catechol oder Pyrogallol gehören zu den industriell relevanten Aromaten. Die kommerzielle Produktion vieler Chemikalien basiert immer noch auf der Synthese von organischen Chemikalien, in der Erdöl-Derivate als Ausgangsmaterial genutzt werden. Diese Prozesse werden als umweltschädigend eingestuft, und darüber hinaus belastet die riesige Ausbeutung die ohnehin limitierte Verfügbarkeit der fossilen Reserven. Daher gilt momentan große Aufmerksamkeit der Entwicklung neuer mikrobieller Anlagen, die für die biologische Produktion industriell relevanter Chemikalien aus erneuerbaren Quellen oder organischen Verunreinigungs-stoffen als Startmaterial genutzt werden können.

Arxula adeninivoras ist eine nicht-konventionelle Hefe, die für die industrielle Anwendung attraktive Eigenschaften besitzt, wie Thermo- und Osmotoleranz. Zusätzlich ist dessen breites Substratspektrum, in dem vor allem Tannine von besonderem Interesse sind, ein großer Vorteil dieses Organismus. Dieses Projekt befasst sich mit den Stoffwechselwegen beim Tanninsäureabbau in *A. adeninivorans*. Zwei Gene, die für die Enzyme Gallussäure-Decarboxylase (*AGDC1*) und Catechol-1,2-Dioxygenase (*ACDO1*) kodieren, wurden näher untersucht. Beide Enzyme wurden charakterisiert und deren Funktion im Tannin-Katabolismus analysiert. Agdc1p ist ein monomeres Protein mit höherer Affinität zu Gallussäure (3,4,5-Trihydroxybenzoesäure) (Km - 0.7 $\pm$ 0.2 mM, k_{cat} - 42.0 $\pm$ 8.2 s^{-1}) als zu Protocatechusäure (3,4-Dihydroxybenzoesäure) (Km - 3.2 $\pm$ 0.2 mM, k_{cat} - 44.0 $\pm$ 3.2 s^{-1}). Andere hydroxylierte Benzoesäuren wurden nicht als Substrat von Agdc1p erkannt. Acdo1p ist ein dimeres Protein mit höherer Affinität zu Catechol (Km - 0.004 ± 0.001 mM, k_{cat} - 15.6 ± 0.4 s^{-1}) als zu Pyrogallol (Km - 0.1 ± 0.02 mM, k_{cat} - 10.6 ± 0.4 s^{-1}). Acdo1p ist eine Intradiol-Dioxygenase und das Produkt, welches während der Reaktion mit Catechol gebildet wird, ist *cis,cis*-Muconsäure. *A. adeninivorans* G1212/YRC102-AYNI1-AGDC1-6H erreicht eine maximale Gallussäure-Decarboxylase Aktivität von 1064.4 U/l und 97.5 U pro g Trocken-Zellgewicht in Hefe gewachsen auf Minimalmedium mit Nitrat als Stickstoffquelle und 2 % Glukose als Kohlenstoffquelle. Entsprechend erreicht *A. adeninivorans* G1212/YIC102-AYNI1-ACDO1-6H eine maximale Catechol-1,2-Dioxygenase Aktivität von 280.6 U/L und 26.9 U pro g Trocken-Zellgewicht in Hefe gewachsen auf

Minimalmedium mit Nitrat als Stickstoffquelle und 1.5 % Glukose als Kohlenstoffquelle. Unter den gleichen Bedingungen wurden bei Verwendung der Kontrollstämme G1212/YRC102 und G1212/YIC102 mit Expression der Gene *AGDC1* bzw. *ACDO1* jeweils unter der Kontrolle der endogenen Promoteren keine Aktivitäten der Enzyme Gallussäure-Decarboxylase bzw. Catechol-1,2-Dioxygenase detektiert. Genexpressions-analysen zeigten, dass *AGDC1* und *ACDO1* in der Präsenz von Gallussäure und Protocatechusäure induziert werden.

Im Unterschied zu G1212/YRC102-AYNI1-AGDC1 und G1212/YRC102 ist *A. adeninivorans* G1234 [*Δagdc1*] nicht in der Lage, auf Medium mit Gallussäure als C-Quelle zu wachsen. Wachstum in Gegenwart von Protocatechusäure jedoch ist möglich. Der Protocatechusäure-Katabolismus via Agdc1p zu Catechol ist nicht der einzige Degradationsstoffwechselweg. Das bedeutet, dass Agdc1p eine essentielle Rolle im Tanninsäure-Katabolismus spielt und für die Produktion von Catechol und *cis,cis*-Muconsäure nützlich sein könnte, welcher ein Vorläuferstoff für die Produktion von Adipinsäure ist (eine der 50 Top Bulk-Chemikalien).

Durch die Kombination von Microarray-Analysen, basierend auf den *A. adeninivorans* Genomsequenzierungsdaten, sowie den Metabolitanalysen konnte eine Karte des Tannindegradationsstoffwechsels in *A. adeninivorans* hergestellt werden. Dieses Projekt hat somit zu einem besseren Verständnis des Tannindegradationsstoffwechsels und seiner Regulation in *A. adeninivorans* beigetragen. Die Identifikation dieses Degradationsstoffwechselwegs bildet eine solide Grundlage für die Verwendung von *A. adeninivorans* bei metabolischen Engineering-Strategien, welche eine Erweiterung der „grünen“ Produktion von aromatischen Chemikalien und deren Derivate ermöglichen wird.

List of abbreviations

% (v/v)	Volume percent
% (w/v)	Mass percent
Amp	Ampicillin
A	Ampere
bp	Base pair
BSA	Bovine serum albumin
°C	Celsius degree
dcw	Dry cell weight
ddH_2O	Double distilled H_2O
DNA	Deoxyribonucleic acid
dNTP	Deoxyribonucleotide triphosphate
DTT	Dithiothreitol
EDTA	Ethylenediaminetetraacetic acid
g	Gravity speed
h	Hour
Kan	Kanamycin
kDa	Kilo Dalton
l	Liter
GC-MS	Gas chromatography–mass spectrometry
IPTG	Isopropyl β-D-1-thiogalactopyranoside
mM	Millimolar
M	Molar
min	Minute
OD	Optical density
PCR	Polymerase chain reaction
pH	Potential hydrogen
PMSF	Phenylmethanesulfonyl fluoride
rDNA	Ribosomal DNA
RNA	Ribonucleic acid
RT	Room temperature (20 – 22 ˚C)
SDS-PAGE	Sodium dodecyl sulphate polyacrylamide gel electrophoresis
TEMED	N,N,N′,N′-Tetramethylethylenediamine
Tris	Tris(hydroxymethyl)aminomethane
U	Unit of enzyme activity
HMM	Yeast minimal media
SOC	Synthetic oral contraceptive
s	Second
V	Volt

1 Introduction

1.1 Diversity of the plant secondary metabolites

Aromatic acids are widely used in many sectors of industry. They are mainly obtained from plants biomass, where they are synthesized via the shikimate and phenylpropanoid pathways as secondary metabolites which have important roles in plant defence mechanisms (Randhir *et al.*, 2004). Most aromatic acids are classified as phenolic compounds. These rarely occur as free forms and instead form the building blocks for more complicated polymers like tannins and lignin. Phenolic compounds vary in chemical structure, molecular mass as well as physical, chemical and biological properties (Proestos and Komaitis, 2013). In a natural environment compounds, such as lignin and tannin, can be converted by certain microorganisms. However, under industrial utilisation of plant biomass the plethora of phenolic compounds with various functional groups like aldehydes, carboxylic acids, ketone and alcoholic can seriously inhibit the growth of microorganisms. This presents a challenge for industrial processes, like biofuel production.

Tannins are a large group of polyphenolic biomolecules with complicated structures and high chemical and biological reactivity. They are usually described as compounds with a molecular mass between 500 and 3000 Da, mostly soluble in water and able to complex proteins, polysaccharides as well as metal ions (Mahadevan and Muthukumar, 1980a, 1980b, Scalbert, 1991). This diversity in size, composition and properties almost defy a general definition. Based on the molecular structures, their origin and role in plants life, Khanbabaee and van Ree (2001) defined tannins as: “polyphenolic secondary metabolites of higher plants, (which) are either galloyl esters and their derivatives, in which galloyl moieties or their derivatives are attached to a variety of polyol-, catechin- and triterpenoid cores (gallotannins, ellagitannins and complex tannins), or they are oligomeric and polymeric proanthocyanidins that can possess different interflavanyl coupling and substitution patterns (condensed tannins).” This definition emphasizes the enormous structural diversity tannins.

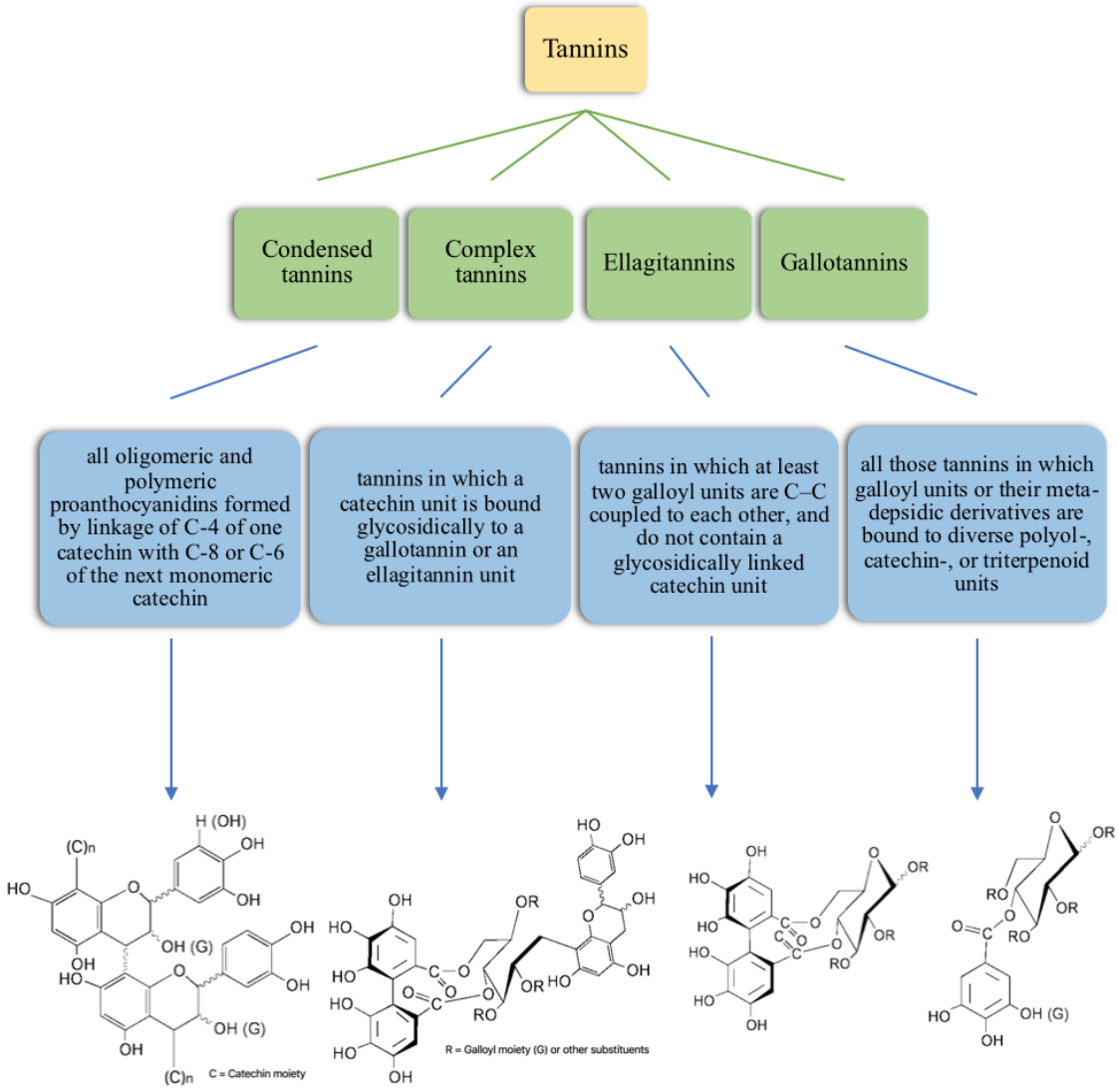

Figure 1 Classification of tannins.

For convenient systematic classification, tannins can be divided in four main classes: gallotannins, ellagitannins, complex tannins and condensed tannins (**Figure 1**). However, to this day tannins are most commonly divided into two main groups: hydrolysable and condensed tannins, yet even this simplification can skip some compounds (Mahadevan and Muthukumar, 1980b, Scalbert, 1991). Hydrolysable tannins comprise of core monosaccharides (e.g. glucose) or other polyols containing hydroxyl groups which are partially or totally esterified with gallic acid or its derivatives. The simplest hydrolysable tannin compound is tannic acid and during its hydrolysis gallic acid and glucose are released (**Figure 2**). In contrast, condensed tannins (proanthocyanidins) are flavonoids derivatives, which possess no carbohydrates units in their structure (Mahadevan and Muthukumar, 1980b).

Tannins are highly resistant to biodegradation. Characteristic is their ability to form highly stable complexes with different minerals and macromolecules, like proteins, cellulose or starch, and to precipitate heavy metals and certain alkaloids. Tannins serve as a defense against diseases caused by fungi, bacteria, and viruses, and protect plant tissues against attack by insects and herbivores (Swain, 1977, Scalbert, 1991).

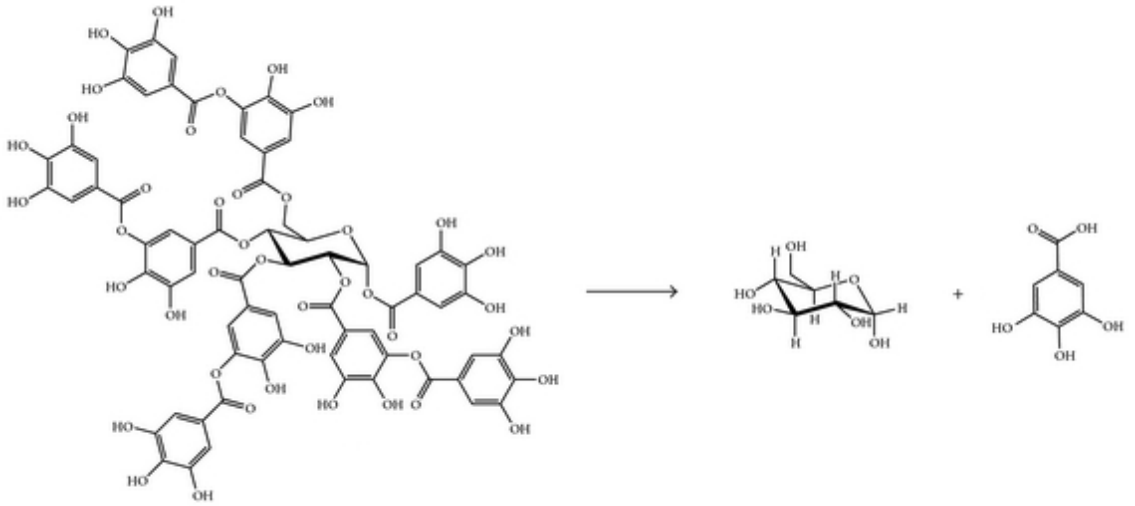

Figure 2 Hydrolysis of tannic acid.

Lignins represent the second most abundant cross-linked phenolic polymer in terrestrial plants. They are composed of phenylpropanoid units derived from three cinnamyl alcohols (monolignols): p-coumaryl, coniferyl and simple alcohols (Boudet *et al.*, 1995, Hatfield and Vermerris, 2001). Because of its robustness against degradation, it was speculated that lignins might have a more complex composition (Erdtman, 1972). Today we know that also other phenolics can be incorporated into lignins (for review, see Sederoff *et al.* (1999)). However, the exact linkage structures are still not completely elucidated. Composition and structure of lignins reflect their functions. Lignins convey strength to cell walls, facilitate water transport, and though impeding the degradation of wall polysaccharides they are also a major line of defence against pathogens, insects, and other herbivores. Though lignins are highly resistant to microbial degradation, some microbes have developed enzymes like lignin peroxidase, manganese peroxidase and laccase which through radical reactions can attack lignin structure (Martinez *et al.*, 2005, Leonowicz *et al.*, 2001).

Microbial degradation of plant biomass releases aromatic compounds which are of major interest to industry as they can be converted to, among others, flavour and antioxidant compounds. However, free (non-polymeric) aromatic compounds are already toxic for most microorganisms at relatively low concentrations (Buswell and Eriksson, 1994, Scalbert, 1991). Therefore, to circumvent this toxicity, microorganisms keep these oligomeric compounds actively out of the cell or efficiently convert them inside the cell into aliphatic non-toxic compounds.

1.2 Properties and industrial applications of phenolic compounds

Tannins and other polyphenolic metabolites as well as their degradation products like gallic acid or protocatechuic acid, are present in almost all parts of higher plants. They not only protect against pathogens and herbivores, but also against unfavourable environmental factors.

There is a strong interest in polyphenolic compounds in the industry. Tannins possess antimicrobial properties and inhibit the growth of many filamentous fungi, yeasts and bacteria already at very low concentrations (Scalbert, 1991, Sikkema *et al.*, 1995, Chung *et al.*, 1998b, 1998c, de Bruyne *et al.*, 1999, Howell *et al.*, 1998). Moreover, they complex proteins, starch and digestive enzymes, thereby producing an astringent, unpleased taste and reducing the nutritional values of foods (Butler, 1992, Badhani *et al.*, 2015). Tobacco mosaic virus, herpes simplex virus, influenza virus, coxsackievirus, echovirus, reoviruses, herpes viruses, and polio viruses can be inactivated by tannins (Chung *et al.*, 1998a). Additionally, many reports attribute tannins an antimutagenic, anticarcinogenic, anti-AIDS or immunomodulatory activity (Chung *et al.*, 1998a, Mizuno *et al.*, 1992). Tannins even found their place in daily used products like antitranspirants and deodorants conferring several patents to the usage of tannins in this field (e.g. DE 20 2015 100 862 U1).

Gallic acid has also become a wanted compound, especially as a raw material in pharmaceutical, food, chemical and electronic industries, because of its, among others, antifungal, bacteriostatic, anticancer, antimelanogenic and antioxidant properties (Badhani *et al.*, 2015). Gallic acid is used e.g. for the synthesis of the food antioxidant propyl gallate, the antibacterial drug trimethoprim (Hadi *et al.*, 1994, Yu *et al.*, 2004) and printing inks (Hadi *et al.*, 1994). The conventional production of gallic acid is an acidic hydrolysis of tannic acid. However, because of costs, low yield and low purity, this

method is not economically preferable. In 2015, the global demand was more than eight thousand tons per year, and according to Global Gallic acid Market Analysis from 2018, with demands growing (Raport, 2018, Aguilar-Zárate *et al.*, 2015). The high requirements have sparked the search for new, more efficient methods of production. The best alternative is fermentation processes involving microorganisms. Since this also enables the use of waste material as starting substrates, this also has ecological advantages (Shete and Chitanaad, 2015).

Protocatechuic acid and catechol are among the phenolic compounds for which there is a growing demand. Protocatechuic acid is similar in structure to gallic acid and is present in more than 500 plants. It has been reported to act as antioxidant, antibacterial, anticancer, antiulcer, antidiabetic, antiageing, antifibrotic, antiviral, anti-inflammatory, analgesic, antiatherosclerotic, cardiac, hepatoprotective agent as well as a neurological and nephro protectant (Kakkar and Bais, 2014). For this reason, protocatechuic acid is often classified as medicine and used in pharmaceutical synthesis. However, it is also used as an organic intermediate, chemical reagent and for dye synthesis. In 2017, the protocatechuic acid market achieved 105 million $ (MarketResearchStore (2018). In the same year, the medicine market shared 72.91% of protocatechuic acid applications. The medical products based on protocatechuic acid are for example erlotinib (antineoplastic), veratridine (sodium channel inactivation inhibitor), hydrochloric acid Mai Pi skin Lin (respiratory drug), Picatin II (treatment of hepatitis B) and itopride hydrochloride (new gastrointestinal motility drug) (QYResearch, 2018).

Growth rates for the second compound, catechol, are also expected to rise steeply. Synthetic catechols are mainly used for the production of pesticides and to a lesser extend in the personal care industry. Here it is used as a precursor for pharmaceuticals and perfumes including the preparations of vanillin and ethyl-vanillin (MarketResearchFuture, 2018, CredenceResearch, 2018).

Another compound with great industrial potential is *cis,cis*-muconic acid, which is an unsaturated six carbon di-carboxylic acid (McKetta, 1977). It can be used for the production of adipic acid. With annual worldwide production approaching 3 million tonnes, adipic acid is among the top 50 of bulk chemicals produced (Polen *et al.*, 2013). It is used mainly in the production of nylons, but also of lubricants and as coatings for the chemical, pharmaceutical and food industries (Burgard *et al.*, 2011, Wu *et al.*, 2011).

The traditional feedstock for the production of adipic acid is benzene and benzene-derived chemicals (Van de Vyver and Román-Leshkov, 2013). This chemical synthesis is extremely energy and cost intensive. More problematic, however, is its use of carcinogenic feedstock and the generation of the potent greenhouse gas nitrous oxide during the production process (Alini *et al.*, 2007, Cavani *et al.*, 2009, Galbraith *et al.*,

2010, Opec., 2012, Van de Vyver and Román-Leshkov, 2013, Faustini *et al.*, 2014, OrbiChem, 2013). Biocatalytic synthesis using genetically optimized microorganisms could eliminate these environmental concerns while at the same time providing a more cost-efficient production pathway. Much research has been devoted to the construction of microbiological strains with modified native pathways for the large scale production of *cis,cis*-muconic acid.

So far, microbiological production has concentrated on engineering the β-ketoadipate pathway, present in most soil bacteria (Collier *et al.*, 1998, Denef *et al.*, 2006, Cao *et al.*, 2008), as well as the chorismate pathway, which is the most common aromatic producing pathway in prokaryotic and eukaryotic microorganisms (Braus, 1991). In case of the second pathway, production of *cis,cis*-muconic acid uses glucose as starting substrate. Initial studies using transformed *Escherichia coli* as host organism produced satisfying amounts of *cis,cis*-muconic acid. Unfortunately, scaling-up proved prohibitively expensive, especially because of high costs, large amount of calcium carbonate waste produced during extraction of un-dissociated *cis,cis*-muconic acid, and high risk of contamination of the fermentation culture (Draths and Frost, 1994, Niu *et al.*, 2002, Gosset, 2009, Wang and Zheng, 2015, Lin *et al.*, 2014, Sun *et al.*, 2013). In search for cheaper solutions, application of more robust organisms like *S. cerevisiae* has been proposed. So far, however, *cis,cis*-muconic acid production in these alternative systems is still challenging (Luttik *et al.*, 2008, Curran *et al.*, 2013, Bruckner *et al.*, 2018, Weber *et al.*, 2012).

1.3 Persistence of phenolic compounds

Aromatic compounds, including phenolics, account for around 25 % of the earth's biomass making them the second most abundant class of organic compounds in nature after carbohydrates (Boll *et al.*, 2002). A substantial amount of these aromatic compounds occurs in the form of plant material. Small wonder that plant biomass is attracting increasing attention as a sustainable source for large-scale production of renewable fuels and chemicals. At least on paper, the use of plant material should be beneficial for the environment. However, large scale use of plant material is bound to set free considerable quantities of phenolics compounds. A general feature of these compounds is their low degradation rate, making them highly persistent and prone to accumulation.

In the case of biofuel production, many efforts are devoted in optimizing biomass conversion processes in order to compete with fossil fuels. The process of biofuel production starts with an aqueous pre-treatment of the plant biomass (Davison *et al.*, 2013). This manufacturing step releases large amounts of phenolic compounds. These not only can have an inhibitory effect on the proliferation of the very microbiome implied in the biodegradation of the plant biomass, but they can also affect biodegradation processes itself and with it the efficiency with which ethanol, acetate and glycerol are produced (Adeboye *et al.*, 2014).

These low degradation rates can also lead to the accumulation of synthetic aromatic compounds in the environment. Di- and trihydroxylated aromatic acids like gallic acid and protocatechuic acid are very persistent and these products therefore often accumulate in water and soil (Zhang et al., 2014).

The two main sources of this environmental pollution are the use of aromatic pesticides in agriculture and in the proscription of medicational products. Although part of the medical substances leaves the body unaltered, a far more significant problem is that unused medication is often discarded in the waste water. Recent studies have indicated that in Germany nearly half of all medicational product is discarded this way (Lubick, 2010).

Increasing the efficiency of biodegradation of aromatic compounds has thus become a major issue in both biofuel production and reducing environmental pollution. This requires the investigation of candidate microorganisms, metabolic pathways as well as enzymes involved in these processes.

1.4 Microbial strategies for biodegradation of aromatic compounds

The main function of plant aromatic compounds is that of protectants. Plant aromatic compounds are e.g., toxic to microorganisms or they polymerize upon exposure to air thus acting as a wound seal. The biodegradability of aromatic compounds largely depends on properties such as solubility in water, volatility, molecular size, number and type of functional groups. But also environmental factors like temperature, moisture, pH, oxygen availability, hydrostatic pressure and salinity play an important role in determining their stability (Berry *et al.*, 1987).

Nowadays, as the industrial production of synthetic aromatic compounds has surged, some have become environmental pollutants. This problem has become serious by the

production of xenobiotics, molecules with little resemblance to their natural pre-templates. It has come somewhat of a surprise that many bacteria and fungi have been able to adapt very quickly their catabolic pathways to also metabolize such aromatic xenobiotics, especially because several compounds have been produced only for the past 30-50 years (Schink *et al.*, 2000).

Microorganisms have developed two major biochemical strategies to degrade aromatic compounds which depend on the presence or absence of oxygen. Whereas the anaerobic degradation involves reductive reactions, the primary reaction step in aerobic breakdown is oxidative attack and ring-cleavage. The key role of both pathways though is to transform aromatic substrates into key intermediate products, through devoted peripheral degradation pathways (catabolic funnel), causing in destabilization and fission of ring structure that can be further channelled into the central metabolism of the cell.

Most organic matter, however, is degraded in an aerobic environment by aerobic bacteria and fungi. The preponderance of aerobic degradation is probably due to the ubiquitous presence of molecular oxygen (Jothimani *et al.*, 2003). The major principle of aerobic degradation is ring cleavage in an oxygenase-dependent step and generation of compounds for energy production such as succinate, acetyl-CoA, and/or pyruvate which are intermediates of the Krebs cycle (Dagley, 1971, Schmauder, 1992). A broad range of aromatic compounds is degraded through peripheral pathways that funnel into a few entry point compounds, which serve as substrates for oxygenase ring fission. These include: catechol, protocatechuic acid, 3,4-dihydroxyphenylacetate, gentisic acid, 2,5-dihydroxyphenylacetate, hydroxyquinol and 3-O-methyl gallate. These pathways are highly exergonic, releasing about 300 kJ/mol which is equivalent to 4 or 5 ATP per reaction (Schink *et al.*, 2000). Ring-cleavage can be carried out by intradiol or extradiol dioxygenases. Intradiol dioxygenases cleave the aromatic nucleus ortho (= between) to the hydroxyl substituents. This involves substrates possessing vicinal hydroxyl groups, i.e. catecholic compounds. Extradiol dioxygenases on the other hand, cleave the aromatic ring meta (adjacent) to the hydroxyl substituents and can thus act on both catecholic and non-catecholic compounds (Vaillancourt *et al.*, 2004, 2006, Nogales *et al.*, 2005).

A further type of ring cleavage occurs when two hydroxyl groups are para to each other. Under this condition, cleavage occurs between the carboxyl-substituted carbon and the adjacent hydroxylated carbon. An example is the degradation of gentisic acid (**Figure 3**). Ortho-cleavage pathways, commonly known as β-ketoadipate pathways, are chromosomally encoded. This is in contrast to meta-cleavage pathways which are plasmid encoded. The *β*-ketoadipate pathway plays a central role in both eukaryotic and

prokaryotic microorganisms as it is involved in the processing and degradation of naturally occurring aromatic compounds derived from lignin and other plant components. As such, the β-ketoadipate is a major utility pathway for degradation of aromatic compounds. In bacteria, this pathway frequently coexists with plasmid-encoded *meta*-pathways (Assinder and Williams, 1990).

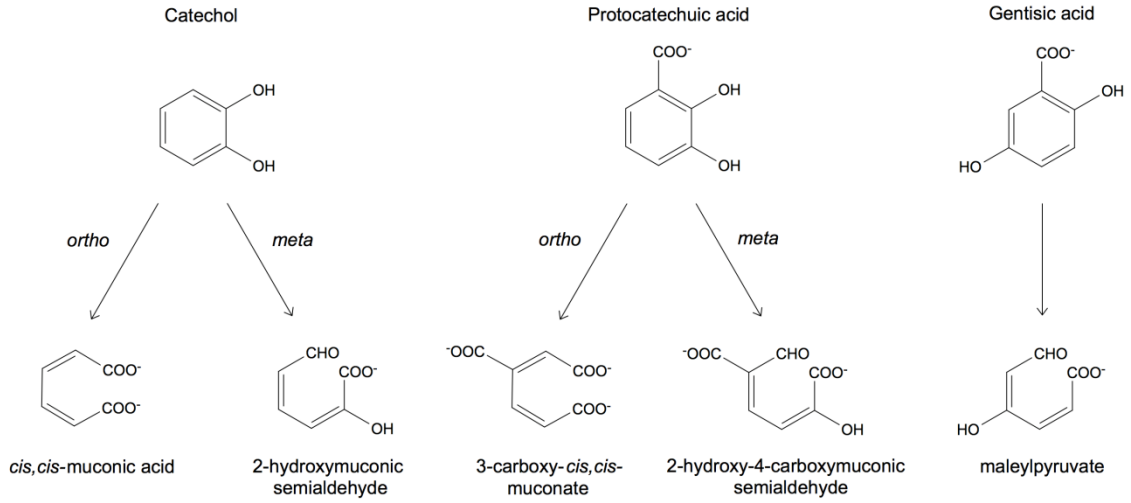

Figure 3 Main strategies of aerobic aromatic ring cleavage: ortho-, metha-, and gentisate pathways.

Aromatic compounds funnelled into the catechol intermediate include: phenanthren, naphthalene, mandelate, toluene, tryptophan, salicylate, benzoate, anthranilate, aniline, cinnamate, benzene and phenol. Compounds channelled into the protocatechuic acid intermediate are for example: 4-coumarate, 4-chlorobenzoate, cyclohexane carboxylate, p-cresol, 4-hydroxybenzoate, shikimate, quinate, 3-hydroxybenzoate, benzoate, ferulate, vanillate, coniferyl alcohol (Andreoni *et al.*, 1991, Ornston, 1971, Petsko *et al.*, 1993, Parke and Ornston, 1984, Hawkins *et al.*, 1993, Blakley, 1974, Bruce and Cain, 1990, Parke *et al.*, 1991, Delneri *et al.*, 1995).

The most common enzymes involved in the biodegradation of aromatic compounds are hydroxylases, dioxygenases, oxidoreductases and decarboxylases. The representative reactions are shown in **Figure 4**. In aerobic degradation, the first reaction step is performed by dioxygenases or oxidoreductases. In non-oxidative decarboxylation, this first reaction step involves a decarboxylase. The direct cleavage of a gallic acid or protocatechuic acid ring can be carried out by protocatechuate-4,5-dioxygenase, leading into the meta fission pathway (**Figure 4 A**) while protocatechuate-3,4-dioxygenase

oxidises gallic acid to 2-pyrone-4,6-dicarboxylic acid (**Figure 4 B**) and protocatechuic acid to β-carboxy-*cis,cis*-muconate following the ortho fission pathway (Ornston, 1971, Ornston and Ornston, 1972).

A. Gallic acid degradation I - aerobic

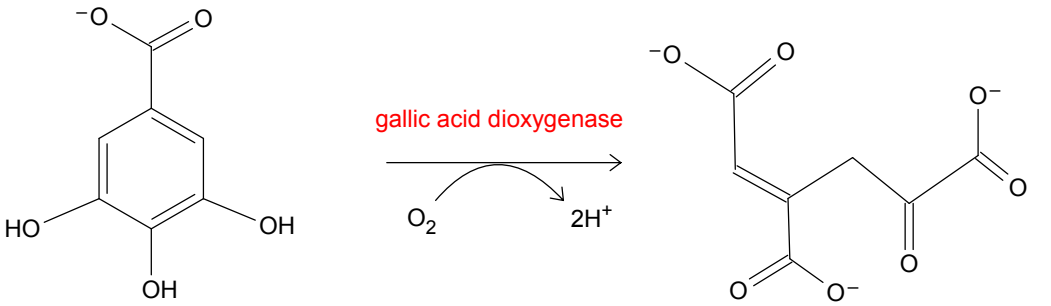

gallic acid (1E)-4-oxobut-1-ene-1,2,4-tricarboxylic acid

B. Gallic acid degradation II - aerobic

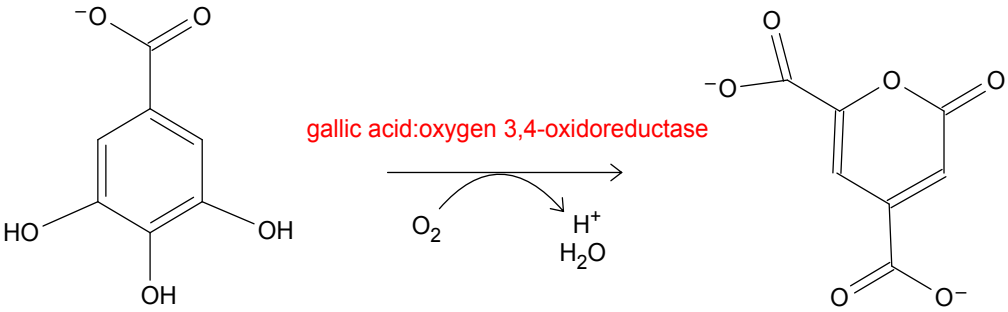

gallic acid 2-pyrone-4,6-dicarboxylic acid

C. Gallic acid degradation III - anaerobic

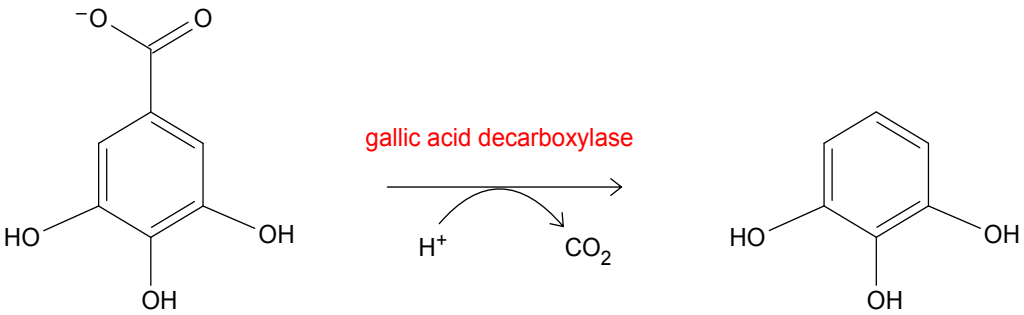

gallic acid pyrogallol

Figure 4 Variants of microbial gallic acid degradation.

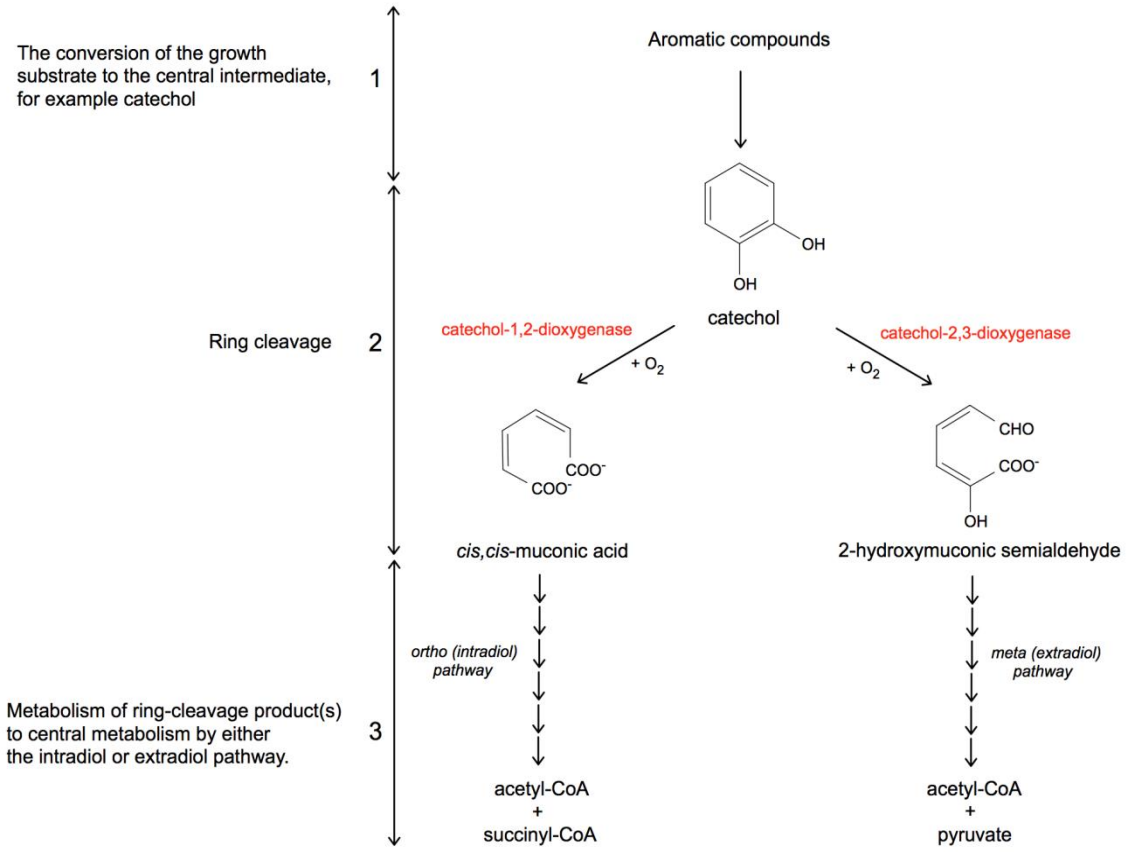

Figure 5 General principles of microbial aerobic catabolism of aromatic compounds with catechol as central intermediate metabolite.

The general pathway of aerobic degradation of aromatic compounds can be divided into three steps. The first step is the conversion of aromatic substrates into central intermediates. In the second step, the aromatic ring is cleaved. Finally, in the last step, the ring-cleavage products enter the central metabolic pathway (**Figure 5**).

1.5 Yeast *Arxula adeninivorans* and its ability to degrade tannin compounds

Arxula adeninivorans (syn. *Blastobotrys adeninivorans*) is a relatively recently discovered non-conventional, non-pathogenic, imperfect, haploid yeast species, belonging to the subphylum *Saccharomycotina*. This new organism was isolated from soil by an enrichment culture method and named *Trichosporon adeninovorans* (Middelhoven *et al.*, 1984). Six years later, Gienow (Gienow *et al.*, 1990) described the second strain, LS3

(PAR-4), isolated from wood hydrolysates in Siberia (Russia). Further strains were isolated from chopped maize herbage in the Netherlands and from humus-rich soil in South Africa (Van der Walt *et al.*, 1990). All of these wild-type isolates were found to possess unusual properties such as nitrate assimilation, xerotolerance and the ability to use adenine, guanine, butylamine, soluble starch, melibiose, uric acid, pentylamine, putrescine, propylamine and hexylamine as sole sources of carbon, nitrogen and energy (Middelhoven *et al.*, 1984).

In 1991, the species was given the name *Arxula adeninivorans* (Middelhoven *et al.*, 1991). Despite a subsequently renaming into *Blastobotrys adeninivorans* (Kurtzman and Fell, 1998), currently the strain genotyping exhibited that various marker sequences actually placed the LS3 group into the *Blastobotrys raffinosifermentans* species (Thomas *et al.*, 2019). Nonetheless, in the current study I have decided to retain the common name *Arxiula adeninivorans*. In this study, *A. adeninivorans* LS3 (Kunze and Kunze, 1994) and the auxotrophic mutant *A. adeninivorans* G1212 (*aleu2 ALEU2::atrp1*) (Steinborn *et al.*, 2007) were employed. Both are deposited in the yeast collection of the Department of Biology of the University of Greifswald (SBUG, Germany).

In 2014, the genome of *A. adeninivorans* LS3 was sequenced. The mitochondrial genome has a size of 31 662 bp and encodes 24 tRNAs and 15 proteins. The nuclear genome has a size of 11.8 Mb and comprises four chromosomes: Arad1A (1 659 397 nt), Arad1B (2 016 785 nt), Arad1C (3 827 910 nt) and Arad1D (4 300 524 nt) with regional centromeres. These four chromosomes house 6116 protein-encoding genes, 33 pseudogenes and 914 introns. A single rDNA cluster which plays an important role in molecular tools of *A. adeninivorans* is located approximately 75 kb upstream of the right subtelomere of the Arad1D chromosome (Kunze *et al.*, 2014, Rösel and Kunze, 1996, Pich and Kunze, 1992).

Although *A. adeninivorans* is phylogenetically distant from *S. cerevisiae*, it reads Leu CUN and Arg CGN codons as in baker's yeast (Kunze *et al.*, 2014). In most cases, this is an additional advantage for heterologous gene expression. Depending on the cultivation temperature, *A. adeninivorans* exhibits different morphological forms (Wartmann *et al.*, 1995, 2002) **(Figure 6**). Various post- translational modifications and protein expression properties are strongly correlated with these two morphologies (Böer *et al.*, 2007, Wartmann *et al.*, 2002).

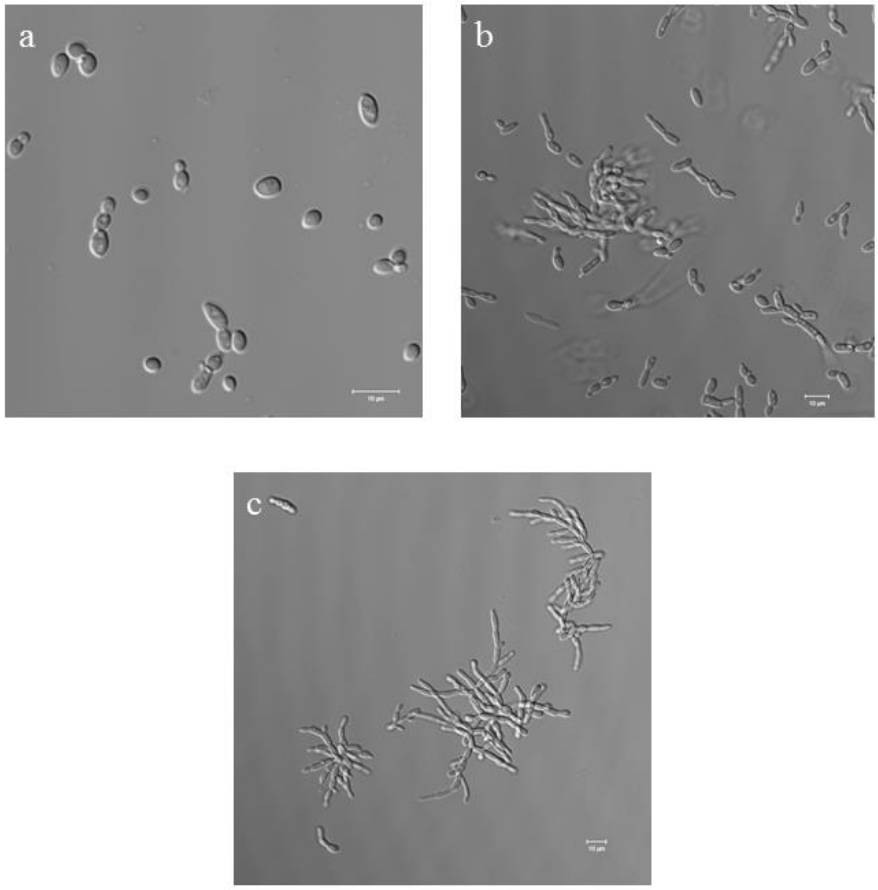

Figure 6 Temperature-dependent dimorphism in *A. adeninivorans* LS3.
A. adeninivorans forms budding cells when cultured at 30 °*C (a),* pseudomycelia when cultured at 42 °C (b) and mycelia when cultured at 45 °C (c). Cells were grown in YEPD medium.

There is already a well-developed transformation/expression platform which makes rapid and simple gene manipulations possible (Terentiev *et al.*, 2004, Böer *et al.*, 2009a). *A. adeninivorans* has shown itself to be a very good host for homologous and heterologous gene expression and to be a useful gene donor (Böer *et al.*, 2004, 2005, 2007, 2009c, Jankowska *et al.*, 2013a, 2013b, Trautwein-Schult *et al.*, 2013, 2014, Bischoff *et al.*, 2015, Kumari *et al.*, 2015). These features make *A. adeninivorans* a good alternative for the most intensively studied yeast species *Saccharomyces cerevisiae* (Meier *et al.*, 2017, Bruckner *et al.*, 2018). In industrial applications, *S. cerevisiae* can have some limitations such as hyperglycosylation, poor secretion and/or incorrect folding of heterologous proteins and a relative sensitivity towards osmotic and temperature stress.

Another interesting feature of *A. adeninivorans* is the presence of many metabolic pathways, including the degradation of n-butanol, purines and tannins. Among the enzymes produced by *A. adeninivorans* LS3 is tannin acyl hydrolase 1 (Atan1p),

catalyzing the first reaction step in tannin degradation (Böer *et al.*, 2009a). The gene encoding a 587-amino acid extracellular protein is preceded by an N-terminal secretion sequence. This sequence contains the consensus pentapeptide motif (–Gly–X–Ser–X–Gly–) which forms part of the catalytic center of serine hydrolases. Expression of *ATAN1* is regulated by the carbon sources tannins or gallic acid (Böer *et al.*, 2009a). Atan1p is a glycosylated protein consisting of four identical subunits and is able to remove gallic acid from both condensed and hydrolysable tannins. Additional genome analysis revealed the presence of a second potential tannin acyl hydrolase (Atan2p) as well as gallic acid decarboxylase (Agdc1p) and catechol-1,2-dioxygenase (Acdo1p), which may also be involved in tannin degradation (Kunze *et al.*, 2014). The transformation of gallic acid and protocatechuic acid by *A. adeninivorans* LS3 wildtype strain (Sietmann *et al.*, 2010) was the first report of a nonoxidative decarboxylation of gallic acid by a eukaryotic microorganism. Cultivation experiments with protocatechuic and gallic acid suggested that the decarboxylation of protocatechuic and gallic acid may be catalyzed by the same enzyme (Sietmann *et al.*, 2010). The authors also proposed a pathway for the transformation of hydroxylated benzoic acid derivatives by the LS3 strain, based on their observation that metabolism of gallic acid lead to the production of pyrogallol and 2-hydroxymuconic acid whereas metabolism of protocatechuic acid produced catechol and *cis,cis*-muconic acid.

Although the information thus gained on the tannic acid metabolic pathway in *A. adeninivorans* was used to optimize *cis,cis*-muconic acid production by *S. cerevisiae*, *A. adeninivorans* itself might be a good alternative to *S. cerevisiae* (Meier *et al.*, 2017, Bruckner *et al.*, 2018).

1.5.1 Gallic acid decarboxylase

Gallic acid decarboxylase (EC 4.1.1.59) belongs to the class of lyases or more precisely that of the carboxy-lyases. Alternative names are gallate decarboxylase, gallate carboxy-lyase and 3,4,5-trihydroxybenzoate carboxy-lyase. The enzyme carries out the non-oxidative decarboxylation of gallic acid, thus producing carbon dioxide and pyrogallol, which has a lower toxicity than gallic acid (**Figure 7**).

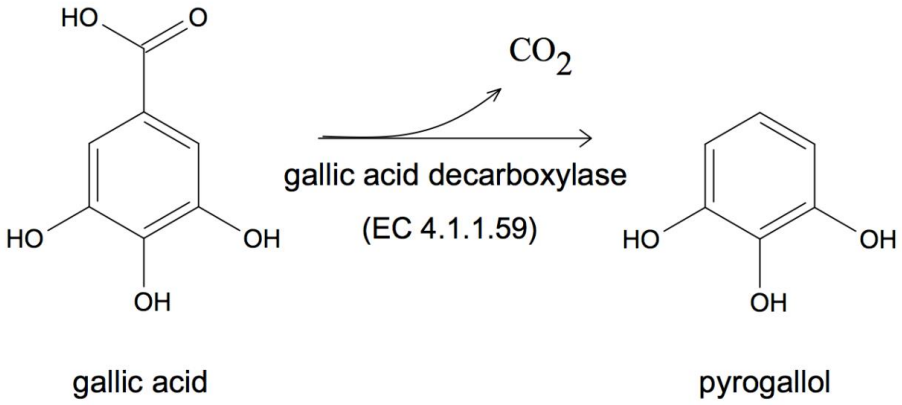

Figure 7 Non-oxidative decarboxylation of gallic acid into carbondioxide and pyrogallol by gallic acid decarboxylase.

Degradation of gallic acid through non-oxidative decarboxylation is observed in many microorganisms, including: *Klebsiella aerogenes* (Grant and Patel, 1969), *Citrobacter* sp. (Yoshida *et al.*, 1982), *Eubacterium oxidoreducens* (Krumholz *et al.*, 1987), *Pleobacter acidigallici* (Samain *et al.*, 1986), *Pelobacter acidigallici* (Brune and Schink, 1992), *Pantoea agglomerans* T71 (Zeida *et al.*, 1998), *Streptococcus gallolyticus* (O'Donovan and Brooker, 2001), *Arxula adeninivorans* (Sietmann *et al.*, 2010), *Enterobacter* spp. (Soni *et al.*, 2012), *Azotobacter* sp. SSB81 (Gauri *et al.*, 2013), *Lactobacillus plantarum* WCFS1 (Jiménez *et al.*, 2013)and *Enterobacter aerogenes* (Li and Wang, 2015). In most of these organisms, the decarboxylase is connected to tannin degradation, since gallic acid is formed during the hydrolysis of tannic acid. Interestingly, some gram-negative bacteria contain tannases but no gallic acid decarboxylase (Nemoto *et al.*, 1995). Bacteria like *S. gallolyticus*, *Selenomonas gallolyticus* and *E. coli* catalyze the decarboxylation of gallic acid to pyrogallol but do not further transform pyrogallol (O'Donovan and Brooker, 2001, Chamkha *et al.*, 2002, Odenyo *et al.*, 2001).

Decarboxylases are often encoded by inducible genes which ensure that the synthesis of the enzymes only occurs in the presence of their substrates. However, the gallic acid decarboxylase in *K. aerogenes* and *K. pneumonia* are constitutive enzymes (Grant and Patel, 1969, Nakajima *et al.*, 1992). Gallic acid decarboxylases are characterized by various substrate specificities. While the enzymes produced by *E. oxidoreducens* and *P. agglomerans* T71 have a high specificity for gallic acid as substrate (Krumholz *et al.*, 1987, Zeida *et al.*, 1998), those of *Citrobacter* sp. and *Clostridium hydroxybenzoicum* have wide range of substrates (He and Wiegel, 1995, Yoshida *et al.*, 1982).

Gallic acid decarboxylases are oxygen-sensitive and relatively unstable. This may be caused by the presence of a metal ion cofactor in the protein structure since enzymes containing iron-sulfur clusters are known to be oxygen-sensitive (Flint and Allen, 1996). However, while gallic acid decarboxylase from *Pantoea agglomerans* T71 requires iron (Zeida *et al.*, 1998) and that of *Pelobacter acidigallici* requires magnesium (Samain *et al.*, 1986), most aromatic acid decarboxylases require no cofactors, yet are still very unstable (Grant and Patel, 1969, Krumholz *et al.*, 1987, Nakajima *et al.*, 1992, Samain *et al.*, 1986, Yoshida *et al.*, 1982, Haddock and Ferry, 1993). Due to this instability, only a few gallic acid decarboxylases have ever been purified and characterized (Jiménez *et al.*, 2013, Nakajima *et al.*, 1992, Yoshida *et al.*, 1982, Zeida *et al.*, 1998). As a consequence, there is still relatively little known about these enzymes.

1.5.2 Catechol-1,2-dioxygenase

Catechol-1,2-dioxygenase (EC 1.13.11.1), an intradiol dioxygenase enzyme belonging to the class of oxidoreductases, is found in many microorganisms. The first report dates from 1950 (Hayaishi and Hashimoto, 1950). These enzymes carry out ring fission of catecholic compounds involving the cleavage and incorporation of molecular oxygen (ortho cleavage). A common example of its reaction is catechol ring cleavage leading to *cis,cis*-muconic acid (**Figure 8**).

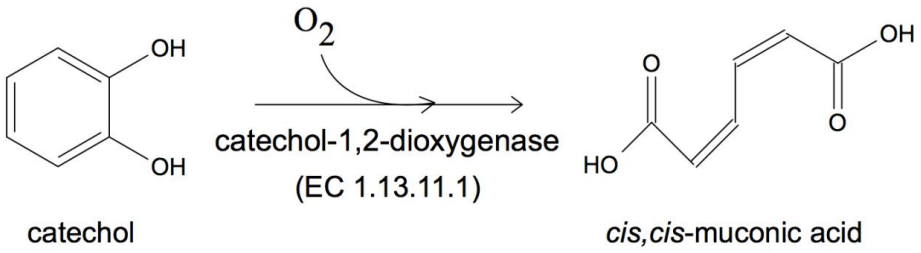

Figure 8 Intradiolic cleavage of catechol by catechol-1,2-dioxygenase.

Cleavage of aromatic rings by dioxygenases is the key reaction in the degradation of aromatic compounds by aerobic microorganisms. An advantage of degrading aromatic compounds through ortho cleavage is that the intermediate products generated are less toxic than those created through meta cleavage (Bartels *et al.*, 1984, El-Sayed *et al.*, 2009). Furthermore, the products generated by catechol-1,2-dioxygenase reactions include some important compounds for the chemical industry like *cis,cis*-muconic acid (Mizuno *et al.*, 1988, Wu *et al.*, 2004).

Based on substrate affinity, intradiol dioxygenases were initially split into two families, catechol-1,2-dioxygenases and protocatechuate-3,4-dioxygenases (Vetting and Ohlendorf, 2000). The former, catechol-1,2-dioxygenases, is further divided into type I dioxygenases with activity against catechol and lack or low affinity against chlorocatechol, and type II dioxygenases with affinity against only chlorocatechols (Caposio *et al.*, 2002). The discovery of a catechol-1,2-dioxygenase from the fungus *Trichosporon cutaneum* with high affinity towards 4-methylcatechol and methyl-substituted aromatic compounds such as p-toluate and p-cresol urged the establishment of a third family of catechol-1,2-dioxygenase, that of the 4-methylcatechol-1,2-dioxygenases (Powlowski and Dagley, 1985).

Catechol-1,2-dioxygenases are homodimeric metalloenzymes containing non-heme iron (III) as a cofactor which is responsible for binding and activating molecular oxygen in the cleavage reaction (Briganti *et al.*, 2000b, Broderick and O'Halloran, 1991, Vetting and Ohlendorf, 2000). The monomers which have a molecular mass of 30-40 kDa contain a single catalytic non-heme ferric ion ($(\alpha Fe^{3+})_2$). The only known exception is catechol-1,2-dioxygenase from *Pseudomonas arvilla* with highly homologous monomers which can associate to form homodimers or heterodimers (Nakai *et al.*, 1979, 1995, 1996, Earhart *et al.*, 2005). The nonheme iron (III) cofactors of intradiol dioxygenases are ligated by four amino acid side chains of two histidine and two tyrosine residues in a trigonal bipyramidal manner with a water molecule occupying the fifth coordination site (see **Figure 9**) (Briganti *et al.*, 2000a, Caposio *et al.*, 2002, Ferraroni *et al.*, 2005, Ohlendorf *et al.*, 1988, Sauret-Ignazi *et al.*, 1996, Vetting and Ohlendorf, 2000, Wang *et al.*, 2006). The arrangement of iron (III) ligands in the active site is very similar to that found in catechol-1,2-dioxygenases (Briganti *et al.*, 2000b, Caposio *et al.*, 2002, Ferraroni *et al.*, 2006, Gou *et al.*, 2009, Guzik *et al.*, 2011, Matera *et al.*, 2010, Pandeeti and Siddavattam, 2011, Sauret-Ignazi *et al.*, 1996, Vetting and Ohlendorf, 2000, Wang *et al.*, 2006). Investigation of the crystal structure of catechol-1,2-dioxygenase from *Acinetobacter* sp. ADP1 revealed a helical zipper motif at the interface of the two subunits next to the presence of two phospholipids (Vetting and Ohlendorf, 2000). The latter were identified as phosphatidylcholine displaying two C14-15/C12-C17

hydrophobic tails, binding the hydrophobic amino acid of the active site. The role of these phospholipids has not yet been clarified (Bugg, 2003, Micalella *et al.*, 2011, Vaillancourt *et al.*, 2006).

Many catechol-1,2-dioxygenases are inducible enzymes, expressed in the presence of phenolics compounds (Ahuatzi-chacón *et al.*, 2004, Caposio *et al.*, 2002, Dorn and Knackmuss, 1978, Haigler *et al.*, 1988, Subbotina *et al.*, 2016, Tsai and Li, 2007). Though they differ in enzyme activity and substrate specificity, all catechol-1,2-dioxygenases have an pH optimum between 7 and 9 (Guzik *et al.*, 2013, Strachan *et al.*, 1998, Tsai and Li, 2007, Wang *et al.*, 2001, Briganti *et al.*, 1997, Dorn and Knackmuss, 1978). Catechol-1,2-dioxygenases require no extra cofactor for activity and the addition of metal ions is often plain inhibitory (Aoki *et al.*, 1984, Briganti *et al.*, 1997, Dorn and Knackmuss, 1978, Itoh, 1981, Tsai and Li, 2007, Wang *et al.*, 2001, Chang-Jun, 2006).

The catalytic cycles of protocatechuate-3,4-dioxygenases and catechol-1,2-dioxygenases have a similar reaction mechanism (Lipscomb *et al.*, 1982, 1980, Que *et al.*, 1977). Borowski and Siegbahn (2006) investigated the mechanism of the catalytic action of intradiol dioxygenases based on protocatechuate-3,4-dioxygenases as representative, using the computational hybrid density functional method B3LYP (**Figure 9**). They suggested that the chemical reactions of the catalytic cycle can be divided into seven steps. The substrate binds as dianion to the iron presented in the catalytic centre. Dioxygen binds to the metal which is aided by an electron transfer from the substrate to O_2. A bridging peroxo intermediate is formed and its conformation is changed, opening the coordination site *trans* to His462. The neutral XOH ligand, H_2O or Tyr447, binds at the open site. The proton from XOH is transferred to the neighboring peroxo ligand and yields the hydroperoxo intermediate. Criegee re-arrangement lead to the anhydride intermediate, hydrolysis of which leads to the final acyclic product (Borowski and Siegbahn, 2006). Guzik *et al.* (2013) took advantage of the results described in the literature and derived a general scheme of the catalytic cycle of the intradiol dioxygenases, precisely describing every catalytic step (**Figure 9**).

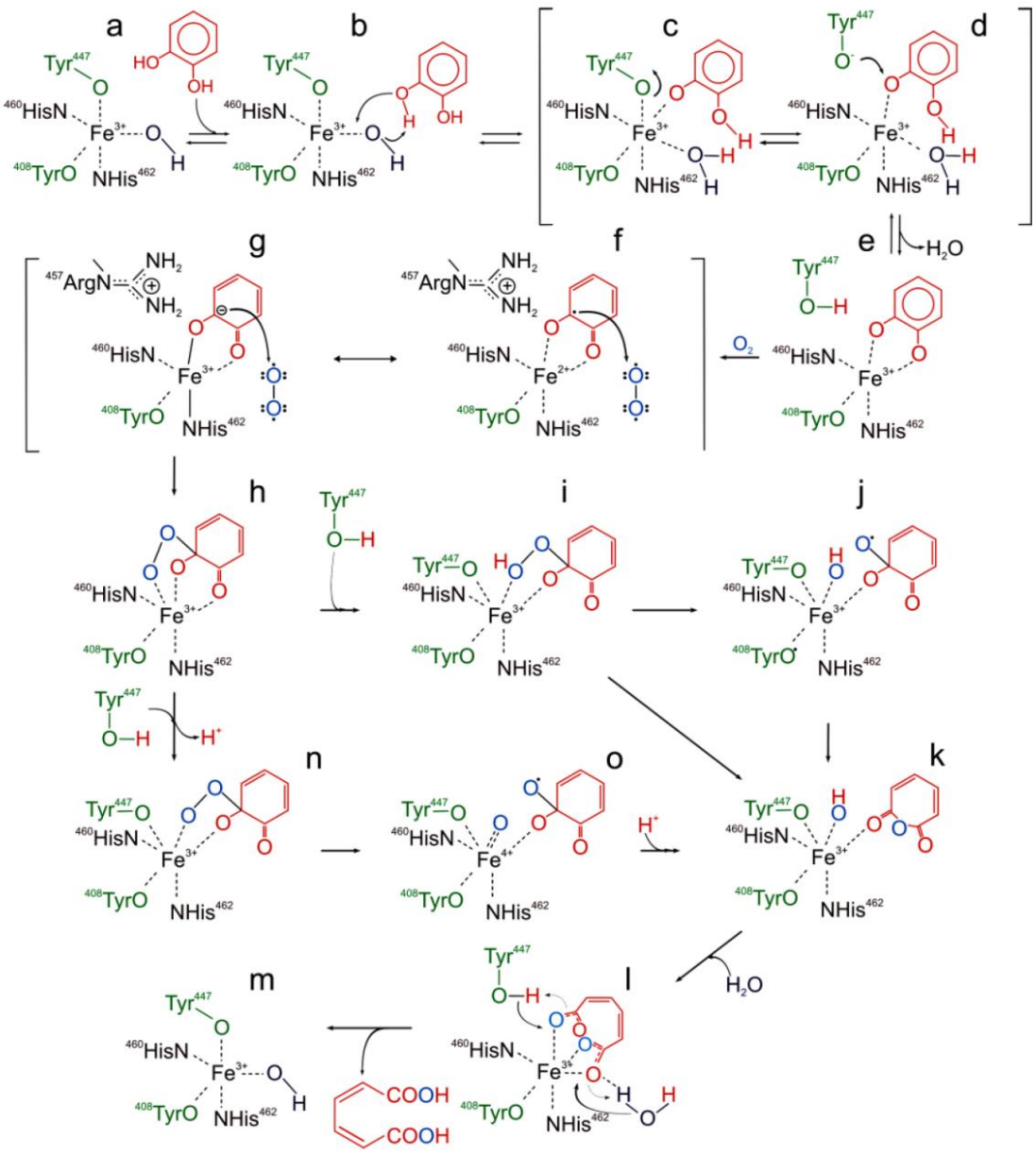

Figure 9 The intradiol dioxygenases catalytic cycle (Guzik et al., 2013).

2 Aim of the project

Aromatic compounds have a wide range of industrial applications, serving as bulk, fine chemicals or pharmaceuticals. Due to the growing awareness of society regarding to fossil resources as well as environmental protection there is increasing demand for “green” approaches as alternatives to traditional chemical synthesis. A big emphasis is putting on developing biotechnological production processes by microbial fermentations. The preferable feedstocks for this alternative organic chemistry are renewable carbon sources like plants biomass, but also organic waste generated by industries or urban societies. Therefore, the main purpose of this study was to investigate the tannic acid degradation pathway in non-conventional yeast *A. adeninivorans*, to create a tool for degrading tannin-containing biomass and convert it into industrially desirable chemicals.

The first aim of this work was the biochemical characterisation of enzymes, investigation of enzyme stabilities, establishment of optimal conditions and kinetics as well as production of recombinant gallic acid decarboxylase (Agdc1p) and catechol-1,2-dioxygenase (Acdo1p) *in vitro*, synthetized in a homologous expression system.

The second aim was the establishment of *in vivo* role of Agdc1p and Acdo1p in *A. adeninivorans* and its expression analysis.

The third aim was the transcriptome analysis of induction of the native promoter by different carbon sources in wildtype *A. adeninivorans* LS3, selection of enzymes involved in the tannic acid degradation pathway and creation of the metabolic map of tannic acid degradation pathway.

The fourth aim of this thesis was the investigation of the metabolite profile of the tannic acid degradation pathway during the degradation of gallic acid and protocatechuic acid. This part of our study was a good supplementation for the transcriptome study.

Finally, Agdc1p and Acdo1p were expressed in *S. cerevisiae* as a heterologous host and *in vitro* properties of recombinant enzymes were investigated.

3 Materials and methods

3.1 Materials

3.1.1 Chemicals

Table 1 List of chemicals used.

Commercial name or chemical formula	Manufacturer	Location
1,2-benzenediol (catechol)	Sigma-Aldrich	Saint Louis, USA
1,2,4-benzenetriol (hydroxyquinol)	Sigma- Aldrich	Saint Louis, USA
1,2,3-benzenetriol (pyrogallol)	Sigma-Aldrich	Saint Louis, USA
1,4-benzenediol (hydroquinone)	Sigma-Aldrich	Saint Louis, USA
1,4-dithiothreitol (DTT)	Roth	Karlsruhe, Germany
2,3-dihydroxybenzoic acid	Sigma-Aldrich	Saint Louis, USA
2,4-dihydroxybenzoic acid	Sigma-Aldrich	Saint Louis, USA
2,5-dihydroxybenzoic acid	Fluka	Buchs, Switzerland
3-hydroxybenzoic acid	Fluka	Buchs, Switzerland
3-mercaptoethanol	Sigma-Aldrich	Saint Louis, USA
3,3',5,5'-tetramethylbenzidine (TMB)	Sigma-Aldrich	Saint Louis, USA
3,4-dihydroxybenzoic acid (protocatechuic acid)	Sigma-Aldrich	Saint Louis, USA
3,4,5-trihydroxybenzoic acid monohydrate (gallic acid monohydrate)	Sigma-Aldrich	Saint Louis, USA
4-hydroxybenzoic acid	Sigma-Aldrich	Saint Louis, USA
acetic acid	Roth	Karlsruhe, Germany
acrylamide solution Rotiphorese®	Roth	Karlsruhe, Germany
agarose	Sigma-Aldrich	Saint Louis, USA
ammonium sulfate	Roth	Karlsruhe, Germany
ammonium persulfate (APS)	Merck	Darmstadt, Germany
benzoic acid	Sigma-Aldrich	Saint Louis, USA
bicine	Roth	Karlsruhe, Germany
biotin	Sigma-Aldrich	Saint Louis, USA
boric acid	Roth	Karlsruhe, Germany
bromophenol blue	Sigma-Aldrich	Saint Louis, USA
bovine serum albumin (BSA)	Sigma-Aldrich	Saint Louis, USA
$Ca(NO_3)_2$	Roth	Karlsruhe, Germany
$CaCl_2$ x $2H_2O$	Sigma- Aldrich	Saint Louis, USA
carrier DNA	Sigma-Aldrich	Saint Louis, USA
cis,cis-muconic acid	Sigma-Aldrich	Saint Louis, USA
citric acid	Roth	Karlsruhe, Germany
cobalt (II) chloride	Fluka	Buchs, Switzerland
$CuSO_4$ x 4 H_2O	Thermo-Fisher Scientific	Saint Louis, USA
DEAE Sephadex A-25	Pharmacia	Uppsala, Sweden
digitonin	Sigma-Aldrich	Saint Louis, USA

dimethylsulfoxide (DMSO)	Thermo-Fisher Scientific	Saint Louis, USA
ethanol	Roth	Karlsruhe, Germany
ethidium bromide	Merck	Darmstadt, Germany
ethylene glycol	Roth	Karlsruhe, Germany
ethylenediaminetetraacetic acid (EDTA)	Roth	Karlsruhe, Germany
$FeCl_3$ x $6H_2O$	Serva	Heidelberg, Germany
glucose 97% pure	Sigma-Aldrich	Saint Louis, USA
glucose	Roth	Karlsruhe, Germany
glycerol	Roth	Karlsruhe, Germany
glycine	Sigma-Aldrich	Saint Louis, USA
imidazole	Sigma-Aldrich	Saint Louis, USA
inositol	Sigma-Aldrich	Saint Louis, USA
isopropanol	Roth	Karlsruhe, Germany
isopropyl β-D-1-thiogalactopyranoside (IPTG)	AppliChem	Darmstadt, Germany
K_2HPO_4	Roth	Karlsruhe, Germany
KCl	Sigma-Aldrich	Saint Louis, USA
KH_2PO_4	Roth	Karlsruhe, Germany
KI	Sigma-Aldrich	Saint Louis, USA
L-ascorbic acid	Serva	Heidelberg, Germany
lysing enzyme from Trichoderma harzianum	Sigma-Aldrich	Saint Louis, USA
methanol	Roth	Karlsruhe, Germany
Methyl tert-butyl ether (MTBE)	Sigma-Aldrich	Saint Louis, USA
$MgCl_2$ x $6H_2O$	Roth	Karlsruhe, Germany
$MgSO_4$ x $7H_2O$	Roth	Karlsruhe, Germany
$MnCl_2$ x $4H_2O$	Roth	Karlsruhe, Germany
$MnSO_4$ x $4H_2O$	Roth	Karlsruhe, Germany
Na_2MoO_4	Ferak	Berlin, Germany
NaCl	Roth	Karlsruhe, Germany
$NaNO_3$	Roth	Karlsruhe, Germany
NaOH	Roth	Karlsruhe, Germany
$NH_4H_2PO_4$	VEB Laborchemie	Apolda, Germany
NH_4OH	Sigma-Aldrich	Saint Louis, USA
nickel (II) chloride hexahydrate	Roth	Karlsruhe, Germany
nickel (II) sulfate hexahydrate	Fluka	Buchs, Switzerland
N,O,-Bis(trimethylsilyl)trifluoro-acetamide (BSTFA)	Sigma-Aldrich	Saint Louis, USA
nonfat dry milk	Roth	Karlsruhe, Germany
pepstatin A	Sigma-Aldrich	Saint Louis, USA
phenol/chloroform/isoamylalcohol solution 25:24:1	Sigma-Aldrich	Saint Louis, USA
phenylmethylsulfonyl fluoride (PMSF)	Serva	Heidelberg, Germany
phosphoric acid	Roth	Karlsruhe, Germany
protein A	GE Healthcare	Munich, Germany
protein G	Thermo-Fisher Scientific	Rockford, USA
pyridine 99% extra pure	Acros organics	New Jersey, USA
sodium acetate	Roth	Karlsruhe, Germany
sodium dodecyl sulfate (SDS)	Roth	Karlsruhe, Germany
sorbitol	Sigma-Aldrich	Saint Louis, USA
sulphuric acid	Roth	Karlsruhe, Germany
synthetic complete mixture (kaiser) drop-out: -URA	ForMedium™	Hunstanton, UK
tannic acid	Sigma-Aldrich	Saint Louis, USA

tetramethylethylenediamine (TEMED)	Sigma-Aldrich	Saint Louis, USA
tris(hydroxymethyl)aminomethane (Tris)	Roth	Karlsruhe, Germany
triton X-100	Boehringer	Mannheim, Germany
tryptone	Sigma-Aldrich	Saint Louis, USA
tryptophan	Sigma-Aldrich	Saint Louis, USA
tween-20	AppliChem	Darmstadt, Germany
xylene	Sigma-Aldrich	Saint Louis, USA
yeast extract	Sigma-Aldrich	Saint Louis, USA
yeast nitrogen base without amino acids (YNB)	Sigma-Aldrich	Saint Louis, USA
$ZnSO_4$ x $7H_2O$	Sigma-Aldrich	Saint Louis, USA

3.1.2 Software

Table 2 List of software applications.

Name	Manufacturer	Location
Biostat®-Aplus Fermentor system	Sartorius Stedim Systems GmbH	Melsungen, Germany
CLC Genomics Workbench	CLC bio, a QIAGEN Company	Aarhus C, Denmark
Endnote	Thomson Reuters	Philadelphia, USA
MagellanTM	Tecan	Männedorf, Switzerland
Microsoft Excel 2013	Microsoft corporation	Redmond, USA
RStudio Server v1.0.143		Boston, USA
Vector NTI®	Thermo-Fisher Scientific	Rockford, USA

3.1.3 Immunolabeling

Table 3 List of antibodies used.

Antibody	Antigen	Host	Manufacturer
Anti-HIS pAb	Polyhistidine sequence	rabbit (polyclonal)	Micromol GmbH (Karlsruhe, Germany)
A8275 Anti-Rabbit IgG (Whole molecule) peroxidase conjugate	Rabbit IgG	goat (polyclonal)	Sigma-Aldrich (Saint Louis, USA)

3.1.4 Kits and enzymes

Table 4 List of commercial kits and enzymes applied.

Name	Manufacturer	Location
BCIP/NBT tablets	Roche diagnostics GmbH	Mannheim, Germany
Bio-Rad protein assay	Bio-Rad	Munich, Germany
Calf intestinal alkaline phosphatase (CIAP)	Promega	Madison, USA
DreamTaq Polymerase	Thermo-scientific	Rockford, USA
Gibson Assembly® Cloning Kit	New England Biolabs	Massachusetts, USA
In-Fusion Cloning Kits - Clontech	Takara Bio USA, Inc.	California, USA
Instantblue TM total protein staining	Expedeon	Harston, UK
Nucleo Spin Gel & PCR Clean-Up	Macherey-Nagel	Düren, Germany
PD10 columns	GE-Healthcare	Munich, Germany
Q5® High-Fidelity DNA Polymerase	New England Biolabs	Massachusetts, USA
Spin Miniprep Kit	Qiagen	Limburg, Netherlands
T4 DNA ligase	Thermo-scientific	Rockford, USA
TOPO®-TA cloning kit	Thermo-Scientific	Rockford, USA

3.1.5 Plasmids and vectors

Table 5 List of plasmids and vectors used.

Name	Features
pCR4®4-TOPO®	promoter *lacI*, Amp^r, Kan^r; used for cloning in *E. coli*
pB25S-ALEU2-ATRP1m-SS	selection *TRP1m*, Kan^r; used for expression in *A. adeninivorans*
pBS-AYNI1-PHO5-SS	*AXOX* gene, Amp^r; used for cloning in *E. coli*
pEVE4912	pCUP1; YEAST ORI: ARS/CEN; eGFP; used for expression in *S. cerevisiae*/ *E. coli*
pEVE2122	pTEF1-tENO2; YEAST ORI: ARS/CEN; used for expression in *S. cerevisiae*/ *E. coli*
pEVE2131	pTEF1-tENO2; YEAST ORI: 2μ; used for expression in *S. cerevisiae*/ *E. coli*

3.2 Biological materials

3.2.1 Bacterial strains

Table 6 List of bacterial strains.

Strain	Description	Company
E. coli XL1 blue	[r*ecA1, endA1, gyrA96, thi-1, hsdR17, supE44, relA1, lac* [F'proABlacI q Z DM15 Tn10 (Tetr)]	Invitrogen (Grand Island, NY, USA)
E. coli DH5α	[F– Φ80d*lac*ZΔM15 Δ(*lac*ZYA-*arg*F) U169, deoR, *rec*A1, *end*A1, *hsd*R17 (r_K–, m_K+) *pho*A *sup*E44, λ⁻, *thi*-1, *gyr*A96 *rel*A1]	Pierce-Thermo-Fisher Scientific (Rockford, USA)

3.2.2 Yeast strains

Table 7 List of yeast strains.

Strain	Description	Source
A. adeninivorans G1212	[*aleu2 atrp1::ALEU2*]	Gatersleben, Germany
S cerevisiae EYS4958	*ura3*	Basel, Switzerland

3.3 Composition of cultivation media

3.3.1 Bacterial media

Table 8 Composition of bacterial medium.

Name	Components	Final concentration
Luria-Bertani	LB-Broth, Sigma (Steinheim, Germany)	2 %
Luria-Bertani agar	LB-Agar, Sigma (Steinheim, Germany)	3.5 %
SOB, pH 7.0	Tryptone (Difco, USA)	2 %
	Yeast extract (Gibco, GB)	0.5 %
	NaCl	8.5 mM
	KCl	2 mM
	$MgCl_2$ x $6H_2O$	10 mM
	$MgSO_4$ x $7H_2O$	10 mM
SOC	SOB	
	Glucose	2 %

For preparation of culture media H_2O_{MQ} was used. All media were autoclaved and stored at 4 °C.

3.3.2 Yeast media

Table 9 Composition of yeast cultivation medium.

	Medium	Components	Final concentration
A. adeninivorans/ S. cerevisiae	Yeast extractpeptone-dextrose medium (YPD)	YPD-Broth (Fluka, Gemany)	6.5 %
A. adeninivorans	Yeast minimal medium with nitrate and glucose (YMM-NO_3^--glucose)	$NaNO_3$	43.5 mM
		KH_2PO_4	50 mM
		K_2HPO_4	10 mM
		$MgSO_4$ x $7H_2O$	8 mM
		mineral mix	0.1 %
		$FeCl_3$ x $6H_2O$	0.012 mM
		$Ca(NO_3)_2$ x $4H_2O$	0.12 mM
	YMM-supplement 1	glucose	variable
	YMM-supplement 2	vitamin mix	0.5 %
	YMM-supplement 3	hydroxylated aromatic acids	variable
	mineral mix	H_3BO_4	6.4 mM
		$CuSO_4$ x $4H_2O$	0.63 mM
		KI	0.6 mM
		$MnSO_4$ x $4H_2O$	2.65 mM
		$ZnSO_4$ x $7H_2O$	2.48 mM
		Na_2MoO_4	0.97 mM
		$CaCl_2$	0.77 mM
	vitamin mix	thiamine hydrochloride	1.19 mM
		inositol	22.2 mM
		nicotinic acid	0.81 mM
		Ca-D-Pantothenate	1.53 mM
S. cerevisiae	Synthetic Complete Medium (SC medium)	YNB	6.8 mg/L
		ammonium sulphate	5 g/L
		L-histidine	10 mg/L
		leucine	60 mg/L
	Supplement 1	glucose	2 % (w/v)
	vitamin mix	vitamin mix	0.5 %
	Supplement 2	Drop-out (-URA)	1.92 g/L

For preparation of culture media H_2O_{MQ} was used. All media were autoclaved and stored at 4 °C.

3.4 Methods

3.4.1 Cultivation conditions

3.4.1.1 Cultivation of bacterial cells

For the cultivation of *E. coli* strains Luria-Bertani (LB) medium supplemented with 50 mg/l ampicillin or kanamycin as antibiotic selection markers was used. After transformation, cells were either grown on agar plates incubated at 37 °C or in liquid cultures incubated at 37 °C under shaking 180 rpm.

3.4.1.2 Cultivation of yeast cells

Strains of *A. adeninivorans* and *S. cerevisiae* were cultivated under non-selective conditions on YPD or under selective conditions on YMM supplemented with vitamin mix and carbon sources. Composition of YMM is shown in **Table 9**. Cultivation temperature for both yeast species was 30 °C. Liquid cultures were shaken at 180 rpm (*A. adeninivorans*) or 150 rpm (*S. cerevisiae*). Preparation of liquid culture mediums required two steps. First 10 ml pre-culture was inoculated and cultivated overnight; this served for the preparation of the final culture with initial OD_{600} = 0.1 which was cultivated for up to 144 h. In case *A. adeninivorans* was grown on YMM supplemented with hydroxylated aromatic acids as carbon source the appropriate culture (YMM-NO_3-glucose) was incubated 24 h; following, cells were centrifuged 3000 *g*, 5 min, washed with YMM without carbon sources and shifted into fresh YMM supplemented with hydroxylated aromatic acid with or without glucose as carbon sources and cultivated for up to 144 h. Initial OD_{600} was ~2.

3.4.2 Techniques used for manipulation of genetic material

3.4.2.1 Agarose gel electrophoresis

DNA fragments were separated on agarose gel. For separation of fragments up to 2000 bp 1 % agarose/TBE solution was prepared. DNA fragments larger than 2000 bp were separated on 0.8 % agarose/TBE solution. DNA fragments were visualized under UV light using 0.5 µg/ml ethidium bromide. For the estimation of DNA length 1 kb Plus DNA ladder (GeneRuler™ 1kb DNA Ladder Plus) was used. Electrophoresis was performed at room temperature in a Biometra electrophorese chamber with TBE buffer as running buffer at constant 90 V.

Table 10 Composition of electrophoresis buffer.

Name	Components	Final concentration [M]	Quantity for 1L solution [g]
TBE buffer	Tris	0.1	12.1
	EDTA	0.0025	0.74
	Boric acid	0.09	5.6

3.4.2.2 DNA extraction from agarose gel

After agarose gel electrophoresis, selected DNA bands were cut from the gel with a scalpel under UV light. DNA was extracted using the gel extraction kit NucleoSpin® Extract II from Marcherey-Nagel (Germany).

3.4.2.3 DNA restriction

Digestion of DNA was performed with *Eco*RI*, Not*I*, Spe*I*, Sac*II*, Hin*dIII (Thermo Fischer Scientific) restriction enzymes according to the manufacturer instructions assuming, that 1 U of the enzyme digest 1 µg of λ-DNA in 1 h under optimum conditions of temperature and buffer.

3.4.2.4 Dephosphorylation of DNA fragments

30 min after the start of the restriction reaction, 1 *µ*l of calf intestinal alkaline phosphatase (CIAP, 1U/µl) was added and incubating continued for an additional 30 min at 37 °C. This step avoids recirculation of the vector after digestion. Reaction was stopped by a final incubation at 65 °C for 15 min.

3.4.2.5 DNA ligation

Before each ligation reaction, relative concentration of insert and vector were quantifying using NanoDrop™ 2000/2000c Spectrophotometer. Ligation of fragments was done using T4-DNA ligase. Depending on the size of each DNA fragment, the ratio insert/vector oscillated between 1:1 and 6:1. First, both fragments were incubated for 10 min at 50 °C before T4-DNA ligase (5 U/µl) and T4-DNA ligase buffer were added followed by incubation for 20 min at 23 °C. Vectors constructed for expression in *S. cerevisiae* were made using In-Fusion Cloning Kit. The procedure was performed according to manufacturers instructions. Vectors constructed for the deletion of gene of interest in *A. adeninivorans* genome were made using Gibson Assembly® Cloning Kit, according to the manufacturer instructions.

3.4.2.6 Mini preparation of plasmid DNA

After transformation of *E. coli* colonies were pick up from the LB agar plate and inoculated in 2 ml LB medium containing ampicillin or kanamycin as antibiotic selection marker and incubated overnight at 37 ºC under vigorous shaking. Each culture was transferred into 2 ml Eppendorfs. Cells were pelleted by 3 min centrifugation at 17,900 *g*, supernatant was rejected, and pellet suspended in 200 *µ*l ice-cold buffer P1 (supplemented with RNase A to final concentration of 20 *µ*g/ml). After vortexing for 1 min, 200 *µ*l buffer P2 was added. Solution was mixed by inverting Eppendorf tubes 6 times followed by 3 min incubation at room temperature. After 200 *µ*l ice-cold P2 buffer was added tubes were gently mixed by inversing in order to optimize protein and chromosomal DNA precipitation. Subsequently the solution was centrifuged for 20 min at 4 ºC, 17,900 *g* and 500 µl of plasmid-DNA rich supernatant transferred in a new tube After adding 350 µl isopropanol (96 %) the solution was kept for 10 min at -20 °C to precipitate DNA. Following centrifugation for 25 min at 17,900 *g* at 4 °C, supernatant was discarded. Precipitated DNA was washed twice with ethanol/H_2O solution (70 %, v/v), centrifuged at 4 °C and 17,900 *g* for 3 min, and supernatant discarded. After drying at RT DNA pellet was resuspended in 50 µl ddH_2O) and, depending on mini preparation efficiency, 1 to 2 µl of DNA (approximately 1 µg) was used for subsequent enzyme restriction.

3.4.2.7 Phenol/chloroform extraction of yeast genomic DNA

Eppendorf tubes containing 2 ml yeast culture were centrifuged for 10 min at 17,900 *g* and 4 °C. Supernatant was rejected and 50 µl phenol/chloroform mixture (1:1) added to the pellet. After vortexing for 1-2 min and centrifugation for 3 min at 17,900 *g* and 4 °C the upper phase was transferred into fresh Eppendorf tubes. Following 6 µl 3 M Na-acetate buffer pH 5.2 and 110 µl ice-cold 96 % ethanol was added. After vortexing for 1-2 min the mixture was incubated at -20 °C for 10 min. Subsequently the mixture was centrifuged for 10 min at 17,900 *g* and 4 °C, the supernatant rejected, and the pellet washed twice with 70 % ethanol, and once with 96 % ethanol. The final DNA pellet was dried at RT. Depending on the efficiency of extraction procedure, DNA pellets were resuspended in 30-50 µl ddH_2O.

3.4.3 Construction of transgenic strains

3.4.3.1 Preparation of chemical competent *E. coli* cells

25 ml pre-cultures of *E. coli* strains (XL1 blue and DH5α) were cultivated for 10 h at 37 °C in SOB medium under vigorous shaking. Cultures were diluted in 250 ml SOB medium and cultivated overnight at 18 °C under mild shaking. Cultures were again diluted in SOB medium to OD_{600} value equal 0.55. After incubation on ice for 15 min, cells were centrifuged for 10 min at 3,000 g and 4 °C, resuspended in 50 ml ice-cold INOUE buffer and centrifuged once again for 10 min at 3,000 *g* and 4 °C. Pelleted cells were resuspended in 20 ml ice-cold INOUE buffer supplemented with 1.5 ml DMSO. After incubation on ice for 10 min the suspension was divided in 50 µl aliquots, frozen in liquid nitrogen and stored at – 80 °C until use.

Table 11 Buffer composition for the preparation of bacterial competent cells.

Buffer	Component	Final concentration
INOUE	$MnCl_2$ x $4H_2O$	55 mM
	$CaCl_2$ x $2H_2O$	15 mM
	KCl	250 mM
	0.5 M PIPES solution (pH=6.7)	10 mM
	Sterile-filtered and stored at 4 °C	
SOB	Tryptone	2 % (w/v)
	Yeast extract	0.5 % (w/v)
	NaCl	8.5 mM
	KCl	2 mM
	$MgCl_2$ x $6H_2O$	10 mM
	$MgSO_4$ x $7H_2O$	10 mM
	Adjusted to pH=7.0 with NaOH, autoclaved and stored at 4 °C	

3.4.3.2 Transformation of chemical competent *E. coli* cells

For the transformation of *E. coli* XL1 blue cells 10-20 µl of constructed plasmid after ligation was added to 100 µl chemical competent cells and incubated for 30 min on ice. Cells were heat-shocked by 90 second incubation in a water bath set at 42 ºC and incubated again on ice for 2 min. Following 800 *µ*l of sterile SOC medium was added and incubation continues at 37 ºC for 1 h with shaking. Transformed cells were speeded on selective LB agar plates containing appropriate antibiotic and incubated overnight at 37 ºC.

3.4.3.3 Preparation of competent *A. adeninivorans* cells

A. adeninivorans G1212 colony was isolated and cultivated overnight in 10 ml yeast total medium (YPD) supplemented with 50 µg/ml tryptophan at 30 °C. This first pre-culture was diluted 1:10 in 10 ml YPD supplemented with 50 µg/ml tryptophan and incubated overnight at 30 °C. To start the main culture with OD_{600nm} of 0.5, an aliquot of the second preculture was transferred into 100 ml YPD supplemented with 20 µg/ml tryptophan and incubation at 30 °C continued until OD_{600nm} reached 1.5.

The culture was centrifuged for 5 min at 5,000 *g* and 4 °C and the pellet resuspended in 50 ml ice-cold sorbitol-based buffer. After a second centrifugation for 5 min at 5,000 *g* and 4 °C, cells were resuspended in 2 ml sorbitol-based buffer, divided into 50 µl aliquots, frozen in liquid nitrogen and stored at -80 °C until use.

Table 12 Buffer composition for the preparation of yeast competent cells and *A. adeninivorans* transformation.

Buffer	Component	Final concentration
Sorbitol based buffer	sorbitol	1 M
	bicine	10 mM
	ethylene glycol	3 % (v/v)
	DMSO	5 % (v/v)
	autoclaved and stored at 4 ºC	
PEG-bicine solution	PEG-1000	40 % (v/v)
	bicine	0.2 M
	adjusted to pH=8.35 with NaOH, autoclaved and stored at 4 °C	
NaCl-bicine solution	NaCl	0.15 mM
	bicine	10 mM
	adjusted to pH = 8.35 with NaOH, autoclaved and stored at 4 °C	

3.4.3.4 Transformation of competent *A. adeninivorans* cells

Yeast transformation was performed according to Dohmen *et al.* (1991). 20 µl of carrier DNA (herring sperm DNA) was denatured at 95 °C for 5 min and placed on ice for 1 min. Denatured carrier DNA supplemented with 10 µl target DNA (previously linearized vector) were added to 50 *µ*l freshly thawed competent cells and incubated in thermomixer at 37 °C for 5 min under vigorous shaking. Following 1 ml of 40 % PEG 1000 (polyethylene glycol) + 0.2 M bicine pH 8.35 was added and the suspension incubated at 30 °C for 1 h without shaking. Afterwards, cells were centrifuged for 5 min at 4,000 *g* at RT, supernatant was discarded, and pellet resuspended in 1 ml sterile 0.15 M NaCl + 0.01 M bicine, pH 8.35 solution. After centrifugation for 5 min at 4,000 g at RT

pellet was resuspended in 500 µl of 0.15 M NaCl + 0.01 M bicine. Suspension was spread on five selective YMM plates (without tryptophan) and incubated at 30 °C.

3.4.3.5 Stabilization of insert in the yeast genomic DNA

Positive transformants were selected on plates with YMM-NO_3-2 % glucose. Single *A. adeninivorans* colonies were stabilized by passaging on selective (YMM-NO_3) and non-selective (YPD) medium to attain a stabile integration of transformation cassette in genomic DNA and high level of protein production (Kuriyama and Nislow, 1992, Klabunde *et al.*, 2003). Stabilization lasted three weeks and was performed in 96 deep-well plates (riplateSW® 2.5 ml of bio-HJ, Mönchengladbach, Germany). Cells were grown for 48 h in 500 µl liquid medium and re-cultivated in the same amount of fresh YMM medium using 10 µl of culture. This process was repeated six times, followed by two additional passages in 500 µl YPD medium for 24 h and a final one in YMM medium for 24 h. Finally, 3 µl aliquots of each culture were dripped onto YMM agar plates and grown for 48 h. All cultivation steps in liquid media were at 30 °C under shaking at 340 rpm.

3.4.3.6 Transformation of competent *S. cerevisiae* cells

Transformation of *S. cerevisiae* cells was done according to the LiAc/ssDNA/PEG transformation protocol described by (Amberg *et al.*, 2005) with modifications added by (Gietz and Schiestl, 2007). After transformation cells were plated on selective SC medium (–URA) and incubated at 30 °C.

3.4.3.7 Construction of knock-out mutant strain of *A. adeninivorans*

To create disruption mutants, a gene disruption cassette containing a minimum 500 bp up and down the ORF of the gene of interest as well as the ATRP1m selection marker module was constructed. All fragments were amplified by PCR (up and down ORF overlapped fragments using chromosomal DNA of *A. adeninivorans* LS3 as template and ATRP1m selection marker module using plasmid pBS-ALEU2-TRP1m as template (Steinborn *et al.*, 2007). Primers used for fragment amplification were created with additional 15 bp overlapping sides (**Table 15**, **Table 21**). This strategy allowed ligation of fragments in one step by using an In-Fusion Cloning Kit (TaKaRa Clontech, USA Inc.). The resulting construct was amplified in *E. coli* DH5a. Finally, complete construct covering overlapping fragment in front of the gene of interest, the *ATRP1m* selection marker module and overlapping fragment behind the gene of interest was amplified using design primers. Resulting product was amplified by PCR and used to transform *A. adeninivorans* G1212 as described in section 2.4.3.4.

3.4.4 Techniques used for work with RNA

3.4.4.1 RNA isolation from yeast cells, quantification and synthesis of cDNA

A. adeninivorans G1212/YRC102 cells were grown in YMM glucose-$NaNO_3$ for 24 h at 30 °C and 180 rpm. Cells were harvested by centrifugation 3,220 *g* at 4 °C, washed with YMM-$NaNO_3$ and resuspended in YMM-$NaNO_3$ containing 0.2 % glucose or hydroxylated aromatic acids. 2 ml of culture samples were collected after 0, 4, 8, 24, and 48 h. After centrifugation 2,300 *g* at 4 °C, cells were disrupted mechanically using silica beads in a Mixer Mill MM400 (RETSCH, Germany) operating for 3 min with vibrational frequency of 30/s. Total RNA was isolated using RNeasy Mini Kit (Qiagen, Germany) according to manufacturer instructions. RNA concentration was analyzed using NanoDrop2000c spectrophotometer (Thermo Fisher, Germany). cDNA was synthesized using RevertAid H Minus First Strand cDNA Synthesis Kit (Fermentas, Germany) with an Oligo(dT)15V-RTA primer.

3.4.4.2 Nested quantitative Real-time PCR

For analysis of temporal gene expression patterns, a nested qRT-PCR assay was applied (Worch and Lemke, 2017). First PCR synthesis was made with cDNA-template (10 cycles) using gene-specific primers and RTA1 primer (Table 1B). PCR product was diluted 1:500 and amplified in the presence of SYBR® Green fluorescent dye (Power SYBR Green PCR Master Mix, Applied Biosystems, Foster City, CA, USA) using ABI 7900HT Fast Sequence Detection System (Applied Biosystems) with gene-specific primers 2 or 4 and RTA primer (**Table 20**, **Table 26**). *TFCI* and *ALG9* were used as reference (housekeeping) genes (Rösel and Kunze, 1995, Teste *et al.*, 2009). Calculations were done using ΔΔct-method (Livak and Schmittgen, 2001).

3.4.4.3 Gene expression analysis using microarray

Gene expression profiling was performed using a microarray produced by Agilent Technologies in 8 x 60 k format. The microarray was based on 6,025 annotated chromosomal sequences and 36 putative mitochondrial gene oligos and was designed using Agilent Technologies eArray software (https:// earray.chem.agilent.com; design number 035454). Depending on sequence length of genes, up to 10 60-mers per gene were created, resulting in a total of 56,312 *A. adeninivorans* specific oligos. *A. adeninivorans* LS3 was cultivated overnight in YMM-glucose-$NaNO_3$. Cells were pelleted by centrifugation for 5 min at 3,220 x *g*, 20 °C and shifted to YMM-$NaNO_3$ containing a mixture of 0.5 % gallic acid plus 1 % glucose or 1 % glucose only. After 15

min, 30 min, 2 and 5 h of cultivation at 30 °C and 180 rpm, cells were harvested, and total RNA isolated using RNeasy Mini Kit (Qiagen, Germany). Samples were labelled and the microarray hybridized according to the Agilent Technologies “One-Color Microarray-Based Gene Expression Analysis (v6.5)” instructions. R package limma was used for microarray data analysis (Smyth, 2005). Background of raw expression data was corrected by “normexp” and normalized between arrays using “quantile.” Differentially expressed genes were detected by fitting a linear model to log2-transformed data by an empirical Bayes method (Smyth, 2005). The Bonferroni method was used to correct for multiple testing.

3.4.5 Yeast cells microscopy

3.4.5.1 Digital Microscope and Emission Scanning Electron Microscopes (FE-SEM)

For a comparative analysis of the phenotype of *A. adeninivorans* control, transgenic and mutant strains, cells were cultivated on agar plates containing YMM-glucose-$NaNO_3$ at 30 °C for 48 h. Colony morphology was investigated using a VHX-5000 Digital Microscope (KEYENCE Deutschland GmbH, Neu-Isenburg, Germany).

For detailed analysis, a FESEM 4100s device (Hitachi High-Technologies Europe GmbH, Krefeld, Germany) was used. Fragments of agar plates containing colonies were dried at 30 °C, attached to carbon-coated aluminum sample blocks and gold-coated in an Edwards S150B sputter coater (Edwards High Vacuum Inc., Clevedon, United Kingdom). Samples were studied under 5 kv acceleration voltage and recordings saved as TIFF files.

3.4.5.2 Confocal leaser scanning microscopy

The localization of eGFP-tagged proteins was performed by confocal leaser scanning microscop (CLSM), LSM 780 T-PMT (Carl Zeiss MicroImaging GmbH, Jena, Germany). GFP-dependent fluorescence was detected by excitation at 488 nm (491−530 nm emission) with an argon laser and filtering the emitting light YFP at 514 nm excitation (517−560 nm emission). The identity of the fluorophores was confirmed by photospectrometric analysis. All confocal sections across samples were recorded with the same microscope settings. Image superimposition and fluorescence quantification were made by means of the Zeiss LSM 510 software version 3.0.

3.4.6 Methods used for work with proteins

3.4.6.1 Determination of protein concentration

The dye-binding method (Bradford, 1976) using Bio-Rad Protein Assay and purified bovine serum albumin as standard was used to determine protein concentration. Reaction mixtures containing sample and Bradford solution were prepared on 96-well microtiter plates (Corning Life Sciences) and measured in a Tecan Infinite M200 microplate reader.

3.4.6.2 Protein electrophoresis on polyacrylamide gel (SDS-PAGE)

Proteins were separated by electrophoresis on polyacrylamide gel under denaturing conditions according to (Laemmli, 1970) using a Dual-Gel Vertical Electrophoresis Systems (Thermo-Fisher Scientific). Composition of separation and stacking gel are shown in **Table 13**. Samples were mixed with Laemmli buffer in a 4:1 ratio, heated for 5 min at 95 °C, chilled on ice and loaded onto the gel applying 25 µl per lane. Electrophoresis ran in 1x Electrophoresis buffer at constant current of 38 mA. Protein marker (PageRuler™ Prestained Protein Ladder, 10 to 180 kDa) was used to estimate molecular mass.

Table 13 Composition of SDS-PAGE.

Components	Gel concentration (%)	
	stacking gel (5 %)	**resolving gel (12 %)**
H_2O_{MQ} [ml]	1.34	2.75
Rotiphorese® Gel 40 (37,5:1) acrylamide [ml]	0.25	1.8
Tris-buffer [ml]	0.4 (0.625 M, pH 6.8)	1.15 (1.88 M, pH 8.8)
SDS 20%(w/v) [µl]	10	30
APS 25%(w/v) [µl]	10	30
TEMED 20%(v/v) [µl]	2	5

3.4.6.3 Gel staining for total protein content

For total protein staining Coomassie staining was used. Gels were immersed in 10 ml Instantblue™ solution for 40 min and washed in 20 ml ddH_2O for 60 min.

3.4.6.4 Western blotting (immunoblotting)

Western blot analysis was performed by transferring the gel to a PVDF (polyvinylidene fluoride) membrane (Immobilon®-P Membrane; EMD Millipore Corporation, Billerica, USA) in Novex™ Semi-Dry Blotter (Invitrogen) using discontinuous transfer buffer for semi-dry blotting Roti®-Blot 1 (Roth). Blotting was performed according the manufacturers instructions.

3.4.6.5 Protein-antibody hybridization

After blotting, the PVDF membrane was washed 2x10 min with TBS, and blocked with 1 % non-fat dry milk for one hour under shaking at RT. After 2x5 min washes with TBS-tween and 1x5 min with TBS, the PVDF membranes was incubated for 60 min at RT under shaking with the appropriate primary antibody. Following 2x5 min washes with TBS-tween and 1x5 min with TBS, the membrane was incubated for 60 min with a secondary antibody under shaking at RT. Finally, the membrane was washed 4x5 min with TBS-tween and bound antibodies visualized by chromogenically detection using BCIP/NBT tablet. Used antibodies are listed in **Table 3**.

3.4.6.6 Cell wall disruption

Enzyme activities in crude extracts were measured using 2 ml culture samples. 2 ml of liquid culture was transfered into the fresh Eppendorf and centrifugated at 17,000 *g* for 5 min, 4 °C. After harvesting cells were washed with H_2O_{MQ} and suspended in 500 µl freshly prepared 50 mM buffer (potassium phosphate buffer pH 6.2 with cOmplete™, EDTA-free Protease Inhibitor Cocktail (Roche) for Agdc1-6hp or Tris-HCl buffer pH 7.5 contained 1 mM PMSF for Acdo1-6hp). Cells were homogenized using 500 µl 0.5 mm silica beads (BioSpec Products) in a Mixer Mill MM 400 (Retsch) for 3 min at 30 Hz, at 4 °C. The protein extract was separated from cell debris and silica beads by centrifugation at 17,000 *g* for 5 min, 4 °C. Crude extract was transferred into the fresh Eppendorf.

For purification purposes, yeast cells from liquid cultivation culture were harvested, suspended in 5-10 ml of 50 mM buffer (potassium phosphate buffer pH 6.2 with cOmplete™, EDTA-free Protease Inhibitor Cocktail (Roche) for Agdc1-6hp or Tris-HCl buffer pH 7.5 contained 1 mM PMSF for Acdo1-6hp) and homogenized using 0.5 mm silica beads (BioSpec Products) in 5 ml vessel in a Mixer Mill MM 400 (Retsch) for 3 min at 30 Hz, at 4 °C. Protein extract was separated from cell debris and silica beads by centrifugation at 25,000 *g* for 15 min, 4 °C. Supernatant was transferred into fresh falcon tubes and 5 ml binding buffer pH 7.9 (**Table 14**) was added. The mixture was ready for protein purification procedure.

3.4.6.7 Protein purification by immobilized metal ion affinity chromatography (IMAC)

Histidine-tagged proteins were purified by column chromatography on HisTrap FF (1 ml) (Novagen, USA) containing nickel ions, using a ÄKTA™ pure chromatography system and buffers listed in **Table 14**.

Table 14 Buffer composition for protein purification.

Component	Final concentration	
	Binding buffer	**Elution buffer**
NaCl	0.5 mM	60 mM
Tris	20 mM	0.5 M
imidazole	5 mM	1 M

All buffers were adjustet to pH 7.9 with HCl, autoclaved and storage at 4 °C.

3.4.6.8 Desalting of protein eluates

After purification, protein fractions were desalted using a Sephadex G-25 in PD-10 Desalting Columns (GE Healthcare, USA) following manufacturers instruction. Elution was performed using potassium phosphate pH 6.2 for gallic acid decarboxylase or PBS pH 7.4 buffer for catechol-1,2-dioxygenase.

3.4.6.9 Size exclusion chromatography

The native molecular mass of the isolated proteins was determined by gel filtration on a HiLoad 16/600 Superdex 200 prep grade column (GE Healthcare, Germany) using the ÄKTApure 150 L Chromatography System. The running buffer used was a 50 mM Tris-HCl pH 8.0 with 150 mM NaCl. It was eluted with 1.5 column volumes at a flow rate of 0.5 mL min^{-1}. Fractions of about 1 ml were collected for 182 min in 96 well plates. For calibration, a protein mixture of blue dextran, ferritin, catalase, bovine albumin, RNAse A and vitamin B12 was used.

3.4.7 Cell growth monitoring

3.4.7.1 OD_{600nm} culture measurement

For optical density measurement, a culture sample was diluted 1:10 or 1:100 to not exceed an OD_{600nm} value of 0.9 and 1 ml pipetted in a 2 ml disposable plastic cuvette (BRAND GMBH, Germany), which was subsequently placed in a Jenway 7305 Spectrophotometer (Jenway, UK) and absorbance measurement at 600 nm. Experiments were performed in triplicate and error bars represent the standard deviation.

3.4.7.2 Determination of dry cell weight (dcw)

2 ml of yeast cultures was pipetted into pre-weighed 2 ml Eppendorfs. Cells were pelleted by centrifugation at 25,000 g for 10 min at 4 °C. Supernatants were discarded. Pellets were dried overnight in oven at 80 °C and weight of the dried cell material determined. Experiments were performed in triplicate; error bars represent standard deviation.

3.4.8 Enzymatic assays

3.4.8.1 Gallic acid decarboxylase

Gallic acid decarboxylase activity was assayed by following gallic acid or protocatechuic acid biotransformation during the enzymatic reaction in 50 mM potassium phosphate buffer pH 6.2. Reactions were carried out in 96-well UV-transparent microtiter plates (Greiner Bio-One GmbH), in a total volume of 100 µl. All measurements were done in triplicates; error bars represent the standard deviation. Reaction was started by adding 0.5 mM substrate solution (190 µl) to the enzyme (10 µl) and monitored 15 min at 40 °C, 259 nm (ε = 7100 [1/M/cm]) and 288 nm (ε = 1,570 [1/M/cm]) for gallic acic and protocatechuic acid, respectively (Krumholz et al., 1987). Blank values were established by assaying using water instead of the enzyme. One Unit (1 U) of enzyme activity was defined as the amount of enzyme required to decarboxylate 1 µmol gallic acid to pyrogallol or 1 µmol protocatechuic acid to catechol per min at 40 °C, pH 6.2. The K_M and V_{max} values for the substrates gallic acid and protocatechuic acid were determined from Michaelis-Menten and Hanes-plot by the linear regression usin Microsoft Excel.

3.4.8.2 Catechol-1,2-dioxygenase

Catechol-1,2-dioxygenase activity was assayed by following *cis,cis*-muconic acid or pyrogallol formation during the enzymatic reaction in 50 mM Tris-HCl buffer pH 7.5. Reactions were in 96-well UV-transparent microtiter plates (Greiner Bio-One GmbH) in a total volume of 100 µl. Experiments were done in triplicates; error bars represent standard deviation. Reaction was started by adding 0.5 mM substrate solution (190 µl) to the enzyme (10 µl) and monitored 15 min at ~20 °C, 260 nm (ε = 16800 [1/M/cm]) and 296 nm (ε = 14500 [1/M/cm]) for *cis,cis*-muconic acid and pyrogallol, respectively (Itoh, 1981). Blank values were established by assaying using water instead of the enzyme. One Unit (1 U) of enzyme activity was defined as the amount of enzyme required to oxydate 1 µmol catechol to *cis,cis*-muconic acid or 1 µmol pyrogallol to 2-hydroxymuconic acid per min at 20 °C, pH 7.5.

Measurement of hydroxyhydroquinone cleavage by catechol-1,2-dioxygenase was assayed by monitoring the reaction between hydroxyhydroquinone and rhodanine which gives rise to a coloured compound (modified method from Sharma *et al.* (2000)). Absorbance was recorded against a water blank at 465 nm (ε = 42000 [1/M/cm]), and hydroxyhydroquinone was used as the standard. One unit of tannase activity was defined as the amount of enzyme required to release 1 mM gallic acid/min at 20 °C and pH 7.5. Activity levels were expressed as U/mg protein or as U/l. The K_M and V_{max} values for the substrates pyrogallol and *cis,cis*-muconic acid were determined from Michaelis-Menten and Hanes-plot by the linear regression usin Microsoft Excel.

3.4.9 Metabolite analysis by gas chromatography – mass spectrometry (GC-MS)

3.4.9.1 Sample collection, extraction and derivatization procedure

Quantitative measurements of hydroxylated aromatic acids, as well as various phenol derivatives were performed by GC-MS (Clarus SQ 8 GC Mass Spectrometers). Prior to these samples were extracted and derivatized. For this purpose, 2 ml yeast culture was centrifuged for 10 min, 16,000 *g*, 4 °C. Supernatant was collected in fresh Eppendorf and pellet was discarded. 500 µl supernatant was adjusted to pH 2 with HCl and compounds were extracted with 2x300 µl and 1x400 µl MTBS (Sigma-Aldrich, USA). The upper extract layer was collected in fresh Eppendorf. Extracts were lyophilized in a Freeze Dryer, Alpha 1-4 LSC plus (Christ) and resuspended in 400 µl pyridine. After adding 100 µl BSTFA (Sigma-Aldrich, USA) samples were incubated overnight at 60 °C.

3.4.9.2 GC-MS measurement

A 1 µl aliquot of sample was injected into an Elite-5MS column, Length 30 m, I.D 0.25 mm, 25 µm (Elite, USA). The injection was performed with a split speed of 10 ml/min. Temperature was kept at 60 °C for 1 min then ramped up to 230 °C at 15 °C/min and held at 230 °C for 11.33 min. Peak areas were calculated by TurboMass 6.1 using data from external quantification standards assayed four times. Experiments were performed in triplicate; error bars represent standard deviation.

4 Results

4.1 Gallic acid tolerance by *A. adeninivorans*

The growth behaviour of *A. adeninivorans* G1212/YRC102 on different gallic acid concentrations was investigated. Cells were cultivated at 30 °C, 180 rpm on YMM-$NaNO_3$ supplemented with 0.05 – 2 % (w/v) gallic acid as the sole source of carbon. Growth occurred in all concentrations. For each condition, the growth profile was characterized by a long adaptation phase of 48 h (**Figure 10**). The OD_{600nm} values strongly correlated with the amount of carbon sources in medium. Despite the long adaptation phase, no growth inhibition was observed. The results also show that cultures grown on gallic acid reached lower final optical densities than cultures grown on medium supplemented with an equal concentration of glucose (**Figure 10**).

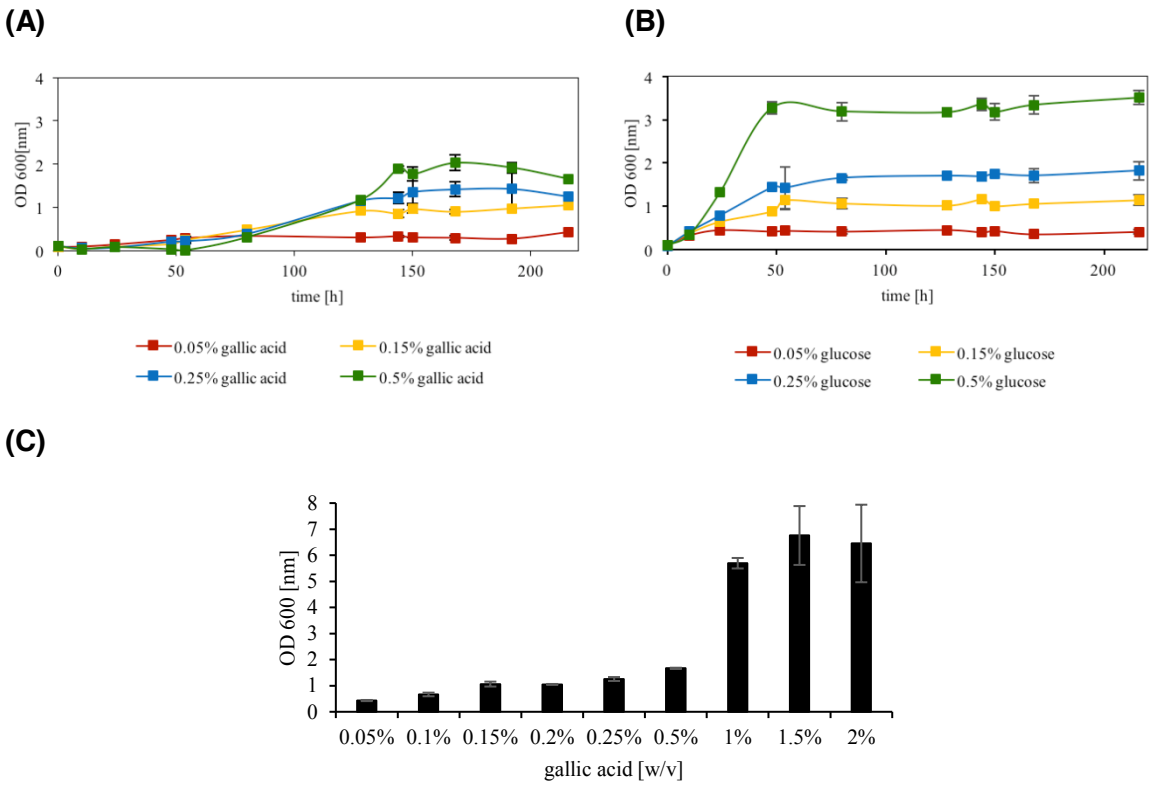

Figure 10 Gallic acid tolerance of *A. adeninivorans* G1212/YRC102.
A. adeninivorans strain G1212/YRC102 was cultivated on YMM-$NaNO_3$ supplemented with: (**A**) different concentrations of gallic acid or (**B**) corresponding concentrations of glucose as a control. (**C**) Optical density of *A. adeninivorans* G1212/YRC102 achieved after 220 h of cultivation on YMM-$NaNO_3$ supplemented with different concentrations of gallic acid.

4.2 *Arxula* gallic acid decarboxylase 1, Agdc1p

4.2.1 Identification of the *A. adeninivorans AGDC1* gene encoding gallic acid decarboxylase (Agdc1p)

A putative *gallic acid decarboxylase* gene (ARAD1C45804g) was annotated in the genome of *A. adeninivorans* LS3. The gene, *Arxula gallic acid decarboxylase 1* (*AGDC1*), is localized on chromosome *Arad1C*, position 3821025 to 3821720. The open reading frame comprises 696 bp without introns encoding a protein with 232 amino acids. Agdc1p has a predicted molecular mass of 27.3 kDa. Protein analysis according to the SignalP (version 4.1) program (http://www.cbs.dtu.dk/services/SignalP/) predicted the absence of a secretion signal sequence.

There are several conserved domains that are fundamental for the catalytic activity and structure of gallic acid decarboxylase. In *Lactobacillus plantarum* WCFS1, gallic acid decarboxylase comprises three subunits whose function is not well known. Jimenez *et al*. (2013) reported that the *in vitro* decarboxylation of gallic acid only occurred when subunit C is present in the reaction mixture. Additional *in vivo* studies with deletion mutants revealed that subunit B and/or C but not D is essential for the decarboxylation reaction.

We performed an alignment of the Agdc1p sequence with several conserved domains that are fundamental for catalytic activity and structure of enzymes such as subunits B and C from *L. plantarum* WCFS1 gallic acid decarboxylase and putative gallic acid decarboxylase protein sequences from other lactic bacteria described by Jiménez *et al*. (2013) (**Figure 11 B,C**). The analysis showed that Agdc1p sequence has a greater similarity to the structures found in subunit B from *L. plantarum* WCFS1 gallic acid decarboxylase (18 identical positions and 60 similar positions) than to subunit C from *L. plantarum* WCFS1 gallic acid decarboxylase (only 5 identical and 8 similar position in the sequence).

Using the Neighbor-Joining method, a phylogenetic tree was established for Agdc1p, gallic acid decarboxylase from *L. plantarum* and putative gallic acid decarboxylase protein sequences from lactic bacteria. It could be demonstrated that the *Lactobacillus sakei* and *Pediococcus pentosaceus* putative enzymes originated from the same ancestral node, which shares a common ancestor with Agdc1p, whereas *Enterococcus faecium*, *Streptococcus gallolyticus*, *Oenococcus oeni*, *L. plantarum, Lactobacillus pentosus* and *Lactobacillus brevis* form other branches with common ancestors (**Figure 11 A**).

(A)

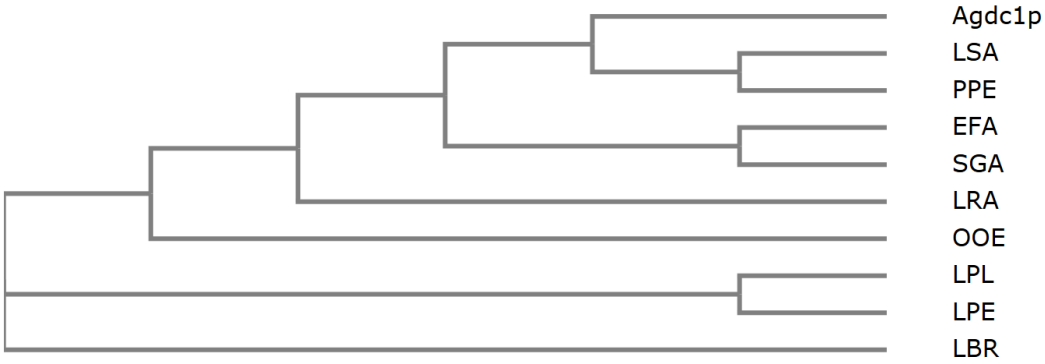

(B)

```
Agdc1p      1 --------MTTSYEPWPQLYSHLNGTNEEVLD--RMKVAELCKGWSVYRDASEWANFKEMFTPDANIWTTWSGAQTIDSFIQISKDGK 78
LSA         1 ---------------MRKIVVGISGASGTIYGIRLLEALHQVPDVETHLVMSRWAKENLAIEK-----TGYTE-KQVVALADFVHPEQ 67
PPE         1 ---------------MKKIVVGISGASGTIYGIRLLEVLHRMPDVETHLVMSRWAKENLAIED-----TGYTE-SQLKDLADFVYSEK 67
LRA         1 ---------------MKRIIVGITGASGTIYAVNLLQHLHRLPDVEVHLVMSAWAKQNLSLE------TDMKQ-SELEALADYVYPVQ 66
OOE         1 -------------MAVKKIIVGVSGASGTIYAVDLLKRLHAISNVEVHLVMSSWAKKNLSLE------SDYSI-DQIKELADYTYNVH 68
LPL         1 MNHNIIINLQKRGDVVMKRIVVGITGASGTIYAVDLLEKLHQRPDVEVHLVMSAWAKKNLELE------TDYSL-AQLTALADATYRAN 81
LPE         1 ---------------MKRIVVGITGASGTIYAVDLLEKLHQLPDVEVHLVMSAWAKKNLELE------TDYSL-AQLTALADATYRAN 66
LBR         1 ---------------MKRIVIGVTGASGTIYAIDLLKKLRDKPGVETHLVMSPWATKNLALE------TSYTL-AQVKAMADYTYSDR 66
EFA         1 --------MEQLAQRKKKIVIGVSGASGTIYAINLVKKLKEYPMIETHGIISPWAKQNLKLE------SDLSL-TEFESLFDYHYSNK 73
SGA         1 -------------MSKKRIVVAISGASGTIYAINLLKKLKEYPDIETHVVMSDWAHENLKLE------LDMSH-DEFASLCDVLYSNK 68
                            ::   :.*:.  :     ::  .     ..:   * **  :  :          .    .  : :     .

Agdc1p     79 DKGAFIMHRECGT-LVDLNPKTQRAIGKMKTTITQRFEYEGVPFDIDCDNYFIFFCLKDSNGDWKARWYKVFYVKDKFVPVGVPTAEN 165
LSA        68 NMGATIASGSFKHDGMVIVPTSMKTLASIATGLGENL---------------I-----ARAADVTLKERRPLIIVPRESPFNQIHLEN 135
PPE        68 NMGATVASGSFIHDGMVIIPASMKTIASVATGLGENL---------------I-----ARAADVTLKEQRQLIVVPRESPFNQIHLEN 135
LRA        67 NQGATIASGSFLTDAMVIVPASMKTIAGIAMGFDDNL---------------I-----GRAADVTIKEQRQLIIVPRETPLSPIHLDN 134
OOE        69 DQGAAIASGSFLNDGMVIVPASMKTVAGIASGFGDNL---------------I-----ARAADVAIKEQRKLILVPRETPLSVIHLEN 136
LPL        82 DQGAAIASGSFLNDGMVIVPASMKTVAGIAYGFGDNL---------------I-----SRAADVTIKEQRKLVIVPRETPLSVIHLEN 149
LPE        67 DQGAAIASGSFLNDGMVIVPASMKTVAGIAYGFGDNL---------------I-----SRAADVTIKEQRKLVIVPRETPLSVIHLEN 134
LBR        67 DQGAKIASGSFLHDGMVIVPASMKTVAGVAYGFGDNL---------------I-----ARAADVTIKEHRQLIIVPRETPLSVIHLEN 134
EFA        74 DLGAAVASGSFLTDGMIIVPASMKTVAGISVGLGDNL---------------I-----ARAADVTMKEQRKLVIVPRETPLNAIHLEN 141
SGA        69 DLGAKIASGSFLTDGMVIVPASMKTVAGIACGFSDNL---------------I-----GRAADVALKEQRKLIIVPRETPLNTIHLEN 136
              : ** :   .     : : * : :::. :   : :.:               *        .*   :  : : :  :  *..    :*

Agdc1p    166 MEKLAKLFSKENLEQYPWGYQYLAVAQANLGYPIDKKLPTWKN-------ELYHTMYDAMKEWMEGKEIDLHW-------------   231
LSA       136 MLKLAQM-----------------------GVAIVPPIPAFYNQPQTIDDIVNHTVMKLLDQLHIETNLGPRWEGLANARQNAR--   196
PPE       136 MLKLSKM-----------------------GVGVIPPIPAFYNNPKTIDDIVNHTVMKILDHLHIQNDVSSRWEGLANARKNNQKK   198
LRA       135 LAKLAHI-----------------------GVQIIPPIPAFYQHPQTIQDLIEHHTMKLLDALHIKTETASRWNGASLR-------   190
OOE       137 LTRLARL-----------------------GVQIIPPIPAFYGHPKTIQDLINHQTMKILDAFSINNNLDNRWEGD----------   189
LPL       150 LTKLAKL-----------------------GAQIIPPIPAFYNHPQSIQDLVNHQTMKILDAFHIHNETDRRWEGD----------   202
LPE       135 LTKLAKL-----------------------GAQIIPPIPAFYNHPTTIQDLVNHQTMKILDAFHIYNETDRRWEGD----------   187
LBR       135 LTKLAKL-----------------------GAQIIPPIPAFYNQPQTIQDLVDHQTMKVLGAFGIQQVTAKRWEGD----------   187
EFA       142 LTKLARL-----------------------GVQIIPPIPAFYNQPQTIQDLVNHHTMKLLDQFEIVNEHSKRWQGD----------   194
SGA       137 LTKLSRM-----------------------GVQVIPPVPAFYNHPKTLQDIIDHNTAKLLDALHIRNDYAGRWDGD----------   189
              : :*:::                       *  :   :*::          : *   . :           :*
```

(C)

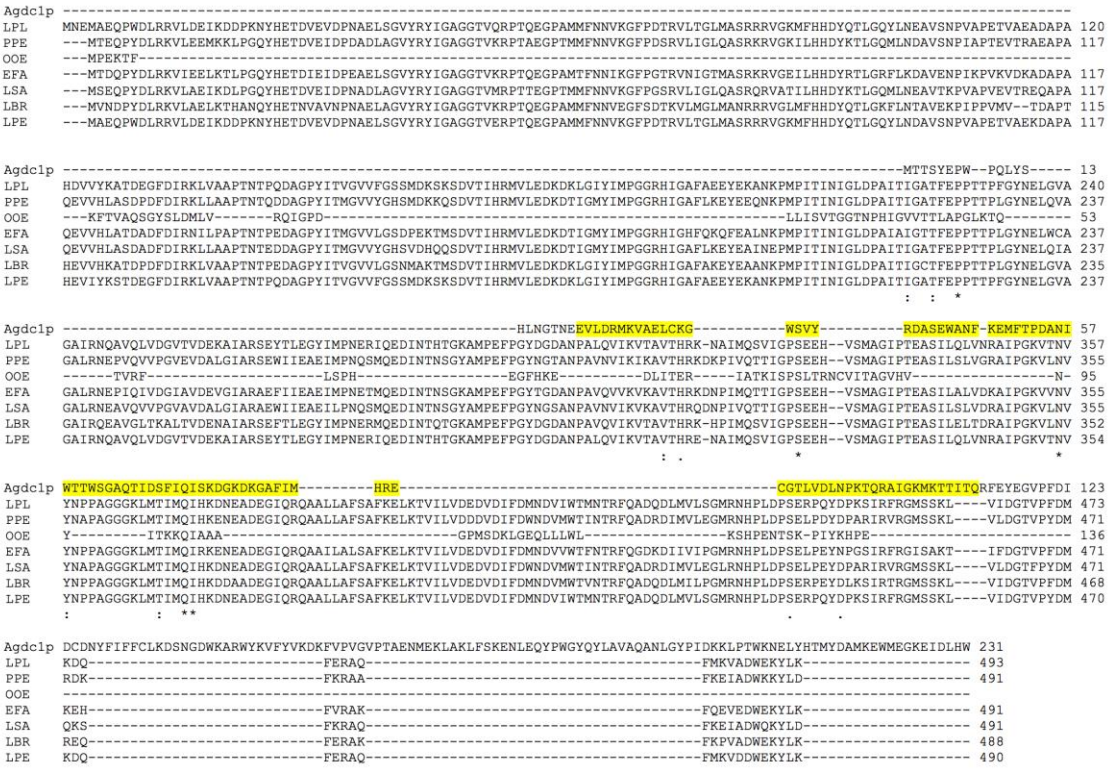

Figure 11 Multiple alignment of Agdc1p with published gallic acid decarboxylase sequences. **(A)** The phylogenetic tree constructed by the neighbour joining method of Agdc1p to selected lactic bacteria without distance corrections. **(B)** Multiple alignment of Agdc1p sequence to subunit B from *L. plantarum* ATCC 14917^T (LPL) (D7V849) and other putative gallic acid decarboxylases from lactic acid bacteria (*L. pentosus* KCA1 (LPE) (I9L531), *L. brevis* ATCC 367 (LBR) (Q03P27), *L. rhamnosus* HN001 (LRA) (B5QPH7), *L. sakei* 23K (LSA) (Q38Y44), *E. faecium* DO (EFA) (Q3Y2U4), *O. oeni* PSU-1 (OOE) (A0NKP0), *P. pentosaceus* ATCC 25745 (PPE) (Q03HH4), and *S. gallolyticus* UCN34 (SGA) (D3HEZ0). **(C)** Multiple alignment of Agdc1p sequence to subunit C from *L. plantarum* ATCC 14917^T (LPL) (D7VDD5) and other putative gallic acid decarboxylases from lactic acid bacteria (*L. pentosus* KCA1 (LPE) (I9KYH7), *L. brevis* ATCC 367 (LBR) (Q03P26), *L. sakei* 23K (LSA) (Q38Y45), *E. faecium* DO (EFA) (Q3Y2U5), *O. oeni* PSU-1 (OOE) (Q04EQ5) and *P. pentosaceus* ATCC 25745 (PPE) (Q03HH5). The alignment was performed using ClustalO software (http://www.ebi.ac.uk/Tools/msa/clustalo/). Residues marked with an asterisk (*) are identical in all sequences in the alignment. A colon (:) indicates conserved substitutions and a dot (.) indicate semi-conserved substitutions. Alignment was done using ClustalOmega. The domains are highlighted in yellow; binding sites in green and nucleotide binding sites in blue.

4.2.2 Generation of an Agdc1-6hp producing yeast strain

A. adeninivorans G1212 [Δ*trp1*] served as a host strain for overexpression of the *AGDC1* gene with a His-Tag encoding sequence fused to the 3´-end of the ORF under control of the nitrate inducible *AYNI1* promoter (*A. adeninivorans* nitrate reductase promoter). Cassettes with the *AGDC1* expression module (YRC102-AYNI1-AGDC1-6H, YIC102-AYNI1-AGDC1-6H (**Figure 12**) and controls (YRC102, YIC102) were prepared as described in "Material and Methods" (3.4.3). After genome integration of the cassettes, a number of selected clones (YICs and YRCs) were passaged to establish high plasmid stability. The transformants were subsequently cultivated in YMM-glucose-$NaNO_3$ at 30 °C for 48 h after which they were harvested, disrupted and screened for gallic acid decarboxylase activity. All stabilized strains of *A. adeninivorans* G1212/YRC102-AYNI1-AGDC1-6H and G1212/YIC102-AYNI1-AGDC1-6H were found to express this enzyme activity. Enzyme activity in transgenic yeast strains with genomically integrated YRCs was approximately 2.2-fold higher than in YIC transformants (**Figure 13**).

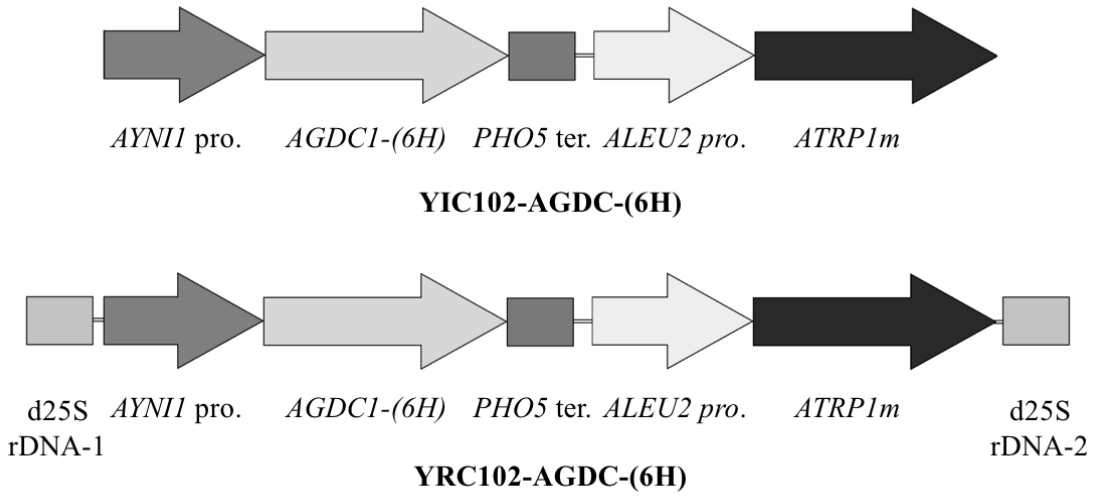

Figure 12 Physical map of the *AGDC1* yeast integrative expression cassettes.
The cassettes contain one copy of the expression module: *AYNI1* promoter-*AGDC-6H-PHO5*-terminator, selection marker *ATRP1m* and *ALEU2* promoter.

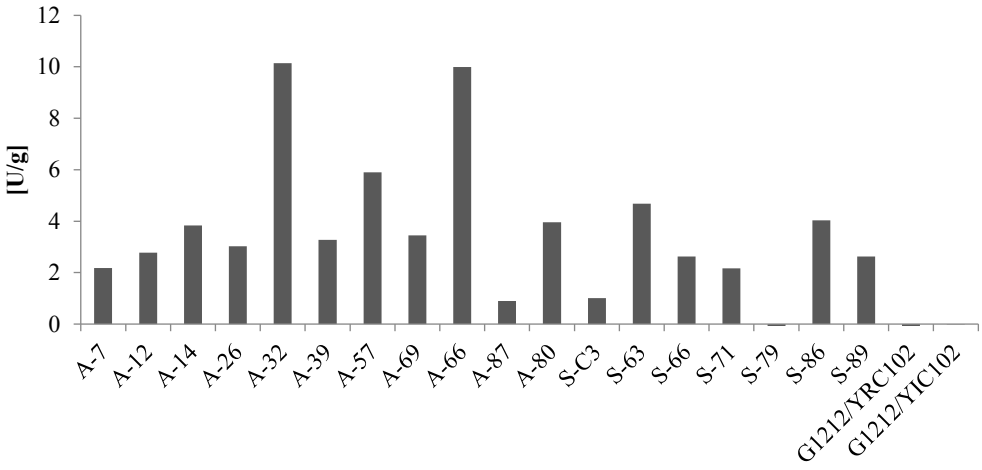

Figure 13 Screening of stabilized transformants after pre-selection analysis.
Gallic acid decarboxylate activities were measured in transformant strains YRC102-AGDC-6H (A-numbers), YIC102-AGDC-6H (S-numbers) as well as control strains G1212/YRC102 and G1212/YIC102. Numbers after letter are the numbers of transformants selected for final analysis. U/g is the U per g of protein.

In a time-course analysis, the *A. adeninivorans* control strain G1212/YRC102 was compared with the transgenic strain G1212/YRC102-AYNI1-AGDC1-6H. Both strains were cultivated in YMM-glucose-$NaNO_3$ at 30 °C and 180 rpm for 144 h. Dry cell weight (dcw), gallic acid decarboxylase activity with gallic acid as substrate and yield [Y(P/X)] (where Y is yield coefficient, P is enzyme formation in U, X is biomass in g) were determined every 24 h. The experiment was performed in triplicate. In the presence of glucose as the sole carbon source, gallic acid decarboxylase activity was detected in the selected transgenic strain (*A. adeninivorans* G1212/YRC102-AYNI1-AGDC1-6H) but not in the control strain *A. adeninivorans* G1212/YRC102. In both yeast strains maximum dcw was reached after 24 h of cultivation and then remained constant until the end of the experiment. The transgenic *A. adeninivorans* strain G1212/YRC102-AYNI1-AGDC1-6H achieved its maximum enzyme activity of 1064.4 U/l and 97.5 U/g dcw after 96 h (**Figure 13**).

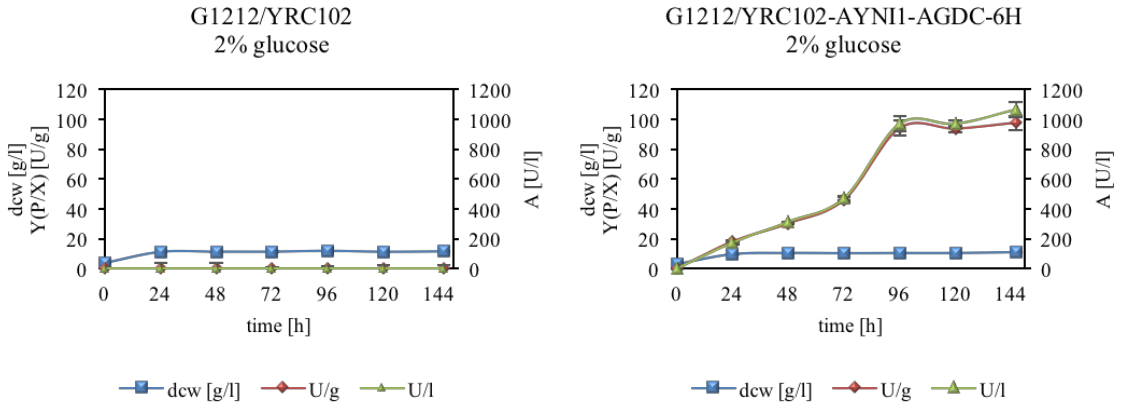

Figure 14 Time-course analysis of gallic acid decarboxylase activity in *A. adeninivorans* control and transgenic strain overexpressing *AGDC-6H*.
The cells were grown on YMM-glucose-$NaNO_3$ in shake flasks at 30 °C for 146 h. Physiological parameters investigated were intracellular Agdc1-6hp activity (triangles) detected with gallic acid as substrate, calculated yield [Y(P/X)] (circles), and dry cell weight (squares). Y - yield coefficient, P - enzyme formation in U, X - biomass in g. Measurements were done in triplicate and error bars represent the standard deviation.

4.2.3 Generation of Δ*agdc1* gene disruption mutant strain

An insight into the function of *AGDC1* in *A. adeninivorans* was obtained through the deletion of the *AGDC1* gene, using gene targeting by homologous recombination. The deletion mutant cassette constructed was 1019 bp upstream and 1032 bp downstream of homology fragments of the ORF of the gene (**Figure 15**).

A. adeninivorans G1212 [Δ*trp1*] served as a host strain for the deletion of *AGDC1*. The deletion cassettes accurately targeted integration into a particular region of the yeast genome, replacing the gene of interest by a selection marker sequence. Efficiency of gene replacement and tagging were checked by PCR. Integration into the target locus was verified by PCR of genomic DNA, using primers amplifying part of the integrated marker and an adjacent area of genomic DNA, thus confirming that the site of integration was correct. Deletion of the ORF was also verified by PCR (**Figure 16**). The strain carrying the correct integrated deletion cassette obtained the number: G1234 [Δ*agdc1*].

(A)

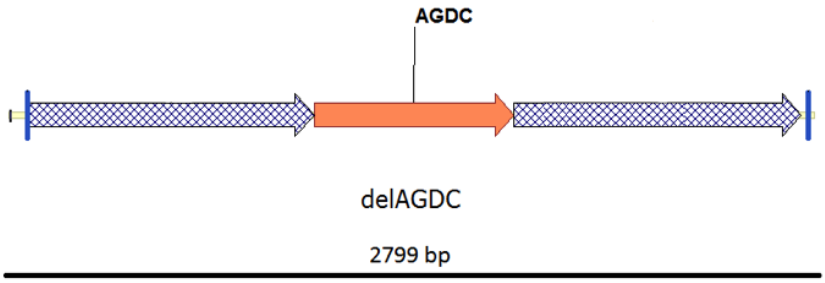

(B)

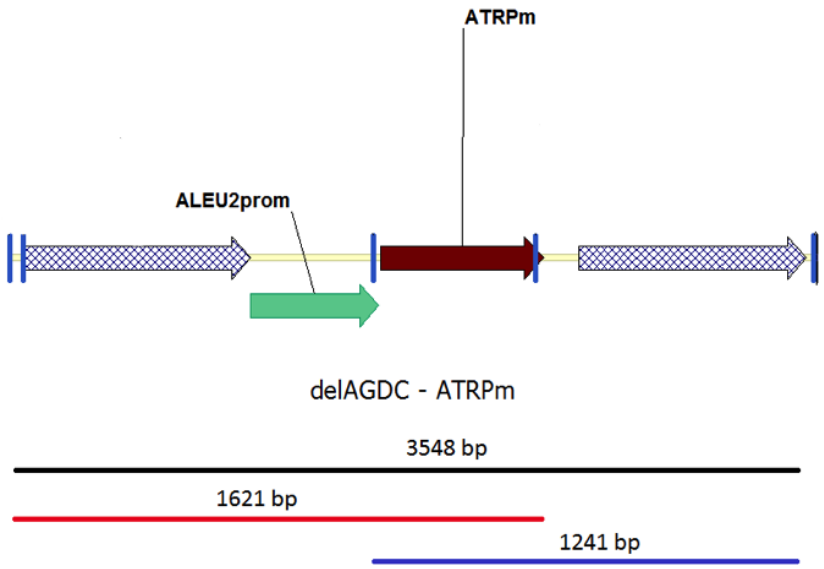

Figure 15 Design of *AGDC1* gene deletion cassettes.
(A) Illustration of genomic DNA fragment length used for construction of *AGDC1* deletion cassette. Arrow with blue checkered pattern - 1019 bp upstream and 1032 bp downstream of homology fragments; orange arrow – *AGDC1* gene. **(B)** Constructed deletion mutant cassette. Arrow with blue checkered pattern - 1019 bp upstream and 1032 bp downstream of homology fragments; green arrow – *ALEU2* promoter; dark red arrow *ATRP1* – selection marker for tryptophan prototrophy; black, red and blue lines – length of fragments obtained by PCR after successful deletion of *AGDC1*.

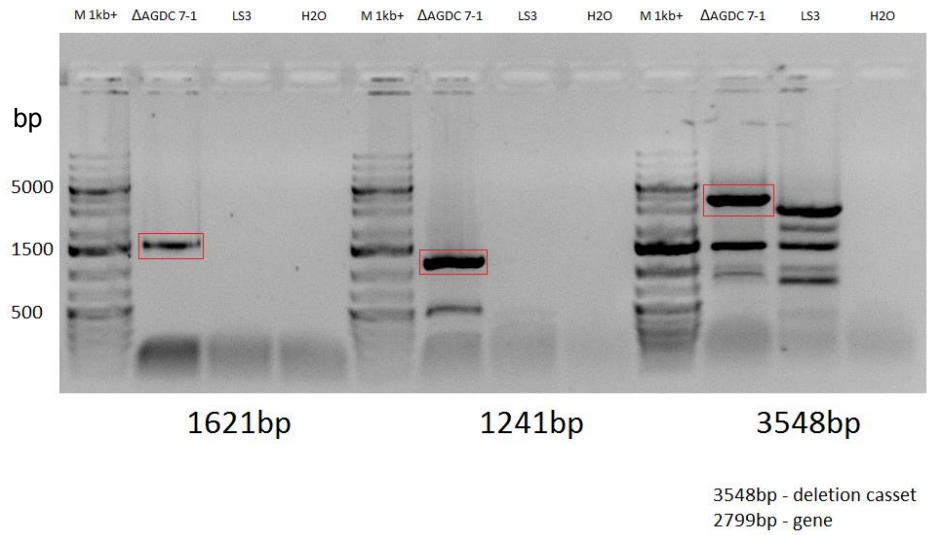

Figure 16 Verification of correctly integrated deletion cassettes by PCR of isolated genomic DNA. Correct integration is characterized by DNA fragments of 1621 bp, 1241 bp and 3548 bp – band marked in red rectangle. Fragment length of 2799 bp – genomic DNA length with AGDC1 gene, serving as a negative control. M1kb+ – 1 Kb Plus DNA Ladder (Thermo Fischer), ΔAGDC1 7-1 – strain number with correctly targeted deletion cassette; LS3 – wild type (control); H2O – no template PCR reaction (control).

Table 15 Primers used for construction of deletion mutant strain G1234 [Δ*agdc1*].

Primers for construction of *A. adeninivorans* G1234 [Δ*agdc1*]	
Primer	Sequence (5‘ → 3‘)
01. 1000bp ΔAGDC left	GTTTTAATTACAAAAAGCTAAATTCTTCTACAGGAAGTCAGG
02. Primer right 1 ΔAGDC	TGTACAATGTTTCTTTCTTGTCTG
03. Marker left ΔAGDC	AAGAAACATTGTACATTTCAATCGACGATTGCAATTGAC
04. Marker right 1 ΔAGDC	GAGTCTGTATTGAAGCTTAGCTTG
05. Primer left 1 ΔAGDC	CTTCAATACAGACTCACAGAACTAGAATATATAACAATGTTATTAAA
06. 1000bp ΔAGDC right	TTAGTTAAAAGCACTCCATTGTTATGCACTATTCGTTAACGG

4.2.4 Phenotypic analysis of *AGDC1* wild type and Δ*agdc1* deletion strains

Yeast strains G1212/YRC102, G1234 (Δ*agdc1*) and G1212/YRC102-AYNI1-AGDC1-6H were grown on agar plates containing YMM-$NaNO_3$ medium supplemented with 2 % glucose as the sole carbon source. Within days, the strains used displayed distinctly different colony growth pattern which were readily visible to the eye. Whereas G1212/YRC102 (control) and G1212/YRC102-AYNI1-AGDC1-6H (overexpression of *AGDC1*) formed spherical whitish colonies, the strain G1234 [Δ*agdc1*] (deletion of *AGDC1*) formed characteristic tubular colonies (**Figure 17 A-C**).

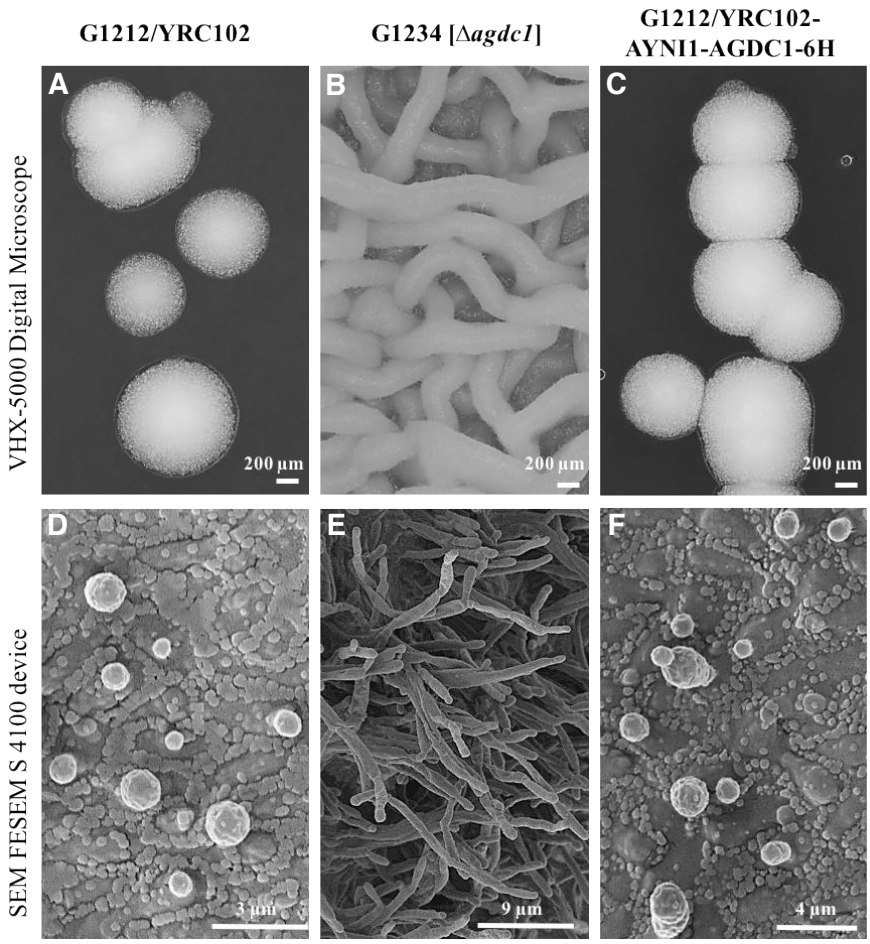

Figure 17 Phenotypic analysis of *A. adeninivorans* strains.
Strain G1212/YRC102 (control), G1234[Δagdc1] (deletion of *AGDC1*) and G1212/YRC102-AYNI1-AGDC1-6H (overexpression of *AGDC1*) were cultivated on agar plates containing YMM-glucose-$NaNO_3$ at 30 °C for 48 h. (A-C) Light microscopic recordings of colony phenotype show the deletion strain to form characteristic tubular structures. Electron microscope analysis reveals that cells of both control and overexpression strains are spherical (D, F) while those of the deletion strain form mycelia (E).

Subsequent analysis under a scanning electron microscope revealed that the cells of the control and overexpression strains were spherical (**Figure 17 D, F**), however, those of the deletion strain were growing as mycelia (**Figure 17 E**). Evidently, deletion of the gallic acid decarboxylase gene has resulted in a change of cells shape and through this, a change in colony morphology.

4.2.5 Generation of Agdc1-eGFP producing yeast strain

A. adeninivorans G1212 [Δ*trp1*] served as a host strain for overexpression of *AGDC1* with a eGFP encoding sequence fused to the 3´-end of the ORF under control of the *TEF1* promoter (translation elongation factor 1). Preparation of cassettes with the *AGDC1* expression module (YRC102-TEF1-AGDC1-eGFP) (**Figure 18**) and control (YRC102) is described under 3.4.2. After genomic integration of the cassettes, selected clones were passaged to establish high construct stability.

Figure 18 Physical map of the *AGDC1-eGFP* yeast integrative expression cassette.
The cassette contains one copy each of the *TEF1* promoter, *AGDC1-eGFP, PHO5* terminator, *ALEU2* promoter and selection marker *ATRP1m*.

4.2.6 Cellular localisation of Agdc1-eGFP

Transformants containing eGFP tagged *AGDC1* were cultivated in YMM-glucose-$NaNO_3$ at 30 °C for 24 h after which they were screened in a confocal laser scanning microscope (CLSM) equipped with appropriate filters for the detection of YFP. Only for cells containing the YRC102-TEF1-AGDC1-eGFP expression cassette displayed cytosolic GFP signals (**Figure 19**).

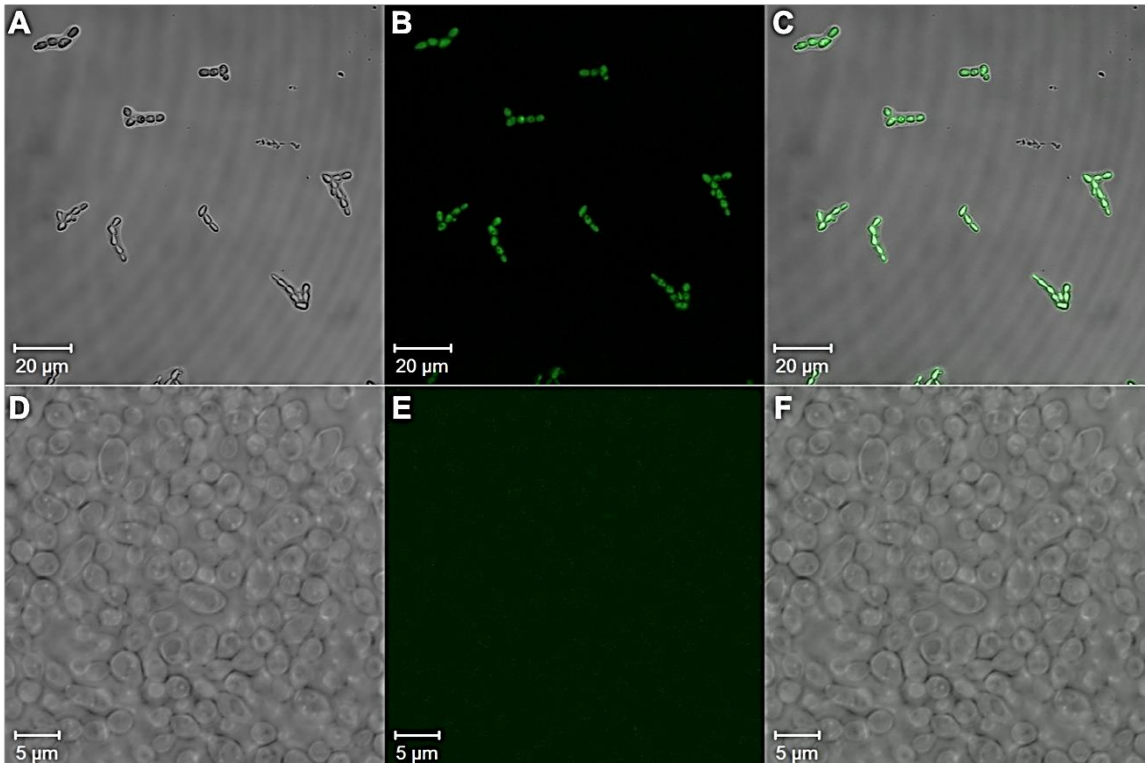

Figure 19 Subcellular localization of Agdc1-eGFP.
CLSM analysis shows a cytosolic distribution of GFP signals in strain G1212/YRC102-TEF1-AGDC1-eGFP **(A-C)** but not in strain *A. adeninivorans* strain G1212/YRC102 **(D-F)**. **(A)** and **(D)** bright field image, **(B)** and **(E)** GFP derived fluorescence. **(C)** Merged image from bright field **(A)** and GFP derived fluorescence **(B). (F)** Merged image from bright field **(D)** and GFP derived fluorescence **(E)**.

4.2.7 Purification of the recombinant Agdc1-6hp

A. adeninivorans strain G1212/YRC102-AYNI1-AGDC1-6H containing a HisTag encoding sequence at the 3´-end of the *AGDC1* ORF was used for synthesis of recombinant Agdc1-6hp. The protein purification process by Immobilized Metal Affinity Chromatography (IMAC) was performed using the ÄKTA Pure System. To achieve the highest possible purification performance, the optimal imidazole concentration was determined. Purified fractions of Agdc-6h were eluted with ~630 mM imidazole (**Figure 20**).

Agdc1-6hp has a predicted mass of 27.3 kDa. For the denatured protein on SDS-PAGE, a molecular weight of approximately 25 kDa in both the crude extract and the purified protein fraction was measured (**Figure 21**).

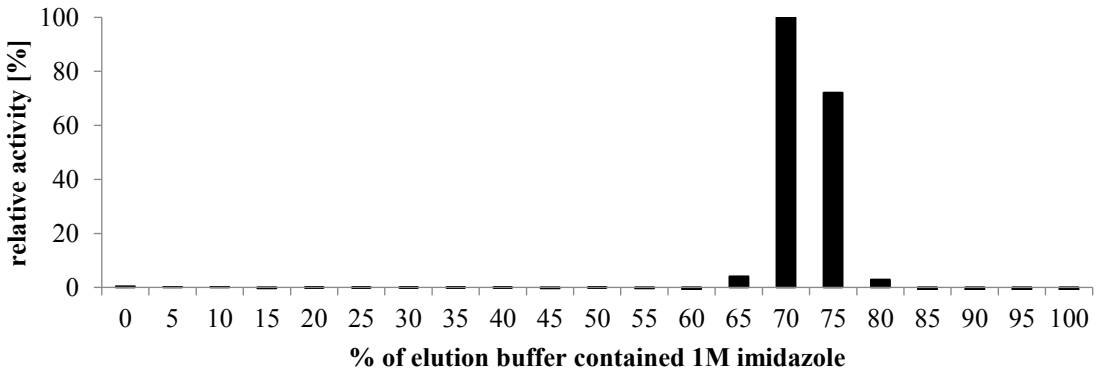

Figure 20 Test for elution of Agdc1-6hp by varying concentrations of imidazole.
Agdc1-6h was purified via IMAC. To established imidazole concentration at which Agdc1-6h is eluting from the column, the protein was washed with elution buffer with a continuous gradient of 0-1 M imidazole. The protein was released from the column at imidazole concentration between 630 and 770 mM as confirmed by enzyme activity assay.

Gallic acid decarboxylase activity was measured for crude extract and purified Agdc1-6hp. The specific activity in crude extract was 1 U/mg whereas it was 5.9 U/mg in the purified Agdc1-6hp fraction, corresponding to 77 % of yield (**Table 16**).

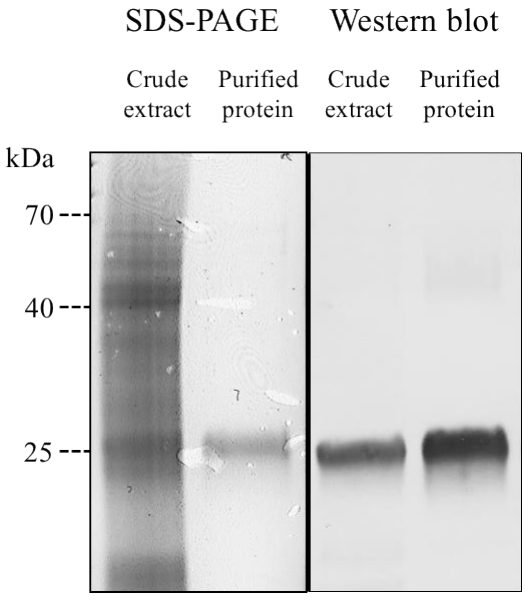

Figure 21 Purification of Agdc1-6hp on Ni-Sepharose.
Crude extract and purified Agdc1-6hp on 12% SDS-PAGE gel after Coomassie-staining. Western blot labelling using anti-polyhistidine antibodies from rabbit and secondary antibodies anti-rabbit from goat confirms the presence of Agdc-1-6hp in crude extract and its enrichment after purification.

Table 16 Summary of the Agdc1-6hp purification.
Protein was purified from 200 ml culture incubated in a shaking flask for 48 h at 30 °C and 180 rpm.

Step	Protein [mg]	A_{total} [U]	$A_{specific}$ [U/mg]	Yield [%]	Purification fold
Crude extract	1.95 ± 0.08	2 ± 0.1	1 ± 0.05	100	1
Purified protein	0.26 ± 0.13	1.55 ± 0.03	5.9 ± 0.12	77	6

4.2.8 Native molecular mass determination of the recombinant gallic acid decarboxylase (Agdc1-6hp)

The indicative molecular mass of native Agdc1-6hp was estimated by gel filtration on a Superdex^{TM} 200 column. A standard curve was prepared using molecules with known molecular masses (Blue Dextran – 20000000 Da, Ferritin – 450000 Da, Catalase – 240000 Da, BSA – 67000 Da, RNAse A - 13700 Da and Vitamin B12 – 1355 Da) (**Figure 22**). The calculated molecular mass of 27.1 kDa for the native enzyme closely follows the predicted molecular mass of 28.1 kDa thus indicating that Agdc1-6hp is a monomeric protein (**Figure 23**).

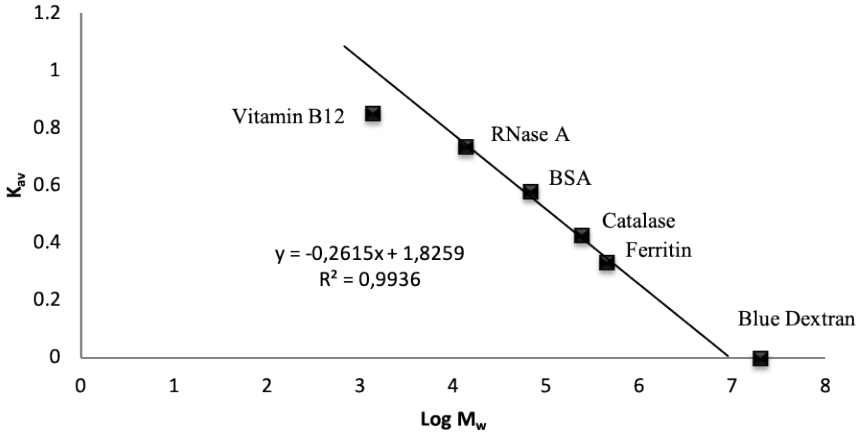

Figure 22 Standard curve for determination of native molecular mass of proteins by gel filtration.
Partition coefficient Kav plotted over the logarithm of molecular mass for selected molecules. The selectivity curve is straight over a range from Kav=0.33 to Kav=0.73. Here, the dimer of Blue Dextran elutes in the void volume V0 (Kav = 0) and the other proteins nicely follow the theoretical Kav curve.

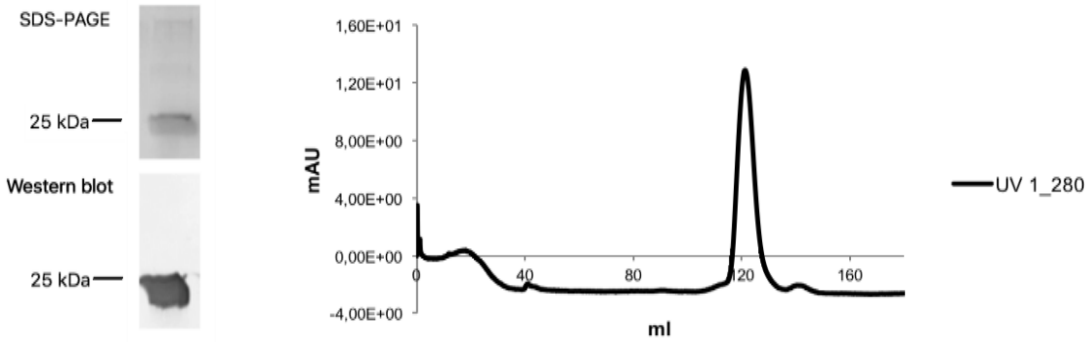

Analyst	Predicted m_M [kDa]	MW [kDa]	Retention volume [mL]	Ratio	
A. adeninivorans G1212-YRC102-AGDC1-6H	27.32	27.05	120.9	99	**Monomer**

Figure 23 Determination of native molecular mass of recombinant gallic acid decarboxylase by size exclusion chromatography.
Sample contained Agdc1-6hp after purification. Gel filtration on a Superdex^{TM} 200 column was prepared on AKTA Pure System. Molecular mass was calculated based on previously prepared standards.

4.2.9 Properties of the recombinant gallic acid decarboxylase

4.2.9.1 Determination of the optimal pH

Optimal conditions for enzymatic activity were established *in vitro* using 0.5 mM gallic acid as substrate. The optimum pH was determined with the following buffers: 50 mM citrate-phosphate (McIlvaine) (pH 2.6 to 8), 50 mM sodium acetate (pH 3 - 6), 50 mM sodium citrate (pH 3.5 to 6.5), 50 mM potassium phosphate buffer (pH 6.2), 50 mM sodium phosphate (pH 5.5 - 8), 50 mM TRIS-HCl (pH 6.5 – 8.8) and CAPS (pH 10.5). Enzyme activity of Agdc1-6hp peaked between pH 5.6 - 7.1 with an optimum at pH 6.2 in 50 mM potassium phosphate buffer (**Figure 24**). Some buffer systems were found to reduce enzyme activity of Agdc1-6hp. Maximum enzyme activity in citrate-phosphate buffer was only 52 %, in sodium-citrate buffer only 15 % of the activity measured in potassium phosphate buffer (**Figure 25**).

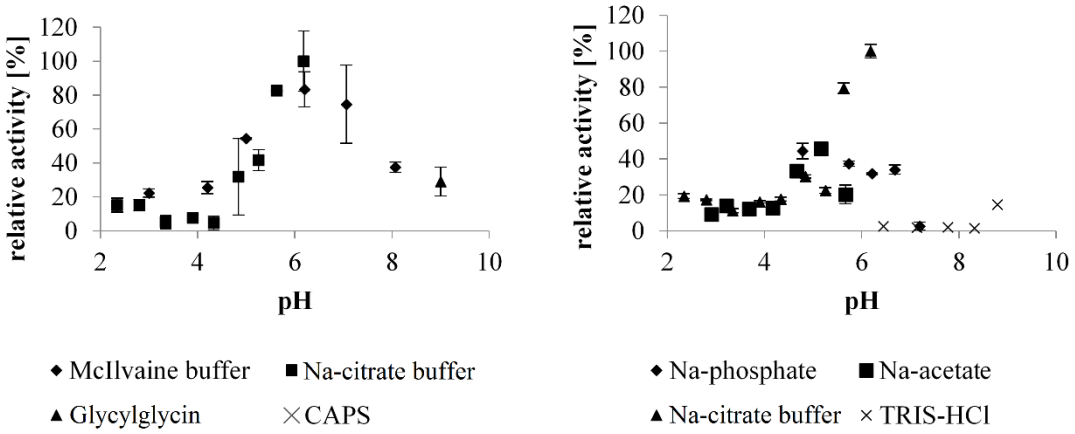

Figure 24 pH spectrum of recombinant gallic acid decarboxylase.
Enzyme activity was measured in 50 mM of different buffers at 30 °C.

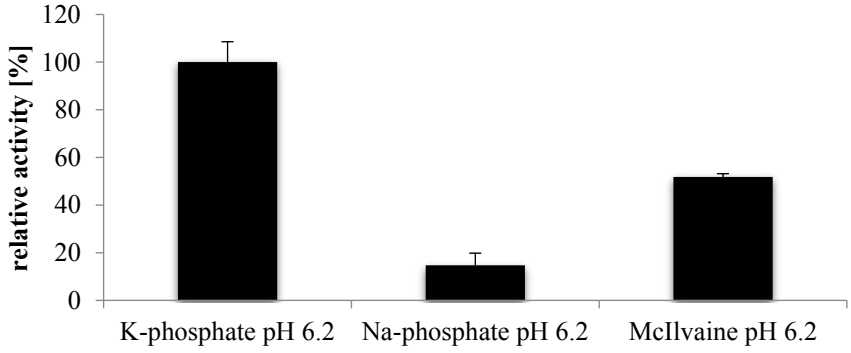

Figure 25 Most favourable buffer for gallic acid decarboxylase activity.

4.2.9.2 Optimal temperature and thermostability of Agdc1-6hp

The effect of temperature on the activity of gallic acid decarboxylase was measured by incubating reaction mixtures at different temperatures under optimal pH conditions. Enzyme activity of Agdc1-6hp peaked between 25 and 45 °C with a maximum observed at 40 °C (**Figure 26**).

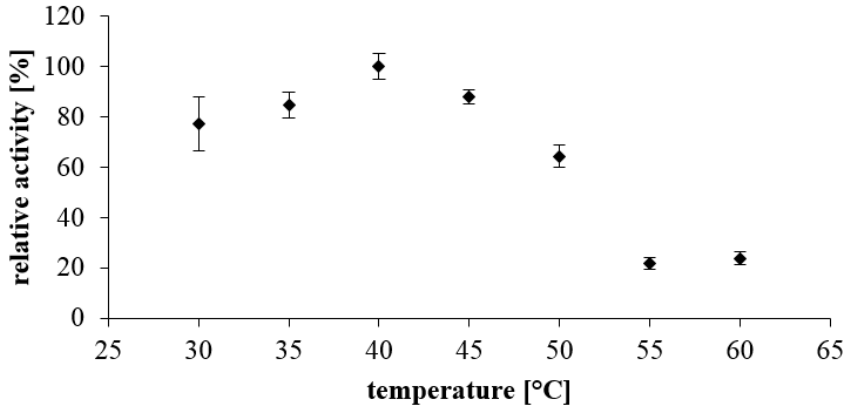

Figure 26 Temperature optimum of recombinant gallic acid decarboxylase activity.

Thermostability of Agdc-1-6hp was tested by monitoring the change in enzyme activity during 24 h incubation at different temperatures. Between 4 and 30 °C, activity of Agdc1-6hp remained unaffected even after 24 h, proving that the enzyme is stable within this temperature range. At 35 °C and 40 °C, enzyme activity initially remained constant but showed a sharp drop after 7 h incubation, eventually falling to 40 % and 10 %, respectively, of the original activity after 24 h. Temperatures above 40 °C led to a complete loss of activity within 6 h (**Figure 27**). Freezing in liquid nitrogen typically resulted in 40 % loss of Agdc1-6hp activity. However, once frozen this way, the enzyme could be stored at -80 °C for one month or more without loosing any further activity (**Figure 28**).

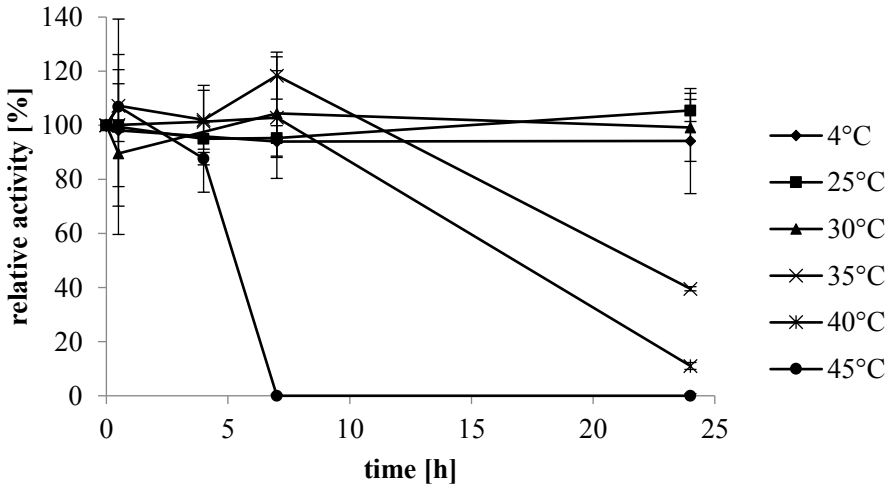

Figure 27 Thermostability of Agdc1-6hp at different temperatures.

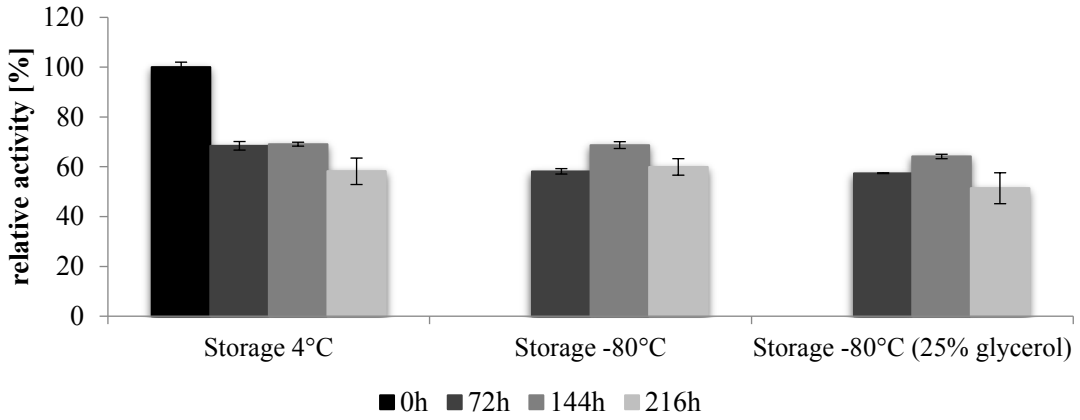

Figure 28 Agdc1-6hp activity during storage under different temperature regimes.
Enzyme activity immediately after protein purification (0 h) was set at 100 %. Before being stored at -80 °C, samples were frozen in liquid nitrogen.

4.2.9.3 Kinetic study

The kinetic parameters of purified Agdc1-6hp were determined photometrically for gallic acid and protocatechuic acid as substrates. The K_m of Agdc1-6hp for gallic acid was found to be one quarter that for protocatechuic acid (0.73 ± 0.15 mM and 3.2 ± 0.24 mM, respectively). Turnover, k_{cat}, was 42 ± 8.24 s^{-1} for gallic acid and 44 ± 3.42 s^{-1} for protocatechuic acid. However, the catalytic efficiency was much lower for protocatechuic acid (14 ± 2 [$mM^{-1}s^{-1}$]) than for gallic acid (57.8 ± 7.6 [$mM^{-1}s^{-1}$]) (**Table 17**).

Table 17 Kinetic constants of purified Agdc1-6hp.
Purified protein was synthetized by G1212/YRC102-AYNI1-AGDC1-6H and kinetic constants were measured by photospectrometry for gallic acid and protocatechuic acid as substrates.

Substrate	K_m [mM]	k_{cat} [s^{-1}]	k_{cat}/Km [$mM^{-1}s^{-1}$]
gallic acid	0.7 ± 0.2	42.0 ± 8.2	57.8 ± 7.6
protocatechuic acid	3.2 ± 0.2	44.4 ± 3.2	14.0 ± 2.0

4.2.9.4 Effect of different additives on Agdc1-6hp activity

A number of metal ions and reagents were tested to identify possible inhibitors and/or cofactors of gallic acid decarboxylase activity. In the presence of 1 mM of either Ni^{2+}, Fe^{2+}, Fe^{3+}, Co^{2+} or Cu^{2+}, enzyme activity was strongly inhibited (relative activity < 30 %). In contrast, addition of 1 mM Mg^{2+}, Mn^{2+}, Ca^{2+}, $Na_2S_2O_3$, PEG4000, PEG6000 or PEG8000 to the reaction mixture had no significant influence on enzyme activity (> 80 % activity of control reaction) (**Table 18).** A slight positive effect was detected in the presence of 1 mM EDTA, ascorbic acid or DTT (**Table 18**).

Table 18 Effect of metal salts and additives on Agdc1-6hp activity.
Relative Agdc1-6hp activity [%] assayed for 0.5 mM gallic acid as substrate and presence of different additives in the reaction mixture.

1 [mM]	Relative activity [%]	1 [mM]	Relative activity [%]	1 [mM]	Relative activity [%]
control (H_2O)	100 ± 7	$ZnSO_4$	52 ± 4	$Na_2S_2O_3$	85 ± 0
$NiSO_4$	0 ± 1	$ZnCl_2$	60 ± 2	PEG4000	91 ± 7
$NiCl_2$	0 ± 4	$AlCl_3$	73 ± 4	PEG6000	95 ± 0
$FeSO_4$	0 ± 3	$MgSO_4$	84 ± 12	PEG8000	95 ± 1
$FeCl_3$	24 ± 11	$MgCl_2$	84 ± 3	Ascorbic acid	107 ± 0
$CoSO_4$	4 ± 3	$MnSO_4$	86 ± 1	DTT	116 ± 2
$CoCl_2$	27 ± 4	$MnCl_2$	94 ± 4	EDTA	146 ± 5
$CuSO_4$	4 ± 6	$CaSO_4$	84 ± 2		
$CuCl_2$	39 ± 1	$CaCl_2$	97 ± 2		

4.2.9.5 Substrate spectrum of Agdc1-6hp

Five additional hydroxylated aromatic acids (3-hydroxybenzoic acid, 4-hydroxybenzoic acid, 2,3-dihydroxybenzoic acid, 2,4-dihydroxybenzoic acid, 2,5-dihydroxybenzoic acid) with different numbers and positions of hydroxyl groups were tested to determine the *in vitro* substrate specificity of Agdc1-6h. However, even after 35 min incubation under optimal conditions, the enzyme failed to catalyse the decarboxylation of these compounds. This shows a high specificity of Agdc1-6hp to decarboxylate only gallic acid and protocatechuic acid (**Table 19**). Hydroxyl groups in the meta and para position on the aromatic ring may be a prerequisite for this enzymatic reaction to occur (**Figure 68 A**).

Table 19 Substrate spectrum for Agdc1-6hp.

	Substrate	Formed product
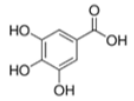	3,4,5-trihydroxybenzoic acid (gallic acid)	1,2,3-trihydroxybenzene (pyrogallol)
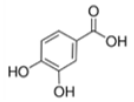	3,4-dihydroxybenzoic acid (protocatechiuc acid)	1,2-dihydroxybenzene (catechol)
	3-hydroxybenzoic acid	-
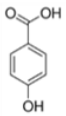	4-hydroxybenzoic acid	-
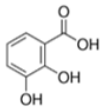	2,3-dihydroxybenzoic acid	-
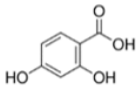	2,4-dihydroxybenzoic acid	-
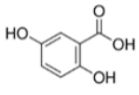	2,5-dihydroxybenzoic acid	-

4.2.9.6 Expression of *AGDC1* in dependence of carbon sources

The expression level of *AGDC1* relative to the housekeeping genes *TFCI* and *ALG9* was analysed by nested quantitative RT-PCR. Primers used for expression analysis of *AGDC1* are listed in **Table 20**. *A. adeninivorans* G1212/YRC102 was cultivated on YMM-$NaNO_3$ supplemented with 0.2 % (w/v) of glucose or a hydroxylated aromatic acid as the sole source of carbon. Samples were collected at different time points and total RNA was isolated. Gene transcription of *AGDC1* significantly rose when cells were cultivated on gallic acid or protocatechuic acid with peak expression reached after 8 h (**Figure 29**). In the presence of other carbon sources (glucose, 3-hydroxybenzoic acid, 4-hydroxybenzoic acid, 2,4-dihydroxybenzoic acid, 2,3-dihydroxybenzoic acid, 2,5-dihydroxybenzoic acid), expression level of *AGDC1* was not increased (**Figure 29**).

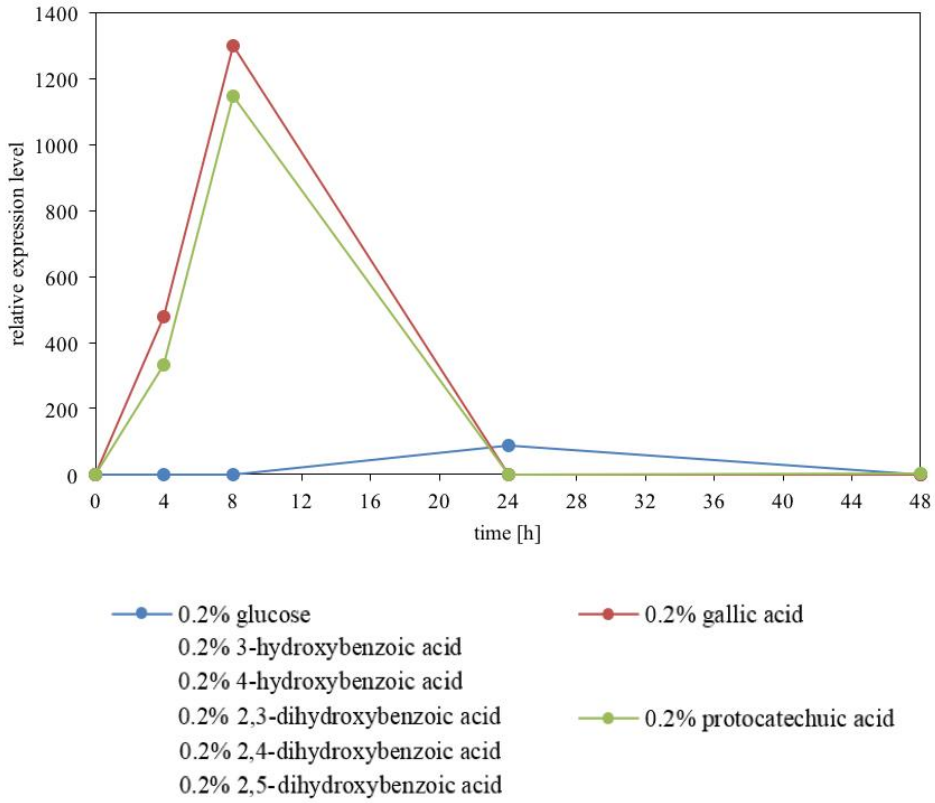

Figure 29 Influence of carbon sources on *AGDC1* expression.
A. adeninivorans G1212/YRC102 was cultivated on YMM-$NaNO_3$ supplemented with 0.2 % (w/v) of either: glucose, gallic acid, protocatechuic acid, 3-hydroxybenzoic acid, 4-hydroxybenzoic acid, 2,3-dihydroxybenzoic acid, 2,4-dihydroxybenzoic acid or 2,5-dihydroxybenzoic acid. Expression analysis was performed by nested quantitative real time PCR.

Table 20 Primers used for analysis of *AGDC1* expression levels.

Primers for nested quantitative RT PCR		
Reaction step	Primer	Sequence (5‘ → 3‘)
Step1 cDNA synthesis	(dT) 15V-RTA	TGA CAG GAT ACC ATA CAG ACA CTA TTT TTT TTT TTT TTT V
Step 2 Second PCR synthesis	RTA-1 rv	TGA CAG GAT ACC ATA CAG ACA C
	AGDC1-V fw	TGC TGT GGC TCA GGC TAA TC
	TFC1-3 fw	TGA AGA AGA GCA CCA AGC A
	ALG9-7	TGGTATCGGTCGCATTCT
Step 3 Second PCR synthesis	RTA rv	TGA CAG GAT ACC ATA CAG ACA CTA
	AGDC1-III fw	ATG TAC GAC GCC ATG AAG GA
	TFC1-1 fw	ACA ACA AGA TGA AAA CGC
	ALG9-8	TCAATTGCAGTGGACTGACTA

4.2.10 Influence of gallic acid on gene expression in *A. adeninivorans* by microarray expression analysis

In order to get information on whole transcriptome variations upon incubation of *A. adeninivorans* with gallic acid, microarray expression analysis was performed. Gene expression of *A. adeninivorans* wildtype strain LS3 cultivated in YMM-$NaNO_3$ supplemented with 1 % glucose was compared with that of the same strain grown on YMM-$NaNO_3$ supplemented with 1 % glucose plus 0.5 % gallic acid. Cells were harvested after 15 min, 30 min, 5 h and 12.5 h of incubation in shaking flasks at 30 °C and 180 rpm. Microarray data analysis of the isolated RNA allowed the identification of candidate genes involved in the tannic acid degradation pathway (**Figure 30**). Significantly upregulated were gallic acid decarboxylase 1 (*AGDC1*) and tannase 1 (*ATAN1*) as well as genes annotated as putative tannase 2 (*ATAN2*), catechol-1,2-dioxygenase, oxalocrotonate decarboxylase, 2-oxopent-4-dienoate hydratase, 4-hydroxy-2-oxovalerate aldolase. These data suggest that additional enzymes are involved in tannic acid degradation. These enzymes convert pyrogallol into pyruvate and acetaldehyde and make them available to the central metabolism (**Figure 30).** Also upregulated were genes involved in the β-oxidation process but those involved in the glyoxylate cycle, the methyl citrate cycle and in the catabolism of the branched-chain amino acids valine, leucine and isoleucine were not upregulated (**Figure 31** - **Figure 34**).

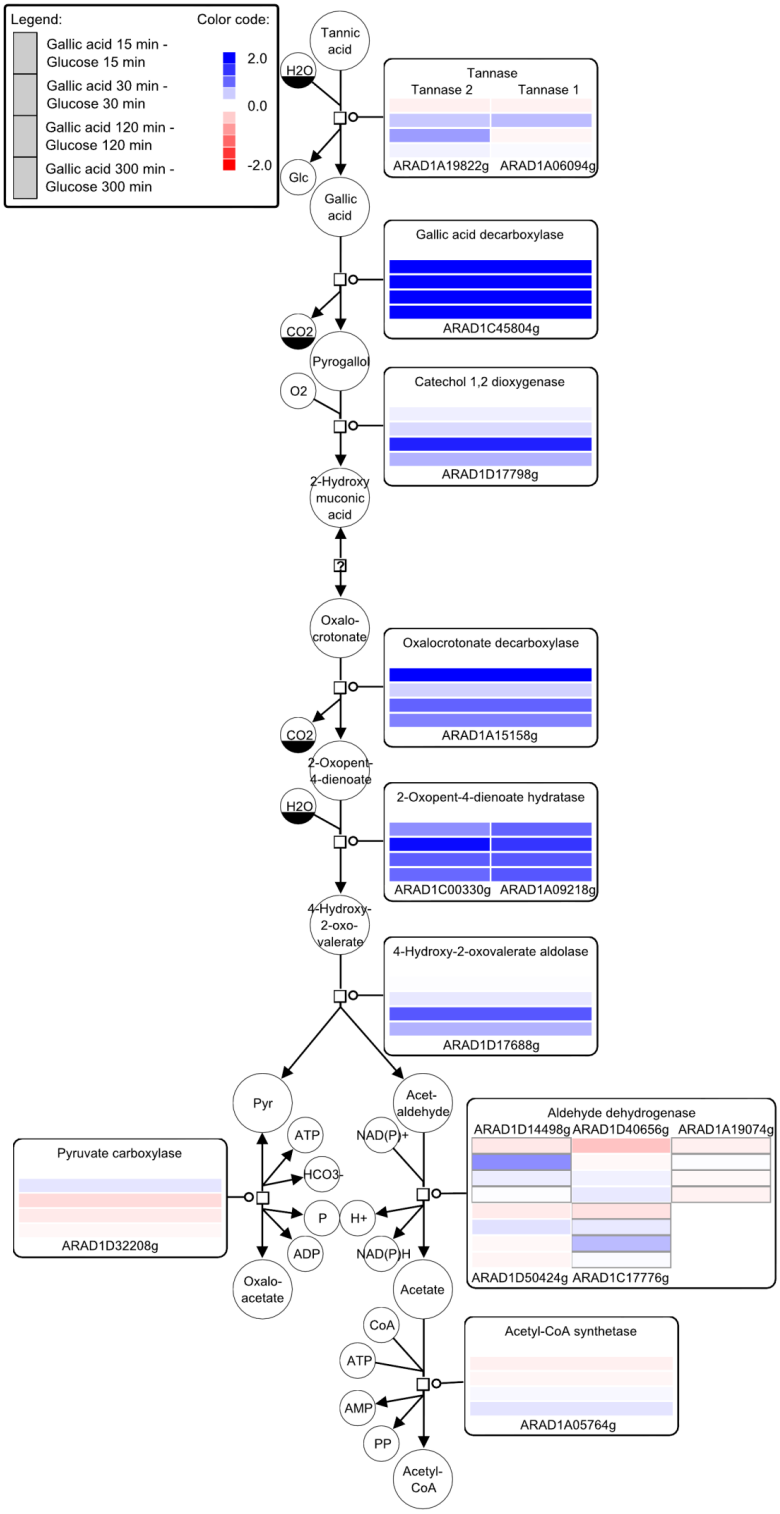

Figure 30 Key compounds of the tannin catabolism revealed by microarray study of gene regulation by gallic acid.
The Systems Biology Graphical Notation (SBGN) of the metabolic network depicts reactions catalyzed by the corresponding enzymes (rectangular square). Enzymes are enriched with colour-coded log2 fold change values of time resolved expression data of the respective genes. The change in gene expression resulting from a shift from a glucose based to a gallic acid based carbon source is colour coded with blue indicating upregulation (dark blue 2-fold upregulation) and red indicating downregulation (dark red 2-fold downregulation). Metabolites or enzymes occurring multiple times in the metabolic network are decorated with a clone marker (e. g. NAD^+) [graph produced with VANTED – (Junker *et al.*, 2012, Rohn *et al.*, 2012)].

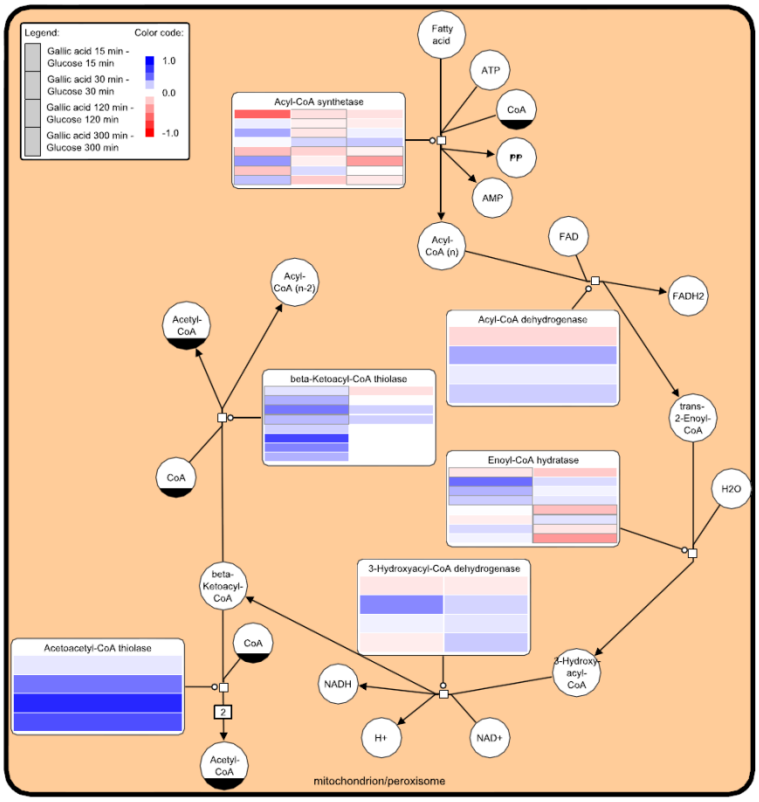

Figure 31 Key compounds of the β-oxidation revealed by microarray study of gene regulation by gallic acid.

The Systems Biology Graphical Notation (SBGN) of the metabolic network depicts reactions catalyzed by the corresponding enzymes (rectangular square). Enzymes are enriched with color-coded log2 fold change values of time resolved expression data of the respective genes. The colours represent upregulation (dark blue 1-fold upregulation) and downregulation (dark red 1-fold downregulation) of genes in cells shifted to a medium containing 0.5 % gallic acid and 1 % glucose as the carbon sources compared to cells grown with 1 % glucose. Metabolites or enzymes occurring multiple times in the metabolic network are decorated with a clone marker (e. g. NAD^+) [graph produced with VANTED – (Junker *et al.*, 2012, Rohn *et al.*, 2012)].

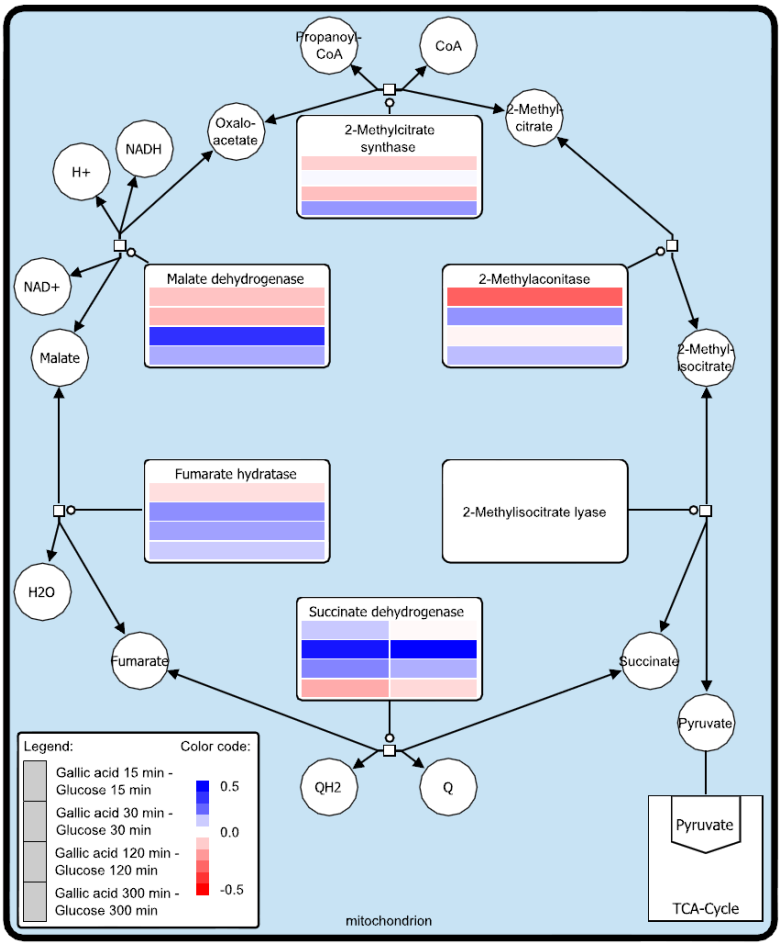

Figure 32 Key compounds of the methyl citrate cycle - microarray studies of gene regulation by gallic acid.

The Systems Biology Graphical Notation (SBGN) of the metabolic network depicts reactions catalysed by the corresponding enzymes (rectangular square). Enzymes are enriched with color-coded log2 fold change values of time resolved expression data of the respective genes. The colours represent upregulation (dark blue 0.5-fold upregulation) and downregulation (dark red 0.5-fold downregulation) of genes in cells shifted to a medium containing 0.5 % gallic acid and 1 % glucose as the carbon sources compared to cells grown with 1 % glucose. Metabolites or enzymes occurring multiple times in the metabolic network are decorated with a clone marker (e. g. NAD^+) [graph produced with VANTED – (Junker *et al.*, 2012, Rohn *et al.*, 2012)].

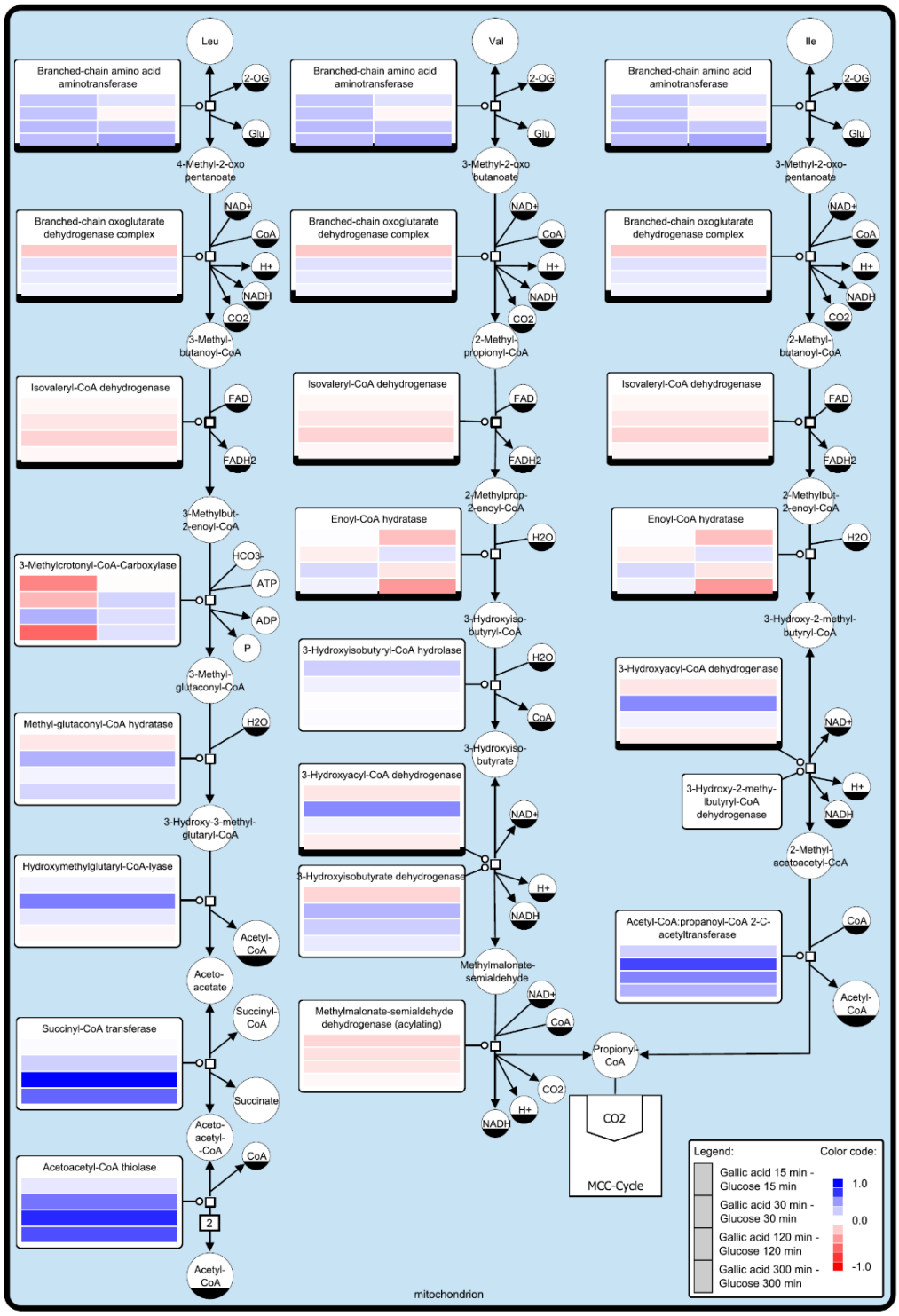

Figure 33 Key compounds of the catabolism of the branched-chain amino acids valine, leucine and isoleucine - microarray studies of gene regulation by gallic acid.
The Systems Biology Graphical Notation (SBGN) of the metabolic network depicts reactions catalyzed by the corresponding enzymes (rectangular square). Enzymes are enriched with color-coded log2 fold change values of time resolved expression data of the respective genes. The colours represent upregulation (dark blue 1-fold upregulation) and downregulation (dark red 1-fold downregulation) of genes in cells shifted to a medium containing 0.5 % gallic acid and 1 % glucose as the carbon sources compared to cells grown with 1 % glucose. Metabolites or enzymes occurring multiple times in the metabolic network are decorated with a clone marker (e. g. NAD^+) [produced using VANTED – (Junker *et al.*, 2012, Rohn *et al.*, 2012)].

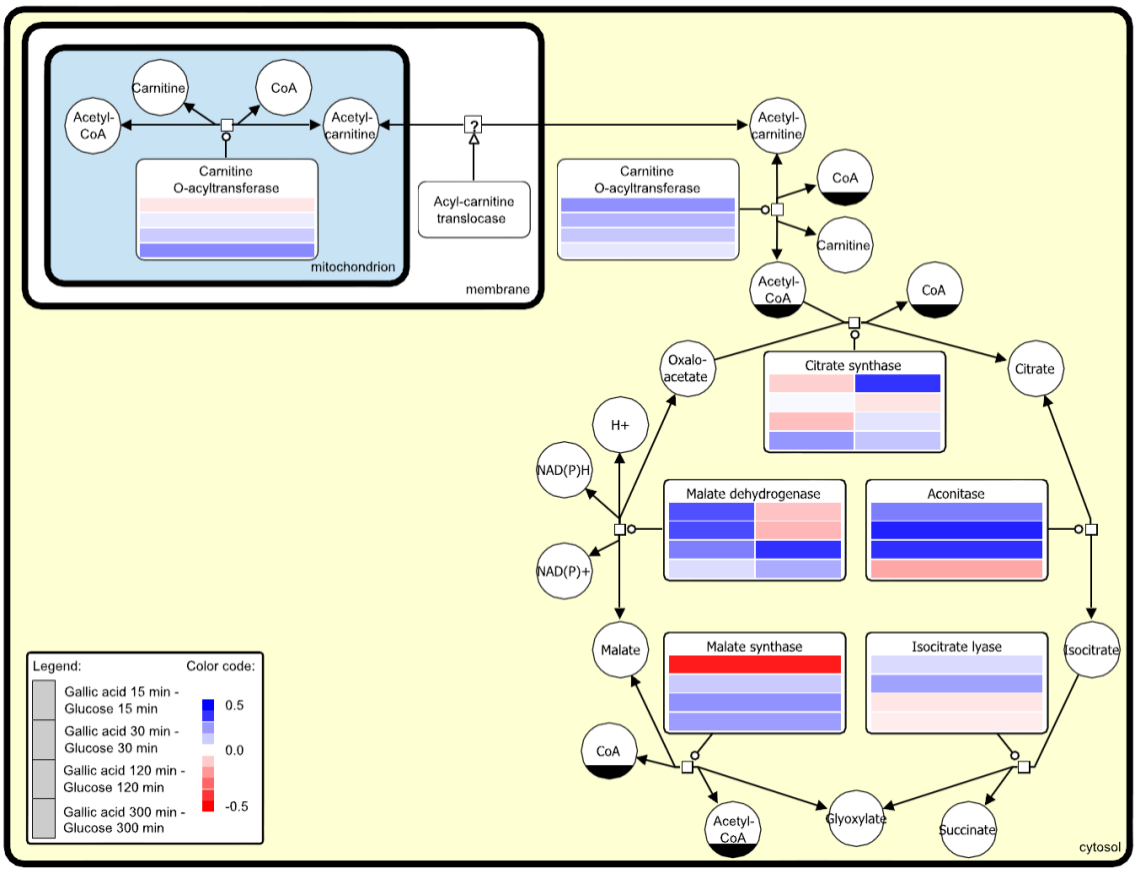

Figure 34 Key compounds of the glyoxylate cycle - microarray studies of gene regulation by gallic acid.
The Systems Biology Graphical Notation (SBGN) of the metabolic network depicts reactions catalysed by the corresponding enzymes (rectangular square). Enzymes are enriched with color-coded log2 fold change values of time resolved expression data of the respective genes. The colours represent upregulation (dark blue 0.5-fold upregulation) and downregulation (dark red 0.5-fold downregulation) of genes in cells shifted to a medium containing 0.5 % gallic acid and 1 % glucose as the carbon sources compared to cells grown with 1 % glucose. Metabolites or enzymes occurring multiple times in the metabolic network are decorated with a clone marker (e. g. NAD^+) [graph produced with VANTED – (Junker *et al.*, 2012, Rohn *et al.*, 2012)].

4.2.11 Role of Agdc1p in *A. adeninivorans* on metabolizing gallic acid

The present work has revealed that Agdc1p is an enzyme expressed by a gallic acid inducible gene. To analyse the *in vivo* role, three *A. adeninivorans* strains G1212/YRC102, G1212/YRC102-AYNI1-AGDC1-6H and G1234 [Δ*agdc1*] were cultivated for up to 146 h on YMM-$NaNO_3$ supplemented with 2 % (w/v) glucose, 2 % (w/v) gallic acid or 1 % (w/v) gallic acid plus 1 % (w/v) glucose at 30 °C. Following, dcw as well as gallic acid decarboxylase activity and yield [Y(P/X)] (Y is yield coefficient, P is enzyme formation in U, X is biomass in g) were determined. The deletion of *AGDC1* caused growth inhibition of *A. adeninivorans* G1234 [Δ*agdc1*] when this strain was grown

in culture medium containing gallic acid (**Figure 36 B**). Crude extract of this strain lacked gallic acid decarboxylase activity under all cultivation conditions tested. As a consequence, gallic acid concentrations in the culture medium remained unaltered during the entire cultivation which was verified by additional metabolite analysis. If, however, protocatechuic acid was supplied as the sole carbon source, its concentration rapidly declined proving that *A. adeninivorans* G1234 [Δ*agdc1*] can metabolize this alternative carbon source (**Figure 35**).

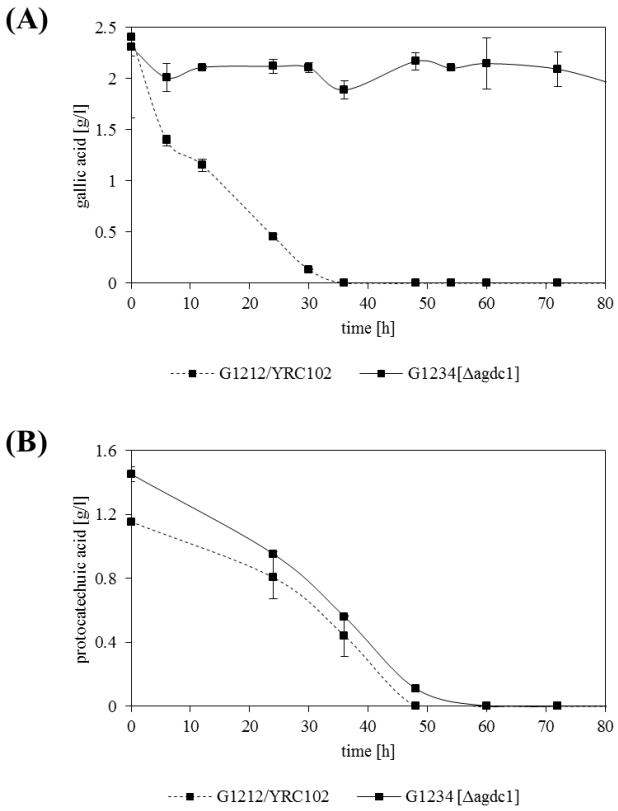

Figure 35 GC-MS analysis of supernatant from cultures of *A. adeninivorans* control strain G1212/YRC102 and deletion mutant G1234 [Δ*agdc1*].
Cells were grown in YMM-$NaNO_3$ supplemented with 0.25 % of **(A)** gallic acid or **(B)** protocatechuic as sole carbon source.

When the control strain *A. adeninivorans* G1212/YRC102 was grown on gallic acid as the sole carbon source, gallic acid decarboxylase was synthesized and accumulated in the cell. In the presence of glucose, the Agdc1 activity in the overexpression strain *A. adeninivorans* G1212/YRC102-AYNI1-AGDC1-6H reached 1,064 U/l and 97.5 U/g between 96 – 146 h of cultivation. An even higher enzyme activity of 1,617 U/l and 148 U/g was detected when this strain was cultivated on a mixture of gallic acid and glucose (**Figure 36 I**). Under the same conditions enzyme activity in the control strain

G1212/YRC102 reached no more than 446.7 U/l and 37.5 U/g. However, the overexpression of *AGDC1* did not significantly improve cell growth on gallic acid (**Figure 36 F**).

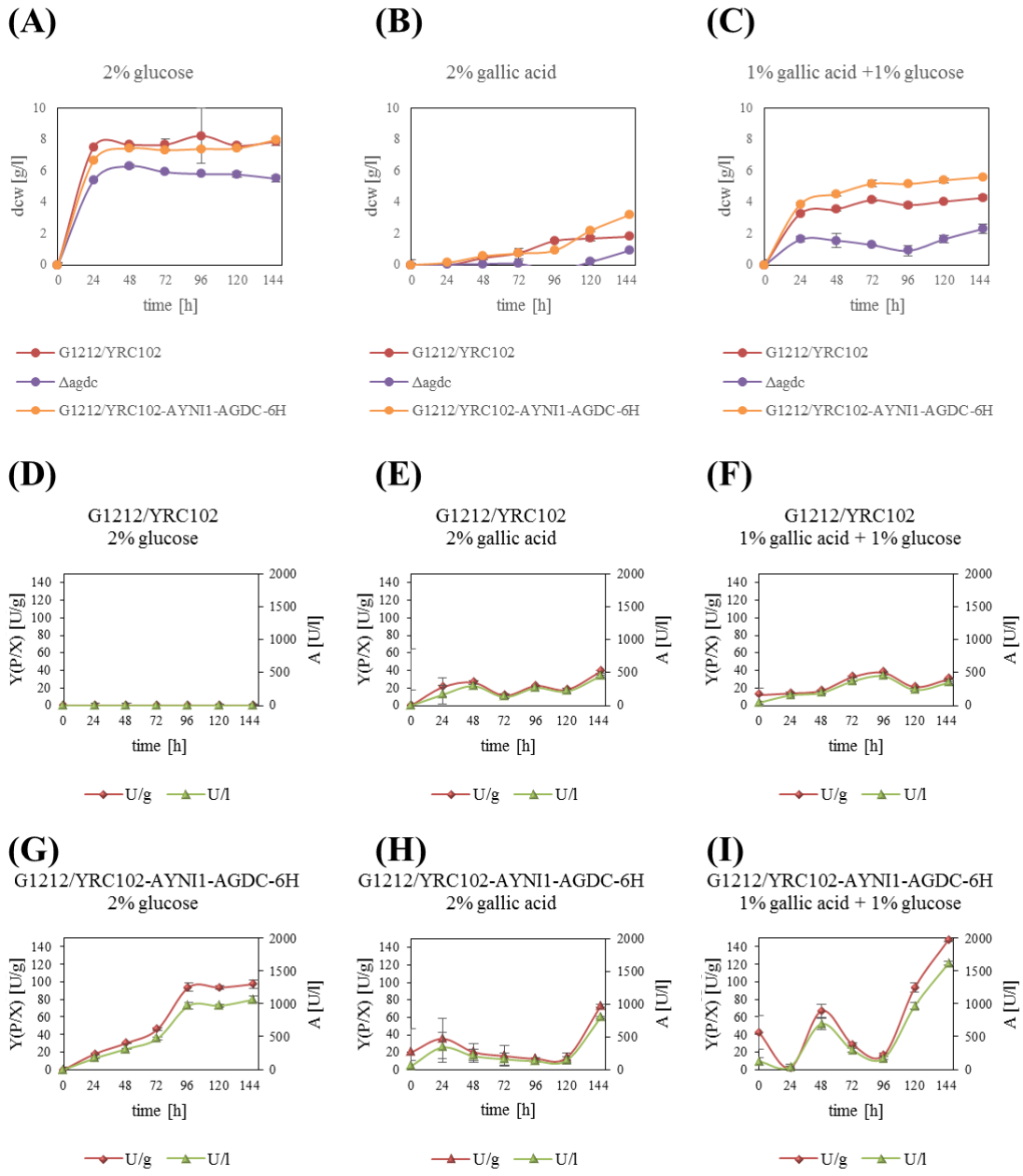

Figure 36 Time course experiment of *A. adeninivorans* G1212/YRC102, G1212/YRC102-AYNI1-AGDC1-6H and G1234 [Δ*agdc1*].
Influence of carbon source on the dry cell weight (**A-C**) as well as Agdc1-6hp activity and yield [Y(P/X)] Y - yield coefficient, P - enzyme formation in U, X - biomass in g. (**D-I**) with cultivation in YMM-$NaNO_3$ with 2 % glucose, 2 % gallic acid or 1 % glucose plus 1 % gallic acid as carbon sources.

4.2.12 Role of Agdc1p in *A. adeninivorans* on metabolizing hydroxylated aromatic acids

To demonstrate that the main role of gallic acid decarboxylase in *A. adeninivorans* is to degrade gallic acid, *A. adeninivorans* strains G1212/YRC102 and G1234 [Δ*agdc1*] were cultivated for 48 h on YMM-$NaNO_3$ supplemented with 0.2 % (w/v) of different hydroxylated aromatic acids (listed in **Figure 37**) as their sole source of carbon.

(A)

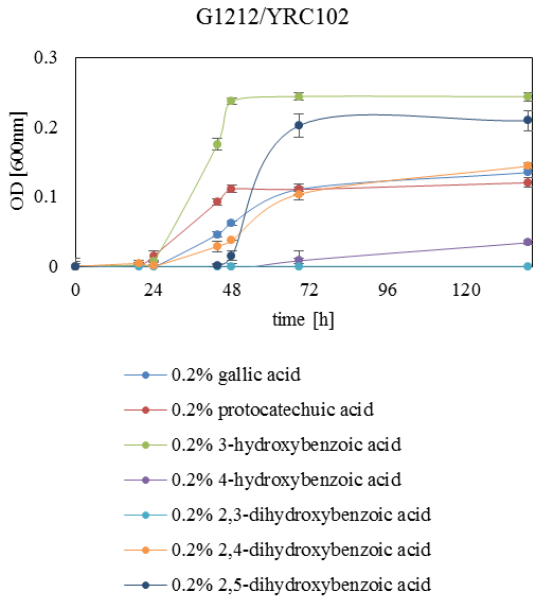

(B)

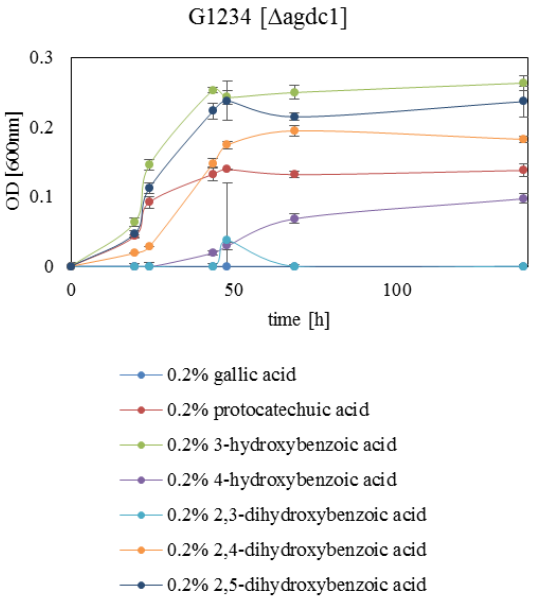

(C)

	Cell Growth	
Carbon source (0.2%)	G1212/YIC102	G1234 [Δ*agdc1*]
gallic acid	yes	**no**
protocatechuic acid	yes	yes
3-hydroxybenzoic acid	yes	yes
4-hydroxybenzoic acid	yes	yes
2,3-dihydroxybenzoic acid	**no**	**no**
2,4-dihydroxybenzoic acid	yes	yes
2,5-dihydroxybenzoic acid	yes	yes

Figure *37* Growth behaviour of *A. adeninivorans* strains, feeding with hydroxylated aromatic acids as sole source for carbon and energy.
(A) *A. adeninivorans* G1212/YRC102; **(B)** *A. adeninivorans* G1234 [Δ*agdc1*]; **(C)** Summarization of growth behaviour. Results show average of three separate experiments.

Samples for metabolite analysis were collected at 0, 30 and 48 h of cultivation. The results showed that with the exception of 2,3-dihydroxybenzoic acid *A. adeninivorans* control strain G1212/YRC102 was able to grow on all carbon sources supplied, i.e. gallic acid, protocatechuic acid, 3-hydroxybenzoic acid, 4-hydroxybenzoic acid, 2,4-dihydroxybenzoic acid and 2,5-dihydroxybenzoic acid, with different adaptation times. In contrast to this, the deletion mutant G1234 [Δ*agdc1*] was not only unable to grow on 2,3-dihydroxybenzoic acid but also failed on gallic acid as carbon source. In all other cases, the adaptation phase of *A. adeninivorans* G1234 [Δ*agdc1*] was shorter and cells grew better compared to the control strain. For both strains, optimal growth was observed with 3-hydroxybenzoic acid and minimum growth with 4-hydroxybenzoic acid (**Figure 37**).

4.2.13 Metabolic conversion of gallic acid and protocatechuic acid by *A. adeninivorans*

A. adeninivorans strains G1212/YRC102 and G1212/YRC102-AYNI1-AGDC1-6H were grown on gallic acid plus glucose as carbon source. Analysis of the medium by GS-MS revealed complete consumption of gallic acid within 48 h of cultivation in the control strain and within 96 h in the G1212/YRC102-AYNI1-AGDC1-6H strain. Pyrogallol was the only product detected in the medium during the metabolic degradation of gallic acid. Maximum extracellular pyrogallol concentration was reached after 24 h incubation. The yield, calculated as the % of gallic acid converted into pyrogallol, was approximately 2.7 % for the control and 2.2 % for the overexpression strain (**Figure 38**).

If, however, gallic acid was replaced by the same amount of protocatechuic acid, the products detected in the culture medium were catechol, *cis,cis*-muconic acid and trace amounts of 3-hydroxybenzoic acid, 4-hydroxybenzoic acid, 1,4-dihydroxybenzene and 1,2,4-benzentriol (**Figure 39**). Both strains completely degraded protocatechuic acid within 48 h. The first metabolite detected was catechol which reached a maximum concentration after 24 h of cultivation (**Figure 39 A, B**). After 24 h, *cis,cis*-muconic acid appeared, reaching a peak at 48 h in strain G1212/YRC102 strain and after 72 h in strain G1212/YRC102-AYNI1-AGDC1-6H. The yield, calculated as the % of protocatechuic acid converted into *cis,cis*-muconic acid was 42.5 % for G1212/YRC102 and 71.2 % for G1212/YRC102-AYNI1-AGDC1-6H (**Figure 39 B**).

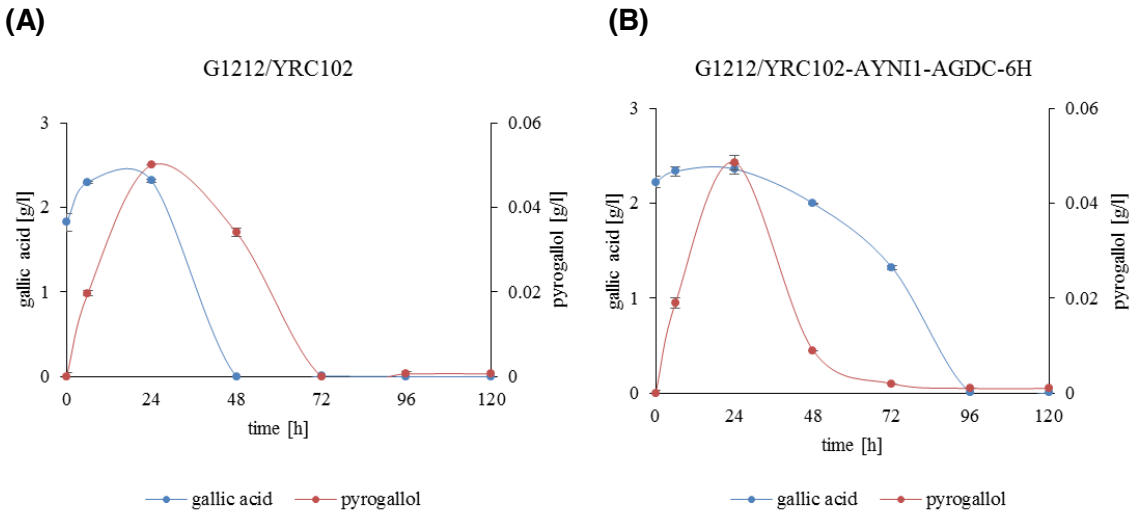

Figure 38 GC-MS analysis of substrate – product conversion during cultivation of *A. adeninivorans* on gallic acid.
Gallic acid degradation (blue line) and pyrogallol production (red line) by **(A)** *A. adeninivorans* G1212/YRC102 and **(B)** G1212/YRC102-AYNI1-AGDC1-6H cultivated on YMM-$NaNO_3$ with 0.25 % gallic acid plus 0.5 % glucose.

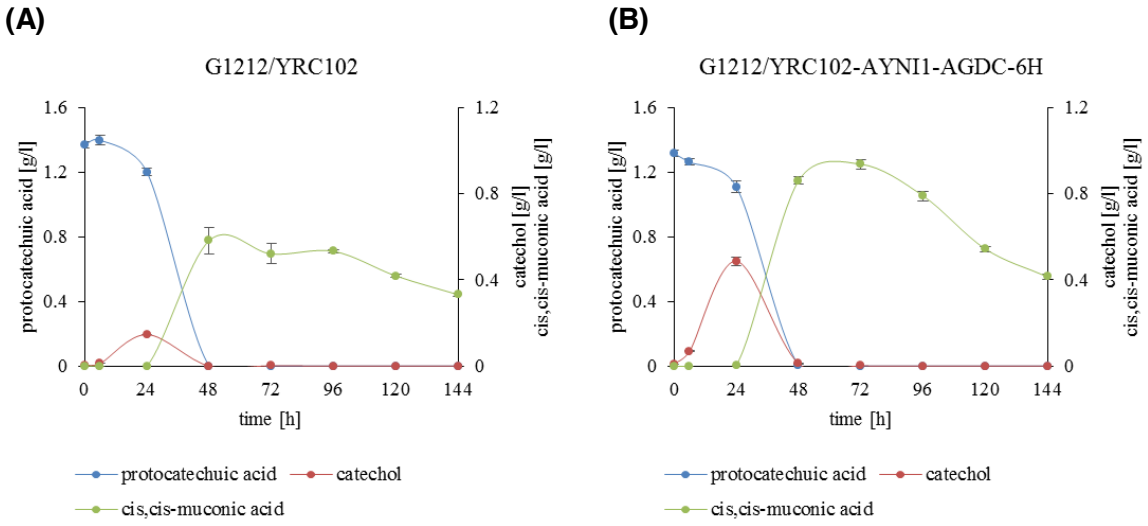

Figure 39 GC-MS analysis of substrate – product conversion during cultivation of *A. adeninivorans* on protocatechuic acid.
Substrate and product accumulation during the degradation of protocatechuic acid by *A. adeninivorans* **(A)** G1212/YRC102 and **(B)** G1212/YRC102-AYNI1-AGDC1-6H. Cells were cultivated on YMM-$NaNO_3$ with 0.25 % protocatechuic acid plus 0.5 % glucose.

4.3 *Arxula* catechol-1,2-dioxygenase 1, Acdo1p

4.3.1 Identification of an *A. adeninivorans ACDO1* gene encoding for catechol-1,2-dioxygenase (Acdo1p)

A putative *catechol-1,2-dioxygease* gene (ARAD1D17798g) was annotated in the genome of *A. adeninivorans* LS3. The gene, *Arxula catechol-1,2-dioxygenase 1* (*ACDO1*), is localized on chromosome *Arad1D*, position 1512070 to 1513071. The 1005 bp open reading frame contains no introns and encodes a protein with 335 amino acids. The predicted subunit molecular mass of Agdc1p is 37.76 kDa. Protein analysis according to the SignalP program (version 4.1; http://www.cbs.dtu.dk/services/SignalP/) predicts the absence of a secretion signal sequence.

(A)

```
Acdo1p -----------------MAGSGLEGYEATSKEDMWDRFFTTQAVEANSKGKDPRMTFIISRLIPHLHDFAREVRLT 59
P86029 ------------------------------------MSQAFTESVKTSLGPNATPRAKKLIASLVQHVHDFARENHLT 42
P07773 MEVKIFNTQDVQDFLRV-AS-----------------------GLEQEGGNPRVKQIIHRVLSDLYKAIEDLNIT 51
O33948 MSIKVFGTKEVQDLLKA-AT-----------------------NLEGKGGNARSKQIVHRLLSDLFKAIDDLDIT 51
O33950 -----MNKQAIDALLQKIND------------------------SAINEGNPRTKQIVNRIVRDLFYTIEDLDVQ 46
Q43984 ---MMMNRQQIDSLVQQMNV-----------------------ATATGEVNLRVQQIVVRLLGDLFQAIEDLNMS 49
P96984 ----------MTDIDTAVATAHASGNAAT------DK-FK--TARVSCDTSPERAAAIYRDVLSALGEVIHRHEVT 57
P95607 ----------------------GSGSAAT------DK-FK--AERATADTSPERLAAIAKDALGALNDVILKHGVT 45
Q8GAY6 MSVKVFDTKEVQDLLKA-AA-----------------------NMGSEDGSARAKQIVNRLLGDLFKAIDDLDMT 51
A7LBQ4 ---------PMFSLLHKVAG------------------------LDHAEGNPRFKQIILRVLQDTARLVEDLEIT 42
                                                     *   :    :          :

Acdo1p FEEWQLGLKFLVDVGKTCTDVRHEFILLSDVLGLSVLVDAMSHVK-----AKNATPGTLLGPFHTEDANVFEQGEC 130
P86029 TEDWLWGVDFINRIGQMSDSRRNEGILVCDIIGLETLVDALTNES----EQSNHTSSAILGPFYLPDSPVYPNGGS 114
P07773 SDEYWAGVAYLNQLGA-----NQEAGLLSPGLGFDHYLDMRMDAEDAALGIENATPRTIEGPLYVAGAPESVGYAR 122
O33948 PDEVWAGVNYLNKLGQ-----DGEATLLAAGSGLEKYLDIRLDAADKAEGIEGGTPRTIEGPLYVAGATVHDGVSK 122
O33950 PDEFWTALNYLGDAGR-----SGELGLLAAGLGFEHFLDLRMDEAEAKAGVEGGTPRTIEGPLYVAGAPVSDGHAR 117
Q43984 QTELWKGLEYLTDAGQ-----ANELGLLAAGLGLEHYLDLRADEADAKAGITGGTPRTIEGPLYVAGAPESVGFAR 120
P96984 YDEYRVLKQWMIDVGE-----YGEWPLW-----LDVFVEHQVEDVNYSRNGLAGTKGSIEGPYYVPDAPQLPAVCT 123
P95607 YPEYRVFKQWLIDVGE-----GGEWPLF-----LDVFIEHSVEEVLA--RSRKGTMGSIEGPYYIENSPELPSKCT 109
Q8GAY6 PDEIWAGVHYFNKLGQ-----DGEAALLAAGLGLEKFLDIRMDAEDKAAEITGGTPRTIEGPLYVAGAPVRDGISK 122
A7LBQ4 EDEFWHAIDYLNRLGG-----RNEAGLLAAGLGIEHFLDLLQDAKDAEAGLGGGTPRTIEGPLYVAGAPLAQGEAR 113
         :      ::   *        *  *      :.  ::   .           *  :: ** :  .:

Acdo1p IVSKENEGD-P-LTLYGTVRDIHGNPIPNVSIDIWETDETGHYDTQYDDRNGP--DYRGIIYTDAEGKYLIKGIVP 202
P86029 IVQKAIPTD-VKCFVRGKVTDTEGKPLGGAQLEVWQCNSAGFYSQQAD-HDGPEFNLRGTFITDDEGNYSFECLRP 188
P07773 MDDGSDPNG-HTLILHGTIFDADGKPLPNAKVEIWHANTKGFYSHFDPTGEQQAFNMRRSIITDENGQYRVRTILP 197
O33948 IDINPDEDA-GPLVIHGTVTGPDGKPVAGAVVECWHANSKGFYSHFDPTGAQSDFNLRGAVKTGADGKYEFRTLMP 197
O33950 LDDGTDPGQ--TLVMRGRVFGEDGKPLANALVEVWHANHLGNYSYFDK--SQPAFNLRRSIRTDAEGKYSFRSVVP 189
Q43984 MDDGSESAHVDALIIEGNVTDTAGQIIPNAKVEIWHANSLGNYSFFDK--SQSAFNLRRSIFTDTQGQYIAQTTMP 194
P96984 MPMREQDRRSTPLVFSGQVTDLDGNGLGGATVELWHADEDGFYSQFAP--NIPEWNLRATIVCDDEGRYEITTIQP 197
P95607 LPMREEDEKITPLVFSGQVTDLDGNGLAGAKVELWHADNDGYYSQFAP--HLPEWNLRGTIIADEEGRYEITTIQP 183
Q8GAY6 IDVNPDEGA-GPLVIRGTVTGPDGKPVANALVECWHANSKGFYSHFDPTGAQSEFNLRGAVSTDVDGKYEFRTLMP 197
A7LBQ4 MDDGTDPGV--VMFLQGQVFDADGKPLAGATVDLWHANTQGTYSYFDS--TQSEYNLRRRIITDAEGRYRARSIVP 185
       :             . * : .  *: : .. :: *. :  * *.          : *  .  . :*.*      *

Acdo1p VSYPIPHDGPVGRFLTYVGRHPYRPAHIHFKLEKEGYDNLITGLYMKGDKYSGEDAVFGEKKELTVEPKKFGDQKL 278
P86029 TSYPIPYDGPAGDLLKIMDRHPNRPSHIHWRVSHPGYHTLITQIYDAECPYTNNDSVYAVKDDIIVHFEKVDNK-- 262
P07773 AGYGCPPEGPTQQLLNQLGRHGNRPAHIHYFVSADGHRKLTTQINVAGDPYTYDDFAYATREGLVVDAVEHTDPEA 273
O33948 VGYGCPPQGATQQLLNVLGRHGNRPAHVHFFVSSDSARKLTTQFNIEGDPLIWDDFAYATREELIPPVTEKKGGTA 273
O33950 VGYSVPPQGQTQLLLDQLGRHGHRPAHIHFFVSAPGFRKLTTQINIDGDPYLWDDFAFATRDGLVPAVRQAEVRKA 265
Q43984 VGYGCPPEGTTQALLNLLGRHGNRPSHVHYFVSAPGYRKLTTQFNIEGDKYLWDDFAFATRDGLIATALDVTDLAK 270
P96984 APYQIPHDGPTGWFIESHGGHPWRPAHLHLMVKAPGRLPITTQLYFRGGDWVETDVATAVKPELVLDPVRGADGVN 273
P95607 APYQIPTDGPTGQFIEAQNGHPWRPAHLHLIVSAPGKESVTTQLYFKGGEWIDSDVASATKPELILDPKTGDDGKN 259
Q8GAY6 VGYGCPPHGATQQLLNVLARHGNRPAHVHFFVTTDKYRKLTTQINIEGDPLIWDDFAYATREDLIPHVVEKTGGTP 273
A7LBQ4 SGYGCEPAGPTQECLDLLGRHGQRPAHVHFFISAPGFRHLTTQINFEGDKYLWDDFAYATRDGLIGELRFVEDAAA 261
         *     * .   :     *  **:*:*  :       : * :          * . . :  :

Acdo1p A-EKYMSNADDYFINFDITLMSTKESMELFDAQSRRDLKTLGIDAKVVNGVPIADLD 334
P86029 --DKDLVGKVEYKLDYDISLATESSIQEARAAAKARQDAEIKL-------------- 303
P07773 -IKANDVEGPFAEMVFDLKLTRLVDGVDNQVVDRPRLAV----------------- 311
O33948 -LGL--KADTYKDIEFNLTLTSLVKGKDNQVVHRLRAEVAA---------------- 311
O33950 NRTAWTVSSR------------------------------------------------ 275
Q43984 -IKQYNLNKAFKHIKFNFQLVQDADQVPLQRLIV----VE----------------- 305
P96984 ------------RVAYDFALDPTP------------------------------- 285
P95607 ------------YVTYNFVLDPA--------------------------------- 270
Q8GAY6 -LGM--KADTYKEIEFNIELTPLVHGKDNQLVSRLRASVTA---------------- 311
A7LBQ4 ARDRGVQGERFAELAFDFHLQAAAAPEAEARSHRPRALQEG---------------- 302
```

(B)

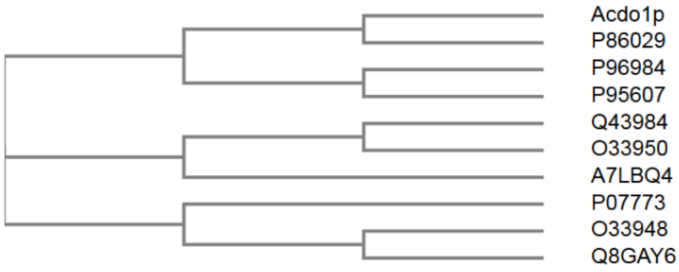

Figure 40 Sequence alignment and phylogenetic tree of catechol-1,2-dioxygenases.
(A) Acdo1p sequence was aligned to predicted catechol-1,2-dioxygenase amino acid sequences of *C. albicans* (P86029), *A. baylyi* (P07773), *A. lwoffii* (O33948), *A. lwoffii* (O33950), *A. guillouiae* (Q43984), *R. erythropolis* (P96984), *R. opacus* (P95607), *Burkholderia* sp. (Q8GAY6), *P. putida* (A7LBQ4) from UniProt database. Alignment was done using ClustalOmega software (http://www.ebi.ac.uk/Tools/msa/clustalo/). Residues marked with an asterisk (*) are identical in all sequences in the alignment. A colon (:) indicates conserved substitutions and a dot (.) indicates semi-conserved substitutions. The predicted catalytic domain is highlight in yellow and metal binding sites in green. **(B)** The phylogenetic tree was constructed by neighbor joining method of Acdo1p to selected catechol-1,2-dioxygenase amino acid sequences without distance corrections.

Sequence alignment of Acdo1p with known catechol-1,2-dioxygenases revealed multiple conserved domains that are fundamental for enzyme catalytic activity and structure, including the highly conserved metal binding sites Tyr171, Tyr205, His229, His231 (**Figure 40 A**). A phylogenetic tree between Acdo1p and catechol-1,2-dioxygenase protein sequences from bacteria and yeast was made using the Neighbor-Joining method (**Figure 40 B)**.

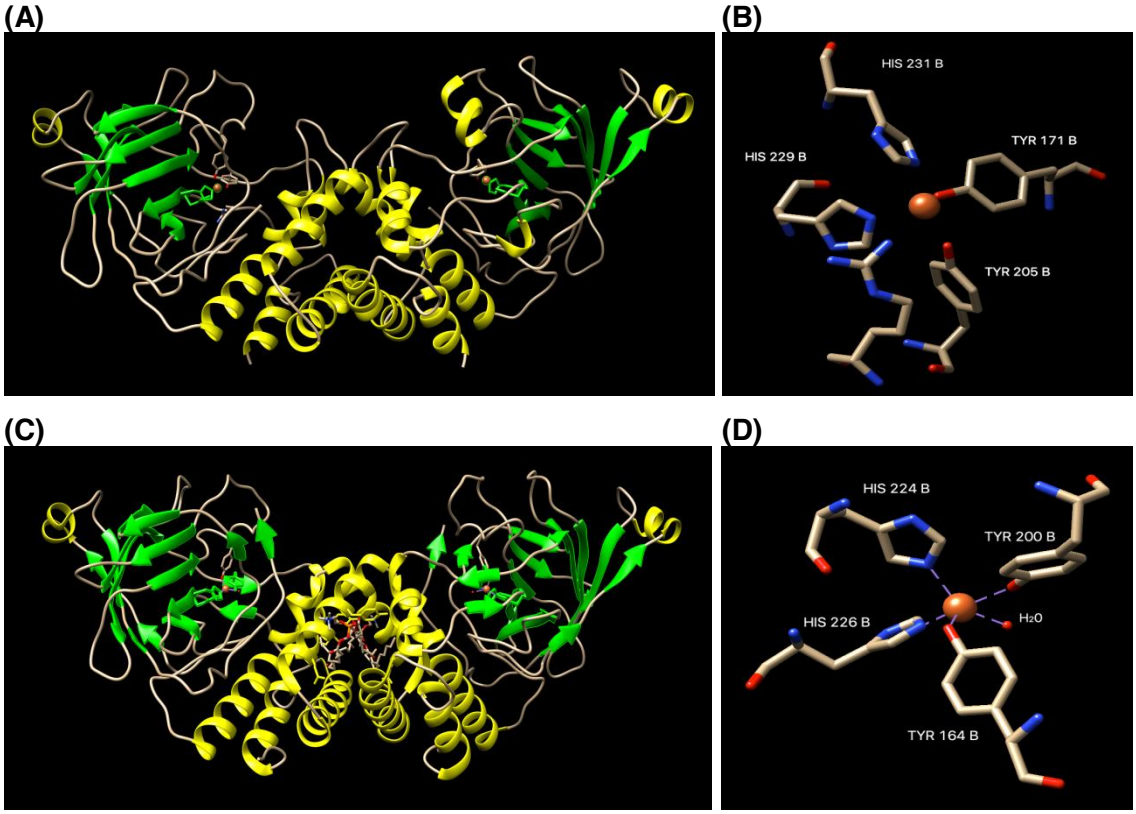

Figure 41 Structure prediction of Acdo1p.
(A) Structure model of catechol-1,2-dioxygenase from *A. adeninivorans*. **(B)** Amino acid residues predicted to be involved in ferric ions coordination. **(C)** Structure model of catechol-1,2-dioxygenase from *Acinetobacter* sp. **(D)** Amino acid residues involved in ferric ions coordination of catechol-1,2-dioxygenase from *Acinetobacter* sp.. Yellow = helix domain; green = strand domain; orange = ion domain.

Crystallographic studies have shown that catechol-1,2-dioxygenases are homodimers which incorporate a non-heme ferric iron atom (Fe^{3+}) as cofactor. A catecholate substrate binds to the Fe atom by means of the deprotonated hydroxyl groups. The iron abstracts an electron to produce a radical on the substrate. This then allows the reaction with dioxygen and a subsequent intradiol cleavage to occur.

Acdo1p shows 24% sequence identity with catechol-1,2-dioxygenase from *Acinetobacter* sp. including 84 identical and 109 similar positions (**Figure 40 A**). Based on the crystal structure of the latter enzyme (Vetting *et al.*(2000), a protein model of Acdo1p was prepared using UCSF Chimera Software (chimera-1.11.2-mac64.dmg) and SWISS-MODEL (https://swissmodel.expasy.org/interactive#structure) (**Figure 41**).

4.3.2 Generation of an Acdo1-6hp producing yeast strain

A. adeninivorans G1212 [Δ*trp1*] was used to construct an Acdo1-6hp producing yeast strain. A HisTag encoding sequence was fused to the 3´-end of the ORF of the *ACDO1* gene under control of the nitrate inducible *AYNI1* promoter (*A. adeninivorans* nitrate reductase promoter). Cassettes with the *ACDO1* expression module (YRC102-AYNI1-ACDO1-6H, YIC102-AYNI1-ACDO1-6H (**Figure 42**) and controls (YRC102, YIC102) were prepared as described in 3.4.3.4. After genome integration, selected clones (YICs and YRCs) were passaged to establish high plasmid stability. After cultivation in YMM-glucose-$NaNO_3$ at 30 °C for 48 h, cells were harvested and screened for catechol-1,2-dioxygenase activity. This activity was present in all stabilized *A. adeninivorans* G1212/YRC102-AYNI1-ACDO1-6H and G1212/YIC102-AYNI1-ACDO1-6H strains. The best transgenic strains belonged to the genome integrated YICs (**Figure 43**).

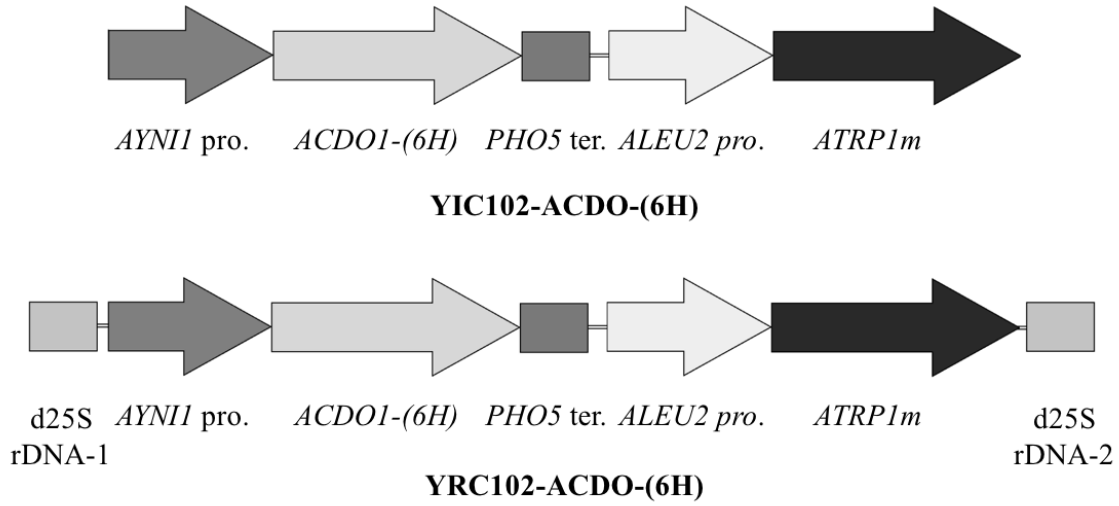

Figure 42 Physical map of the *ACDO1* yeast integrative expression cassettes.
The cassettes contain one copy of the expression module: *AYNI1* promoter-*ACDO*-6H-*PHO5*-terminator, selection marker *ATRP1m* together with the *ALEU2* promoter.

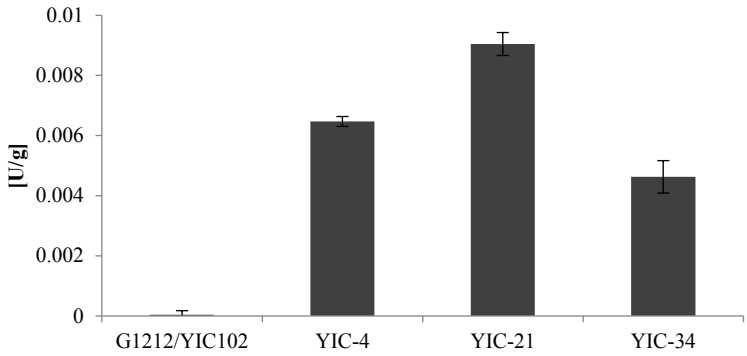

Figure 43 Acdo1 enzyme activity in control (G1212/YIC102) and most productive transformant strains.

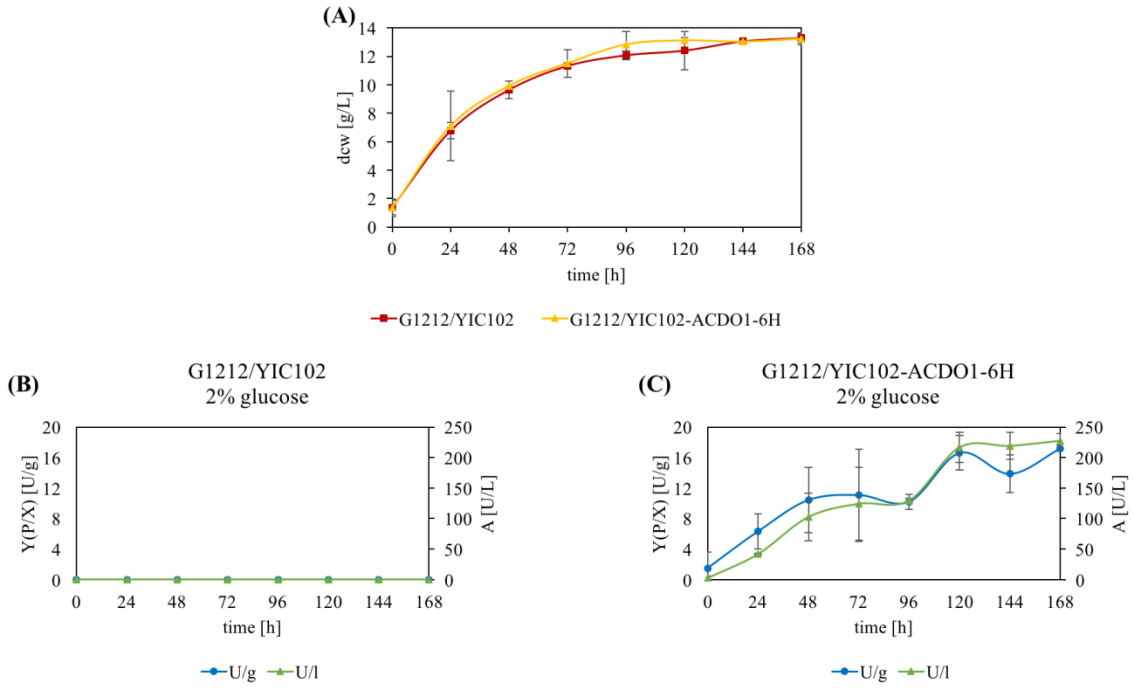

Figure 44 Time-course analysis of catechol-1,2-dioxygenase activity in *A. adeninivorans* control strain and strain with overexpression of ACDO1-6H.
The cells were grown on YMM-glucose-$NaNO_3$ in shake flasks at 30 °C for 168 h. Measurement of cells growth **(A)**. Intracellular Acdo1-6hp activity (triangles) detected with protocatechuic acid as substrate and calculated yield [Y(P/X)] (circles) for G1212/YIC102 **(B)** as well as for G1212/YIC102-ACDO1-6H **(C)** Measurements were done in triplicate and error bars represent the standard deviation.

A. adeninivorans strains G1212/YIC102 and G1212/YIC102-AYNI1-ACDO1-6H were cultivated in YMM-glucose-$NaNO_3$ at 30 °C and 180 rpm for 168 h. Dry cell weight (dcw), catechol-1,2-dioxygenase activity with catechol as substrate and yield [Y(P/X)] (Y - yield coefficient, P - enzyme formation in U, X - biomass in g) were determined each 24 h. The

experiment was performed in triplicate. Catechol-1,2-dioxygenase activity was detectable in the selected transgenic strain (*A. adeninivorans* G1212/YIC102-AYNI1-ACDO1-6H) but not in the control strain *A. adeninivorans* G1212/YIC102 when glucose served as sole carbon source. Both yeast strains reached a maximum dcw after 72 h of cultivation and then remained constant until the end of the experiment. Transgenic strain *A. adeninivorans* G1212/YIC102-AYNI1-ACDO1-6H achieved its maximum enzyme activity of ≈ 220 U/l and ≈ 17 U/g dcw after 120 h (**Figure 44**).

4.3.3 Generation of Acdo1-eGFP producing yeast strain

A. adeninivorans G1212 [Δ*trp1*] served as a host strain for overexpression of *ACDO1* gene containing an eGFP encoding sequence fused to the 3´-end of the ORF under control of the *TEF1* promoter (translation elongation factor 1). The cassette with the *ACDO1* expression module (YRC102-TEF1-ACDO1-eGFP) (**Figure 45**) and control (YRC102, YIC102) were prepared as described in 3.4.2.. After genome integration clones were passaged to establish high plasmid stability.

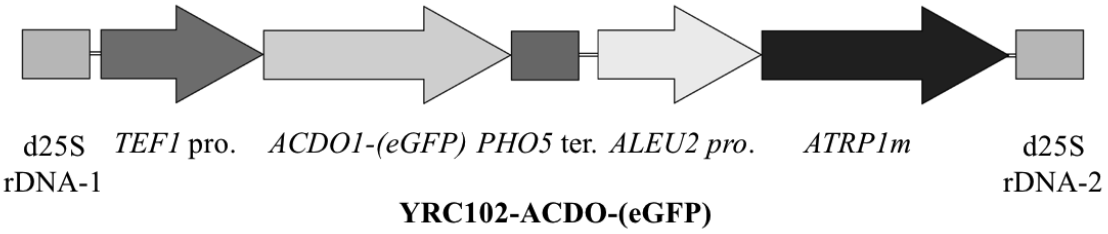

Figure 45 Physical map of the *ACDO1-eGFP* yeast integrative expression cassettes.
The cassettes contain one copy of the expression module: *TEF1* promoter-ACDO-eGFP-PHO5-terminator, selection marker *ATRP1m* together with the *ALEU2* promoter.

4.3.4 Cellular localisation of Acdo1-eGFP

After cultivation in YMM-glucose-$NaNO_3$ at 30 °C for 24 h, cells were screened by fluorescence microscopy for the presence of GFP signals. GFP fluorescence was only found in the cytosol of cells containing the YRC102-TEF1-ACDO1-eGFP expression cassette (**Figure 46**).

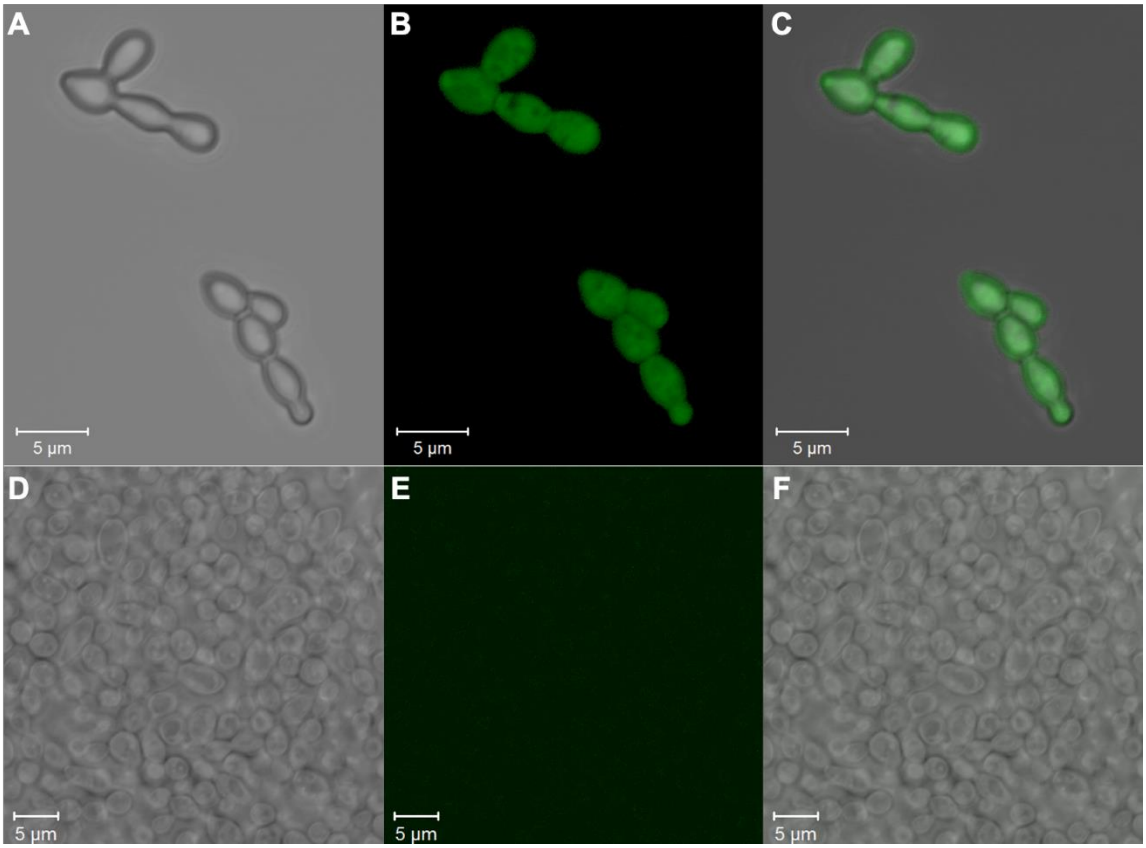

Figure 46 Subcellular localization of Acdo1-eGFP.
CLSM analysis shows a cytosolic distribution of GFP signals in strain G1212/YRC102-TEF1-AGDC1-eGFP **(A-C)** but not in strain *A. adeninivorans* strain G1212/YRC102 **(D-F)**.Pictures made under: bright light **(A,D)**, fluorescence filter **(B,E),** bright light and fluorescence filter **(C,F)**.

4.3.5 Generation of Δ*acdo1* gene disruption mutant strain

To analyse the function of *ACDO1*, the gene was deleted by homologous recombination using *A. adeninivorans* G1212 [Δ*trp1*] as a host strain. To avoid affecting any possible nearby genes, the deletion mutant cassette was constructed using 381 bp of upstream homology fragment + 142 bp of the 5' gene coding sequence and 158 bp of downstream homology fragment + 361 bp of the 3' gene coding sequence (**Figure 47**). After the selection marker indicated integration of the cassette, the correct integration locus was verified by PCR using primers (listed in **Table 21**) amplifying part of the integrated marker and an adjacent area of genomic DNA (**Figure 48**). The strain with a correctly integrated deletion cassette was labelled G1235 [Δ*acdo1*].

(A)

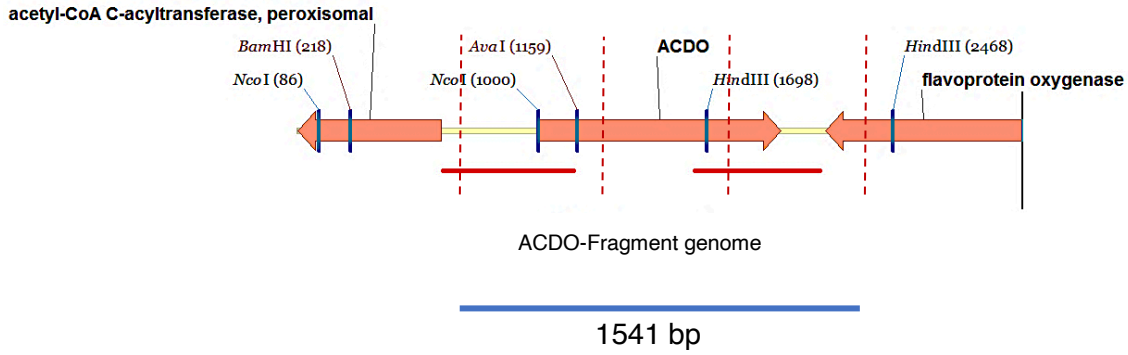

(B)

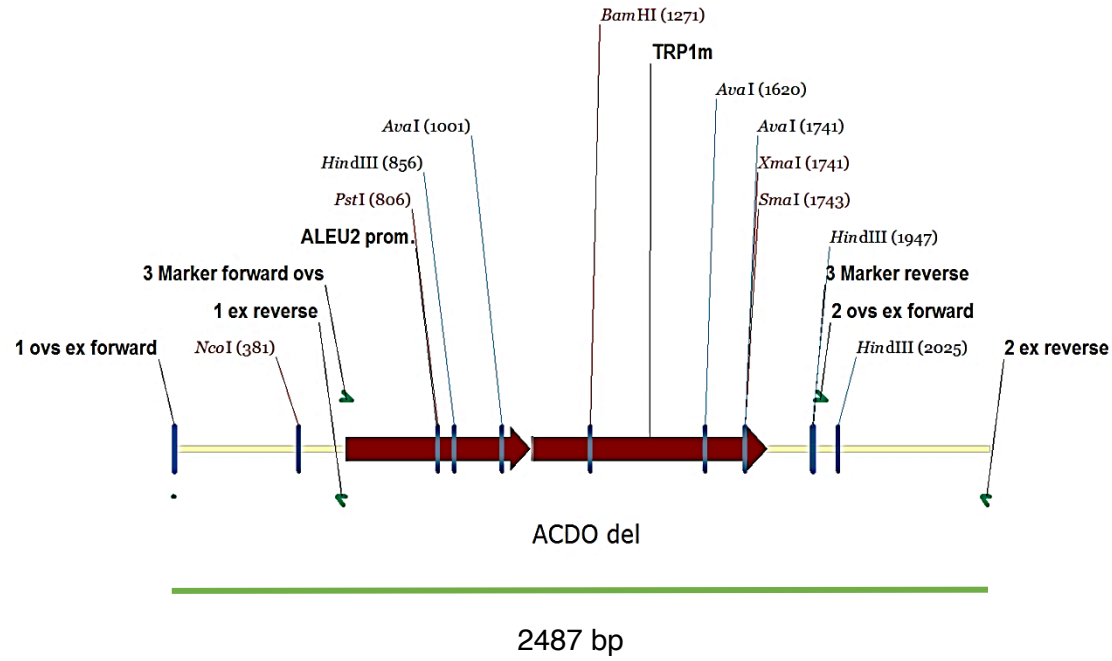

Figure 47 Design of *ACDO1* gene deletion cassettes.
(A) DNA fragment used for construction of *ACDO1* deletion cassette. To avoid affecting putative nearby genes, deletion was restricted to a 995 bp fragment of *ACDO1*: left red line = 381 bp upstream homology fragment + 142 bp of the 5' gene fragment; right red line = 158 bp downstream homology fragment + 361 bp of the 3' gene fragment. Blue line = fragments obtained by PCR after unsuccessful deletion of *ACDO1*. **(B)** Deletion mutant cassette. Yellow line = 523 bp upstream and 519 bp downstream homology fragments; red arrows = *ALEU2* promoter; *ATRP1* = tryptophan marker; green line = fragment obtained by PCR after successful deletion of *ACDO1*.

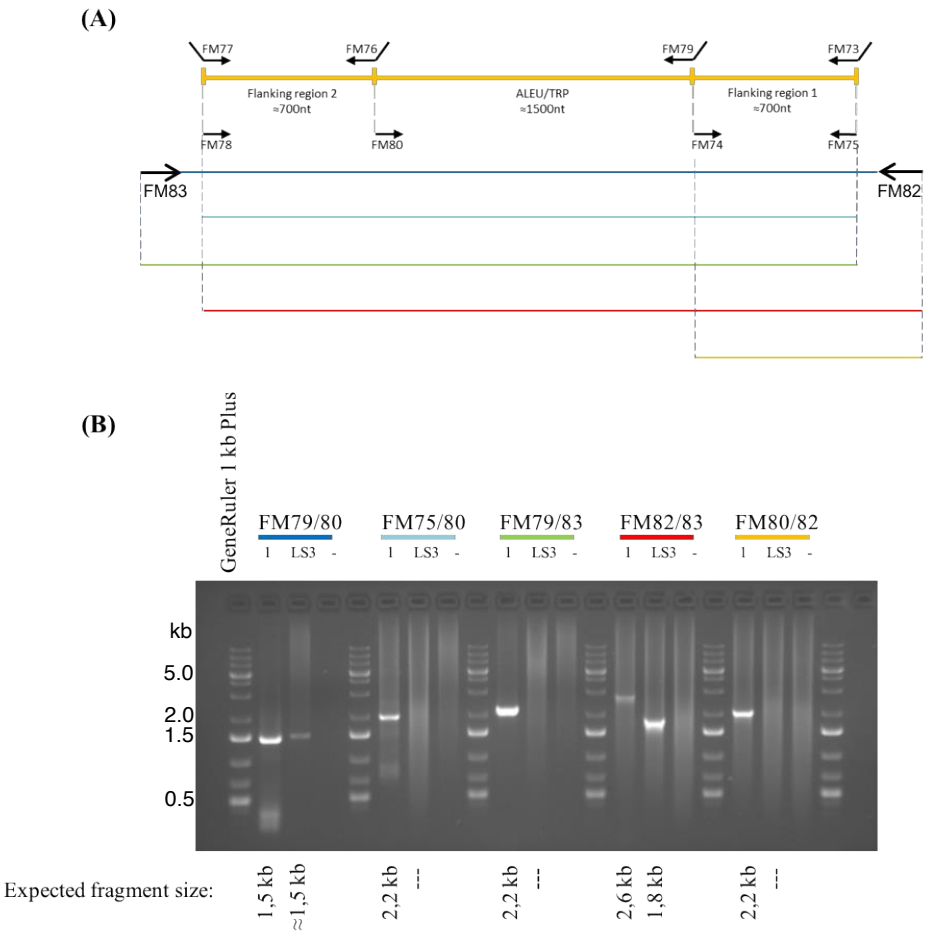

Figure 48 Verification of correct integration of *ACDO1* deletion cassettes by PCR.
Integration into the target locus was verified by PCR of isolated genomic DNA. **(A)** Fragments design for verification of correct integration of the deletion cassette into the genome. **(B)** Correct integration yielding a 2487 bp DNA fragment whereas a 1541 bp long fragment represents the unaffected *ACDO1* gene, serving as negative control. 1 – strain number with correct targeted deletion cassette (Δacdo1); LS3 – wild type (control); "–" – no template PCR reaction (control).

Table 21 Primers used for construction of deletion mutant strain G1235 [Δ*acdo1*]

Primers for construction of *A. adeninivorans* G1235 [Δ*acdo1*]	
Primer	Sequence (5' → 3')
1_ovs_ex_forward	TAATCAACAGAATT TGACTAT TGATTTCCCCACC
1_ex_reverse	GGGGAATCAATCGAGAAATAATAAA
2_ovs_ex_forward	ATACAGACTCGATCGACGATTCCTTACCTATGTAGG
2_ex_reverse	GGGAATTAGCGGCC TGTAATCAATGTAAAGGACCAGG
3_Marker_forvard_ovs	CTCGATTGATTCCCCTTTCAATCGACGATTGCA
3_Marker_reverse	CGATCGAGTCTGTATTGAAG
ACDO_screen_fwd	CAGCGTCTTTGCCCCTGATA
ACDO_screen_rev	GCCAAGCTGCTTCCAGTTTC

4.3.6 Colony phenotype analysis of control strain (G1212/YRC102) and mutant strain G1235 [Δ*acdo1*]

When grown on agar plates with YMM-$NaNO_3$ supplemented with 2 % glucose as the sole source of carbon and incubated at 30 °C, the colony phenotype of the deletion strain G1235 [Δ*acdo1*]) proved to be identical to that of the control strain *A. adeninivorans* G1212/YIC102 (**Figure 49**).

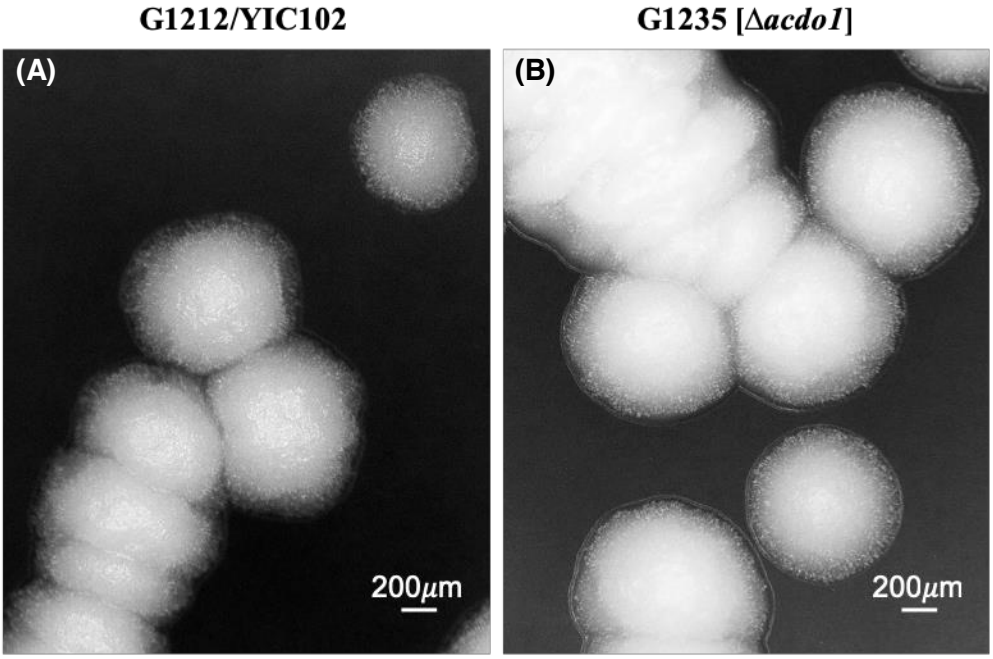

Figure 49 Phenotype of *A. adeninivorans* colonies.
Control strain *A. adeninivorans* G1212/YIC102 (**A**) and mutant strain G1235 [Δ*acdo1*] (**B**) were cultivated on agar plates containing YMM-glucose-$NaNO_3$ at 30 °C for 48 h before microscopic analysis using a VHX-5000 Digital Microscope. Bar = 200 μm.

4.3.7 Purification of the recombinant Acdo1-6hp

A. adeninivorans G1212/YIC102-AYNI1-ACDO1-6H with HisTag encoding sequence at the 3´-end of the *ACDO1* ORF was selected for synthesis of recombinant Acdo1-6hp. Purification was done by Immobilized Metal Affinity Chromatography (IMAC) using ÄKTA Pure System. At approximately 860 mM imidazole Acdo1-6h was eluted (**Figure 50**).

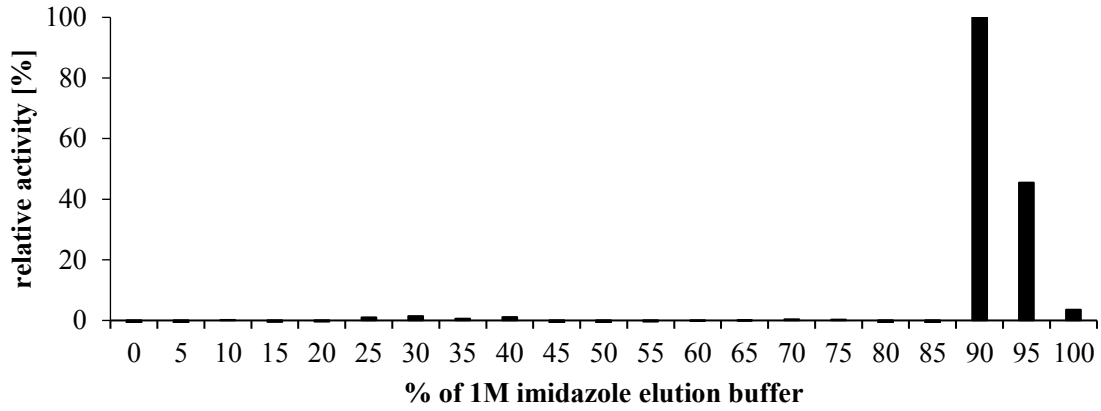

Figure 50 Test for elution of of Acdo1-6hp by varying concentrations of imidazole.
Acdo1-6h was purified via IMAC. To established imidazole concentration at which Acdo1-6h is eluting from the column, the protein was washed with elution buffer with a continuous gradient of 0-1 M imidazole. The protein was released from the column at an imidazole concentration around 860 mM as confirmed by enzyme activity assay.

Acdo1-6hp has a predicted molecular mass of 37.76 kDa. The denatured protein in both crude extract and purified protein fraction was visible at a position of 40 kDa on SDS-PAGE and Western blot (**Figure 51**).

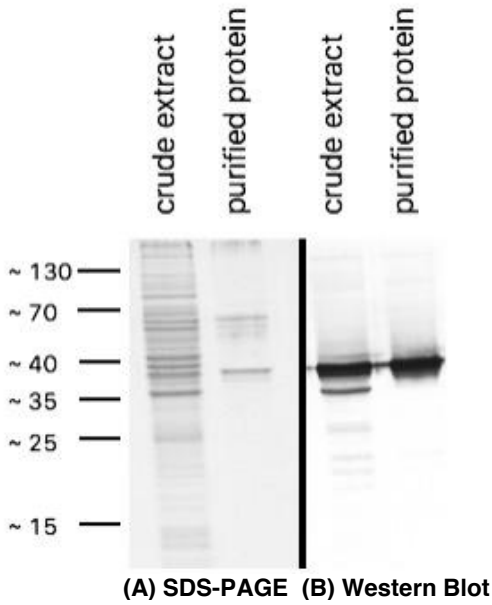

Figure 51 Purification of Acdo1-6hp on Ni Sepharose.
(A) SDS-PAGE of crude extract and purified Acdo1-6hp. (B) Western blot analysis, using primary antibodies anti-polyhistidine from rabbit and secondary antibodies anti-rabbit from goat, confirms the identity of the Acdo1-6hp.

Catechol-1,2-dioxygenase total activity was 0.92 ± 0.02 U in crude extract and 0.85 ± 0.02 U in the purified fraction, with a specific activity of 0.82 ± 0.02 U/mg for the crude extract and 5.39 ± 0.13 U/mg for the purified fraction. Purification yield was approximately 93 % (**Table 22**).

Table 22 Summary of Acdo1-6hp purification.
The protein was purified from 200 ml culture incubated in shaking flask for 48 h at 30 °C and 180 rpm.

Step	Protein [mg]	A_{total} [U]	$A_{specific}$ [U/mg]	Yield [%]	Purification fold
Crude extract	1.13 ± 0.01	0.92 ± 0.2	0.82 ± 0.02	100	1
Purified protein	0.16 ± 0.01	0.85 ± 0.02	5.39 ± 0.13	92.62	6.61

4.3.8 Native molecular mass of recombinant catechol-1,2-dioxygenase (Acdo1-6hp)

The molecular mass of native Acdo1-6hp was estimated by gel filtration on a Superdex™ 200 column and compared to a standard curve using molecules with known molecular masses (Blue Dextran – 20000000 Da, Ferritin – 450000 Da, Catalase – 240000 Da, BSA – 67000 Da, RNAse A - 13700 Da and Vitamin B12 – 1355 Da) (see **Figure 22**). Accordingly, the native enzyme had a calculated mass of 37.76 kDa. Since the predicted molecular mass of the His-tagged Acdo1-6hp is 79.67 kDa, this indicates that Acdo1-6hp is a dimeric protein (**Figure 52 C**).

(A)

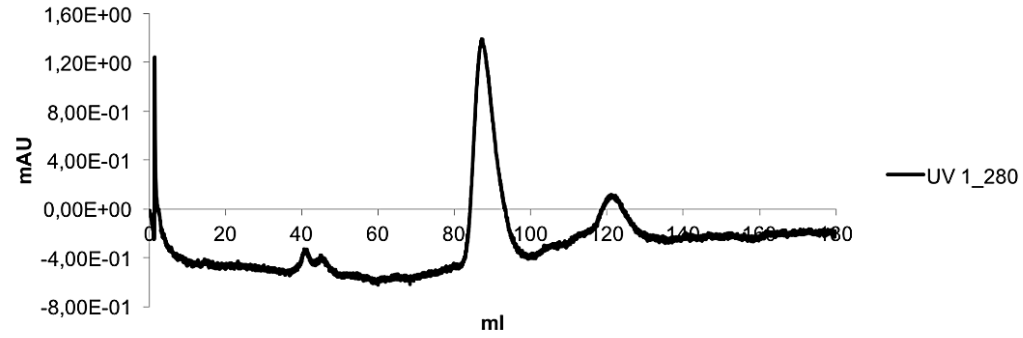

(B)

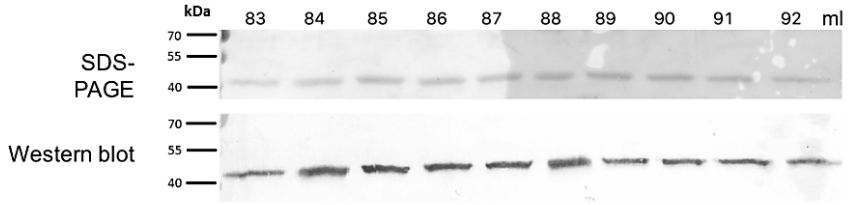

(C)

Analyst	Predicted m_M [kDa]	MW [kDa]	Retention volume [mL]	Ratio	
A. adeninivorans G1212-YIC102-ACDO1-6H	37.76	79.67	84.5	2.1	Dimer

Figure 52 Determination of native molecular mass of recombinant catechol-1,2-dioxygenase by size exclusion chromatography.
(A) Gel filtration of purified Acdo1-6hp on a Superdex^{TM} 200. **(B)** SDS-PAGE and Western blot analysis of Acdo1-6hp enriched elution fractions. **(C)** Calculated and predicted molecular mass of Acdo1-6hp.

4.3.9 Properties of recombinant catechol-1,2-dioxygenase

4.3.9.1 Determination of the optimal pH

The optimal pH conditions for Acdo1-6hp activity were established *in vitro* using 0.5 mM catechol as substrate and following buffers: 50 mM sodium citrate (pH 2.5 – 6.5), 50 mM sodium acetate (pH 3.5 to 6), 50 mM sodium phosphate (pH 5.5 - 8) and 50 mM TRIS-HCl (pH 7 – 9). Highest relative enzyme activity of 80 % and more was observed in the range pH 7 – 8.5 with an absolute peak (100%) at pH 7.5 (**Figure 53**).

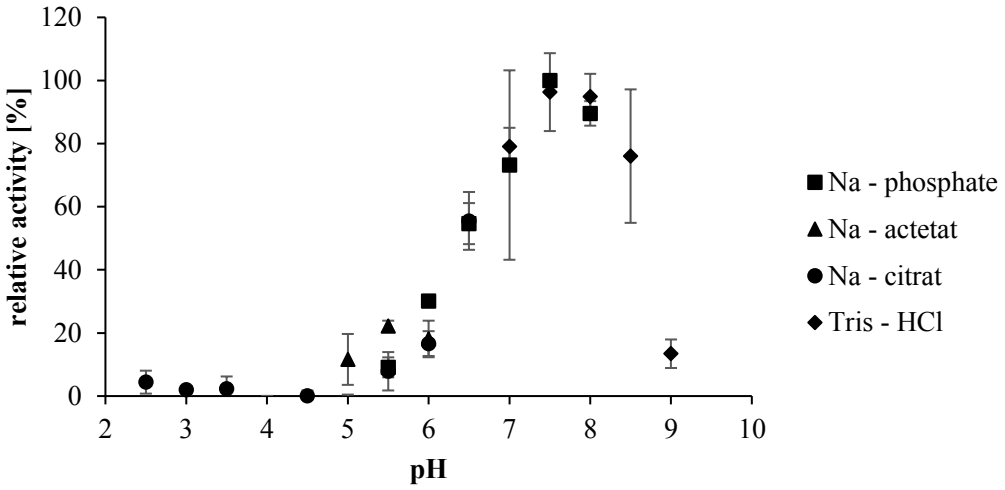

Figure 53 pH spectrum of recombinant catechol-1,2-dioxygenase activity.
Relative activity was measured at 30°C and shows highest value at pH 7.5.

4.3.9.2 Determination of optimal temperature and thermostability of Acdo1-6hp

The effect of temperature on the activity of catechol-1,2-dioxygenase was measured by incubating the reaction mixture at different temperatures under optimal pH conditions. Relative enzyme activity in excess of 80 % was observed at temperatures between 25 and 40 °C. Acdo1-6hp was most active at 25 °C (**Figure 54**).

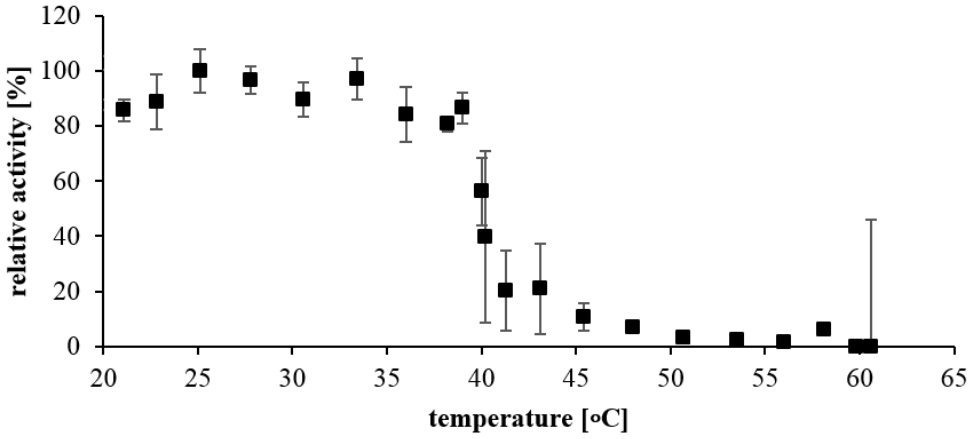

Figure 54 Influence of temperature on recombinant catechol-1,2-dioxygenase activity.

Acdo1-6hp is stable between 4 and 30 °C, shown by the fact that enzyme activity after 23 h of incubation at these temperatures remained at 100 % of the initial value (**Figure 55**). Increasing the temperature to 40 °C resulted in a decrease of enzyme activity to 85 % after 7 h and complete loss of activity after 23 h. At 50 °C, enzyme activity fell to 60 % within 1 h and was completely abolished after 7 h of incubation (**Figure 55**).

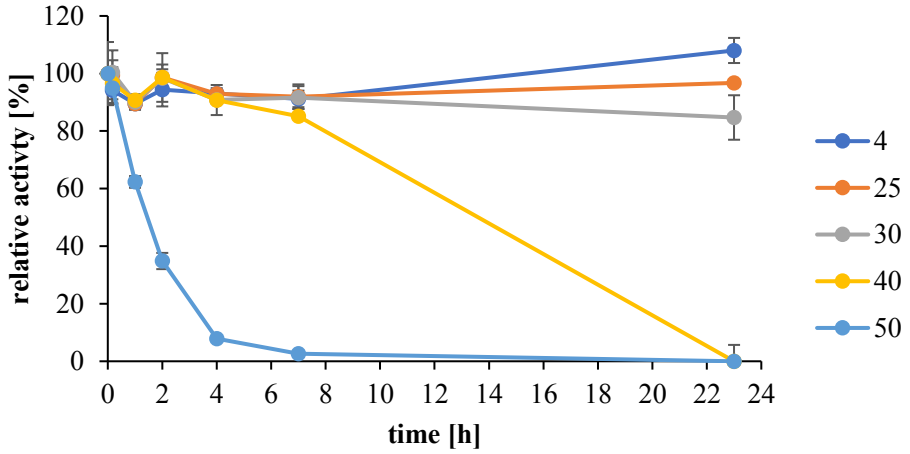

Figure 55 Stability of Acdo1-6hp under different temperature regimes.

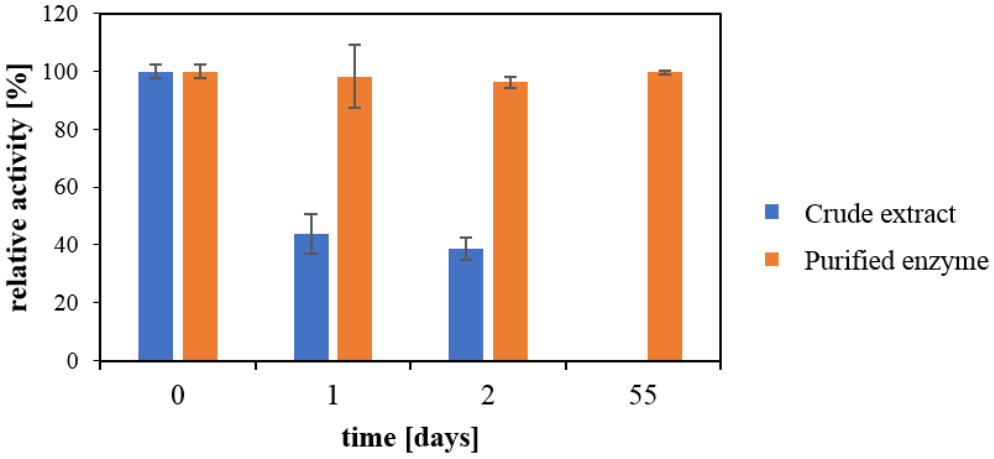

Figure 56 Acdo1-6hp activity upon storage at 4 °C.
Diagram bars show the effect of storage at 4 °C on relative enzyme activity in crude extract and purified enzyme. Initial activity was measured directly after protein purification and set to 100 %.

In a crude extract kept at 4 °C, Acdo1-6hp enzyme activity rapidly declined with time, showing 50% and 60% loss after 24 h and 48h of storage, respectively. After 55 days of storage, no enzyme activity was detected in the crude extract anymore (**Figure 55**). In contrast to the crude extract, enzyme activity in the purified fraction remained far more stable, still exhibiting 99 % of initial activity after 55 days at 4 °C (**Figure 56**). Freezing samples in liquid nitrogen resulted in complete loss of Acdo1-6hp activity in both crude extract and purified fraction (results not shown).

4.3.9.3 Effect of different additives on Acdo1-6hp activity

To identify possible inhibitors and/or cofactors of Acdo1-6hp, the enzyme was incubated in reaction mixtures containing a variety of supplements at 1 mM final concentration. Strong enzyme inhibition (relative activity < 30 %) was observed in the presence of Ni^{2+}, Al^{3+}, Zn^{2+}, PEG4000, PEG6000, PEG8000 or EDTA. In contrast, addition of Mg^{2+}, Ca^{2+} and Fe^{3+} to the reaction mixture had no significant influence on catechol-1,2-dioxygenase activity (relative activity > 80 %). None of these additives tested had a positive effect on catechol-1,2-dioxygenase activity. During the experiments it was observed that addition of cOmplete™ (EDTA-free Protease Inhibitor Cocktail) to the lysis buffer during the purification procedure caused an almost complete inhibition of Acdo1-6hp activity (**Table 23**).

Table 23 Effect of metal salts and additives on Acdo1-6hp activity.
Relative Acdo1-6hp activity [%] was analysed in the presence of 0.5 mM catechol as substrate.

1 [mM]	Relative activity [%]	1 [mM]	Relative activity [%]	1 [mM]	Relative activity [%]
control (H_2O)	100 ± 4	**$ZnSO_4$**	5 ± 3	**PEG4000**	12 ± 2
$NiSO_4$	19 ± 2	**$ZnCl_2$**	14 ± 2	**PEG6000**	11 ± 2
$NiCl_2$	25 ± 1	**$AlCl_3$**	0 ± 48	**PEG8000**	13 ± 2
$FeSO_4$	46 ± 3	**$MgSO_4$**	84 ± 12	**EDTA**	12 ± 4
$FeCl_3$	98 ± 7	**$MgCl_2$**	108 ± 13	**cOmplete™, EDTA-free Protease Inhibitor Cocktail**	6 ± 3
$CoSO_4$	48 ± 3	**$MnSO_4$**	80 ± 5		
$CoCl_2$	63 ± 6	**$MnCl_2$**	37 ± 9		
$CuSO_4$	38 ± 8	**$CaSO_4$**	105 ± 5		
$CuCl_2$	55 ± 7	**$CaCl_2$**	103 ± 1		

4.3.9.4 Kinetic study

The kinetic parameters of purified Acdo1-6hp were determined photometrically using pyrogallol and catechol as substrates. The K_m of Acdo1-6hp for pyrogallol (0.1 ± 0.02 mM) was found to be 25 times higher than for catechol (0.004 ± 0.001 mM). Turnover (k_{cat}) was 10.6 ± 0.4 s^{-1} for pyrogallol and 15.6 ± 0.4 s^{-1} for catechol. With a value of 118.6 ± 18.3 [mM^{-1} s^{-1}]) the catalytic efficiency for pyrogallol was found to be much lower than for catechol for which a value of 3946.9 ± 930.3 [mM^{-1} s^{-1}] was measured (**Table 24**).

Table 24 Kinetic constants of purified Acdo1-6hp using pyrogallol and catechol as substrates. Measurements were assayed spectrophotometrically.

Substrate	K_m [mM]	k_{cat} [s^{-1}]	k_{cat}/Km [$mM^{-1}s^{-1}$]
pyrogallol	0.1 ± 0.02	10.6 ± 0.4	118.6 ± 18.3
catechol	0.004 ± 0.001	15.6 ± 0.4	3946.9 ± 930.3

4.3.9.5 Substrate spectrum of Acdo1-6hp

Several substrates differing in the number and positions of hydroxyl groups were tested to determine the *in vitro* substrate specificity of Acdo1-6h. The enzymatic reactions were carried out under optimal conditions for catechol-1,2-dioxygenase. Reactions were monitored spectrophotometrically under differed wavelengths depending on the tested substrates (**Table 26**). The results not only showed the specificity of Acdo1-6hp for pyrogallol, catechol and hydroxyquinol but also confirmed that Acdo1-6hp is a catechol-1,2-dioxygenase but not a catechol-2,3-dioxygenase. The reaction carried out for the catechol-2,3-dioxygenase activity (monitored at a wavelength of 375 nm) failed to show formation of 2-hydroxymuconic semialdehyde as the expected product. Evidently, the positions of hydroxyl groups on the aromatic ring are crucial for the enzymatic reaction by Acdo1-6hp (**Figure 68 B**), which is similar to the results found for gallic acid decarboxylase (see 4.2.9.5).

Table 25 Spectrophotometric substrate analysis for Acdo1-6hp.

substrate	product	λ	U_{sp} [U g^{-1}]
catechol	*cis,cis*-muconic acid	260 nm	0.57 ± 0.03
catechol	2-hydroxymuconic semialdehyde	375 nm	0.00 ± 0.00
hydroquinone	4-hydroxymuconic acid semialdehyde	320 nm	0.00 ± 0.00
hydroxyquinol	3-hydroxy-*cis,cis*-muconic acid	465 nm	2.78 ± 0.49
pyrogallol	2-hydroxymuconic acid	296 nm	0.59 ± 0.01
protocatechuic acid	3-carboxy-*cis,cis*-muconate	290 nm	0.02 ± 0.00
gallic acid	4-carboxy-2-hydroxymuconic semialdehyde	259 nm	0.02 ± 0.05
2,3 DHBA	3-carboxy-2-hydroxymuconate semialdehyde	268 nm	0.00 ± 0.00
2,5 DHBA	maleyl pyruvate	334 nm	0.00 ± 0.03

4.3.10 Expression analysis of *ACDO1* on various carbon sources

The expression level of *ACDO1* relative to the housekeeping gene *TFCI* was analyzed by nested quantitative RT-PCR. Primers used for expression analysis of *AGDC1* are shown in **Table 26**. *A. adeninivorans* G1212/YIC102 was cultivated on YMM-$NaNO_3$ supplemented with 0.2 % (w/v) of either glucose or different hydroxylated aromatic acids as the sole source of carbon. Samples were collected at different times and total RNA was isolated. An increase of gene transcription of *ACDO1* was observed when cells were cultivated on gallic acid and protocatechuic acid. The highest expression level was detected after 8 h of cultivation (**Figure 57**). In contrast, none of the other carbon sources (glucose, 3-hydroxybenzoic acid, 4-hydroxybenzoic acid, 2,4-dihydroxybenzoic acid, 2,3-dihydroxybenzoic acid, 2,5-dihydroxybenzoic acid) altered the expression of *ACDO1*.

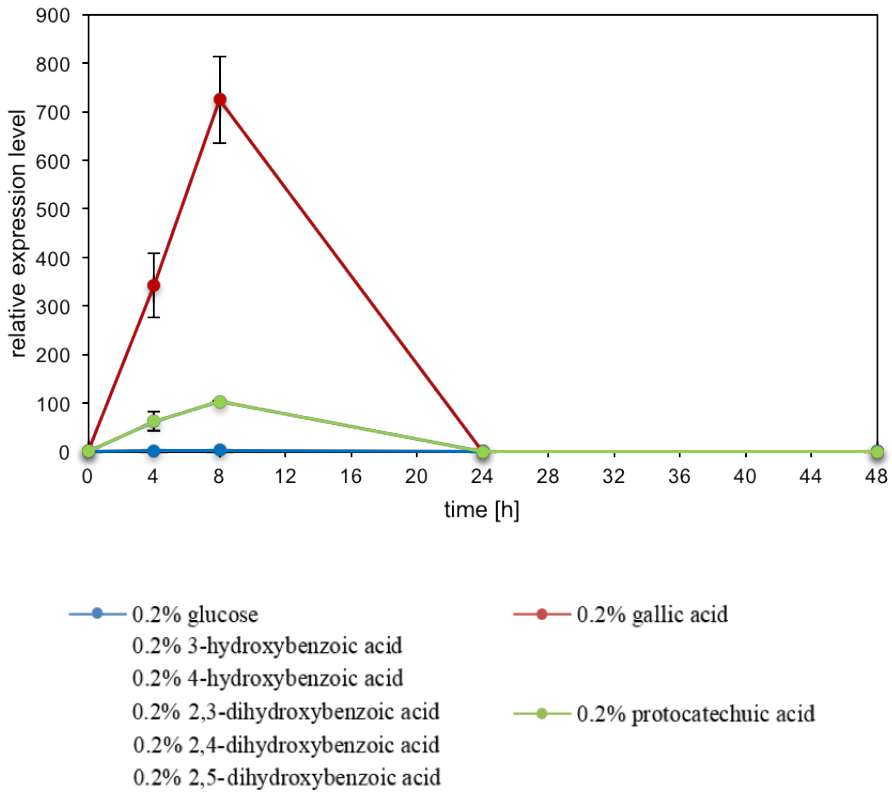

Figure 57 Influence of carbon sources on *ACDO1* expression.
Gene expression of *ACDO1* was analysed in *A. adeninivorans* G1212/YRC102 cultivated on YMM-$NaNO_3$ supplemented with 0.2 % of either glucose, gallic acid, protocatechuic acid, 3-hydroxybenzoic acid, 4-hydroxybenzoic acid, 2,3-dihydroxybenzoic acid, 2,4-dihydroxybenzoic acid or 2,5-dihydroxybenzoic acid as the sole source of carbon. Expression analysis was performed by nested quantitative real time PCR.

Table 26 Primers used for analysis of *ACDO1* expression levels.

Primers for nested quantitative RT PCR		
Reaction step	Primer	Sequence (5‘ → 3‘)
Step1 cDNA synthesis	(dT) 15V-RTA	TGA CAG GAT ACC ATA CAG ACA CTA TTT TTT TTT TTT TTT V
Step 2 Second PCR synthesis	RTA-1 rv	TGA CAG GAT ACC ATA CAG ACA C
	ACDO1-V fw	TTC GAT GCT CAG AGC CGA C
	TFC1-3 fw	TGA AGA AGA GCA CCA AGC A
Step 3 Second PCR synthesis	RTA rv	TGA CAG GAT ACC ATA CAG ACA CTA
	ACDO1-III fw	AAG GTT GTC AAC GGA GTC CC
	TFC1-1 fw	ACA ACA AGA TGA AAA CGC

4.3.11 Influence of protocatechuic acid on gene expression in *A. adeninivorans* by microarray expression analysis

To evaluate whole transcriptome variations upon incubation of *A. adeninivorans* with protocatechuic acid, microarray expression analysis was performed. Changes in gene expression of wildtype strain, *A. adeninivorans* LS3, cultivated in YMM-$NaNO_3$ supplemented with 1 % glucose and YMM-$NaNO_3$ supplemented with 1 % glucose plus 0.5 % protocatechuic acid were analyzed over time. For this, cells were harvested after 15 min, 30 min, 5 h and 12.5 h of incubation in shaking flasks at 30 °C and 180 rpm. After RNA isolation, microarray data were used to identify main candidate genes involved in tannic acid degradation (**Figure 58**) as well as candidate genes and/or reactions, which may be involved in the degradation of protocatechuic acid (**Figure 59**). Significant upregulation was observed for genes of gallic acid decarboxylase 1 (*AGDC1*), catechol-1,2-dioxygenase *(ACDO1)* and tannase 1 (*ATAN1*) as well as for genes annotated as putative tannase 2 (*ATAN2*), oxalocrotonate decarboxylase, 2-oxopent-4-dienoate hydratase and 4-hydroxy-2-oxovalerate aldolase. These data suggest that additional enzymes are involved in tannic acid degradation. In **Figure 59**, an alternative protocatechuic acid degradation pathway is presented based on data obtained from these microarray experiments as well as actually available gene annotations. The constructed pathway schemes suggest that catechol is converted into pyruvate and acetaldehyde thus allowing entry into the central metabolism (**Figure 58** and **Figure 59**). In addition, microarray data further showed that whereas genes involved in β-oxidation were upregulated, those involved in the glyoxylate cycle, methyl citrate cycle and in the catabolism of the branched-chain amino acids valine, leucine and isoleucine were not upregulated (**Figure 60** - **Figure 61**).

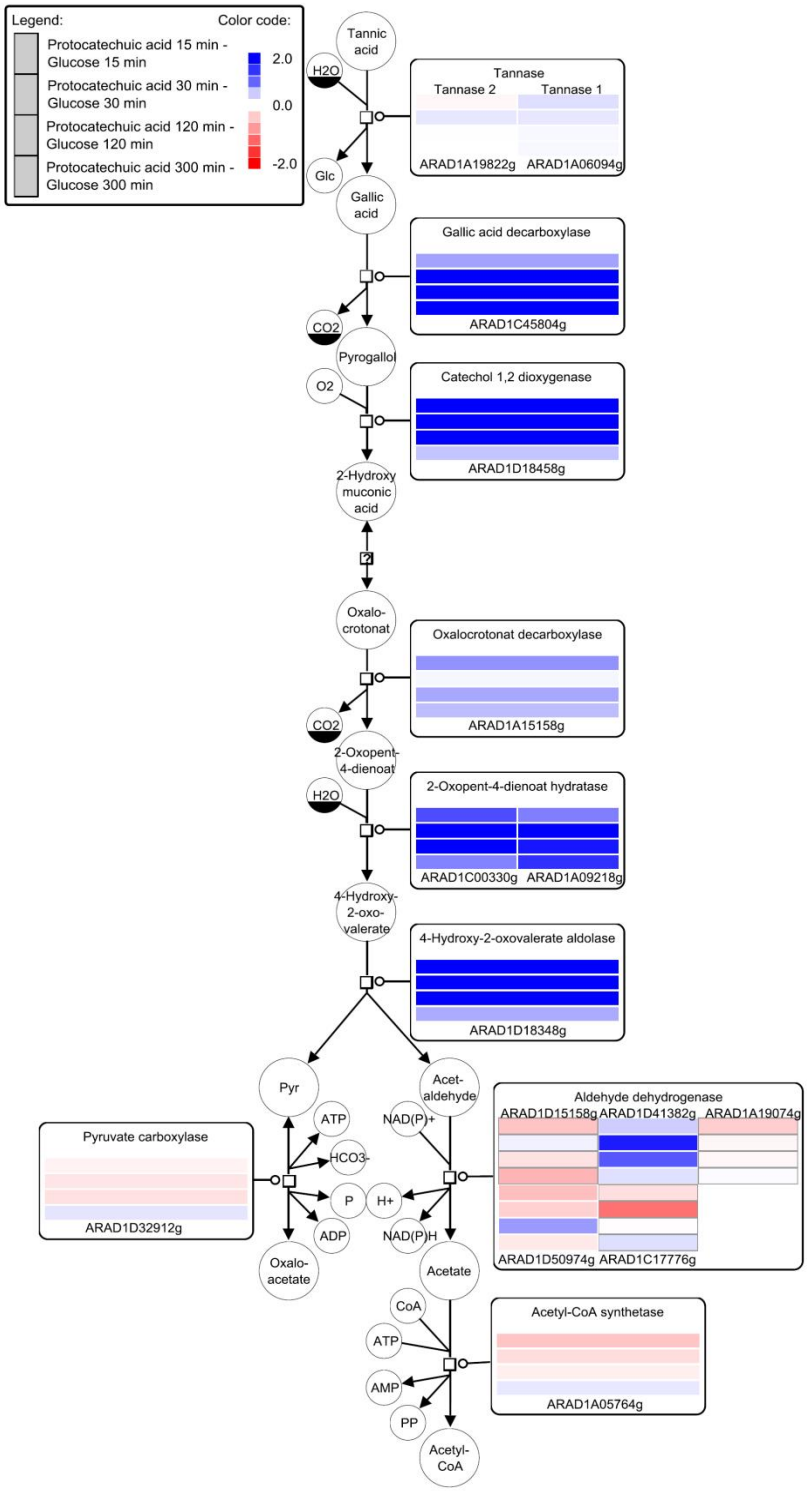

Figure 58 Key compounds of the tannin catabolism based on microarray studies of gene regulation by protocatechuic acid.
The Systems Biology Graphical Notation (SBGN) of the metabolic network depicts reactions catalysed by the corresponding enzymes (rectangular square). Enzymes are enriched with colour-coded log2 fold change values of time-resolved expression data of the respective genes. The colours represent upregulation (dark blue 2-fold upregulation) and downregulation (dark red 2-fold downregulation) of genes in cells shifted to a medium containing gallic acid as the carbon source compared to cells grown on glucose. Metabolites or enzymes occurring multiple times in the metabolic network are decorated with a clone marker (e.g. NAD^+) [graph produced with VANTED – (Junker *et al.*, 2012, Rohn *et al.*, 2012)].

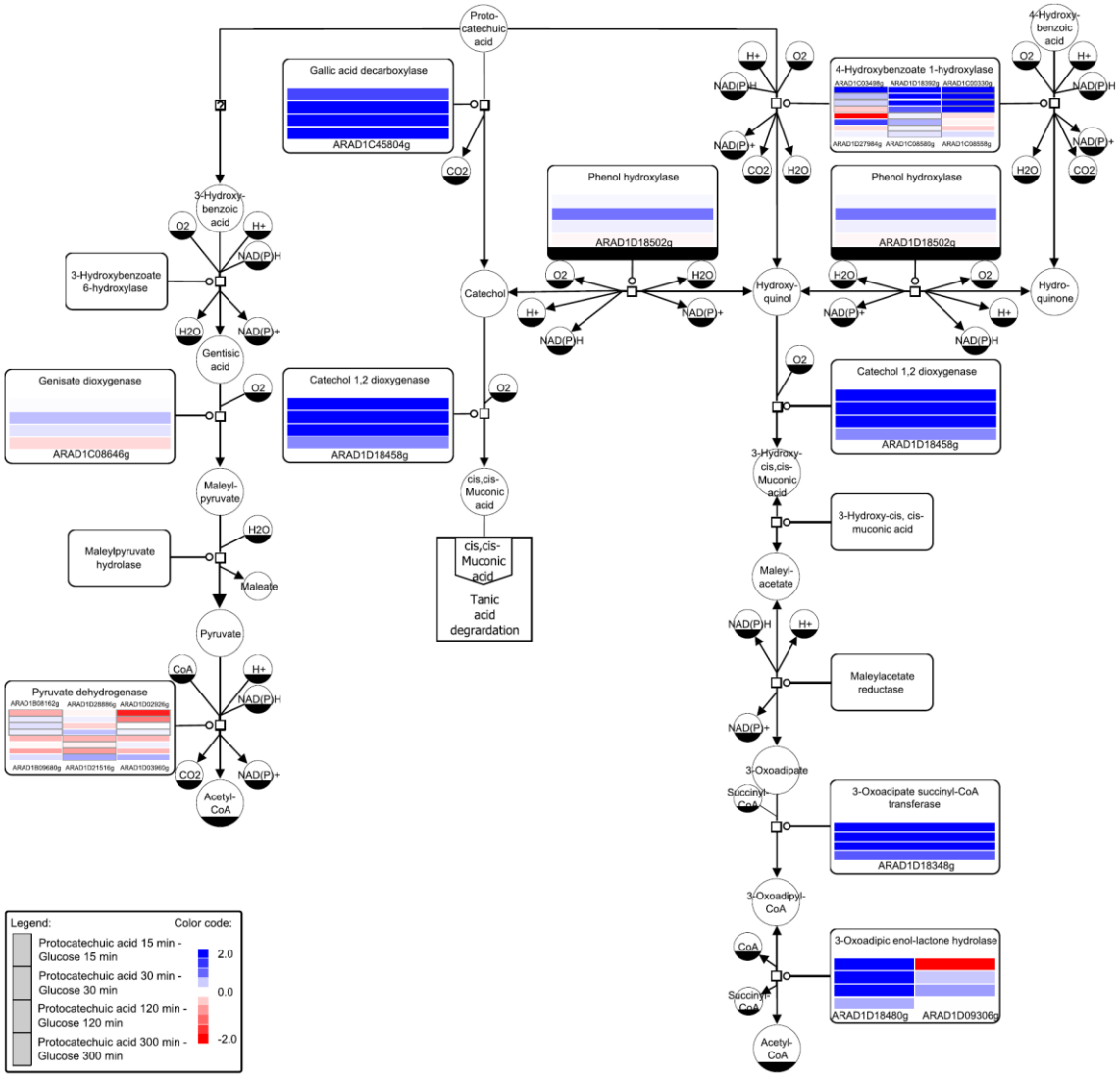

Figure 59 Expanded scheme of potential key compounds involved in tannin catabolism based on microarray studies of gene regulation by protocatechuic acid.
The Systems Biology Graphical Notation (SBGN) of the metabolic network depicts reactions catalysed by the corresponding enzymes (rectangular square). Enzymes are enriched with colour-coded log2 fold change values of time resolved expression data of the respective genes. The colours represent upregulation (dark blue 2-fold upregulation) and downregulation (dark red 2-fold downregulation) of genes in cells shifted to a medium containing gallic acid as the carbon source compared to cells grown with glucose. Metabolites or enzymes occurring multiple times in the metabolic network are decorated with a clone marker (e. g. NAD^+) [graph produced with VANTED – (Junker *et al.*, 2012, Rohn *et al.*, 2012)].

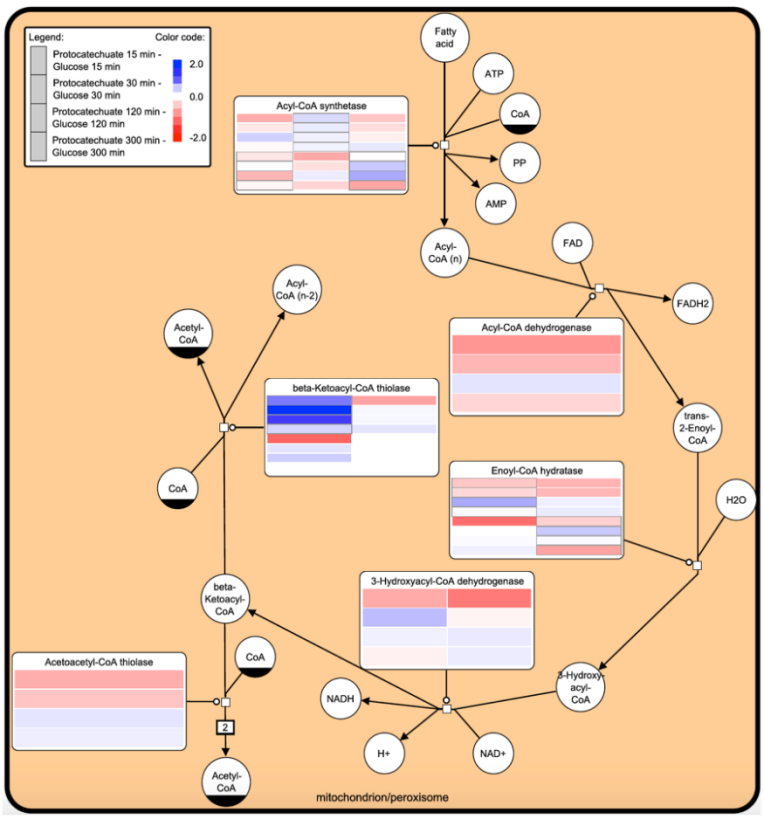

Figure 60 Key compounds of the β-oxidation - Microarray studies of gene regulation by protocatechuic acid.
The Systems Biology Graphical Notation (SBGN) of the metabolic network depicts reactions catalyzed by the corresponding enzymes (rectangular square). Enzymes are enriched with color-coded log2 fold change values of time resolved expression data of the respective genes. The colors represent upregulation (dark blue 2-fold upregulation) and downregulation (dark red 2-fold downregulation) of genes in cells shifted to a medium containing 0.5 % protocatechuic acid and 1 % glucose as the carbon sources compared to cells grown with 1 % glucose. Metabolites or enzymes occurring multiple times in the metabolic network are decorated with a clone marker (e. g. NAD^+) [graph produced with VANTED – (Junker *et al.*, 2012, Rohn *et al.*, 2012)].

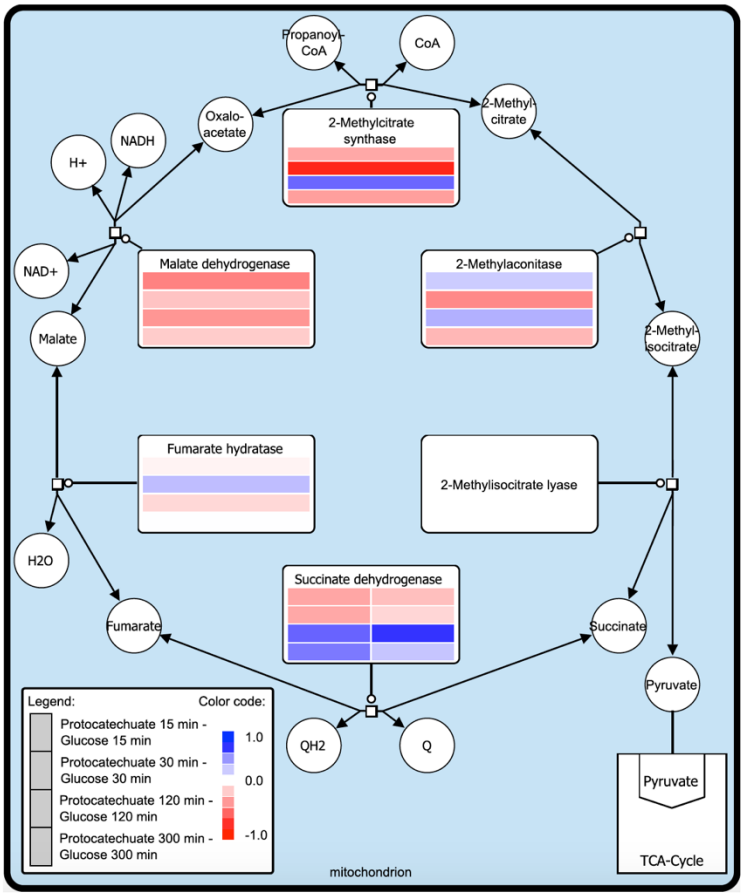

Figure 61 Key compounds of the methyl citrate cycle – based on microarray studies of gene regulation by protocatechuic acid.
The Systems Biology Graphical Notation (SBGN) of the metabolic network depicts reactions catalysed by the corresponding enzymes (rectangular square). Enzymes are enriched with color-coded log2 fold change values of time resolved expression data of the respective genes. The colours represent upregulation (dark blue 1-fold upregulation) and downregulation (dark red 1-fold downregulation) of genes in cells shifted to a medium containing 0.5 % protocatechuic acid and 1 % glucose as the carbon sources compared to cells grown with 1 % glucose. Metabolites or enzymes occurring multiple times in the metabolic network are decorated with a clone marker (e. g. NAD^+) [graph produced with VANTED – (Junker *et al.*, 2012, Rohn *et al.*, 2012)].

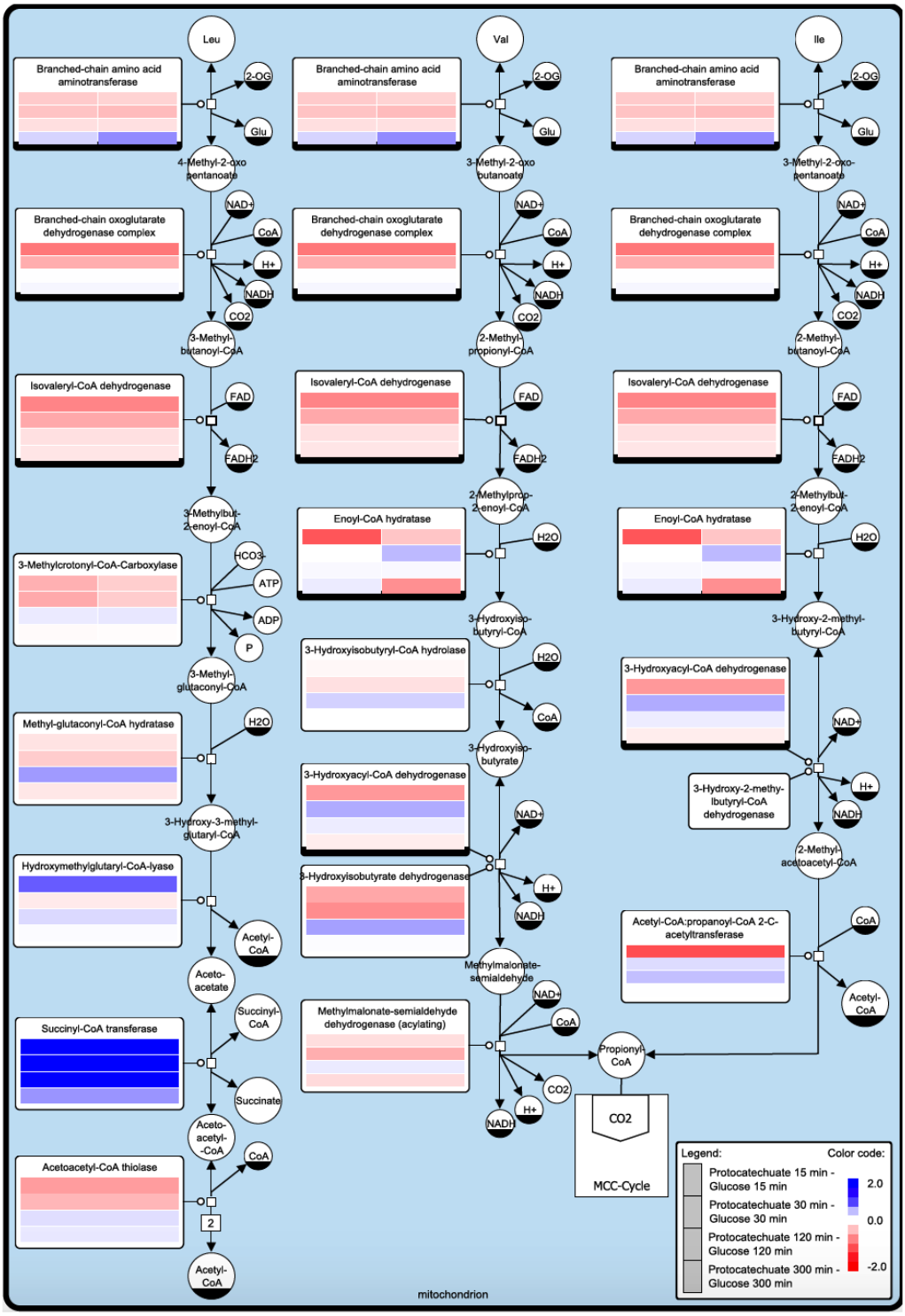

Figure 62 Key compounds of the catabolism of the branched-chain amino acids valine, leucine and isoleucine based on microarray studies of gene regulation by gallic acid.
The Systems Biology Graphical Notation (SBGN) of the metabolic network depicts reactions catalyzed by the corresponding enzymes (rectangular square). Enzymes are enriched with colour-coded log2 fold change values of time resolved expression data of the respective genes. The colours represent upregulation (dark blue 2-fold upregulation) and downregulation (dark red 2-fold downregulation) of genes in cells shifted to a medium containing 0.5 % protocatechuic acid and 1 % glucose as the carbon sources compared to cells grown with 1 % glucose. Metabolites or enzymes occurring multiple times in the metabolic network are decorated with a clone marker (e. g. NAD^+) [produced using VANTED – (Junker *et al.*, 2012, Rohn *et al.*, 2012)].

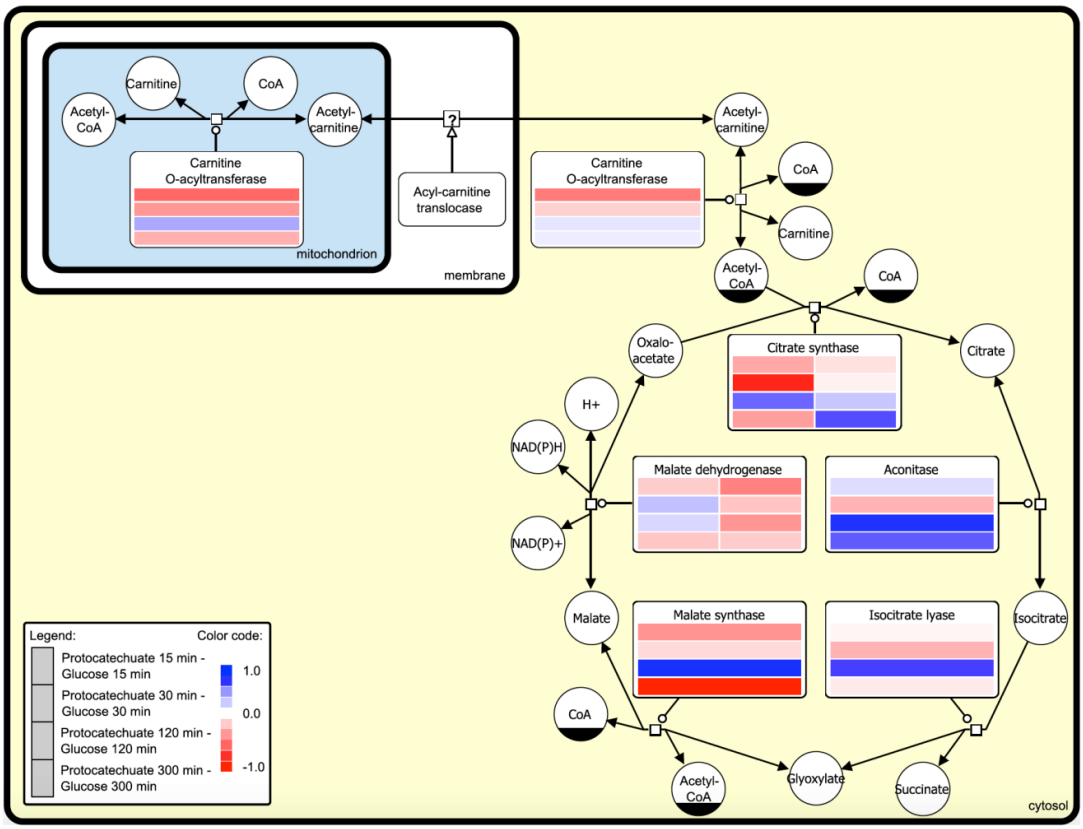

Figure 63 Key compounds of the glyoxylate cycle based on microarray studies of gene regulation by protocatechuic acid.
The Systems Biology Graphical Notation (SBGN) of the metabolic network depicts reactions catalysed by the corresponding enzymes (rectangular square). Enzymes are enriched with color-coded log2 fold change values of time resolved expression data of the respective genes. The colours represent upregulation (dark blue 1-fold upregulation) and downregulation (dark red 1-fold downregulation) of genes in cells shifted to a medium containing 0.5 % protocatechuic acid and 1 % glucose as the carbon sources compared to cells grown with 1 % glucose. Metabolites or enzymes occurring multiple times in the metabolic network are decorated with a clone marker (e. g. NAD^+) [graph produced with VANTED – (Junker *et al.*, 2012, Rohn *et al.*, 2012)].

4.3.12 Role of Acdo1p in metabolism of protocatechuic acid in *A. adeninivorans*

The enzyme Acdo1p is, similar to *Arxula* gallic acid decarboxylase 1, encoded by an inducible gene. The induction occurs in the presence of gallic acid as well as protocatechuic acid. The analysis of its *in vivo* role was enabled by the generation of the *A. adeninivorans* strains G1212/YIC102, G1212/YIC102-AYNI1-ACDO1-6H and G1235 [Δ*acdo1*]. The strains were cultivated at 30 °C and 180 rpm on YMM-$NaNO_3$ supplemented with 0.75 % glucose, 0.25 % gallic acid, 0.25 % gallic acid + 0.5 % glucose, 0.25 % protocatechuic acid and 0.25 % protocatechuic acid + 0.5 % glucose as

the sole sources of carbon and energy. Growth behaviour was monitored by dcw measurement (**Figure 64**). All strains performed best in medium supplemented with glucose as the sole source of carbon. Growth was not affected by the deletion of *ACDO1* (**Figure 64 A,D**).

Growth of all strains was reduced by nearly 50 % in medium containing 0.25 % gallic acid or 0.25 % protocatechuic acid + 0.5 % glucose (**Figure 64 C**). Under the same conditions, the *ACDO1* deletion strain G1235 [Δ*acdo1*] initially performed similar to the other strains. However, from 24 h onwards, the dcw of G1235 [Δ*acdo1*] dropped by nearly 50 % whereas dcw of the other strains remained more or less constant (**Figure 64 C,F**). Weakest growth was observed in medium supplemented with 0.25 % gallic acid or 0.25 % protocatechuic acid as the sole source of carbon (**Figure 64 B,E**). Under these conditions, the *ACDO1* overexpressing strain G1212/YIC102-AYNI1-ACDO1-6H performed slightly better that the control strain, whereas growth of the *ACDO1* deletion strain G1235 [Δ*acdo1*] was completely inhibited.

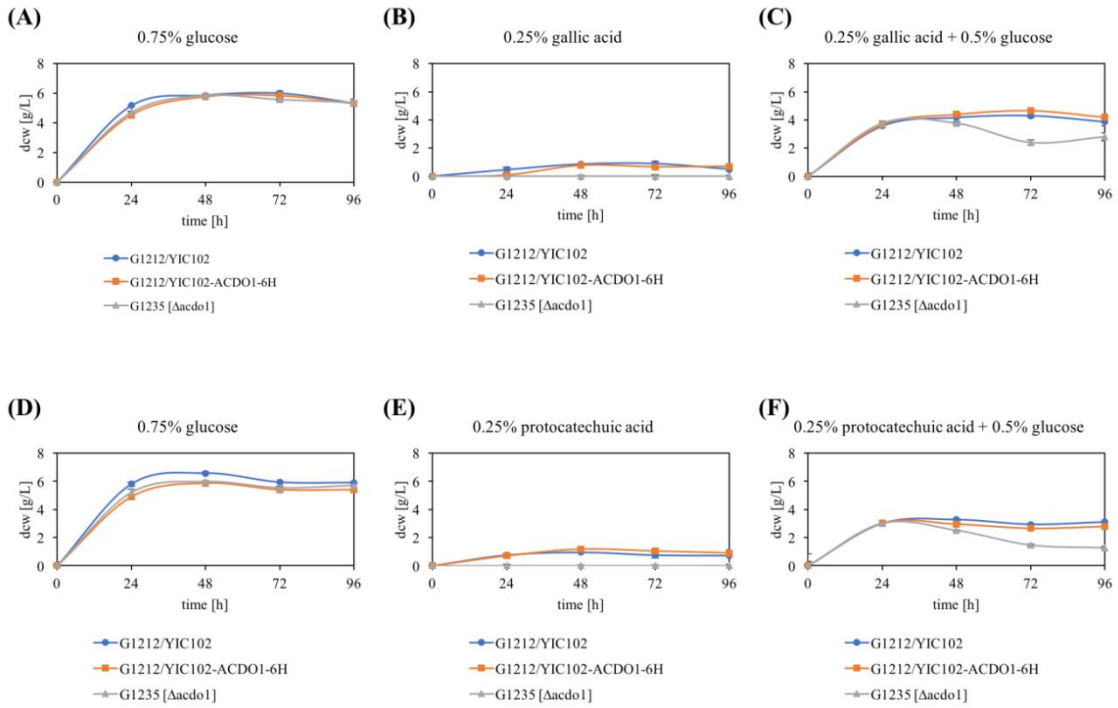

Figure 64 Growth behaviour of *A. adeninivorans* strains G1212/YRC102 (control), G1212/YIC102-AYNI1-ACDO1-6H (*ACDO1-6H* overexpression) and G1235 [Δ*acdo1*] (*ACDO1* deletion).
Strains ware cultivated on HMM-NO_3 supplemented with **(A,D)** 0.75 % glucose, **(B)** 0.25 % gallic acid, **(C)** 0.25 % gallic acid + 0.5 % glucose, **(E)** 0.25 % protocatechuic acid and **(F)** 0.25 % protocatechuic acid + 0.5 % glucose as the sole source of carbon.

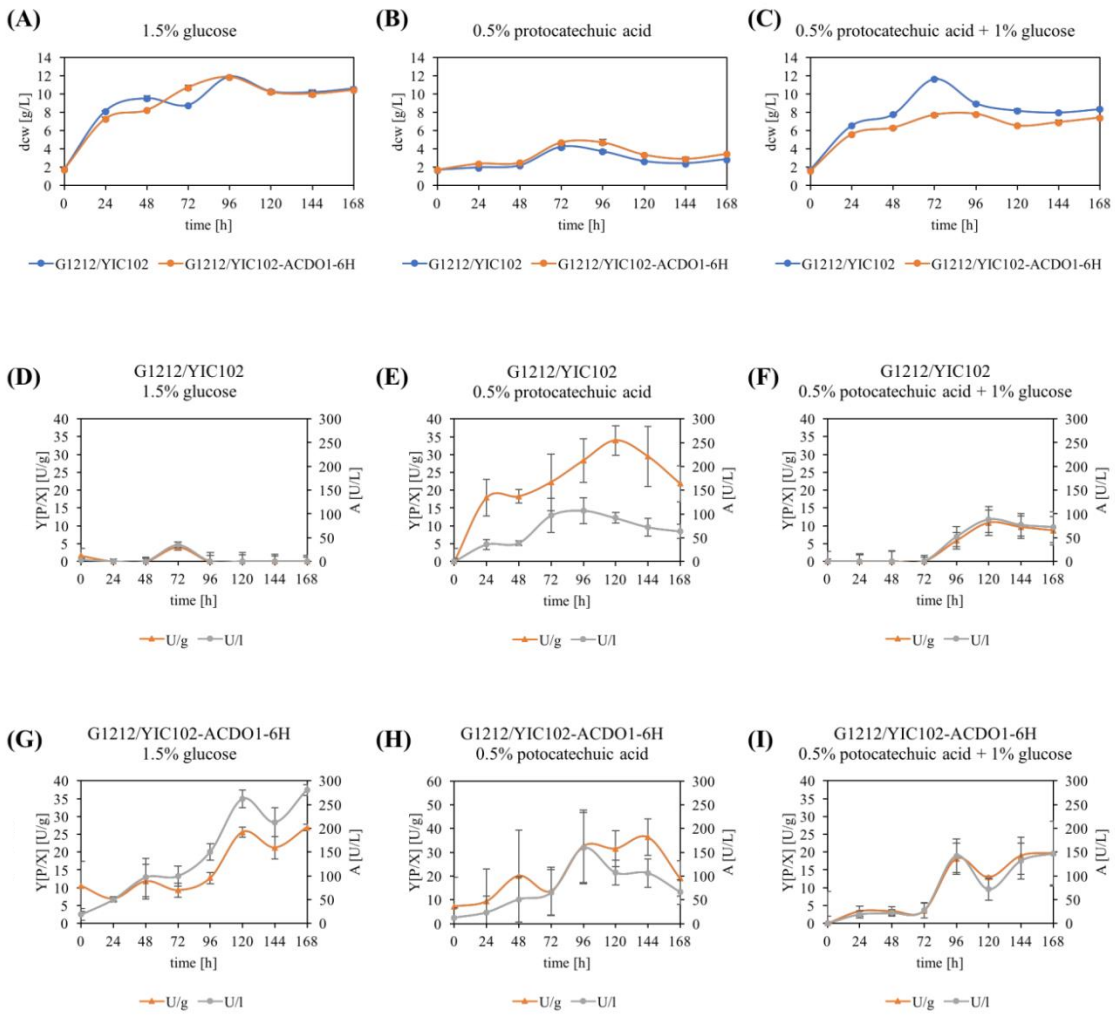

Figure 65 Growth behaviour and Acdo1-6hp activity in *A. adeninivorans* strains G1212/YRC102 (control) and G1212/YIC102-AYNI1-ACDO1-6H (*ACDO1-6H* overexpression).
(A-C) Influence of carbon source on the dry cell weight; **(D-I)** Acdo1-6hp activity in relation to carbon source and yield [Y(P/X)] (Y - yield coefficient, P - enzyme formation in U, X - biomass in g). Strains were cultivated in YMM-$NaNO_3$ with 1.5 % glucose, 0.5 % protocatechuic acid or 1 % glucose plus 0.5 % protocatechuic acid as carbon source.

In a time course experiment using catechol as a growth substrate, variations in catechol-1,2-dioxygenase activity and yield [Y(P/X)] (Y is yield coefficient, P is enzyme formation in U and X is biomass in g) (**Figure 65**) were measured for the control strain G1212/YIC102 and the ACDO1-6H overexpressing strain G1212/YIC102-ACDO1-6H. Both strains were cultivated at 30 °C in shacking flask on YMM-$NaNO_3$ supplemented with 1.5 % (w/v) glucose, 0.5 % (w/v) protocatechuic acid or 0.5 % (w/v) protocatechuic acid + 1% (w/v) glucose for up to 168 h (**Figure 65**). Growth behaviour of the two strains was largely identical under the culture conditions employed (**Figure 65 A-C**). In the presence of glucose as the sole carbon source, catechol-1,2-dioxygenase activity was

virtually absent from crude extract of *A. adeninivorans* G1212/YIC102 (**Figure 65 D**) but was prominently present and showing a strong increase in time in strain G1212/YIC102-ACDO1-6H ultimately reaching 280.6 U/L and 26.9 U/g of dry cell weight (**Figure 65 G**). When protocatechuic acid was the sole carbon source, both control strain G1212/YRC102 and overexpressing strain G1212/YIC102-ACDO1-6H showed a similar strong increase of catechol-1,2-dioxygenase activity with time (**Figure 65 E,H**). In medium containing 0.5 % protocatechuic acid and 1 % glucose, enzyme activity in strains initially remained low before a distinct increase after 72 h of incubation (**Figure 65 F,I**). Whereas in the control strain enzyme activity reached 76 U/L, in the overexpressing strain it reached 150 U/L.

4.3.13 Metabolite analysis during degradation of gallic acid and protocatechuic acid by *A. adeninivorans*

To investigate the *in vivo* transformation of protocatechuic acid, *A. adeninivorans* strains G1212/YIC102 (control), G1212/YIC102-AYNI1-ACDO1-6H (overexpression of *ACDO1-6H*) and G1235 [Δ*acdo1*] (*ACDO1* deletion) were cultivated on HMM-$NaNO_3$ supplemented with 0.25 % protocatechuic acid or with 0.25 % protocatechuic acid + 0.5 % glucose (**Figure 66**). In the presence of protocatechuic acid as the sole source of carbon, control and G1212/YIC102-AYNI1-ACDO1-6H strain achieved complete consumption of protocatechuic acid within 48 h of cultivation while consumption in the deletion strain G1235 [Δ*acdo1*] remained incomplete (**Figure 66 A-C**). In medium supplemented with 0.25 % protocatechuic acid + 0.5 % glucose, control and G1212/YIC102-AYNI1-ACDO1-6H strain achieved complete consumption of protocatechuic acid not before 72 h of cultivation (**Figure 66 D,E**). Under the same conditions, deletion strain G1235 [Δ*acdo1*] started protocatechuic acid consumption after 24 h of cultivation reaching complete degradation at the end of the cultivation period (**Figure 66 F**). The degradation products identified during cultivation differed for all strains. In the control and overexpressing strain G1212/YIC102-AYNI1-ACDO1-6H catechol, *cis,cis*-muconic acid and 3-hydroxybenzic acid were detected. In the control strain grown on medium containing 0.25 % protocatechuic acid, catechol reached a maximum concentration of ~0.27 g/L after 24 h of cultivation while 3-hydroxybenzoic acid reached a maximum concentration of ~0.3 g/L after 48 h of cultivation at which timepoint also *cis,cis*-muconic acid peaked at ~0.04 g/L (**Figure 66 A**). When the control strain was grown on 0.25 % protocatechuic acid + 0.5 % glucose maximum values for catechol

(~0.23 g/L) was reached after 48 h of cultivation, whereas 3-hydroxybenzoic acid (~0.36 g/L) and *cis,cis*-muconic acid (0.06 g/L) were reached after 72 h of cultivation (**Figure 66 D**). For the overexpression strain grown on medium supplemented with 0.25 % protocatechuic acid, the maximum values were 0.09 g/L catechol after 24 h, 0.35 g/L 3-hydroxybenzoic acid after 48 h and 0.04 g/L *cis,cis*-muconic acid after 48 h (**Figure 66 B**). In the presence of 0.25 % protocatechuic acid and 0.5 % glucose, the results were 0.07 g/L catechol after 48 h, 0.45 g/L 3-hydroxybenzoic acid after 72 h, and 0.07 g/L *cis,cis*-muconic acid after 72 h (**Figure 66 E**). During cultivation of deletion strain G1235 [Δ*acdo1*] in the presence of 0.25 % protocatechuic acid, hydroxyquinol (maximum 0.24 g/L after 24 h) and catechol (maximum 0.185 g/L after 48 h) were detected (**Figure 66 C**). When the same strain was cultivated on medium supplemented with 0.25 % protocatechuic acid + 0.5 % glucose, catechol (maximum 0.28 g/L after 72 h) and hydroxyquinol (maximum 0.09 g/L after 24 h) were identified (**Figure 66 F**). In contrast to the other two strains, 3-hydroxybenzoic acid was absent from G1235 [Δ*acdo1*] cultures (**Figure 66 C,F**). In an additional experiment, *A. adeninivorans* strains G1212/YIC102, G1212/YIC102-AYNI1-ACDO1-6H and G1235 [Δ*acdo1*] were cultivated on HMM-$NaNO_3$ supplemented with either 0.25 % gallic acid or with 0.25 % gallic acid + 0.5 % glucose. When gallic acid was the sole source of carbon, the control and G1212/YIC102-AYNI1-ACDO1-6H strain achieved complete degradation of gallic acid within 48 h and within 72 h when glucose was added (**Figure 67 A,D**). Similar to the experiments using protocatechuic acid (**Figure 66 C,F**), the deletion mutant G1235 [Δ*acdo1*] failed to completely degrade gallic acid under both culture conditions (**Figure 67 C,F**).

For the control strain grown in gallic acid-containing medium without and with 0.5 % glucose, ~0.3 g/L and ~0.55 g/L, respectively, of the gallic acid breakdown product pyrogallol was detected (**Figure 67 A,D**). In contrast, pyrogallol was not detected in cultures of the overexpressing strain G1212/YIC102-AYNI1-ACDO1-6H (**Figure 67 B,E**).

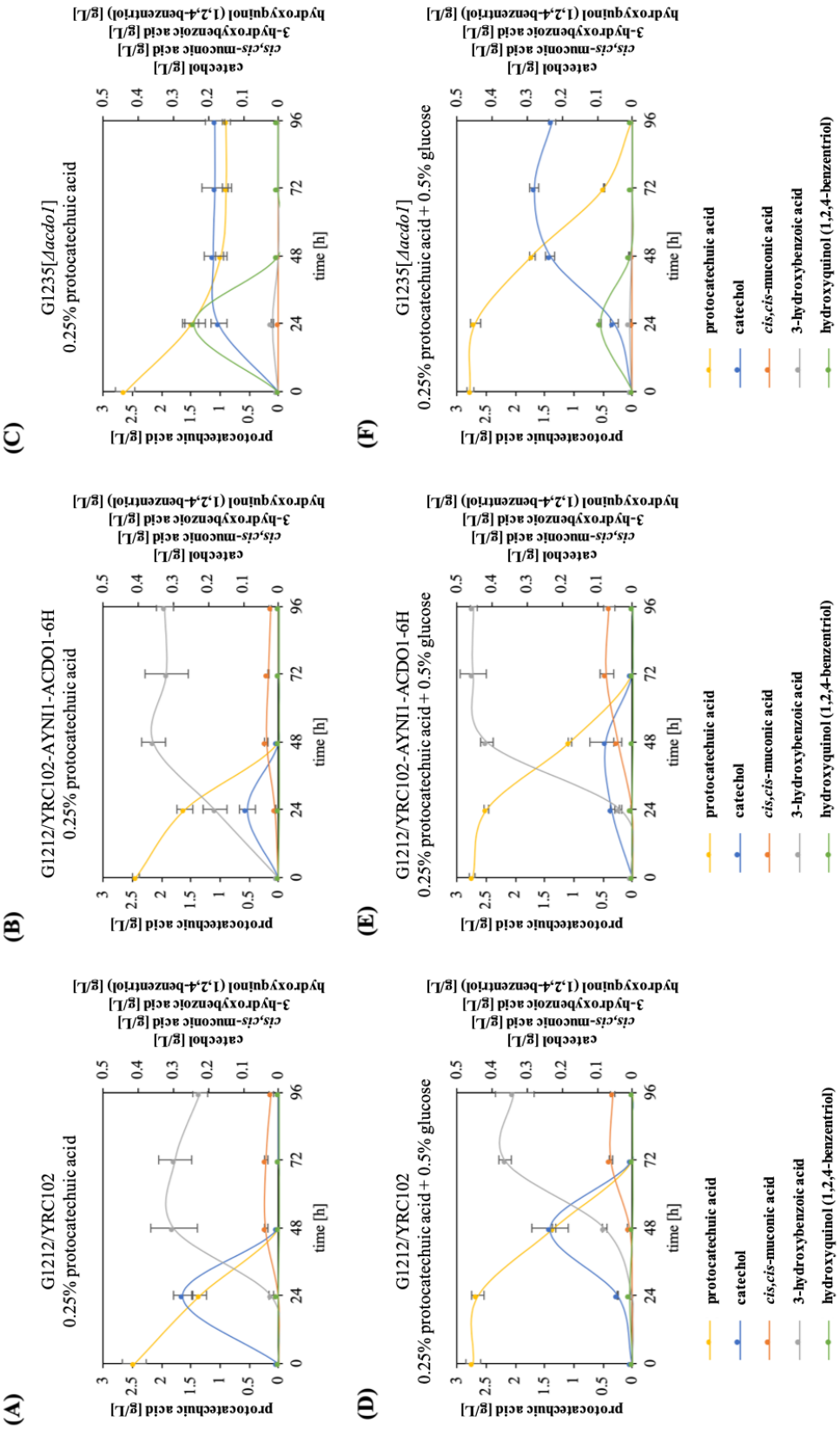

Figure 66 GC-MS analysis of substrate – product conversion during cultivation of *A. adeninivorans* on protocatechuic acid. **(A,D)** *A. adeninivorans* G1212/YIC102; **(B,E)** *A. adeninivorans* G1212/YIC102-AYNI1-ACDO1-6H; **(C,F)** *A. adeninivorans* G1235 [*Δacdo1*]. Strains were cultivated on HMM-$NaNO_3$ supplemented with 0.25 % protocatechuic acid **(A,B,C)** or with 0.25 % protocatechuic acid plus 0.5 % glucose **(D,E,F)**.

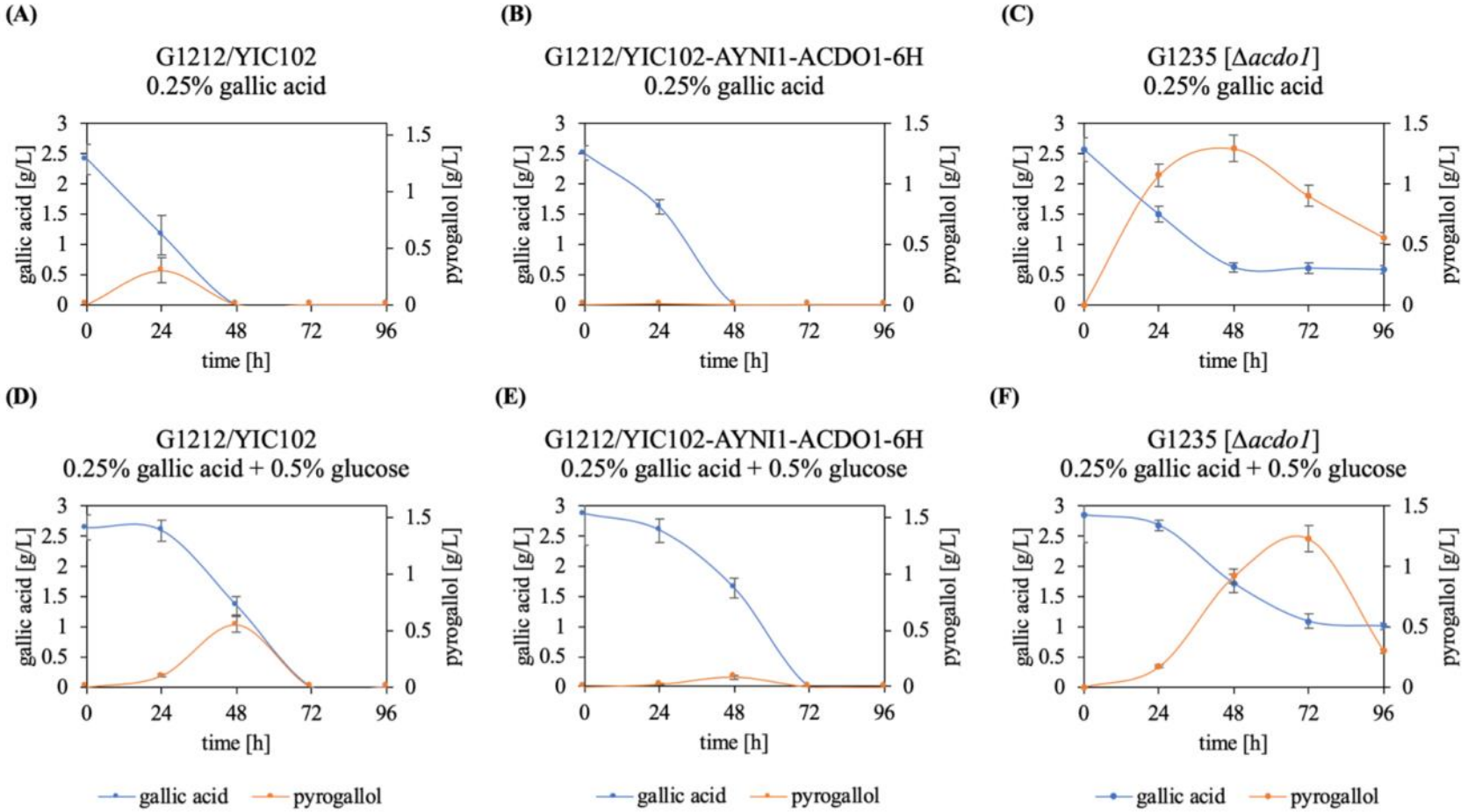

Figure 67 GC-MS analysis of substrate – product conversion during cultivation of *A. adeninivorans* on gallic acid.
A. adeninivorans G1212/YIC102 **(A,D)**; *A. adeninivorans* G1212/YIC102-AYNI1-ACDO1-6H **(B,E)**; *A. adeninivorans* G1235 [Δ*acdo1*] **(C,F)**.Strains were cultivated on YMM-$NaNO_3$ supplemented with 0.25 % gallic acid **(A,B,C)** or with 0.25 % gallic acid plus 0.5 % glucose **(D,E,F)**.

4.4 Expression of gallic acid decarboxylase (Agdc1p) and catechol-1,2-dioxygenase (Acdo1p) in *Saccharomyces cerevisiae*

Strain EYS4958 from the strain collection of the Biotech company EVOLVA was selected to create new *S. cerevisiae* strains using plasmids with *URA3* as selection marker. Genes encoding gallic acid decarboxylase (*AGDC1*) and catechol-1,2-dioxygenase (*ACDO1*) were amplified from genomic DNA of *A. adeninivorans* strain LS3 by PCR reaction, cloned into the plasmids from the EVOLVA collection and expressed in *S. cerevisiae.* Two type of plasmids (ARS/CEN and 2μ) were used for the cloning procedures. Genes were expressed in three combinations:

a) eGFP-tagged genes – enabling visualization and localization of proteins
b) untagged genes
c) His-tagged genes – enabling protein purification

4.4.1 Cellular localization of Acdo1-eGFP and Acdo1-eGFP in *S. cerevisiae*

The expression of heterologous eGFP-tagged genes enabled the localisation of *Arxula* enzymes in *S. cerevisiae*. Genes were expressed under control of the copper-inducible *CUP1* promoter. Final concentration of $CuSO_4$ in SC-Ura medium was 600 μM. Fluorescence analysis by confocal laser scanning microscopy (CLSM) confirmed that all transgenic strains had incorporated the pCUP1-GENE-eGFP construct. The GFP signals indicate that both Agdc1p and Acdo1p have a cytosolic distribution (**Figure 68**).

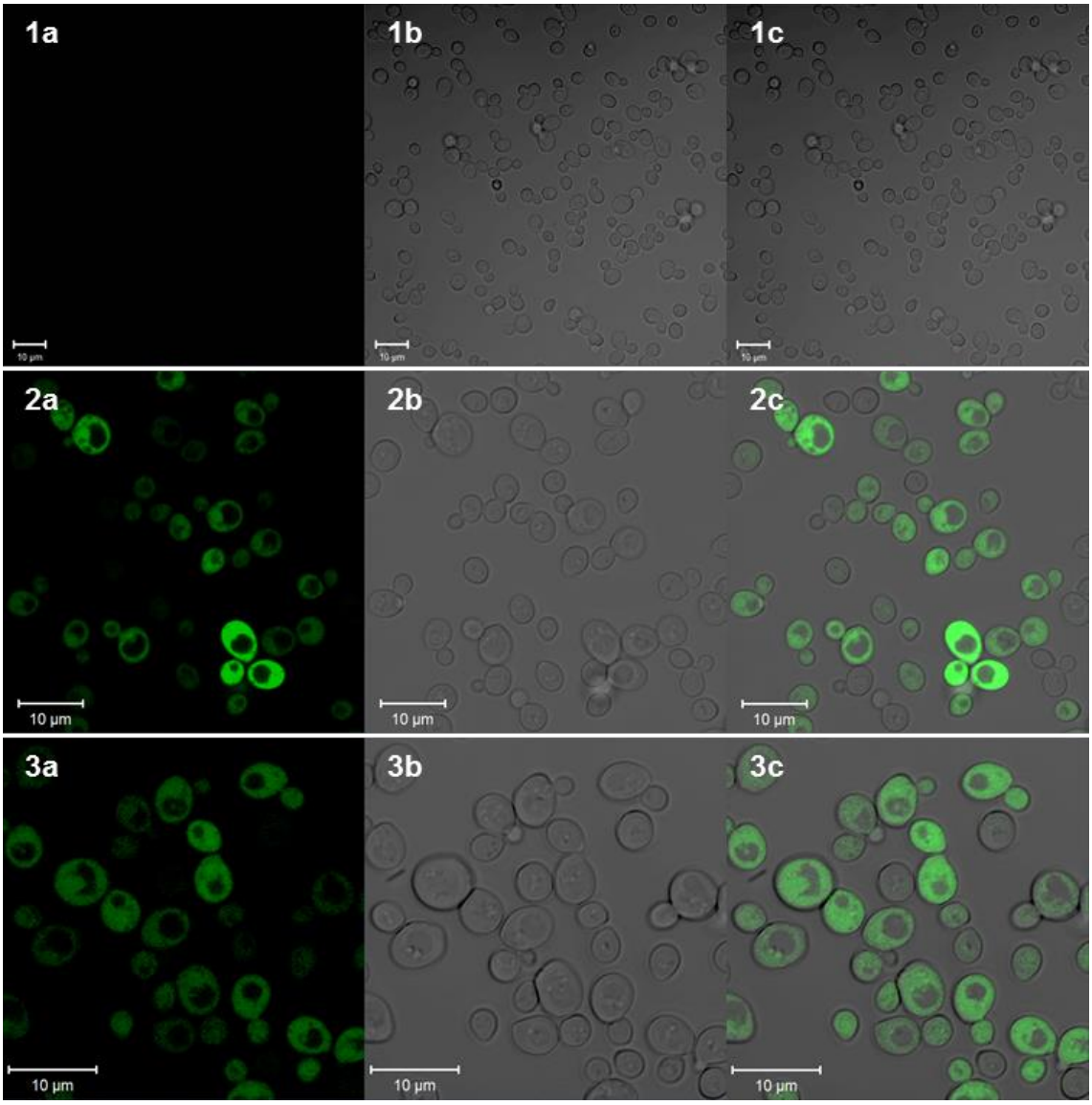

Figure 68 Subcellular localization of Agdc1-eGFP and Acdo1-eGFP in *S. cerevisiae*.
CLSM analysis shows a cytosolic distribution of GFP signals in transgenic *S. cerevisiae* strains expressing Agdc1p-eGFP **(2 a-c)** and Acdo1p-eGFP **(3 a-c)** but not in *S. cerevisiae* control strain **(1 a-c)**. Pictures were made under: fluorescence filter **(1 a, 2 a, 3 a),** bright light **(1 b, 2 b, 3 b)**, merged bright light and fluorescence filter **(1 c, 2 c, 3 c)**.

4.4.2 Screening of transgenic *S. cerevisiae* strains as potential producer for recombinant *Arxula* catechol-1,2-dioxygenase

Several *S. cerevisiae* strains were screened for the production of *Arxula* catechol-1,2-dioxygenase. According to SDS-PAGE analysis of crude extract, Acdo1p was present in all strains tested which was confirmed by Western blot of tagged proteins (**Figure 69**). Cells transformed with 2μ plasmid exhibited a higher expression rate of *ACDO1*. Catechol-1,2-dioxygenase activity was measured in crude extracts from *S. cerevisiae* cultures incubated for 24 h at 30 °C. Not only were recombinant proteins found to be active, higher activity was observed for strains containing the 2μ plasmid, indicating a higher level of expression (**Figure 70**). Further research is required not only to obtain more information about the biochemical properties and the optimal conditions of the recombinant *Arxula* catechol-1,2-dioxygenase expressed in *S. cerevisiae* but also to compare purity and yield to the results obtained with *A. adeninivorans*.

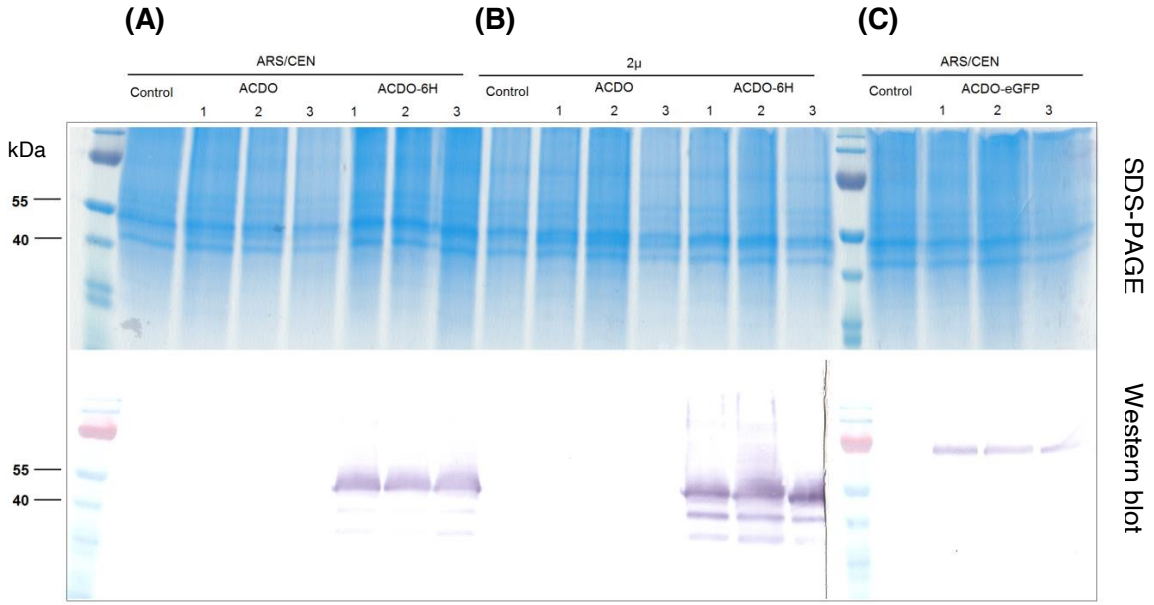

Figure 69 SDS-PAGE and Western blot analysis of catechol-1,2-dioxygenase production in crude extracts of transgenic *S. cerevisiae* strains expressing the *ACDO1* gene from *A. adeninivorans*. **(A)** *S. cerevisiae* transformed with ARS/CEN plasmid expressing *ACDO1* and *ACDO1-6H*; **(B)** *S. cerevisiae* transformed with 2μ plasmid expressing *ACDO1* and *ACDO1-6H*; **(C)** *S. cerevisiae* transformed with ARS/CEN plasmid expressing *ACDO1-eGFP*. Western blots were performed with primary anti-polyhistidine antibodies from rabbit **(A, B)** and anti-eGFP **(C)** and secondary antibodies anti-rabbit from goat.

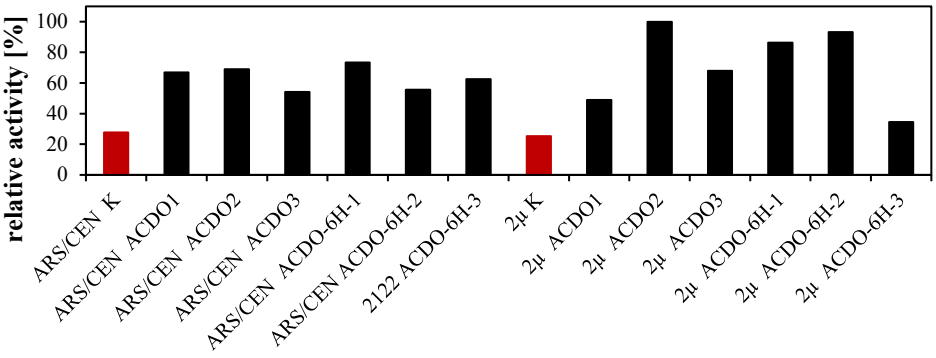

Figure 70 Screening of catechol-1,2-dioxygenase activity in transgenic *S. cerevisiae* strains with expression of *ACDO1* gene from *A. adeninivorans.*

4.4.3 Purification of recombinant Acdo1-6hp and Agdc1-6hp from *S. cerevisiae*

S. cerevisiae strains transformed with 2µ plasmid constructs containing the His-tag at the 3´-end of the respective ORF were selected for synthesis of recombinant Acdo1-6hp and Agdc1-6hp. Recombinant Acdo1-6hp and Agdc1-6hp was purified by Immobilized Metal Affinity Chromatography (IMAC). SDS-PAGE analysis showed a band for Acdo1-6hp (predicted molecular mass 37.76 kDa) around 40 kDa while Agdc1-6hp (predicted molecular mass 27,3 kDa) showed a band around 27 kDa (**Figure 71**). Additional experiments will be required to define the efficiency of purification and further optimize the procedure conditions.

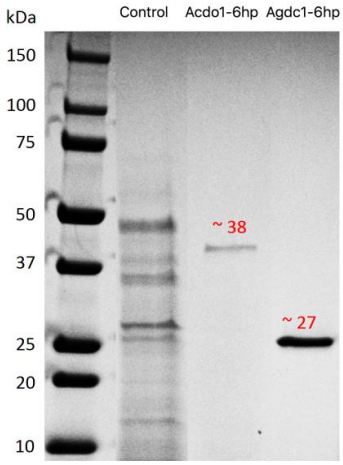

Figure 71 SDS-PAGE analysis of purified Acdo1-6hp and Agdc1-6hp produced by *S. cerevisiae*. Crude extract served as control.

5 Discussion

Petroleum products are far more than just fuel, they are also important feedstocks for the chemical and pharmaceutical industry. To this day, there is a big competition between fuels and chemical feedstocks for a share of oil production. Thus, the global economy strongly depends on fossil fuels, especially on oil, which have a huge influence on our daily life. Though the availability of fossil reserves is eventually limited, commercial production of many chemicals still rely on organic chemical synthesis, using petroleum-derivatives as starting material. On top of this, many of these substances, like benzene, are considered as environmental unfriendly (Frumkin *et al.*, 2009).

Nowadays people are more aware of the consequences posed by uncontrolled usage of fossil feedstocks. One solution would be to transform the chemical industry into a sustainable sector. Before this can be achieved, however, it is necessary to provide an attractive range of renewable carbon sources to replace fossil raw materials such as crude oil, natural gas and coal. Great emphasis is placed on research focusing on developing such “green” synthetic approaches as alternatives to traditional chemical synthesis. In the spotlight are microbial chemical factories which convert biomass into desired feedstock product(s). To this purpose, metabolic engineering is an indispensable tool not only to introduce heterologous or non-natural biosynthetic pathways into genetically advantageous microbial hosts but also to modify and improve existing microbial pathways. Genetic engineering has already become an integral part of the large scale resource-efficient production of specific enzymes (Lubick, 2010, Sun *et al.*, 2015).

Also, with biomass as feedstock, the ultimate goal is to achieve the highest possible concentrations of a given product in the shortest possible time. However, because of its non-well defined composition, the conversion of biomass is still a challenge. Prior knowledge of the biochemical pathways are just as important as selection of the microorganisms involved and defining culture conditions.

E. coli and *S. cerevisiae* are among the best studied and most widely used microorganisms in the biotechnological industry. Multiple improved strains with modified metabolic pathways or newly introduced heterologous pathways are in commercial use. Nonetheless, the spectrum of compounds produced is still rather limited and bioproduction of certain chemical compounds, like *cis,cis*-muconic acid, is still a challenge (Lin *et al.*, 2014, Wang & Zheng, 2015, Weber *et al.*, 2012, Curran *et al.*, 2013, Bruckner *et al.*, 2018).

The goal of the present project was to investigate the metabolic pathway with which the non-conventional yeast *A. adeninivorans* catabolizes tannin-rich biomass. Based on

whole genome sequencing (Kunze *et al.*, 2014), the annotated genes potentially encoding gallic acid decarboxylase (ARAD1C45804g) and catechol-1,2-dioxygenase (ARAD1D17798g), enzymes involved in tannin degradation pathway, were selected and investigated. To this purpose, the amino acid sequences of the Agdc1p and Acdo1p gene products were compared with the amino acid sequences of gallic acid decarboxylases and catechol-1,2-dioxygenases known from other microbial sources. Based on their similarity, potential conserved domains were identified and their putative influence on activity of the active centre as well as on enzyme stability was analyzed. The transformation/expression platform, Xplor®2 (Böer *et al.*, 2009b), which allows rapid and simple gene manipulations in *A. adeninivorans*, was used to construct recombinant strains showing overexpression of *AGDC1* and *ACDO1*. These recombinant enzymes were purified, their *in vitro* biochemical properties characterized, and optimal working conditions established. Moreover, corresponding knock-out mutants lacking *AGDC1* or *ACDO1* genes were created. Metabolite analysis of supernatants from recombinant knock-out mutants as well as control strains allowed it to establish the *in vivo* functions and to determine the enzymatic reactions carried out by these two enzymes. Expression analysis of *A. adeninivorans* wildtype LS3 shed light on the regulation of *AGDC1* and *ACDO1* as well as on the tannin degradation pathway. Finally, the microarray whole-genome gene expression dataset allowed the identification of transcripts and gene interactions taking part in the tannin degradation pathway. Based on these results, a first simple map of metabolic pathways was created for tannin degradation in *A. adeninivorans*. In a pilot experiment for possible future work, *AGDC1* and *ACDO1* genes were also successfully expressed in *S. cerevisiae* as the host cell.

The findings reported in this thesis are a contribution to the development of an innovative approach for the bioproduction of industrially relevant chemicals such as *cis,cis*-muconic acid, gallic acid, protocatechuic acid, catechol and pyrogallol by new microbial factories, as well as for the production of sought after enzymes.

5.1 Morphology of *A. adeninivorans* deletion mutants

During the work for this thesis it was demonstrated that deletion of the gene encoding for gallic acid decarboxylase causes changes in the morphology of *A. adeninivorans* cells. *A. adeninivorans* is a dimorphic microorganism but the exact physiological regulation of its dimorphism has remained elusive. So far, the only factor known to initiate a change of cell shape from budding cells to mycelia was a temperature above 42 °C. It is not clear

why the lack of gallic acid decarboxylase causes an identical change in morphology and it is also not known whether deletion of other enzymes may have a similar effect. Gallic acid decarboxylase plays a very important role in the metabolism of tannins and phenol derivatives. Since the latter substances are toxic for cells, lack of gallic acid decarboxylase may cause stress and changes in cell phenotype. However, in contrast to this hypothesis, deletion of catechol-1,2-dioxygenase as an enzyme also involved in tannin metabolism does not influence cells morphology. Alternatively, this enzyme may be somehow connected to a signalling pathway which is controlled by temperature, allowing mycelia to form at 30 °C. Possibly, the position of *AGDC1* in the genome is connected to a regulatory sequence affecting morphological changes of *A. adeninivorans*. However, further investigations and additional evidence are required to support this hypothesis. Finally, it is possible that this enzyme possesses other not yet known functions affecting the dimorphism of *A. adeninivorans*.

5.2 Gallic acid decarboxylase

Decarboxylation of hydroxylated aromatic acids has been reported for bacteria and fungi. A well-known example is the non-oxidative decarboxylation of gallic acid which leads to the synthesis of pyrogallol (Grant and Patel, 1969, Yoshida *et al.*, 1982, Li and Wang, 2015). The yeast *A. adeninivorans* LS3 has been described as a microorganism able to utilize hydroxylated aromatic acids such as tannic acid, gallic acid or protocatechuic acid as a sole source of carbon and energy (Sietmann *et al.*, 2010). The same authors also described the degradation of gallic acid, protocatechuic acid and 4-hydroxybenzoic acid by the LS3 wildtype strain. However, the enzymes involved were neither identified nor characterized.

Gallic acid decarboxylase is an enzyme of the tannic acid decarboxylase pathway that transforms gallic acid into pyrogallol and protocatechuic acid into catechol. The gallic acid decarboxylases described so far are known for their instability due to their high oxygen sensitivity. As a consequence, only some have been successfully purified (Jiménez *et al.*, 2013, Zeida *et al.*, 1998) and few have been partially characterized as most display a complete loss of activity after purification (Grant and Patel, 1969, Brune and Schink, 1992, Yoshida *et al.*, 2010).

In this thesis, gallic acid decarboxylase from *A. adeninivorans* fused with a C-terminal HisTag region (Agdc1-6hp) was successfully purified and characterized for the first time. Selection of appropriate buffer and pH were crucial for long term storage of purified

Agdc1-6hp without loss of activity. When present in crude extract, the enzyme lost 42% of its activity when stored for 5 days at 4 ºC. A similar loss in activity was reported by Zeida *et al.* (1998). Stored in 50 mM potassium phosphate buffer (pH 6.0), the purified enzyme retained 60 % activity after 9 days at 4 ºC. Best results were obtained when enzymes were stored at -80 °C (4.2.9.2). Under these conditions, activity remained virtually unaltered even after one-month storage. This shows that Agdc1-6hp can be stored for prolonged times without loss of activity.

With a measured molecular mass of approximately 27 kDa, gallic acid decarboxylase probably is a monomeric enzyme. This seems rather unusual since gallic acid decarboxylases from bacterial sources are always multimeric, consisting of up to six subunits (Zeida *et al.*, 1998, Jiménez *et al.*, 2013) while decarboxylases from *Bacillus megaterium* and *Clostridium hydroxybenzoicum* also possess a minimum two subunits (He and Wiegel, 1995, 1996, Omura *et al.*, 1998).

Several metal ions were tested as potential cofactors for Agdc1p. In the presence of most metal ions, enzyme activity was decreased with complete inhibition caused by Fe^{2+} and Ni^{2+}. In contrast to this, addition of DTT and ascorbic acid increased relative enzyme activity to 107 and 116 %, respectively, of the control activity. $Na_2S_2O_3$ used to stabilize gallic acid decarboxylases from *Pantotea agglomerans* T71 or *Lactobacillus plantarum* WCFS1 (Zeida *et al.*, 1998, Jiménez *et al.*, 2013) did not show any stabilization effect on Agdc1p. Instead, enzyme activity went down by 85 %. On the other hand, addition of EDTA caused a rise in relative activity to 146% which is in stark contrast to the inhibitory effect EDTA has on gallic acid decarboxylase from *P. agglomerans* T71 (Zeida *et al.*, 1998).

Because the purification procedure was carried out on Ni Sepharose column, it is possible that the EDTA does not directly affect the enzyme but acts by chelating the nickel residues after purification which could have inhibitory effects on the enzyme activity. However, it is also possible that EDTA positively affects the enzyme.

In vitro investigation of kinetic and substrate specificity of Agdc1-6hp indicated that the enzyme affinity for gallic acid (K_m 0.7 $\pm$ 0.2 mM) is four times higher than that for protocatechuic acid (K_m 3.2 $\pm$ 0.2 mM). In comparison, gallic acid decarboxylase from *P. agglomerans* T71 has a K_m for gallic acid of 0.96 mM (Zeida *et al.*, 1998). Most gallic acid decarboxylases have a limited substrate spectrum (He and Wiegel, 1995, 1996, Zeida *et al.*, 1998). Gallic acid is the only known substrate for gallic acid decarboxylase from *P. agglomerans* T71 (Zeida *et al.*, 1998) while the 3,4-dihydroxybenzoate decarboxylase from *Enterobacter cloacae* P can decarboxylate protocatechuic acid but not gallic acid (Yoshida *et al.*, 2010). Whether Agdc1-6hp is able to *in vitro* decarboxylate

hydroxylated aromatic acids other than gallic acid and protocatechuic acid has not been confirmed.

5.3 Catechol-1,2-dioxygenase

The delocalization of π orbitals makes aromatic compounds very stable (Greń *et al.*, 2010). The degradation of aromatic compounds is therefore greatly facilitated by ring-cleavage. Ring fission by oxygenases is considered as the main strategy in the degradation of aromatic structures (Zhang *et al.*, 2012, Fetzner, 2012, Hu and Wu, 2012). Depending on the exact position of cleavage, two groups of dioxygenases are distinguished: intradiol and extradiol dioxygenases. Both belong to the metalloenzymes containing a non-heme iron which plays a crucial role in the binding and activating of dioxygen in the cleavage reaction. While catechol-1,2-dioxygenases use Fe^{3+} as a cofactor, catechol-2,3-dioxygenase uses Fe^{2+} (Cox and Que, 1988, Vetting and Ohlendorf, 2000, Murakami *et al.*, 1997, Briganti *et al.*, 2000b).

In the *A. adeninivorans* genome, a single gene could be annotated as catechol-1,2-dioxygenase. Protein sequence alignment to catechol-1,2-dioxygenase sequences from *Candida albicans* (P86029), *Acinetobacter baylyi* (P07773), *Acinetobacter lwoffii* (O33948), *Acinetobacter lwoffii* (O33950), *Acinetobacter guillouiae* (Q43984), *Rhodococcus erythropolis* (P96984), *Rhodococcus opacus* (P95607), *Burkholderia* sp. (Q8GAY6), *Pseudomonas putida* (A7LBQ4) exhibited 19 identical and 31 similar positions in the sequences.

Catechol-1,2-dioxygenase belongs to the family of intradiol dioxygenases, forming dimers with identical or similar structures $(\alpha Fe^{3+})_2$. Analysis of the *A. adeninivorans* catechol-1,2-dioxygenase protein sequence revealed the presence of conserved metal binding sites (Tyr171, Tyr205, His229, His231). The iron ions within the enzyme structure play an important role for the correct enzyme function. The essential step in the catalytic reaction of catechol-1,2-dioxygenase is the electrophilic attack of molecular oxygen on iron (III)-bound catecholate, whereas the nucleophilic attack of the aromatic π electrons of the iron (III)-bound catecholate on the oxygen molecule is an important step in the cleavage reaction (Matera *et al.*, 2010).

Based on crystal structure studies of catechol-1,2-dioxygenase from *Acinetobacter* sp. it was possible to create a structural model of Acdo1p (**Figure 41**). The subunits are connected with helical zipper motifs. Vetting and Ohlendorf (2000) described the unique helical N-terminal domain of catechol-1,2-dioxygenase from *Acinetobacter calcoaceticus*

ADP1. Sequence alignments indicate that this helical domain is conserved among all members of the catechol-1,2-dioxygenase class. The enzyme from *Acinetobacter calcoaceticus* ADP1 is composed of α helices and β sheets and can be divided into one central linker domain composed of several helices and two catalytic domains at each end of two β sheets of mixed topologies. The 3D model of Acdo1p created here exhibited a very similar enzyme structure.

According to literature, catechol-1,2-dioxygenase subunits contain two molecules of phospholipids bound into a hydrophobic cavity at the dimeric interface (Briganti *et al.*, 2000b, Ferraroni *et al.*, 2006, Earhart *et al.*, 2005, Wang *et al.*, 2006, Guzik *et al.*, 2011, Matera *et al.*, 2010, Caposio *et al.*, 2002, Sauret-Ignazi *et al.*, 1996, Gou *et al.*, 2009, Pandeeti and Siddavattam, 2011). The real role of these molecules is still discussed. It is possible that the phospholipid chains increase the local concentration of substrate and therefore modulate the activity of the enzyme. The lipids may also act as effector molecules. Binding of these molecules to the hydrophobic amino acids of the active site may induce a conformational change. Alternatively, enzyme molecules may alter the phospholipid bilayer as a protection response to toxic levels of aromatic compounds (Vetting and Ohlendorf, 2000, Ferraroni *et al.*, 2006). Nevertheless, the presence of phospholipids and their eventual role for *A. adeninivorans* catechol-1,2-dioxygenase still have to be confirmed. To ultimately unravel the tertiary structure of Acdo1p, more research, especially in the field of crystallography, is necessary.

The *in vitro* analysis of *Arxula* catechol-1,2-dioxygenase properties was possible thanks to the construction of the *A. adeninivorans* strain G1212/YIC102-AYNI1-ACDO1-6H, overproducing recombinant protein with a C-terminal HisTag (Acdo1-6hp). The enzyme was successfully purified and characterized. SDS-PAGE and Western Blot analysis confirmed a predicted molecular mass of 37.76 kDa for the denatured protein. Size exclusion chromatography of the native protein showed a molecular mass of 79.67 kDa thus indicating that Acdo1-6hp is a dimeric protein, similar to most catechol-1,2-dioxygenases (Briganti *et al.*, 1997, Strachan *et al.*, 1998, Potrawfke *et al.*, 2001, Tsai and Li, 2007). Similar to other catechol-1,2-dioxygenases, optimum pH for *Arxula* catechol-1,2-dioxygenase is between pH 7 – 8.5 with highest activity measured at pH 7.5 (Briganti *et al.*, 1997, Guzik *et al.*, 2013, Camargo *et al.*, 2012, Wang *et al.*, 2001).

Acdo1-6hp can be stored for prolonged time at temperatures up to 30 °C without losing activity. Even at 40 °C, activity initially remains stable before gradually declining after 7 h of incubation. At 50 °C, enzyme activity rapidly declined with just 40 % left after 2h. This behaviour was also observed in *Candida albicans* TL3 (Tsai & Li, 2007). Purified Acdo1-6hp, stored at 4 °C in PBS buffer pH 7.4, retained 99 % activity after 55 days. In

contrast, stored as crude extract at 4 °C, the enzyme loses 60 % of initial activity within 2 days. A similar behaviour was reported for catechol-1,2-dioxygenases from *Acinetobacter radioresistens* (Briganti *et al.*, 1997) and *Rhodococcus rhodochrous* NCIMB 13259 (Strachan *et al.*, 1998). Freezing of the enzyme, however, results in complete loss of activity.

A number of potential cofactors, mainly metal ions, were tested for their ability to influence Acdo1-6hp activity. Strongest inhibiting effect was exerted by $AlCl_3$ and $ZnSO_4$. However, also the commercial protease inhibitor cocktail (cOmplete™, EDTA-free Protease Inhibitor Cocktail) initially used during the purification procedure almost completely abolished enzyme activity. This is a reminder that protease inhibitors for the purification procedure have to be selected with care. Addition of iron salts to the reaction mixture also had a negative impact on Acdo1-6hp activity. In general, sulphate salts, with the exception of manganese-sulphate, increased activity of catechol-1,2-dioxygenase more effective than chloride salts. The minor (<10 %) increase in Acdo1-6hp activity observed in the presence of $MgCl_2$, $CaSO_4$ and $CaCl_2$ make it doubtful whether these substances had any effect at all.

Of the hydroxylated aromatic compounds used in a substrate specificity test, catechol-1,2-dioxygenase was only able to degrade catechol, pyrogallol and hydroxyquinol. Additionally, degradation of catechol leads to the production of *cis,cis*-muconic acid which indicates that Acdo1-6hp is an intradiol dioxygenase and is not able to cut the aromatic ring in position 3,4. This shows that gallic acid decarboxylase and catechol-1,2-dioxygenase require a similar conformation of constituents for proper function (

Figure *72*). The kinetic parameters of the *in vitro* degradation of catechol and pyrogallol by catechol-1,2-dioxygenase revealed a 25-times higher affinity for catechol (K_m 0.004 ± 0.001 mM) than for pyrogallol (K_m 0.1 ± 0.02 mM). In comparison, the K_m value for the enzyme from *Candida albicans* TL3 is 9.3 μM, that of *Rhodococcus rhodochrous* NCIMB13259 is 1.1 μM and for *Stenotrophomonas maltophilia* KB2 a K_m 12.18 μM has been reported (Guzik *et al.*, 2013, Strachan *et al.*, 1998, Tsai and Li, 2007). Although these latter K_m values were obtained with non-pyrogallol substrates, several studies indicate (Wang *et al.*, 2006, Fujiwara *et al.*, 1975, Mayer and Que, 1984) that pyrogallol may be a general substrate for all catechol-1,2-dioxygenases.

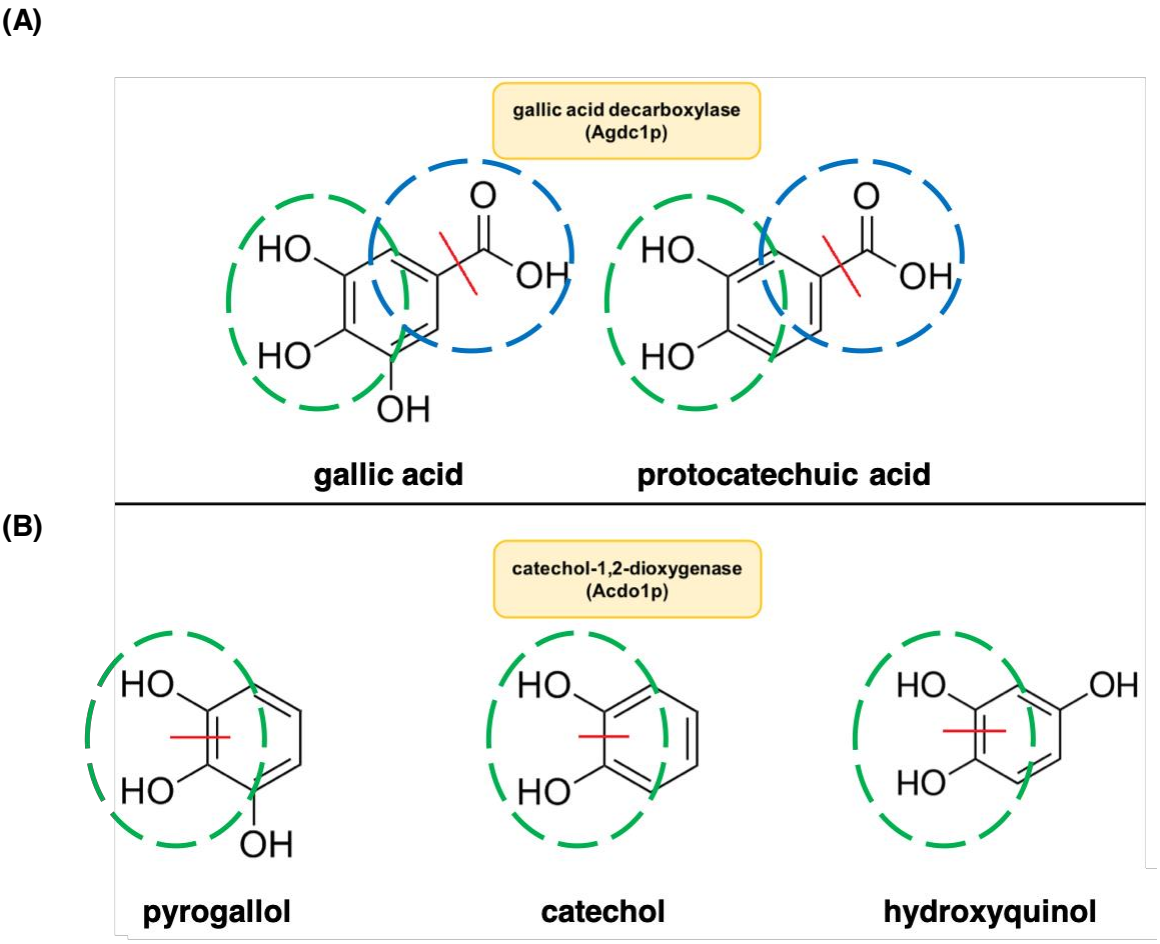

Figure 72 Hydroxyl group conformation required for enzymatic activity of gallic acid decarboxylase and catechol dioxygenase.
(A) Hydroxyl and carboxyl group_position in the aromatic ring required for decarboxylation of hydroxylated aromatic acids by Agdc1-6hp (green dotted circle – -OH group positions; blue dotted circle – -COOH group position) with cleavage position shown as red line. **(B)** Hydroxyl group position in the aromatic ring required for oxidation of hydroxylated aromatic compounds by Acdo1-6hp (green dotted circle – -OH group positions) with cleavage position shown as red line.

5.4 Expression of *AGDC1* and *ACDO1* in *A. adeninivorans*

Enzymes involved in the catabolism of gallic acid and its derivatives, including most reaction products, are considered to be encoded by inducible genes. This means that exposition of microorganisms to different phenolic compounds leads to regulated induction of enzyme transcription. By ensuring that enzymes are only produced when substrates are present microorganisms optimize their energy consumption.

During cultivation of the *A. adeninivorans* control strain G1212/YRC102 on YMM-glucose-$NaNO_3$, gallic acid decarboxylase activity was absent. This suggests that Agdc1p is an enzyme encoded by an inducible gene. Nested qRT-PCR assays

confirmed the inducibility of the *AGDC1* gene in the presence of gallic acid or protocatechuic acid. In contrast, glucose and other selected hydroxybenzoic acid compounds were not able to induce the *AGDC1* gene. The most vigorous gallic acid degrading microorganisms contain inducible *GDC* genes (Jiménez *et al.*, 2013, Reveron *et al.*, 2015, Li and Wang, 2015, Gauri *et al.*, 2013, Yoshida and Yamada, 1985, O'Donovan and Brooker, 2001). An exception to this rule is *Klebsiella aerogenes* where decarboxylation of gallic acid, protocatechuic acid and 2,5-dihydroxybenzoic acid were shown to be constitutive (Grant and Patel, 1969).

When *A. adeninivorans* control strain G1212/YIC102 and overexpression strain G1212/YIC102-AYNI1-ACDO1-6H were cultivated on YMM-glucose-$NaNO_3$, catechol-1,2-dioxygenase activity was only detected in G1212/YIC102-AYNI1-ACDO1-6H. This finding indicating that Acdo1p is also an enzyme encoded by an inducible gene was subsequently confirmed by nested qRT-PCR assay. Similar to *AGDC1*, the *ACDO1* gene was also found to be induced by the presence of gallic acid and protocatechuic acid, the direct precursors of pyrogallol and catechol in the tannic acid metabolic pathway of *Arxula*. For both genes *AGDC1* and *ACDO1*, highest relative induction levels were observed after 8 h cultivation. The relative expression level of *AGDC1* was almost identical for both substrates, whereas in case of *ACDO1* the relative expression level for protocatechuic acid was approximately 86 % lower than that for gallic acid. The promotors of *AGDC1* and *ACDO1* share no identical sequences. It is therefore possible that they are activated differently by specific regulatory proteins. Glucose and other hydroxylated aromatic acids tested did not show any positive effect on *ACDO1* expression. A similar result was also found for *Arxula* gallic acid decarboxylase, where non-substrate substances had no effect on gene expression. Induced expression by the presence of enzyme substrates seems to be a common feature of most recently identified genes encoding catechol-1,2-dioxygenases (Wojcieszyńska *et al.*, 2011, Suzuki *et al.*, 2002, McFall *et al.*, 1998).

5.5 The role of Agdc1p in *Arxula* tannic acid degradation pathway

A. adeninivorans tolerates as much as 2 % (w/v) gallic acid. However, regardless of the gallic acid concentration the growth curves always exhibit long lag phases. Since gallic acid is a weak acid, its presence results in lowering of the pH of the culture medium. It was found that adding 1 % (w/v) gallic acid to the YMM-glucose-$NaNO_3$ medium will cause a drop in pH from 6.1 to 3.8. At this latter pH, gallic acid is undissociated and can go across the yeast cell membrane. As the higher pH of the cell interior causes the gallic acid to dissociate again, the pH_i can fall below the physiological range of the cell and thus interferes with homeostasis. This feature gives hydroxylated aromatic acids their antimicrobial properties, generating cell stress, extending the lag phase and inhibiting cell growth (Restaino *et al.*, 1982, Noda *et al.*, 1982, Ibraheem and Ndimba, 2013, Beales, 2004) . Similar effects are caused by protocatechuic acid.

Cultivation of *A. adeninivorans* in a medium with a constant pH 6 (optimal for growth of *A. adeninivorans*) showed that cells were unable to degrade gallic acid resulting in cell death (data not showed). The overexpression of *AGDC1* did not shorten the lag phase or increase the cell growth period significantly over 144 h (**Figure 36**). In comparison to cultures grown on glucose, Agdc1p activity was lower and the enzyme appeared later when cells were cultivated on gallic acid. These results suggest the existence of a stress response at the level of gene expression generated by gallic acid. A long log phase seen when cells were cultivated on gallic acid was also observed when gallic acid was replaced by other hydroxylated aromatic acids (**Figure 37**).

Cells of the *AGDC1* deletion strain G1234 [Δ*agdc1*] died when cultivated on gallic acid, suggesting the presence of a single pathway only to degrade gallic acid. This is supported by extracellular metabolite analysis of the *A. adeninivorans* control strain G1212/YRC102, which revealed formation of only pyrogallol. According to Sietmann *et al.* (2010), oxidative and non-oxidative decarboxylation of protocatechuic acid occur simultaneously in *A. adeninivorans*. This is confirmed by the fact that the deletion strain G1234 [Δ*agdc1*] was still able to grow on 0.2% protocatechuic acid with a 24 h shorter lag phase compared to the control strain (**Figure 37**).

Analysis of the metabolites in the culture medium showed that both control and *AGDC1* overexpression strain G1212/YIC102-AYNI1-ACDO1-6H produced catechol and *cis,cis*-muconic acid next to trace amounts of 3-hydroxybenzoic acid, 4-hydroxybenzoic acid, 1,4-dihydroxybenzene and 1,2,4-benzentriol.

The present investigations have confirmed that degradation of protocatechuic acid involves gallic acid decarboxylase and other enzymes. Cultivation of the deletion strain

G1234 [Δ*agdc1*] on media containing different hydroxylated aromatic acids as the sole source of carbon revealed that only cultivation on gallic acid led to cell death (**Figure 37**). This indicates that gallic acid decarboxylase is the key enzyme in the degradation of gallic acid by *A. adeninivorans*. It was also established that all of the tested aromatic acids with the exception of 2,3-dihydroxybenzoic acid can serve as sole source of carbon for *A. adeninivorans*. However, the first degradation step is not carried out by gallic acid decarboxylase. Considering all aspects of growth and gene expression analysis, it appears that the tannic acid degradation pathway is used exclusively for tannins and gallic acid. Though protocatechuic acid can also be degraded by this pathway, other aromatic acids are degraded through (a) separate pathway(s).

Overexpression of *AGDC1* did lead to an accumulation of extracellular pyrogallol when cells were cultivated on glucose and gallic acid with a yield similar for control and *AGDC1* overexpression strain. A reason could be that most extracellular pyrogallol accumulates in the first 24 h of cultivation. During this time, the gallic acid places the cells under strong stress conditions, resulting in low gene expression and low recombinant enzyme content. It is conceivable that pre-adaptation of cells on low gallic acid concentration may increase the yield of pyrogallol in the *AGDC1* overexpression strain. Increasing the yield of extracellular pyrogallol requires additional engineering of *A. adeninivorans* and further optimization of cultivation conditions. Unexpectedly, the *AGDC1* overexpression strain generated an accumulation of *cis,cis*-muconic acid. A yield increase of 71.2 % over the control suggests that *A. adeninivorans* could be an efficient producer of this molecule which is difficult to synthesize. This exciting possibility should endorse further investigations.

5.6 The role of Acdo1p in the *Arxula* tannic acid degradation pathway

Aromatic acids are an important source of carbon and energy for soil-dwelling microorganisms. Accumulation of these compounds is mainly the result of the degradation of plant-derived molecules, including lignin. As already mentioned, oxygenases play a crucial role in the catabolism of aromatic compounds, because they are responsible for the conversion of aromatic rings into aliphatic structures. The most intensively studied aromatic degradation pathway in microorganisms is the β-ketoadipate pathway which is a key metabolic pathway involved in the catabolism of the aromatic compounds protocatechuate and catechol (Harwood and Parales, 1996). These

compounds are further degraded by catechol-1,2-dioxygenase and protocatechuate-3,4-dioxygenase, respectively.

In the *A. adeninivorans* genome, a single catechol-1,2-dioxygenase (Acdo1p) has been annotated. *In vitro,* Acdo1p is specific for the ortho ring fission of pyrogallol, catechol and hydroxyquinol. To investigate the *in vivo* role of Acdo1p in tannin catabolism by *A. adeninivorans,* a deletion mutant strain, G1235 [Δ*acdo1*] as well as an overexpressing *ACDO1* strain (G1212/YIC102-AYNI1-ACDO1-6H) were constructed.

Overexpression of *ACDO1* did not affect the growth behaviour of *A. adeninivorans* cells, growing on HMM-$NaNO_3$ supplemented with 0.25 % gallic acid or 0.25 % protocatechuic acid, with or without 0.5% glucose as the sole source of carbon (**Figure 64**). The deletion mutant G1235 [Δ*acdo1*] which did not grow on medium supplemented with only gallic acid or protocatechuic acid as the sole source of carbon showed growth for 24 h when 0,5% glucose was added (**Figure 64 B,E**). This confirms the importance of Acdo1p in the catabolism of at least these two hydroxylated aromatic acids.

GC-MS analysis of the supernatant revealed that when gallic acid was the sole source of carbon, it was completely metabolized by control and overexpression strain G1212/YIC102-AYNI1-ACDO1-6H within 48 h of cultivation, whereas incomplete metabolization was measured for the deletion mutant (**Figure 67**). Supplementing glucose as an additional carbon source delayed the degradation of gallic acid by about 24 h. In the medium of control and deletion mutant strain the only degradation product detected was pyrogallol. Further degradation of pyrogallol by G1235 [Δ*acdo1*] was very slow as a consequence of which it could be detected during the whole cultivation process (**Figure 67 C,F**). The culture medium of overexpression strain G1212/YIC102-AYNI1-ACDO1-6H contained only trace amount of pyrogallol, indicating a significantly accelerated degradation process (**Figure 67 B,E**). Brune & Schink (1992) proposed the phloroglucinol pathway for the anaerobic degradation of gallic acid by *Pelobacter acidigalici*. In this pathway, the first reaction step which involves gallic acid decarboxylase (like in *A. adeninivorans*) is followed by a second reaction step by pyrogallol transhydrolase accomplishing the degradation of pyrogallol. A similar pathway for the degradation of gallic acid seems unlikely for *A. adeninivorans* for various reasons. First, *A. adeninivorans* is an aerobic microorganism and in aerobic conditions oxygenase reactions are preferred. Further, *in vitro* analysis confirmed the affinity of Acdo1-6hp for pyrogallol and nested quantitative RT-PCR as well as microarray analysis confirmed the induction of *Arxula* catechol-1,2-dioxygenase by gallic acid. When Sietmann *et al.* (2010) investigated pyrogallol transformation by wild type *A. adeninivorans* by GC-MS analysis, they detected a product showing similarities with *cis,cis*-muconic acid. They proposed 2-

hydroxymuconic acid as a transformation product which fits to our *in vitro* enzyme analysis of purified Acdo1-6hp. Therefore, although pyrogallol degradation products were not identified, a conversion into 2-hydroxymuconic acid remains most likely. However, an enzyme responsible for the further degradation of 2-hydroxymuconic acid has not been identified. Also, a possible spontaneous isomerization of 2-hydroxymuconic acid into oxalocrotonate puts a small questionmark at the proposed tannic acid degradation pathway (**Figure 30**). Further investigations will be indispensable to identify these so far elusive degradation products.

A. adeninivorans gallic acid decarboxylase is involved in the decarboxylation of both gallic acid and protocatechuic acid. Degradation of the latter compound produces catechol. Investigations of the *in vivo* role of Agdc1p in *A. adeninivorans* revealed that removal of the carboxylic group is not the only path for the degradation of protocatechuic acid (**Figure 35, Figure 37**). The culture media of the strains G1212/YIC102, G1212/YIC102-AYNI1-ACDO1-6H and G1235 [Δ*acdo1*] grown on HMM-$NaNO_3$ supplemented with 0.25 % protocatechuic acid or 0.25 % protocatechuic acid and 0.5 % glucose were screened by means of GC-MS analysis for the presence of possible protocatechuic acid degradation products. The reaction products detected during cultivation of control strain G1212/YIC102 and overexpression strain G1212/YIC102-AYNI1-ACDO1-6H were catechol, *cis,cis*-muconic acid and 3-hydroxybenzoic acid. Compared to the control strain, the medium of the overexpressing strain contained significantly less catechol and *cis,cis*-muconic acid and slightly more 3-hydroxybenzoic acid. This indicates that overexpression of *ACDO1* accelerates the turn-over of protocatechuic acid, thus resulting in a lower accumulation of reactions products in the culture medium. An accelerated degradation of protocatechuic acid into catechol and *cis,cis*-muconic acid accounts for the decrease of extracellular 3-hydroxybenzoic acid concentration. The maximum concentration of *cis,cis*-muconic acid was similar for both strains but the time course of accumulation differed, most clearly during culture on medium containing protocatechuic acid and glucose as carbon sources. While in the overexpressing strain accumulation of *cis,cis*-muconic acid started after 24 h of cultivation, in the control strain it started after 48 h cultivation (**Figure 65 D,E**).

In most cases 3-hydroxybenzoic acid was detected approximately 24 h after the first detection of catechol. However, in the overexpression strain cultivated on 0.25 % protocatechuic acid, production of 3-hydroxybenzoic acid and catechol started simultaneously.

Degradation of protocatechuic acid by the G1235 [Δ*acdo1*] deletion mutant was incomplete when this served as the sole source of carbon. In the supernatant, catechol,

hydroxyquinol and trace amounts of 3-hydroxybenzoic acid were found. The catechol produced remained in the culture medium when glucose was absent, while in the presence of glucose a slow decrease in catechol content began after 72 h. An accumulation of catechol (or pyrogallol in case of gallic acid as a substrate) may slowdown cells growth in culture medium. C*is,cis*-muconic acid was not detected in the G1235 [Δ*acdo1*] culture medium.

These results indicated that degradation of protocatechuic acid through catechol in *A. adeninivorans* is the preferable but not the only metabolic route. The normal microbial strategy of direct ring cleavage of protocatechuic acid has to be excluded. An alternative route leads to the production of 3-hydroxybenzoic acid. We propose that 3-hydroxybenzoic acid can be further converted to gentisic acid (2,5-dihydroxybenzoic acid) by monooxygenase reaction and is probably further degraded through the gentisate pathway. Using *A. adeninivorans* CBS8244, Middelhoven *et al.* (1992) observed that cultivation with 3-hydroxybenzoic acid resulted in a high activity of specific 3-hydroxybenzoate monooxygenase(s) converting this substrate into gentisic acid. Microarray analysis did not allow us the identification of candidate enzymes converting 3-hydroxybenzoic acid into gentisic acid. The reason can be incomplete gene annotations of the *A. adeninivorans* genome. However, a gene annotated as gentisate dioxygenase (ARAD1C08646g) is probably also involved in the ring cleavage of gentisic acid with maleylpyruvate as a reaction substrate. However, this hypothesis has yet to be confirmed.

The strains of *A. adeninivorans* displayed a similar growth behaviour when cultivated on 3-hydroxybenzoic acid and 2,5-dihydroxybenzoic acid as the only source of carbon (**Figure 37**). Enzymatic conversion of 3-hydroxybenzoic acid into protocatechuic acid catalyzed by 3-hydroxybenzoate 4-monooxygenase (3-hydroxybenzoate 4-hydroxylase) is known from bacterial and fungal strains such as *Pseudomonas testosterone* and *Aspergillus niger* (Michalover and Ribbons, 1973, Premkumar *et al.*, 1969). The reaction is known to be reversible but the main role of this enzyme, however, is to introduce 3-hydroxybenzoic acid into the protocatechuic acid catabolic pathway. In the case of *A. adeninivorans*, it is not really clear which enzyme is responsible for the opposite reaction, i.e. introducing protocatechuic acid into the gentisate pathway. The gentisate pathway is one of the most important pathways in the catabolism of a large number of aromatic compounds, among others 3-hydroxybenzoic acid. The pathway has been found in species like *Corynebacterium glutamicum*, *Trichosporon cutaneum*, *Burkholderia xenovorans* or *Candida parapsilosis* (Middelhoven *et al.*, 1992, Romero-Silva *et al.*, 2013, Anderson and Dagley, 1980, Chao and Zhou, 2013).

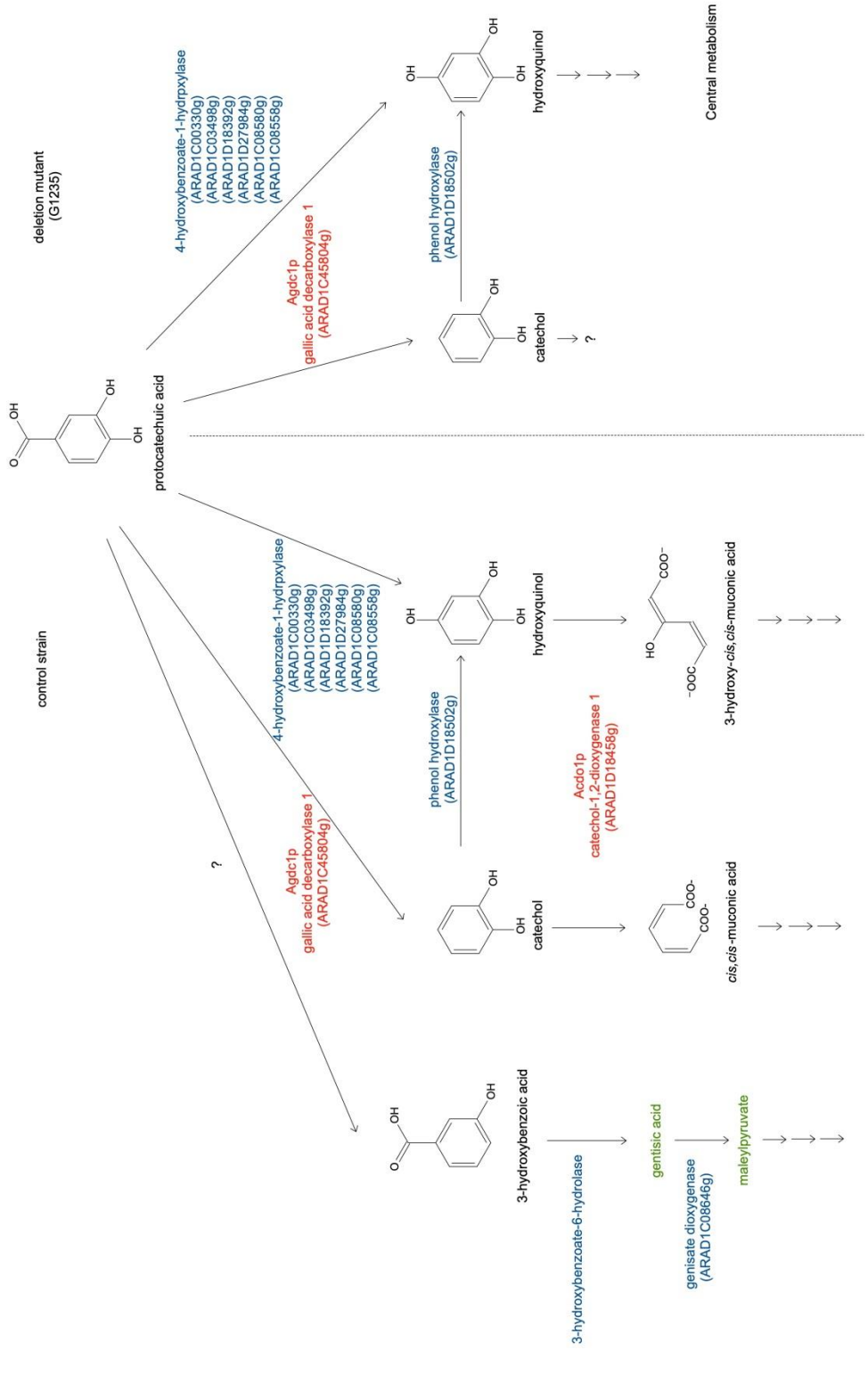

Figure 73 Proposed pathway for the degradation of protocatechuic acid in *A. adeninivorans* control strain (left) and deletion mutant (right). Scheme shows compounds detected by GC-MS analysis; proposed compounds in further degradation steps are in green, proposed enzymes involved in putative reactions are in blue. Agdc1p = gallic acid decarboxylase, Acdo1p = catechol-1,2-dioxygenase are in red.

Deleting the gene encoding catechol-1,2-dioxygenase from the *A. adeninivorans* genome caused the accumulation of hydroxyquinol but not of 3-hydroxybenzoic acid in the culture medium. Hydroxyquinol has also been detected in the supernatant of *A. adeninivorans* LS3 cultures (Sietmann *et al.*, 2010), indicating a simultaneous oxidative and non-oxidative decarboxylation of protocatechuic acid. The oxidative decarboxylation of protocatechuic acid through hydroxyquinol was already described for the pathogenic yeasts *Candida parapsilosis* and *Rhodotorula rubra* (Eppink *et al.*, 1997, Holesova *et al.*, 2011). GC-MS analysis of supernatant metabolites showed trace amounts of hydroxyquinol in case of the *A. adeninivorans* control strain. Microarray data analysis pointed to ARAD1C00330g as the gene encoding 4-hydroxybenzoate 1-hydroxylase converting protocatechuic acid into hydroxyquinol. However, a number of candidate enzymes converting protocatechuic acid into hydroxyquinol, annotated as potential 4-hydroxybenzoate-1-hydroxylase ARAD1C03498g, ARAD1D18392g, ARAD1D27984g, ARAD1C08580g and ARAD1C08558g have been identified. Another selected gene annotated as phenol hydroxylase, ARAD1D18502g, is probably also involved in this degradation pathway and catalyzes conversion of hydroxyquinol into catechol. Further research is needed to find out whether the degradation pathways of 3-hydroxybenzoic acid and hydroxyquinol overlap and whether gentisic acid is the intermediate for one or both of these compounds. A proposed pathway for the degradation of protocatechuic acid by *A. adeninivorans* is shown in **Figure 73**.

5.7 Microarray data analysis

Microarray data revealed genes involved in the degradation of gallic acid and protocatechuic acid. The genes *AGDC1* and *ACDO1* encode the first two enzymes involved in the degradation of gallic acid and protocatechuic acid. Cleavage products of the aromatic ring are ultimately degraded to pyruvate and acetaldehyde. The same occurs in *Eubacterium oxidoreducens* and *Pelobacter acidigallici* (Krumholz *et al.*, 1987, Brune and Schink, 1992). Genes encoding enzymes involved in the main tannic acid degradation pathway steps were identified as putative oxalocrotonate decarboxylase (ARAD1A15158g), 2-oxopent-4-dienoate hydrolase (ARAD1C00330g, ARAD1A09218g), 4-hydroxy-2-oxovalerate aldolase (ARAD1D17688g), aldehyde dehydrogenase (ARAD1D40656g, ARAD1D50424g and ARAD1C17776g), pyruvate carboxylase (ARAD1D32208g) and acyl-CoA synthetase (ARAD1A05764g). Upregulation by

protocatechuic acid was highest for genes related to the β-oxidation pathway with a particular high expression observed for β-ketoacyl-CoA thiolase which mainly catalyzes the final step in the β-oxidation pathway.

It is still an open question whether transporters are involved in the transport of gallic acid and protocatechuic acid into *A. adeninivorans* cells. Microarray data did not reveal any potential specific transporter for gallic acid and/or protocatechuic acid and literature on this topic is scarce. *A. adeninivorans* may not have specific transporters, which means that gallic acid cannot enter the cells at pH 6 because it is in the dissociated form. Alternatively, pH-dependent transporter(s) which are not specific for gallic/protocatechuic acid may exist. A list of potential transporter genes selected for further investigations is given in the Appendix. As a third hypothesis, specific transporter genes may be not yet annotated in the *Arxula* genome.

5.8 Expression of *AGDC1* and *ACDO1* in *S. cerevisiae*

Due to the high industrial demand for aromatic chemicals, several commercial microbial strains have been engineered for their production. The commercially relevant aromatic compounds catechol and pyrogallol as well as *cis,cis*-muconic acid can be synthesized via the shikimic acid pathway. In *E. coli* and *S. cerevisiae*, this pathway has been the target of diverse metabolic engineering strategies. Several limitations still exist, preventing the effective scaling up and commercialization of the created strains (Draths & Frost, 1994, Niu *et al.*, 2002, Gosset, 2009, Sun *et al.*, 2013, Lin *et al.*, 2014, Wang & Zheng, 2015, (Luttik *et al.*, 2008, Curran *et al.*, 2013, Bruckner *et al.*, 2018, Weber *et al.*, 2012). An important bottleneck in the shikimic acid pathway is the decarboxylase reaction converting protocatechuic acid into catechol.

A. adeninivorans is a good gene donor with successful expression in other species (Bui *et al.*, 1996a, 1996b). In this thesis it was demonstrated that *Arxula* gallic acid decarboxylase is specific to gallic acid and protocatechuic acid, whereas catechol-1,2-dioxygenase is specific to catechols pyrogallol and hydroxyquinol. The limitations regarding the expression of bacterial gallic acid decarboxylase in *S. cerevisiae* lead to the idea to express these enzymes in baker's yeast. This resulted in the successful expression of gallic acid decarboxylase (Agdc1p) and catechol-1,2-dioxygenase (Acdo1p). Tagged with eGFP, both enzymes showed a cytosolic distribution. Although both enzymes were purified, cultivation as well as purification procedures need to be optimized before large scale production of Agdc1p and Acdo1p in *S. cerevisie* can be

attempted. Nevertheless, the Acdo1p synthetized in *S. cerevisiae* by recombinant strains *S. cerevisiae*-2μ-ACDO1-2 and *S. cerevisiae*-2μ-ACDO1-6H-2 is active. In the case of Agdc1p synthetized in *S. cerevisiae*, enzyme activity has yet to be investigated. To improve the production of *cis,cis*-muconic acid and gallic acid in a strain of *S. cerevisiae*, Bruckner *et al.* (2018) solved the problem of low active, cofactor-depended gallic acid decarboxylase from *Klebsiella pneumoniae* by introducing *AGDC1* from *A. adeninivorans* instead. The enzyme was considered as active. Again, it will need additional studies to establish the enzyme activity, substrate specificity, optimal culture conditions as well as purification yields of Agdc1p or Acdo1p synthetized in *S. cerevisiae* to allow a comparison with the properties of enzymes synthetized in *A. adeninivorans*.

5.9 Conclusions

In this study, physiological and transcriptome analysis was used to unravel the catabolism of hydroxylated aromatic acids in *A. adeninivorans*. The results confirmed that the genes encoding enzymes involved in the catabolic pathway of gallic acid and protocatechuic acid are induced and that aromatic acid substrates are the inducers. The construction of gallic acid decarboxylase disruption mutants made it possible to prove that gallic acid decarboxylase (Agdc1p) is the only enzyme responsible for transformation of gallic acid. In contrast to this, investigations with catechol-1,2-dioxygenase disruption mutants showed that in the absence of Acdo1p an alternative pathway takes over the degradation of protocatechuic acid.

During the study of cell morphology, an additional difference was observed. While the Agdc1p deletion mutant G1234 [*Δagdc1*] transformed into mycelia at 30 °C, the Acdo1p deletion mutant G1235 [*Δacdo1*] remained a budding cell when grown at 30 °C.

Both the substrate specificity and capabilities for long-term storage without loss of activity make gallic acid decarboxylase (Agdc1p) and catechol-1,2-dioxygenase (Acdo1p) candidate enzymes for commercial use. The enzymes can have useful industrial applications e.g. in bioremediation processes or in chemical synthesis. Further culture optimization as well as strain engineering could also contribute to a more efficient conversion of protocatechuic acid to *cis,cis*-muconic acid. *A. adeninivorans* has proven itself to be a good alternative to *S. cerevisiae*, especially if chemical synthesis should be combined with bioremediation processes.

In addition, both Agdc1 and Acdo1p were also expressed in *S. cerevisiae*. As already described by Bruckner *et al.* (2018), replacement of the currently expressed gallic acid decarboxylase enzyme by the gene encoding Agdc1 enzyme from *A. adeninivorans* may help to improve the production of *cis,cis*-muconic acid and other chemicals.

6 List of Figures and Tables

6.1 Figures

Figure 1 Classification of tannins. 13

Figure 2 Hydrolysis of tannic acid. 14

Figure 3 Main strategies of aerobic aromatic ring cleavage: ortho-, metha-, and gentisate pathways. 20

Figure 4 Variants of microbial gallic acid degradation. 21

Figure 5 General principles of microbial aerobic catabolism of aromatic compounds with catechol as central intermediate metabolite. 22

Figure 6 Temperature-dependent dimorphism in A. adeninivorans LS3. 24

Figure 7 Non-oxidative decarboxylation of gallic acid into carbondioxide and pyrogallol by gallic acid decarboxylase. 26

Figure 8 Intradiolic cleavage of catechol by catechol-1,2-dioxygenase. 27

Figure 9 The intradiol dioxygenases catalytic cycle (Guzik et al., 2013). 30

Figure 10 Gallic acid tolerance of A. adeninivorans G1212/YRC102. 52

Figure 11 Multiple alignment of Agdc1p with published gallic acid decarboxylase sequences. 55

Figure 12 Physical map of the AGDC1 yeast integrative expression cassettes. 56

Figure 13 Screening of stabilized transformants after pre-selection analysis. 57

Figure 14 Time-course analysis of gallic acid decarboxylase activity in *A. adeninivorans* control and transgenic strain overexpressing *AGDC-6H*. 58

Figure 15 Design of AGDC1 gene deletion cassettes. 59

Figure 16 Verification of correctly integrated deletion cassettes by PCR of isolated genomic DNA. 60

Figure 17 Phenotypic analysis of A. adeninivorans strains. 61

Figure 18 Physical map of the AGDC1-eGFP yeast integrative expression cassette. 62

Figure 19 Subcellular localization of Agdc1-eGFP. 63

Figure 20 Test for elution of Agdc1-6hp by varying concentrations of imidazole. 64

Figure 21 Purification of Agdc1-6hp on Ni-Sepharose. 64

Figure 22 Standard curve for determination of native molecular mass of proteins by gel filtration..... 65

Figure 23 Determination of native molecular mass of recombinant gallic acid decarboxylase by size exclusion chromatography..... 66

Figure 24 pH spectrum of recombinant gallic acid decarboxylase..... 67

Figure 25 Most favourable buffer for gallic acid decarboxylase activity. 67

Figure 26 Temperature optimum of recombinant gallic acid decarboxylase activity. ... 68

Figure 27 Thermostability of Agdc1-6hp at different temperatures..... 68

Figure 28 Agdc1-6hp activity during storage under different temperature regimes. 69

Figure 29 Influence of carbon sources on AGDC1 expression..... 72

Figure 30 Key compounds of the tannin catabolism revealed by microarray study of gene regulation by gallic acid. 74

Figure 31 Key compounds of the β-oxidation revealed by microarray study of gene regulation by gallic acid..... 75

Figure 32 Key compounds of the methyl citrate cycle - microarray studies of gene regulation by gallic acid..... 75

Figure 33 Key compounds of the catabolism of the branched-chain amino acids valine, leucine and isoleucine - microarray studies of gene regulation by gallic acid..... 76

Figure 34 Key compounds of the glyoxylate cycle - microarray studies of gene regulation by gallic acid..... 77

Figure 35 GC-MS analysis of supernatant from cultures of A. adeninivorans control strain G1212/YRC102 and deletion mutant G1234 [Δagdc1]. 78

Figure 36 Time course experiment of A. adeninivorans G1212/YRC102, G1212/YRC102-AYNI1-AGDC1-6H and G1234 [Δagdc1]. 79

Figure 37 Growth behaviour of A. adeninivorans strains, feeding with hydroxylated aromatic acids as sole source for carbon and energy. 80

Figure 38 GC-MS analysis of substrate – product conversion during cultivation of A. adeninivorans on gallic acid. 82

Figure 39 GC-MS analysis of substrate – product conversion during cultivation of A. adeninivorans on protocatechuic acid. 82

Figure 40 Sequence alignment and phylogenetic tree of catechol-1,2-dioxygenases. 84

Figure 41 Structure prediction of Acdo1p. 85

Figure 42 Physical map of the *ACDO1* yeast integrative expression cassettes. 86

Figure 43 Acdo1 enzyme activity in control (G1212/YIC102) and most productive transformant strains. 87

Figure 44 Time-course analysis of catechol-1,2-dioxygenase activity in *A. adeninivorans* control strain and strain with overexpression of ACDO1-6H. 87

Figure 45 Physical map of the ACDO1-eGFP yeast integrative expression cassettes. 88

Figure 46 Subcellular localization of Acdo1-eGFP. 89

Figure 47 Design of *ACDO1* gene deletion cassettes. 90

Figure 48 Verification of correct integration of ACDO1 deletion cassettes by PCR. 91

Figure 49 Phenotype of *A. adeninivorans* colonies. 92

Figure 50 Test for elution of of Acdo1-6hp by varying concentrations of imidazole. 93

Figure 51 Purification of Acdo1-6hp on Ni Sepharose. 93

Figure 52 Determination of native molecular mass of recombinant catechol-1,2-dioxygenase by size exclusion chromatography. 95

Figure 53 pH spectrum of recombinant catechol-1,2-dioxygenase activity. 96

Figure 54 Influence of temperature on recombinant catechol-1,2-dioxygenase activity. 96

Figure 55 Stability of Acdo1-6hp under different temperature regimes. 97

Figure 56 Acdo1-6hp activity upon storage at 4 °C. 97

Figure 57 Influence of carbon sources on ACDO1 expression. 101

Figure 58 Key compounds of the tannin catabolism based on microarray studies of gene regulation by protocatechuic acid. 103

Figure 59 Expanded scheme of potential key compounds involved in tannin catabolism based on microarray studies of gene regulation by protocatechuic acid. 104

Figure 60 Key compounds of the β-oxidation - Microarray studies of gene regulation by protocatechuic acid. 105

Figure 61 Key compounds of the methyl citrate cycle – based on microarray studies of gene regulation by protocatechuic acid. 105

Figure 62 Key compounds of the catabolism of the branched-chain amino acids valine, leucine and isoleucine based on microarray studies of gene regulation by gallic acid. 106

Figure 63 Key compounds of the glyoxylate cycle based on microarray studies of gene regulation by protocatechuic acid. 107

Figure 64 Growth behaviour of *A. adeninivorans* strains G1212/YRC102 (control), G1212/YIC102-AYNI1-ACDO1-6H (*ACDO1-6H* overexpression) and G1235 [Δ*acdo1*] (*ACDO1* deletion). 108

Figure 65 Growth behaviour and Acdo1-6hp activity in A. adeninivorans strains G1212/YRC102 (control) and G1212/YIC102-AYNI1-ACDO1-6H (ACDO1-6H overexpression). 109

Figure 66 GC-MS analysis of substrate – product conversion during cultivation of *A. adeninivorans* on protocatechuic acid. 112

Figure 67 GC-MS analysis of substrate – product conversion during cultivation of *A. adeninivorans* on gallic acid. 113

Figure 68 Subcellular localization of Agdc1-eGFP and Acdo1-eGFP in S. cerevisiae. 115

Figure 69 SDS-PAGE and Western blot analysis of catechol-1,2-dioxygenase production in crude extracts of transgenic S. cerevisiae strains expressing the ACDO1 gene from A. adeninivorans. 116

Figure 70 Screening of catechol-1,2-dioxygenase activity in transgenic S. cerevisiae strains with expression of ACDO1 gene from A. adeninivorans. 117

Figure 71 SDS-PAGE analysis of purified Acdo1-6hp and Agdc1-6hp produced by S. cerevisiae. 117

Figure 72 Hydroxyl group conformation required for enzymatic activity of gallic acid decarboxylase and catechol dioxygenase..... 125

Figure 73 Proposed pathway for the degradation of protocatechuic acid in A. adeninivorans control strain (left) and deletion mutant (right). 132

Figure 74 Substrate – product conversion during cultivation of A. adeninivorans on protocatechuic acid in shaking flask culture**.**..... 158

Figure 75 Substrate – product conversion during cultivation of A. adeninivorans on gallic acid in shaking flask culture**.** 159

Figure 76 Expression analysis of ABC transporters. 160

Figure 77 Expression analysis of MFS transporters. 162

6.2 Tables

Table 1 List of chemicals used 32

Table 2 List of software applications 34

Table 3 List of antibodies used 34

Table 4 List of commercial kits and enzymes applied 35

Table 5 List of plasmids and vectors used 35

Table 6 List of bacterial strains 36

Table 7 List of yeast strains 36

Table 8 Composition of bacterial medium 36

Table 9 Composition of yeast cultivation medium 37

Table 10 Composition of electrophoresis buffer 39

Table 11 Buffer composition for the preparation of bacterial competent cells 41

Table 12 Buffer composition for the preparation of yeast competent cells and A. adeninivorans transformation 42

Table 13 Composition of SDS-PAGE 46

Table 14 Buffer composition for protein purification 48

Table 15 Primers used for construction of deletion mutant strain G1234 [Δagdc1] 60

Table 16 Summary of the Agdc1-6hp purification 65

Table 17 Kinetic constants of purified Agdc1-6hp 69

Table 18 Effect of metal salts and additives on Agdc1-6hp activity 70

Table 19 Substrate spectrum for Agdc1-6hp 71

Table 20 Primers used for analysis of AGDC1 expression levels 73

Table 21 Primers used for construction of deletion mutant strain G1235 [Δacdo1] 91

Table 22 Summary of Acdo1-6hp purification 94

Table 23 Effect of metal salts and additives on Acdo1-6hp activity. 98

Table 24 Kinetic constants of purified Acdo1-6hp using pyrogallol and catechol as substrates. 99

Table 25 Spectrophotometric substrate analysis for Acdo1-6hp 100

Table 26 Primers used for analysis of ACDO1 expression levels 101

7 References

ADEBOYE, P. T., BETTIGA, M. & OLSSON, L. 2014. The chemical nature of phenolic compounds determines their toxicity and induces distinct physiological responses in *Saccharomyces cerevisiae* in lignocellulose hydrolysates. *AMB Express,* 4**,** 46.

AGUILAR-ZÁRATE, P., CRUZ, M. A., MONTAÑEZ, J., RODRÍGUEZ-HERRERA, R., WONG-PAZ, J. E., BELMARES, R. E. & AGUILAR, C. N. 2015. Gallic acid production under anaerobic submerged fermentation by two bacilli strains. *Microb Cell Fact,* 14**,** 209.

AHUATZI-CHACÓN, D., ORDORICA-MORALES, G., RUIZ-ORDAZ, N., CRISTIANI-URBINA, E., JUÁREZ-RAMÍREZ, C. & GALÍNDEZ-MAYER, J. J. W. J. O. M. 2004. Kinetic study of phenol hydroxylase and catechol 1,2-dioxygenase biosynthesis by *Candida tropicalis* cells grown on different phenolic substrates. *World Journal of Microbiology Biotechnology,* 20**,** 695-702.

ALINI, S., BASILE, F., BLASIOLI, S., RINALDI, C. & VACCARI, A. 2007. Development of new catalysts for N2O-decomposition from adipic acid plant. *Applied Catalysis B: Environmental,* 70**,** 323-329.

AMBERG, D. C., BURKE, D. J., BURKE, D., STRATHERN, J. N. & LABORATORY, C. S. H. 2005. *Methods in Yeast Genetics: A Cold Spring Harbor Laboratory Course Manual*, Cold Spring Harbor Laboratory Press.

ANDERSON, J. J. & DAGLEY, S. 1980. Catabolism of aromatic acids in *Trichosporon cutaneum*. *J Bacteriol,* 141**,** 534-43.

ANDREONI, V., BERNASCONI, S., BESTETTI, P. & VILLA, M. 1991. Metabolism of lignin-related compounds by Rhodococcus rhodochrous: bioconversion of anisoin. *J Applied Microbiology Biotechnology,* 36**,** 410-415.

AOKI, K., KONOHANA, T., SHINKE, R. & NISHIRA, H. 1984. Purification and Characterization of Catechol 1,2-Dioxygenase from Aniline-assimilating *Rhodococcus erythropolis* AN-13†. *Agricultural and Biological Chemistry,* 48**,** 2087-2095.

ASSINDER, S. J. & WILLIAMS, P. A. 1990. The TOL Plasmids: Determinants of the Catabolism of Toluene and the Xylenes. *In:* ROSE, A. H. & TEMPEST, D. W. (eds.) *Advances in Microbial Physiology.* Academic Press.

BADHANI, B., SHARMA, N. & KAKKAR, R. 2015. Gallic acid: a versatile antioxidant with promising therapeutic and industrial applications. *RSC Advances,* 5**,** 27540-27557.

BARTELS, I., KNACKMUSS, H.-J. & REINEKE, W. 1984. Suicide Inactivation of Catechol 2,3-Dioxygenase from *Pseudomonas putida* mt-2 by 3-Halocatechols. *Appl. Environ. Microbiol.,* 47**,** 500-505.

BEALES, N. 2004. Adaptation of Microorganisms to Cold Temperatures, Weak Acid Preservatives, Low pH, and Osmotic Stress: A Review. *Comprehensive Reviews in Food Science and Food Safety,* 3**,** 1-20.

BERRY, D. F., FRANCIS, A. J. & BOLLAG, J. M. 1987. Microbial metabolism of homocyclic and heterocyclic aromatic compounds under anaerobic conditions. *Microbiol Rev,* 51**,** 43-59.

BISCHOFF, F., LITWINSKA, K., CORDES, A., BARONIAN, K., BODE, R., SCHAUER, F. & KUNZE, G. 2015. Three New Cutinases from the Yeast *Arxula adeninivorans* That Are Suitable for Biotechnological Applications. *Appl Environ Microbiol,* 81**,** 5497-510.

BLAKLEY, E. R. 1974. The microbial degradation of cyclohexanecarboxylic acid: a pathway involving aromatization to form p-hydroxybenzoic acid. *Canadian Journal of Microbiology,* 20**,** 1297-1306.

BÖER, E., BODE, R., MOCK, H. P., PIONTEK, M. & KUNZE, G. 2009a. Atan1p – an extracellular tannase from the dimorphic yeast *Arxula adeninivorans*: molecular cloning of the ATAN1 gene and characterization of the recombinant enzyme. *Yeast,* 26**,** 323-37.

BÖER, E., PIONTEK, M. & KUNZE, G. 2009b. Xplor 2 – an optimized transformation/expression system for recombinant protein production in the yeast *Arxula adeninivorans*. *Appl Microbiol Biotechnol,* 84**,** 583-94.

BÖER, E., SCHROTER, A., BODE, R., PIONTEK, M. & KUNZE, G. 2009c. Characterization and expression analysis of a gene cluster for nitrate assimilation from the yeast Arxula adeninivorans. *Yeast,* 26**,** 83-93.

BÖER, E., STEINBORN, G., MATROS, A., MOCK, H. P., GELLISSEN, G. & KUNZE, G. 2007. Production of interleukin – 6 in *Arxula adeninivorans*, Hansenula polymorpha and Saccharomyces cerevisiae by applying the wide-range yeast vector (CoMed) system to simultaneous comparative assessment. *FEMS Yeast Res,* 7**,** 1181-7.

BÖER, E., WARTMANN, T., LUTHER, B., MANTEUFFEL, R., BODE, R., GELLISSEN, G. & KUNZE, G. 2004. Characterization of the AINV gene and the encoded invertase from the dimorphic yeast Arxula adeninivorans. *Antonie Van Leeuwenhoek,* 86**,** 121-34.

BÖER, E., WARTMANN, T., SCHMIDT, S., BODE, R., GELLISSEN, G. & KUNZE, G. 2005. Characterization of the AXDH gene and the encoded xylitol dehydrogenase from the dimorphic yeast Arxula adeninivorans. *Antonie Van Leeuwenhoek,* 87**,** 233-43.

BOLL, M., FUCHS, G. & HEIDER, J. 2002. Anaerobic oxidation of aromatic compounds and hydrocarbons. *Curr Opin Chem Biol,* 6**,** 604-11.

BOROWSKI, T. & SIEGBAHN, P. E. 2006. Mechanism for catechol ring cleavage by non-heme iron intradiol dioxygenases: a hybrid DFT study. *J Am Chem Soc,* 128**,** 12941-53.

BOUDET, A. M., LAPIERRE, C. & GRIMA-PETTENATI, J. 1995. Biochemistry and molecular biology of lignification. *New Phytologist,* 129**,** 203-236.

BRADFORD, M. M. 1976. A rapid and sensitive method for the quantitation of microgram quantities of protein utilizing the principle of protein-dye binding. *Anal Biochem,* 72**,** 248-54.

BRAUS, G. H. 1991. Aromatic amino acid biosynthesis in the yeast Saccharomyces cerevisiae: a model system for the regulation of a eukaryotic biosynthetic pathway. *Microbiol Rev,* 55**,** 349-70.

BRIGANTI, F., PESSIONE, E., GIUNTA, C., MAZZOLI, R. & SCOZZAFAVA, A. 2000a. Purification and Catalytic Properties of Two Catechol 1,2-Dioxygenase Isozymes from Benzoate-Grown Cells of *Acinetobacter radioresistens*. *Journal of Protein Chemistry,* 19**,** 709-716.

BRIGANTI, F., PESSIONE, E., GIUNTA, C., MAZZOLI, R. & SCOZZAFAVA, A. 2000b. Purification and catalytic properties of two catechol 1,2-dioxygenase isozymes from benzoate-grown cells of *Acinetobacter radioresistens*. *J Protein Chem,* 19**,** 709-16.

BRIGANTI, F., PESSIONE, E., GIUNTA, C. & SCOZZAFAVA, A. 1997. Purification, biochemical properties and substrate specificity of a catechol 1,2-dioxygenase from a phenol degrading *Acinetobacter radioresistens*. *FEBS Lett,* 416**,** 61-4.

BRODERICK, J. B. & O'HALLORAN, T. V. 1991. Overproduction, purification, and characterization of chlorocatechol dioxygenase, a non-heme iron dioxygenase with broad substrate tolerance. *Biochemistry,* 30**,** 7349-58.

BRUCE, N. C. & CAIN, R. B. 1990. Hydroaromatic metabolism in *Rhodococcus rhodochrous*: purification and characterisation of its NAD-dependent quinate dehydrogenase. *Archives of Microbiology,* 154**,** 179-186.

BRUCKNER, C., OREB, M., KUNZE, G., BOLES, E. & TRIPP, J. 2018. An expanded enzyme toolbox for production of *cis,cis*-muconic acid and other shikimate pathway derivatives in *Saccharomyces cerevisiae*. *FEMS Yeast Res,* 18.

BRUNE, A. & SCHINK, B. 1992. Phloroglucinol pathway in the strictly anaerobic *Pelobacter acidigallici*: fermentation of trihydroxybenzenes to acetate via triacetic acid. *Archives of Microbiology,* 157**,** 417-424.

BUGG, T. D. H. 2003. Dioxygenase enzymes: catalytic mechanisms and chemical models. *Tetrahedron,* 59**,** 7075-7101.

BUI, D. M., KUNZE, I., FÖRSTER, S., WARTMANN, T., HORSTMANN, C., MANTEUFFEL, R. & KUNZE, G. 1996a. Cloning and expression of an *Arxula adeninivorans* glucoamylase gene in *Saccharomyces cerevisiae*. *Applied Microbiology Biotechnology,* 44**,** 610-619.

BUI, D. M., KUNZE, I., HORSTMANN, C., SCHMIDT, T., BREUNIG, K. D. & KUNZE, G. 1996b. Expression of the *Arxula adeninivorans* glucoamylase gene in *Kluyveromyces lactis*. *Appl Microbiol Biotechnol,* 45**,** 102-6.

BURGARD, P., PHARKYA, P. & OSTERHOUT, R. E. 2011. Microorganisms for the production of adipic acid and other compounds. *US8088607B2*.

BUSWELL, J. A. & ERIKSSON, K.-E. L. 1994. Effect of lignin-related phenols and their methylated derivatives on the growth of eight white-rot fungi. *World Journal of Microbiology Biotechnology,* 10**,** 169-174.

BUTLER, L. G. 1992. Antinutritional effects of condensed and hydrolyzable tannins. *Basic Life Sci,* 59**,** 693-8.

CAMARGO, A., ANDREAZZA, R., BALDONI, R. & BENTO, F. 2012. Enzymatic activity of catechol 1,2-dioxygenase and catechol 2,3-dioxygenase produced by *Gordonia polyisoprenivorans*. *Quim. Nova,* 35**,** 1587-1592.

CAO, B., GENG, A. & LOH, K. C. 2008. Induction of ortho- and meta-cleavage pathways in *Pseudomonas* in biodegradation of high benzoate concentration: MS identification of catabolic enzymes. *Appl Microbiol Biotechnol,* 81**,** 99-107.

CAPOSIO, P., PESSIONE, E., GIUFFRIDA, G., CONTI, A., LANDOLFO, S., GIUNTA, C. & GRIBAUDO, G. 2002. Cloning and characterization of two catechol 1,2-dioxygenase genes from *Acinetobacter radioresistens* S13. *Res Microbiol,* 153**,** 69-74.

CAVANI, F., CENTI, G., PERATHONER, S. & TRIFIRÒ, F. 2009. *Sustainable Industrial Chemistry: Principles, Tools and Industrial Examples*, Wiley.

CHAMKHA, M., RECORD, E., GARCIA, J. L., ASTHER, M. & LABAT, M. 2002. Isolation from a shea cake digester of a tannin-tolerant *Escherichia coli* strain decarboxylating p-hydroxybenzoic and vanillic acids. *Curr Microbiol,* 44**,** 341-9.

CHANG-JUN, C. 2006. Catechol 1,2-Dioxygenase from *Rhodococcus rhodochrous* N75 Capable of Metabolizing Alkyl-Substituted Catechols. *J. Microbiol. Biotechnol.,* 16**,** 778-785.

CHAO, H. & ZHOU, N. Y. 2013. GenR, an IclR-type regulator, activates and represses the transcription of gen genes involved in 3-hydroxybenzoate and gentisate catabolism in *Corynebacterium glutamicum*. *J Bacteriol,* 195**,** 1598-609.

CHUNG, K.-T., WEI, C.-I. & JOHNSON, M. G. 1998a. Are tannins a double-edged sword in biology and health? *Trends in Food Science & Technology,* 9**,** 168-175.

CHUNG, K. T., LU, Z. & CHOU, M. W. 1998b. Mechanism of inhibition of tannic acid and related compounds on the growth of intestinal bacteria. *Food Chem Toxicol,* 36**,** 1053-60.

CHUNG, K. T., WONG, T. Y., WEI, C. I., HUANG, Y. W. & LIN, Y. 1998c. Tannins and human health: a review. *Crit Rev Food Sci Nutr,* 38**,** 421-64.

COLLIER, L. S., GAINES, G. L., 3RD & NEIDLE, E. L. 1998. Regulation of benzoate degradation in *Acinetobacter* sp. strain ADP1 by BenM, a LysR-type transcriptional activator. *J Bacteriol,* 180**,** 2493-501.

COX, D. D. & QUE, L. 1988. Functional models for catechol 1,2-dioxygenase. The role of the iron(III) center. *Journal of the American Chemical Society,* 110**,** 8085-8092.

CREDENCERESEARCH 2018. Catechol: Market Growth, Future Prospects, Competitive Analysis and Forecast, 2016 - 2023. *https://www.credenceresearch.com/report/catechol-market*.

CURRAN, K. A., LEAVITT, J. M., KARIM, A. S. & ALPER, H. S. 2013. Metabolic engineering of muconic acid production in *Saccharomyces cerevisiae*. *Metab Eng,* 15**,** 55-66.

DAGLEY, S. 1971. Catabolism of Aromatic Compounds by Microorganisms. *In:* ROSE, A. H. & WILKINSON, J. F. (eds.) *Advances in Microbial Physiology.* Academic Press.

DAVISON, B. H., PARKS, J., DAVIS, M. F. & DONOHOE, B. S. 2013. Plant Cell Walls: Basics of Structure, Chemistry, Accessibility and the Influence on Conversion. *Aqueous Pretreatment of Plant Biomass for Biological and Chemical Conversion to Fuels and Chemicals.*

DE BRUYNE, M. C., HOES, A. W., KORS, J. A., HOFMAN, A., VAN BEMMEL, J. H. & GROBBEE, D. E. 1999. Prolonged QT interval predicts cardiac and all-cause mortality in the elderly. The Rotterdam Study. *Eur Heart J,* 20**,** 278-84.

DELNERI, D., DEGRASSI, G., RIZZO, R. & BRUSCHI, C. V. 1995. Degradation of trans-ferulic and p-coumaric acid by *Acinetobacter calcoaceticus* DSM 586. *Biochim Biophys Acta,* 1244**,** 363-7.

DENEF, V. J., KLAPPENBACH, J. A., PATRAUCHAN, M. A., FLORIZONE, C., RODRIGUES, J. L., TSOI, T. V., VERSTRAETE, W., ELTIS, L. D. & TIEDJE, J. M. 2006. Genetic and genomic insights into the role of benzoate-catabolic pathway redundancy in *Burkholderia xenovorans* LB400. *Appl Environ Microbiol,* 72**,** 585-95.

DOHMEN, R. J., MADURA, K., BARTEL, B. & VARSHAVSKY, A. 1991. The N-end rule is mediated by the UBC2(RAD6) ubiquitin-conjugating enzyme. *Proceedings of the National Academy of Sciences,* 88**,** 7351-7355.

DORN, E. & KNACKMUSS, H. J. 1978. Chemical structure and biodegradability of halogenated aromatic compounds. Substituent effects on 1,2-dioxygenation of catechol. *Biochem J,* 174**,** 85-94.

DRATHS, K. M. & FROST, J. W. 1994. Environmentally compatible synthesis of adipic acid from D-glucose. *Journal of the American Chemical Society,* 116**,** 399-400.

EARHART, C. A., VETTING, M. W., GOSU, R., MICHAUD-SORET, I., QUE, L., JR. & OHLENDORF, D. H. 2005. Structure of catechol 1,2-dioxygenase from *Pseudomonas arvilla*. *Biochem Biophys Res Commun,* 338**,** 198-205.

EL-SAYED, W. S., ISMAEIL, M. & EL-BEIH, F. 2009. Isolation of 4-chlorophenol-degrading bacteria, *Bacillus subtilis* OS1 and *Alcaligenes* sp. OS2 from petroleum

oil-contaminated soil and characterization of its catabolic pathway. *Australian Journal of Basic and Applied Sciences,* 3**,** 776-783.

EPPINK, M. H., BOEREN, S. A., VERVOORT, J. & VAN BERKEL, W. J. 1997. Purification and properties of 4-hydroxybenzoate 1-hydroxylase (decarboxylating), a novel flavin adenine dinucleotide-dependent monooxygenase from *Candida parapsilosis* CBS604. *J Bacteriol,* 179**,** 6680-7.

ERDTMAN, H. 1972. Lignins: Occurrence, formation, structure and reactions. *K. V. Sarkanen and C. H. Ludwig, Eds., John Wiley & Sons, Inc.,* 10**,** 228-230.

FAUSTINI, A., RAPP, R. & FORASTIERE, F. 2014. Nitrogen dioxide and mortality: review and meta-analysis of long-term studies. *Eur Respir J,* 44**,** 744-53.

FERRARONI, M., KOLOMYTSEVA, M. P., SOLYANIKOVA, I. P., SCOZZAFAVA, A., GOLOVLEVA, L. A. & BRIGANTI, F. 2006. Crystal structure of 3-chlorocatechol 1,2-dioxygenase key enzyme of a new modified ortho-pathway from the Gram-positive *Rhodococcus opacus* 1CP grown on 2-chlorophenol. *J Mol Biol,* 360**,** 788-99.

FERRARONI, M., SEIFERT, J., TRAVKIN, V. M., THIEL, M., KASCHABEK, S., SCOZZAFAVA, A., GOLOVLEVA, L., SCHLOMANN, M. & BRIGANTI, F. 2005. Crystal structure of the hydroxyquinol 1,2-dioxygenase from *Nocardioides simplex* 3E, a key enzyme involved in polychlorinated aromatics biodegradation. *J Biol Chem,* 280**,** 21144-54.

FETZNER, S. 2012. Ring-cleaving dioxygenases with a cupin fold. *Appl Environ Microbiol,* 78**,** 2505-14.

FLINT, D. H. & ALLEN, R. M. 1996. Ironminus signSulfur Proteins with Nonredox Functions. *Chem Rev,* 96**,** 2315-2334.

FRUMKIN, H., HESS, J. & VINDIGNI, S. 2009. Energy and public health: the challenge of peak petroleum. *Public health reports (Washington, D.C. : 1974),* 124**,** 5-19.

FUJIWARA, M., GOLOVLEVA, L. A., SAEKI, Y., NOZAKI, M. & HAYAISHI, O. 1975. Extradiol cleavage of 3-substituted catechols by an intradiol dioxygenase, pyrocatechase, from a *Pseudomonad*. *J Biol Chem,* 250**,** 4848-55.

GALBRAITH, D., GROSS, S. A. & PAUSTENBACH, D. 2010. Benzene and human health: A historical review and appraisal of associations with various diseases. *Crit Rev Toxicol,* 40 Suppl 2**,** 1-46.

GAURI, S. S., MANDAL, S. M., ATTA, S., DEY, S. & PATI, B. R. 2013. Novel route of tannic acid biotransformation and their effect on major biopolymer synthesis in *Azotobacter* sp. SSB81. *J Appl Microbiol,* 114**,** 84-95.

GIENOW, U., KUNZE, G., SCHAUER, F., BODE, R. & HOFEMEISTER, J. 1990. The yeast genus *Trichosporon* spec. LS3; molecular characterization of genomic complexity. *Zentralbl Mikrobiol,* 145**,** 3-12.

GIETZ, R. D. & SCHIESTL, R. H. 2007. High-efficiency yeast transformation using the LiAc/SS carrier DNA/PEG method. *Nat Protoc,* 2**,** 31-4.

GOSSET, G. 2009. Production of aromatic compounds in bacteria. *Curr Opin Biotechnol,* 20**,** 651-8.

GOU, M., QU, Y., ZHOU, J., LI, A. & SALAH UDDIN, M. 2009. Characterization of catechol 1,2-dioxygenase from cell extracts of *Sphingomonas xenophaga* QYY. *J Science in China Series B: Chemistry,* 52**,** 615-620.

GRANT, D. J. & PATEL, J. C. 1969. The non-oxidative decarboxylation of p-hydroxybenzoic acid, gentisic acid, protocatechuic acid and gallic acid by *Klebsiella aerogenes* (*Aerobacter aerogenes*). *Antonie Van Leeuwenhoek,* 35**,** 325-43.

GREŃ, I., WOJCIESZYŃSKA, D., GUZIK, U., PERKOSZ, M. & HUPERT-KOCUREK, K. 2010. Enhanced biotransformation of mononitrophenols by *Stenotrophomonas maltophilia* KB2 in the presence of aromatic compounds of plant origin. *World Journal of Microbiology Biotechnology,* 26**,** 289-295.

GUZIK, U., GREŃ, I., HUPERT-KOCUREK, K. & WOJCIESZYŃSKA, D. 2011. Catechol 1,2-dioxygenase from the new aromatic compounds – Degrading *Pseudomonas putida* strain N6. *International Biodeterioration & Biodegradation,* 65**,** 504-512.

GUZIK, U., HUPERT-KOCUREK, K., SITNIK, M. & WOJCIESZYŃSKA, D. 2013. High activity catechol 1,2-dioxygenase from *Stenotrophomonas maltophilia* strain KB2 as a useful tool in cis,cis-muconic acid production. *Antonie Van Leeuwenhoek,* 103**,** 1297-307.

HADDOCK, J. D. & FERRY, J. G. 1993. Initial steps in the anaerobic degradation of 3,4,5-trihydroxybenzoate by Eubacterium oxidoreducens: characterization of mutants and role of 1,2,3,5-tetrahydroxybenzene. *J Bacteriol,* 175**,** 669-73.

HADI, T. A., BANERJEE, R. & BHATTACHARYYA, B. C. 1994. Optimization of tannase biosynthesis by a newly isolated *Rhizopus oryzae*. *Bioprocess Engineering,* 11**,** 239-243.

HAIGLER, B. E., NISHINO, S. F. & SPAIN, J. C. 1988. Degradation of 1,2-dichlorobenzene by a *Pseudomonas* sp. *Appl Environ Microbiol,* 54**,** 294-301.

HARWOOD, C. S. & PARALES, R. E. 1996. The beta-ketoadipate pathway and the biology of self-identity. *Annu Rev Microbiol,* 50**,** 553-90.

HATFIELD, R. & VERMERRIS, W. 2001. Lignin Formation in Plants. The Dilemma of Linkage Specificity. *Plant Physiology,* 126**,** 1351.

HAWKINS, A. R., LAMB, H. K., MOORE, J. D., CHARLES, I. G. & ROBERTS, C. F. 1993. The pre-chorismate (shikimate) and quinate pathways in filamentous fungi: theoretical and practical aspects. *J Gen Microbiol,* 139**,** 2891-9.

HAYAISHI, O. & HASHIMOTO, K. 1950. Pyrocatecase. A new enzyme catalizing oxidative breakdown of pyrocatechin. *The Journal of Biochemistry,* 37**,** 371-374.

HE, Z. & WIEGEL, J. 1995. Purification and characterization of an oxygen-sensitive reversible 4-hydroxybenzoate decarboxylase from Clostridium hydroxybenzoicum. *Eur J Biochem,* 229**,** 77-82.

HE, Z. & WIEGEL, J. 1996. Purification and characterization of an oxygen-sensitive, reversible 3,4-dihydroxybenzoate decarboxylase from *Clostridium hydroxybenzoicum*. *J Bacteriol,* 178**,** 3539-43.

HOLESOVA, Z., JAKUBKOVA, M., ZAVADIAKOVA, I., ZEMAN, I., TOMASKA, L. & NOSEK, J. 2011. Gentisate and 3-oxoadipate pathways in the yeast *Candida parapsilosis*: identification and functional analysis of the genes coding for 3-hydroxybenzoate 6-hydroxylase and 4-hydroxybenzoate 1-hydroxylase. *Microbiology,* 157**,** 2152-63.

HOWELL, A. B., VORSA, N., DER MARDEROSIAN, A. & FOO, L. Y. 1998. Inhibition of the adherence of P-fimbriated *Escherichia coli* to uroepithelial-cell surfaces by proanthocyanidin extracts from cranberries. *N Engl J Med,* 339**,** 1085-6.

HU, X.-F. & WU, L. 2012. Oxidation of 3,5-di-tert-butylcatechol in the presence of V-polyoxometalate. *Chemical Papers,* 66**,** 211-215.

IBRAHEEM, O. & NDIMBA, B. K. 2013. Molecular adaptation mechanisms employed by ethanologenic bacteria in response to lignocellulose-derived inhibitory compounds. *Int J Biol Sci,* 9**,** 598-612.

ITOH, M. 1981. Characteristics of a New Catechol 1,2-Oxygenase from *Trichosporon cutaneum* WY 2-2. *Agricultural and Biological Chemistry,* 45**,** 2787-2796.

JANKOWSKA, D. A., FAULWASSER, K., TRAUTWEIN-SCHULT, A., CORDES, A., HOFERICHTER, P., KLEIN, C., BODE, R., BARONIAN, K. & KUNZE, G. 2013a. *Arxula adeninivorans* recombinant adenine deaminase and its application in the production of food with low purine content. *J Appl Microbiol,* 115**,** 1134-46.

JANKOWSKA, D. A., TRAUTWEIN-SCHULT, A., CORDES, A., HOFERICHTER, P., KLEIN, C., BODE, R., BARONIAN, K. & KUNZE, G. 2013b. *Arxula adeninivorans* xanthine oxidoreductase and its application in the production of food with low purine content. *J Appl Microbiol,* 115**,** 796-807.

JIMÉNEZ, N., CURIEL, J. A., REVERON, I., DE LAS RIVAS, B. & MUNOZ, R. 2013. Uncovering the *Lactobacillus plantarum* WCFS1 gallate decarboxylase involved in tannin degradation. *Appl Environ Microbiol,* 79**,** 4253-63.

JOTHIMANI, P., KALAICHELVAN, G., BHASKARAN, A., SELVASEELAN, D. A. & RAMASAMY, K. 2003. Anaerobic biodegradation of aromatic compounds. *Indian J Exp Biol,* 41**,** 1046-67.

JUNKER, A., ROHN, H., CZAUDERNA, T., KLUKAS, C., HARTMANN, A. & SCHREIBER, F. 2012. Creating interactive, web-based and data-enriched maps with the Systems Biology Graphical Notation. *Nat Protoc,* 7**,** 579-93.

KAKKAR, S. & BAIS, S. 2014. A Review on Protocatechuic Acid and Its Pharmacological Potential. *ISRN Pharmacology,* 2014**,** 9.

KLABUNDE, J., KUNZE, G., GELLISSEN, G. & HOLLENBERG, C. P. 2003. Integration of heterologous genes in several yeast species using vectors containing a Hansenula polymorpha-derived rDNA-targeting element. *FEMS Yeast Research,* 4**,** 185-193.

KRUMHOLZ, L. R., CRAWFORD, R. L., HEMLING, M. E. & BRYANT, M. P. 1987. Metabolism of gallate and phloroglucinol in *Eubacterium oxidoreducens* via 3-hydroxy-5-oxohexanoate. *J Bacteriol,* 169**,** 1886-90.

KUMARI, A., BARONIAN, K., KUNZE, G. & GUPTA, R. 2015. Extracellular expression of YlLip11 with a native signal peptide from *Yarrowia lipolytica* MSR80 in three different yeast hosts. *Protein Expr Purif,* 110**,** 138-44.

KUNZE, G., GAILLARDIN, C., CZERNICKA, M., DURRENS, P., MARTIN, T., BÖER, E., GABALDON, T., CRUZ, J. A., TALLA, E., MARCK, C., GOFFEAU, A., BARBE, V., BARET, P., BARONIAN, K., BEIER, S., BLEYKASTEN, C., BODE, R., CASAREGOLA, S., DESPONS, L., FAIRHEAD, C., GIERSBERG, M., GIERSKI, P. P., HAHNEL, U., HARTMANN, A., JANKOWSKA, D., JUBIN, C., JUNG, P., LAFONTAINE, I., LEH-LOUIS, V., LEMAIRE, M., MARCET-HOUBEN, M., MASCHER, M., MOREL, G., RICHARD, G. F., RIECHEN, J., SACERDOT, C., SARKAR, A., SAVEL, G., SCHACHERER, J., SHERMAN, D. J., STEIN, N., STRAUB, M. L., THIERRY, A., TRAUTWEIN-SCHULT, A., VACHERIE, B., WESTHOF, E., WORCH, S., DUJON, B., SOUCIET, J. L., WINCKER, P., SCHOLZ, U. & NEUVEGLISE, C. 2014. The complete genome of *Blastobotrys* (*Arxula*) *adeninivorans* LS3 - a yeast of biotechnological interest. *Biotechnol Biofuels,* 7**,** 66.

KUNZE, G. & KUNZE, I. 1994. Characterization of *Arxula adeninivorans* strains from different habitats. *Antonie Van Leeuwenhoek,* 65**,** 29-34.

KURIYAMA, R. & NISLOW, C. 1992. Molecular components of the mitotic spindle. *BioEssays,* 14**,** 81-88.

KURTZMAN, C. & FELL, J. W. 1998. *The Yeasts - A Taxonomic Study*, Elsevier Science.

LAEMMLI, U. K. 1970. Cleavage of structural proteins during the assembly of the head of bacteriophage T4. *Nature,* 227**,** 680-5.

LEONOWICZ, A., CHO, N. S., LUTEREK, J., WILKOLAZKA, A., WOJTAS-WASILEWSKA, M., MATUSZEWSKA, A., HOFRICHTER, M., WESENBERG, D. & ROGALSKI, J. 2001. Fungal laccase: properties and activity on lignin. *J Basic Microbiol,* 41**,** 185-227.

LI, W. & WANG, C. 2015. Biodegradation of gallic acid to prepare pyrogallol by *Enterobacter aerogenes* through substrate induction. *BioRes.,* 10**,** 3027-3044.

LIN, Y., SUN, X., YUAN, Q. & YAN, Y. 2014. Extending shikimate pathway for the production of muconic acid and its precursor salicylic acid in *Escherichia coli*. *Metab Eng,* 23**,** 62-9.

LIPSCOMB, J. D., J.B., H. & WOOD, J. M. 1982. *Protocatechuate dioxygenases. Structural and mechanistic studies.*

LIVAK, K. J. & SCHMITTGEN, T. D. 2001. Analysis of relative gene expression data using real-time quantitative PCR and the 2(-Delta Delta C(T)) Method. *Methods,* 25**,** 402-8.

LUBICK, N. 2010. Drugs in the environment: do pharmaceutical take-back programs make a difference? *Environmental health perspectives,* 118**,** A210-A214.

LUTTIK, M. A., VURALHAN, Z., SUIR, E., BRAUS, G. H., PRONK, J. T. & DARAN, J. M. 2008. Alleviation of feedback inhibition in *Saccharomyces cerevisiae* aromatic amino acid biosynthesis: quantification of metabolic impact. *Metab Eng,* 10**,** 141-53.

MAHADEVAN, A. & MUTHUKUMAR, G. 1980a. Aquatic Microbiology with Reference to Tannin Degradation. *Hydrobiologia,* 72**,** 73-79.

MAHADEVAN, A. & MUTHUKUMAR, G. 1980b. Aquatic Microbiology with Reference to Tannin Degradation. *Hydrobiologia,* 72**,** 73-79.

MARKETRESEARCHFUTURE 2018. Catechol market analysis, growth by companies, trends by types and application, forecast analysis to 2022 *http://www.abnewswire.com/pressreleases/catechol-market-analysis-growth-by-companies-trends-by-types-and-application-forecast-analysis-to-2022_192506.html*.

MARKETRESEARCHSTORE 2018. Global Protocatechuic Acid (CAS 99-50-3) Market Research Report 2018. *https://www.marketresearchstore.com/report/global-protocatechuic-acid-cas-99-50-3-market-259357*.

MARTINEZ, A. T., SPERANZA, M., RUIZ-DUENAS, F. J., FERREIRA, P., CAMARERO, S., GUILLEN, F., MARTINEZ, M. J., GUTIERREZ, A. & DEL RIO, J. C. 2005. Biodegradation of lignocellulosics: microbial, chemical, and enzymatic aspects of the fungal attack of lignin. *Int Microbiol,* 8**,** 195-204.

MATERA, I., FERRARONI, M., KOLOMYTSEVA, M., GOLOVLEVA, L., SCOZZAFAVA, A. & BRIGANTI, F. 2010. Catechol 1,2-dioxygenase from the Gram-positive *Rhodococcus opacus* 1CP: quantitative structure/activity relationship and the crystal structures of native enzyme and catechols adducts. *J Struct Biol,* 170**,** 548-64.

MAYER, R. J. & QUE, L., JR. 1984. 18O studies of pyrogallol cleavage by catechol 1,2-dioxygenase. *J Biol Chem,* 259**,** 13056-60.

MCFALL, S. M., CHUGANI, S. A. & CHAKRABARTY, A. M. 1998. Transcriptional activation of the catechol and chlorocatechol operons: variations on a theme. *Gene,* 223**,** 257-67.

MCKETTA, J. J. 1977. *Encyclopedia of Chemical Processing and Design: Volume 2 - Additives to Alpha*, Taylor & Francis.

MEIER, A. K., WORCH, S., BÖER, E., HARTMANN, A., MASCHER, M., MARZEC, M., SCHOLZ, U., RIECHEN, J., BARONIAN, K., SCHAUER, F., BODE, R. & KUNZE, G. 2017. Agdc1p - a Gallic Acid Decarboxylase Involved in the Degradation of Tannic Acid in the Yeast *Blastobotrys* (*Arxula*) *adeninivorans*. *Front Microbiol,* 8**,** 1777.

MICALELLA, C., MARTIGNON, S., BRUNO, S., PIOSELLI, B., CAGLIO, R., VALETTI, F., PESSIONE, E., GIUNTA, C. & RIZZI, M. 2011. X-ray crystallography, mass spectrometry and single crystal microspectrophotometry: a multidisciplinary characterization of catechol 1,2 dioxygenase. *Biochim Biophys Acta,* 1814**,** 817-23.

MICHALOVER, J. L. & RIBBONS, D. W. 1973. 3-Hydroxybenzoate 4-hydroxylase from *Pseudomonas testosteroni*. *Biochemical and Biophysical Research Communications,* 55**,** 888-896.

MIDDELHOVEN, W. J., COENEN, A., KRAAKMAN, B. & SOLLEWIJN GELPKE, M. D. 1992. Degradation of some phenols and hydroxybenzoates by the imperfect ascomycetous yeasts *Candida parapsilosis* and *Arxula adeninivorans*: evidence for an operative gentisate pathway. *Antonie Van Leeuwenhoek,* 62**,** 181-7.

MIDDELHOVEN, W. J., DE JONG, I. M. & DE WINTER, M. 1991. *Arxula adeninivorans*, a yeast assimilating many nitrogenous and aromatic compounds. *Antonie Van Leeuwenhoek,* 59**,** 129-37.

MIDDELHOVEN, W. J., HOOGKAMER-TE NIET, M. C. & KREGER-VAN RIJ, N. J. 1984. *Trichosporon adeninovorans* sp. nov., a yeast species utilizing adenine, xanthine, uric acid, putrescine and primary n-alkylamines as the sole source of carbon, nitrogen and energy. *Antonie Van Leeuwenhoek,* 50**,** 369-78.

MIZUNO, S., YOSHIKAWA, N., SEKI, M., MIKAWA, T. & IMADA, Y. 1988. Microbial production of *cis,cis*-muconic acid from benzoic acid. *Applied Microbiology Biotechnology,* 28**,** 20-25.

MIZUNO, T., UCHINO, K., TOUKAIRIN, T., TANABE, A., NAKASHIMA, H., YAMAMOTO, N. & OGAWARA, H. 1992. Inhibitory effect of tannic acid sulfate and related sulfates on infectivity, cytopathic effect, and giant cell formation of human immunodeficiency virus. *Planta Med,* 58**,** 535-9.

MURAKAMI, S., KODAMA, N., SHINKE, R. & AOKI, K. 1997. Classification of catechol 1,2-dioxygenase family: sequence analysis of a gene for the catechol 1,2-dioxygenase showing high specificity for methylcatechols from Gram+ aniline-assimilating *Rhodococcus erythropolis* AN-13. *Gene,* 185**,** 49-54.

NAKAI, C., KAGAMIYAMA, H., SAEKI, Y. & NOZAKI, M. 1979. Nonidentical subunits of pyrocatechase from *Pseudomonas arvilla* C-1. *Arch Biochem Biophys,* 195**,** 12-22.

NAKAI, C., UYEYAMA, H., KAGAMIYAMA, H., NAKAZAWA, T., INOUYE, S., KISHI, F., NAKAZAWA, A. & NOZAKI, M. 1995. Cloning, DNA sequencing, and amino acid sequencing of catechol 1,2-dioxygenases (pyrocatechase) from *Pseudomonas putida* mt-2 and *Pseudomonas arvilla* C-1. *Arch Biochem Biophys,* 321**,** 353-62.

NAKAI, C., YAMAZAKI, G., KAGAMIYAMA, H. & NOZAKI, M. 1996. Amino acid sequence of catechol 1,2-dioxygenase (pyrocatechase) isozyme αα from *Pseudomonas arvilla* C-1. *IUBMB Life,* 39**,** 781-788.

NAKAJIMA, H., OTANI, C. & NIIMURA, T. 1992. Decarboxylation of Gallate by Cell-Free Extracts of *Streptococcus faecalis* and *Klebsiella pneumoniae* Isolated from

Rat Feces. *Food Hygiene and Safety Science (Shokuhin Eiseigaku Zasshi),* 33**,** 371-377_1.

NEMOTO, K., OSAWA, R., HIROTA, K., ONO, T. & MIYAKE, Y. 1995. An investigation of gram-negative tannin-protein complex degrading bacteria in fecal flora of various mammals. *J Vet Med Sci,* 57**,** 921-6.

NIU, W., DRATHS, K. M. & FROST, J. W. 2002. Benzene-free synthesis of adipic acid. *Biotechnol Prog,* 18**,** 201-11.

NODA, F., HAYASHI, K. & MIZUNUMA, T. 1982. Influence of pH on Inhibitory Activity of Acetic Acid on Osmophilic Yeasts Used in Brine Fermentation of Soy Sauce. *Appl Environ Microbiol,* 43**,** 245-6.

NOGALES, J., CANALES, A., JIMENEZ-BARBERO, J., GARCIA, J. L. & DIAZ, E. 2005. Molecular characterization of the gallate dioxygenase from *Pseudomonas putida* KT2440. The prototype of a new subgroup of extradiol dioxygenases. *J Biol Chem,* 280**,** 35382-90.

O'DONOVAN, L. & BROOKER, J. D. 2001. Effect of hydrolysable and condensed tannins on growth, morphology and metabolism of *Streptococcus gallolyticus* (*S. caprinus*) and *Streptococcus bovis*. *Microbiology,* 147**,** 1025-33.

ODENYO, A. A., BISHOP, R., ASEFA, G., JAMNADASS, R., ODONGO, D. & OSUJI, P. 2001. Characterization of Tannin-tolerant Bacterial Isolates from East African Ruminants. *Anaerobe,* 7**,** 5-15.

OHLENDORF, D. H., LIPSCOMB, J. D. & WEBER, P. C. 1988. Structure and assembly of protocatechuate 3,4-dioxygenase. *Nature,* 336**,** 403-5.

OMURA, H., WIESER, M. & NAGASAWA, T. 1998. Pyrrole-2-carboxylate decarboxylase from *Bacillus megaterium* PYR2910, an organic-acid-requiring enzyme. *Eur J Biochem,* 253**,** 480-4.

OPEC. 2012. World Oil Outlook 2012.

ORBICHEM, T. 2013. T. Chemical Market Insight and Foresight - Adipic Acid. *<http://www.orbichem.com/userfiles/CNF/Samples/ada_13_11.pdf>*.

ORNSTON, L. N. 1971. Regulation of catabolic pathways in *Pseudomonas*. *Bacteriol Rev,* 35**,** 87-116.

ORNSTON, M. K. & ORNSTON, L. N. 1972. The regulation of the -ketoadipate pathway in *Pseudomonas acidovorans* and *Pseudomonas testosteroni*. *J Gen Microbiol,* 73**,** 455-64.

PANDEETI, E. V. & SIDDAVATTAM, D. 2011. Purification and Characterization of Catechol 1,2-Dioxygenase from *Acinetobacter* sp. DS002 and Cloning, Sequencing of Partial catA Gene. *Indian J Microbiol,* 51**,** 312-8.

PARKE, D. & ORNSTON, L. N. 1984. Nutritional Diversity of *Rhizobiaceae* Revealed by Auxanography. *Journal of General Microbiology,* 130**,** 1743-1750.

PARKE, D., RYNNE, F. & GLENN, A. 1991. Regulation of phenolic catabolism in *Rhizobium leguminosarum* biovar trifolii. *J Bacteriol,* 173**,** 5546-50.

PETSKO, G. A., KENYON, G. L., GERLT, J. A., RINGE, D. & KOZARICH, J. W. 1993. On the origin of enzymatic species. *Trends Biochem Sci,* 18**,** 372-6.

PICH, U. & KUNZE, G. 1992. Genome organization of mitochondrial DNA from the non-saccharomycete yeast *Arxula adeninivorans* LS3. *Curr Genet,* 22**,** 505-6.

POLEN, T., SPELBERG, M. & BOTT, M. 2013. Toward biotechnological production of adipic acid and precursors from biorenewables. *J Biotechnol,* 167**,** 75-84.

POTRAWFKE, T., ARMENGAUD, J. & WITTICH, R. M. 2001. Chlorocatechols substituted at positions 4 and 5 are substrates of the broad-spectrum chlorocatechol 1,2-dioxygenase of *Pseudomonas chlororaphis* RW71. *J Bacteriol,* 183**,** 997-1011.

POWLOWSKI, J. B. & DAGLEY, S. 1985. beta-Ketoadipate pathway in *Trichosporon cutaneum* modified for methyl-substituted metabolites. *J Bacteriol,* 163**,** 1126-35.

PREMKUMAR, R., RAO, P. V., SREELEELA, N. S. & VAIDYANATHAN, C. S. 1969. m-Hydroxybenzoic acid 4-hydroxylase from *Aspergillus niger*. *Can J Biochem,* 47**,** 825-7.

PROESTOS, C. & KOMAITIS, M. 2013. Analysis of Naturally Occurring Phenolic Compounds in Aromatic Plants by RP-HPLC Coupled to Diode Array Detector (DAD) and GC-MS after Silylation. *Foods,* 2**,** 90-99.

QUE, L., JR., HEISTAND, R. H., 2ND, MAYER, R. & ROE, A. L. 1980. Resonance Raman studies of pyrocatechase-inhibitor complexes. *Biochemistry,* 19**,** 2588-93.

QUE, L., JR., LIPSCOMB, J. D., MUNCK, E. & WOOD, J. M. 1977. Protocatechuate 3,4-dioxygenase. Inhibitor studies and mechanistic implications. *Biochim Biophys Acta,* 485**,** 60-74.

QYRESEARCH 2018. Global Protocatechuic Acid (CAS 99-50-3) Market Expected to Witness a Sustainable Growth over 2025. *https://surveyandmarket.wordpress.com/2018/07/13/global-protocatechuic-acid-cas-99-50-3-market-expected-to-witness-a-sustainable-growth-over-2025-qy-research/*.

RANDHIR, R., LIN, Y. T. & SHETTY, K. 2004. Phenolics, their antioxidant and antimicrobial activity in dark germinated fenugreek sprouts in response to peptide and phytochemical elicitors. *Asia Pac J Clin Nutr,* 13**,** 295-307.

RAPORT 2018. Global Gallic Acid Market Size, Share, Growth, Forecast and Trends to 2023. *Research cosmos***,** 93.

RESTAINO, L., LENOVICH, L. M. & BILLS, S. 1982. Effect of Acids and Sorbate Combinations on the Growth of Four Osmophilic Yeasts. *Journal of Food Protection,* 45**,** 1138-1142.

REVERON, I., DE LAS RIVAS, B., MATESANZ, R., MUNOZ, R. & LOPEZ DE FELIPE, F. 2015. Molecular adaptation of *Lactobacillus plantarum* WCFS1 to gallic acid revealed by genome-scale transcriptomic signature and physiological analysis. *Microb Cell Fact,* 14**,** 160.

ROHN, H., JUNKER, A., HARTMANN, A., GRAFAHREND-BELAU, E., TREUTLER, H., KLAPPERSTÜCK, M., CZAUDERNA, T., KLUKAS, C. & SCHREIBER, F. 2012. VANTED v2: a framework for systems biology applications. *BMC Systems Biology,* 6**,** 139.

ROMERO-SILVA, M. J., MENDEZ, V., AGULLO, L. & SEEGER, M. 2013. Genomic and functional analyses of the gentisate and protocatechuate ring-cleavage pathways and related 3-hydroxybenzoate and 4-hydroxybenzoate peripheral pathways in *Burkholderia xenovorans* LB400. *PLoS One,* 8**,** e56038.

RÖSEL, H. & KUNZE, G. 1995. Cloning and characterization of a TEF gene for elongation factor 1α from the yeast Arxula adeninivorans. *Current Genetics,* 28**,** 360-366.

RÖSEL, H. & KUNZE, G. 1996. Identification of a group-I intron within the 25S rDNA from the yeast *Arxula adeninivorans*. *Yeast,* 12**,** 1201-8.

SAMAIN, E., ALBAGNAC, G. & DUBOURGUIER, H. C. 1986. Initial steps of catabolism of trihydroxybenzenes in *Pelobacter acidigallici*. *Archives of Microbiology,* 144**,** 242-244.

SAURET-IGNAZI, G., GAGNON, J., BEGUIN, C., BARRELLE, M., MARKOWICZ, Y., PELMONT, J. & TOUSSAINT, A. 1996. Characterisation of a chromosomally encoded catechol 1,2-dioxygenase (E.C. 1.13.11.1) from *Alcaligenes eutrophus* CH34. *Arch Microbiol,* 166**,** 42-50.

SCALBERT, A. 1991. Antimicrobial properties of tannins. *Phytochemistry,* 30**,** 3875-3883.

SCHINK, B., PHILIPP, B. & MULLER, J. 2000. Anaerobic degradation of phenolic compounds. *Naturwissenschaften,* 87**,** 12-23.

SCHMAUDER, H.-P. 1992. Hans G. Schlegel (unter Mitarbeit von Christiane Zaborosch), Allgemeine Mikrobiologie (7. überarbeitete Auflage). XIV + 634 S., 263 Abb., 41 Tab. Stuttgart–New York 1992. Georg Thieme Verlag. DM 48,00. ISBN: 3-13-444607-3. 32**,** 429-430.

SEDEROFF, R. R., MACKAY, J. J., RALPH, J. & HATFIELD, R. D. 1999. Unexpected variation in lignin. *Current Opinion in Plant Biology,* 2**,** 145-152.

SHARMA, S., BHAT, T. K. & DAWRA, R. K. 2000. A spectrophotometric method for assay of tannase using rhodanine. *Anal Biochem,* 279**,** 85-9.

SHETE, H. G. & CHITANAAD, M. P. 2015. Bioconversion of Naturally Occurring Tannins into a Value Added Pharmaceutical Intermediate Gallic Acid a New Approach. *International Journal of Current Microbiology and Applied Sciences,* 4**,** 597-604.

SIETMANN, R., UEBE, R., BÖER, E., BODE, R., KUNZE, G. & SCHAUER, F. 2010. Novel metabolic routes during the oxidation of hydroxylated aromatic acids by the yeast *Arxula adeninivorans*. *J Appl Microbiol,* 108**,** 789-99.

SIKKEMA, J., DE BONT, J. A. & POOLMAN, B. 1995. Mechanisms of membrane toxicity of hydrocarbons. *Microbiol Rev,* 59**,** 201-22.

SMYTH, G. K. 2005. limma: Linear Models for Microarray Data. *In:* GENTLEMAN, R., CAREY, V. J., HUBER, W., IRIZARRY, R. A. & DUDOIT, S. (eds.) *Bioinformatics and Computational Biology Solutions Using R and Bioconductor.* New York, NY: Springer New York.

SONI, M., SHARMA, K. P. & JOHN, P. J. 2012. Characterization of Pyrogallol Production from Gallic acid by *Enterobacter* spp. *J. Microbiol. Biotech. Res.,* 2**,** 327-336.

STEINBORN, G., GELLISSEN, G. & KUNZE, G. 2007. A novel vector element providing multicopy vector integration in Arxula adeninivorans. *FEMS Yeast Res,* 7**,** 1197-205.

STRACHAN, P. D., FREER, A. A. & FEWSON, C. A. 1998. Purification and characterization of catechol 1,2-dioxygenase from Rhodococcus rhodochrous NCIMB 13259 and cloning and sequencing of its catA gene. *Biochem J,* 333 (Pt 3)**,** 741-7.

SUBBOTINA, N. M., KOLOMYTSEVA, M. P., BASKUNOV, B. P. & GOLOVLEV, L. A. 2016. Catechol 1,2-dioxygenase induced in *Rhodococcus opacus* strain 1CP cultured in the presence of 3-hydroxybenzoate. *Microbiology,* 85**,** 638-641.

SUN, X., LIN, Y., HUANG, Q., YUAN, Q. & YAN, Y. 2013. A Novel Muconic Acid Biosynthesis Approach by Shunting Tryptophan Biosynthesis via Anthranilate. *Applied and Environmental Microbiology,* 79**,** 4024.

SUN, X., SHEN, X., JAIN, R., LIN, Y., WANG, J., SUN, J., WANG, J., YAN, Y. & YUAN, Q. 2015. Synthesis of chemicals by metabolic engineering of microbes. *Chemical Society Reviews,* 44**,** 3760-3785.

SUZUKI, K., ICHIMURA, A., OGAWA, N., HASEBE, A. & MIYASHITA, K. 2002. Differential Expression of Two Catechol 1,2-Dioxygenases in *Burkholderia* sp. Strain TH2. *Journal of Bacteriology,* 184**,** 5714.

SWAIN, T. 1977. Secondary Compounds as Protective Agents. *Ann. Rev. Plant Physiol.,* 28**,** 479-501.

TERENTIEV, Y., PICO, A. H., BÖER, E., WARTMANN, T., KLABUNDE, J., BREUER, U., BABEL, W., SUCKOW, M., GELLISSEN, G. & KUNZE, G. 2004. A wide-range integrative yeast expression vector system based on *Arxula adeninivorans*-derived elements. *J Ind Microbiol Biotechnol,* 31**,** 223-8.

TESTE, M.-A., DUQUENNE, M., FRANÇOIS, J. M. & PARROU, J.-L. 2009. Validation of reference genes for quantitative expression analysis by real-time RT-PCR in Saccharomyces cerevisiae. *BMC Molecular Biology,* 10**,** 99.

THOMAS, S., SANYA, D. R. A., FOUCHARD, F., NGUYEN, H. V., KUNZE, G., NEUVEGLISE, C. & CRUTZ-LE COQ, A. M. 2019. Blastobotrys adeninivorans and B. raffinosifermentans, two sibling yeast species which accumulate lipids at elevated temperatures and from diverse sugars. 12**,** 154.

TRAUTWEIN-SCHULT, A., JANKOWSKA, D., CORDES, A., HOFERICHTER, P., KLEIN, C., MATROS, A., MOCK, H. P., BARONIAN, K., BODE, R. & KUNZE, G. 2013. *Arxula adeninivorans* recombinant urate oxidase and its application in the production of food with low uric acid content. *J Mol Microbiol Biotechnol,* 23**,** 418-30.

TRAUTWEIN-SCHULT, A., JANKOWSKA, D., CORDES, A., HOFERICHTER, P., KLEIN, C., MATROS, A., MOCK, H. P., BARONIAN, K., BODE, R. & KUNZE, G. 2014. *Arxula adeninivorans* recombinant guanine deaminase and its application in the production of food with low purine content. *J Mol Microbiol Biotechnol,* 24**,** 67-81.

TSAI, S. C. & LI, Y. K. 2007. Purification and characterization of a catechol 1,2-dioxygenase from a phenol degrading Candida albicans TL3. *Arch Microbiol,* 187**,** 199-206.

VAILLANCOURT, F. H., BOLIN, J. T. & ELTIS, L. D. 2004. Ring-Cleavage Dioxygenases. *In:* RAMOS, J.-L. (ed.) *Pseudomonas: Volume 3 Biosynthesis of Macromolecules and Molecular Metabolism.* Boston, MA: Springer US.

VAILLANCOURT, F. H., BOLIN, J. T. & ELTIS, L. D. 2006. The ins and outs of ring-cleaving dioxygenases. *Crit Rev Biochem Mol Biol,* 41**,** 241-67.

VAN DE VYVER, S. & ROMÁN-LESHKOV, Y. 2013. Emerging catalytic processes for the production of adipic acid. *Catalysis Science & Technology,* 3**,** 1465-1479.

VAN DER WALT, J. P., SMITH, M. T. & YAMADA, Y. 1990. *Arxula* gen. nov. (*Candidaceae*), a new anamorphic, arthroconidial yeast genus. *Antonie Van Leeuwenhoek,* 57**,** 59-61.

VETTING, M. W. & OHLENDORF, D. H. 2000. The 1.8 A crystal structure of catechol 1,2-dioxygenase reveals a novel hydrophobic helical zipper as a subunit linker. *Structure,* 8**,** 429-440.

WANG, C.-L., YOU, S.-L. & WANG, S.-L. 2006. Purification and characterization of a novel catechol 1,2-dioxygenase from *Pseudomonas aeruginosa* with benzoic acid as a carbon source. *Process Biochemistry,* 41**,** 1594-1601.

WANG, C. L., TAKENAKA, S., MURAKAMI, S. & AOKI, K. 2001. Production of catechol from benzoate by the wild strain Ralstonia species Ba-0323 and characterization of its catechol 1,2-dioxygenase. *Biosci Biotechnol Biochem,* 65**,** 1957-64.

WANG, J. & ZHENG, P. 2015. Muconic acid production from glucose using enterobactin precursors in *Escherichia coli*. *J Ind Microbiol Biotechnol,* 42**,** 701-9.

WARTMANN, T., KRUGER, A., ADLER, K., DUC, B. M., KUNZE, I. & KUNZE, G. 1995. Temperature-dependent dimorphism of the yeast *Arxula adeninivorans* Ls3. *Antonie Van Leeuwenhoek,* 68**,** 215-23.

WARTMANN, T., STEPHAN, U. W., BUBE, I., BÖER, E., MELZER, M., MANTEUFFEL, R., STOLTENBURG, R., GUENGERICH, L., GELLISSEN, G. & KUNZE, G. 2002. Post-translational modifications of the AFET3 gene product: a component of the iron transport system in budding cells and mycelia of the yeast *Arxula adeninivorans*. *Yeast,* 19**,** 849-62.

WEBER, C., BRUCKNER, C., WEINREB, S., LEHR, C., ESSL, C. & BOLES, E. 2012. Biosynthesis of cis,cis-muconic acid and its aromatic precursors, catechol and protocatechuic acid, from renewable feedstocks by *Saccharomyces cerevisiae*. *Appl Environ Microbiol,* 78**,** 8421-30.

WOJCIESZYŃSKA, D., GUZIK, U., GREŃ, I., PERKOSZ, M. & HUPERT-KOCUREK, K. 2011. Induction of aromatic ring: cleavage dioxygenases in *Stenotrophomonas maltophilia* strain KB2 in cometabolic systems. *World J Microbiol Biotechnol,* 27**,** 805-811.

WORCH, S. & LEMKE, I. 2017. Gene expression analysis in Arxula adeninivorans: a nested quantitative real time PCR approach.

WU, C.-M., LEE, T.-H., LEE, S.-N., LEE, Y.-A. & WU, J.-Y. 2004. Microbial synthesis of *cis,cis*-muconic acid by *Sphingobacterium* sp. GCG generated from effluent of a styrene monomer (SM) production plant. *Enzyme and Microbial Technology,* 35**,** 598-604.

WU, L., DE WILDEMAN, S. M. A., VAN DEN BERG, M. A. & TREFZER, A. C. 2011. Adipate (ester or thioester) synthesis. *US20110091944*.

YOSHIDA, H., TANI, Y. & YAMADA, H. 1982. Isolation and Identification of a Pyrogallol Producing Bacterium from Soil. *Agricultural and Biological Chemistry,* 46**,** 2539-2546.

YOSHIDA, H. & YAMADA, H. 1985. Microbial Production of Pyrogallol through Decarboxylation of Gallic Acid. *Agricultural and Biological Chemistry,* 49**,** 659-663.

YOSHIDA, T., INAMI, Y., MATSUI, T. & NAGASAWA, T. 2010. Regioselective carboxylation of catechol by 3,4-dihydroxybenzoate decarboxylase of *Enterobacter cloacae* P. *Biotechnol Lett,* 32**,** 701-5.

YU, X., LI, Y. K., WANG, C. & WU, D. 2004. Immobilization of *Aspergillus niger* tannase by microencapsulation and its kinetic characteristics. *Biotechnol Appl Biochem.,* 40**,** 151-155.

ZEIDA, M., WIESER, M., YOSHIDA, T., SUGIO, T. & NAGASAWA, T. 1998. Purification and characterization of gallic acid decarboxylase from *pantoea agglomerans* T71. *Appl Environ Microbiol,* 64**,** 4743-7.

ZHANG, S., SUN, W., XU, L., ZHENG, X., CHU, X., TIAN, J., WU, N. & FAN, Y. 2012. Identification of the para-nitrophenol catabolic pathway, and characterization of three enzymes involved in the hydroquinone pathway, in *Peudomonas* sp. 1-7. *BMC Microbiol,* 12**,** 27.

8 Appendix

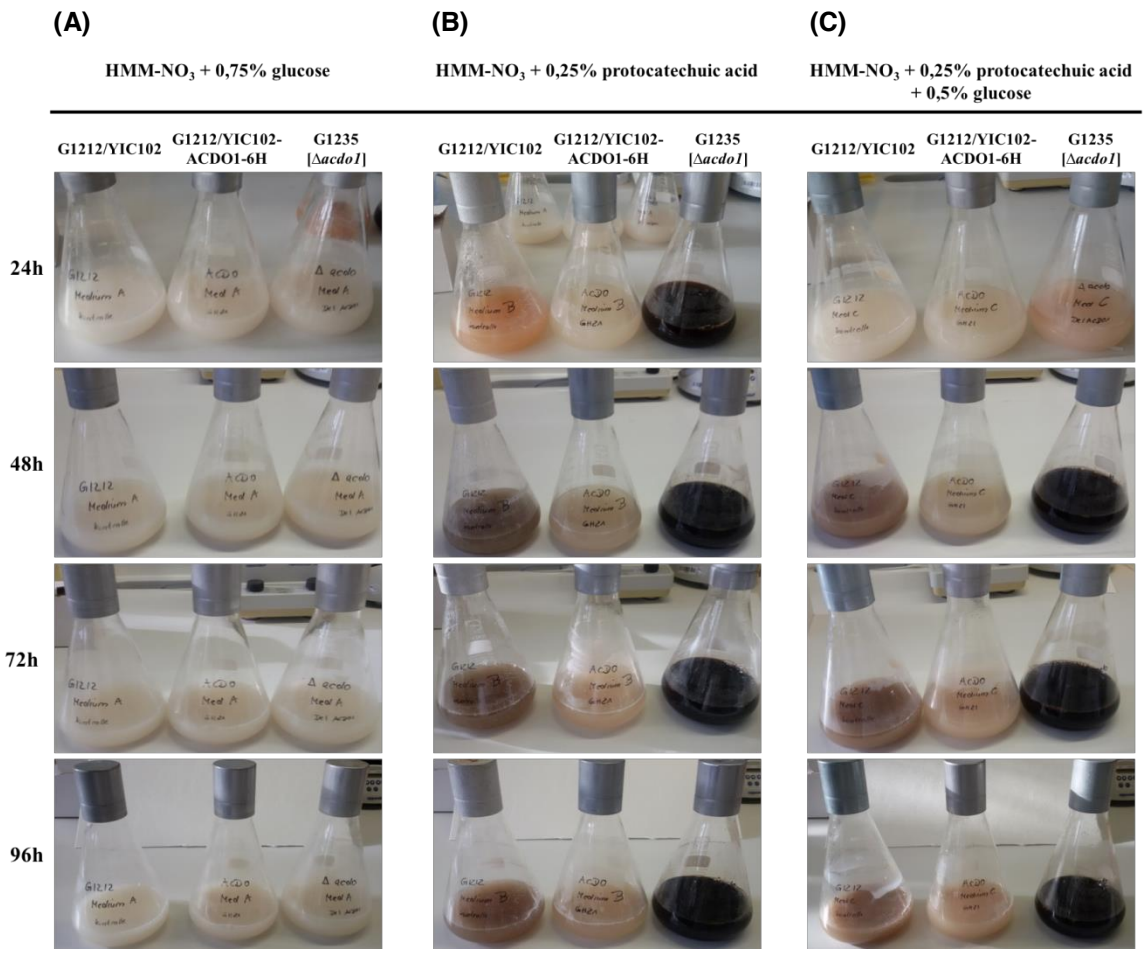

Figure 74 Substrate – product conversion during cultivation of *A. adeninivorans* on protocatechuic acid in shaking flask culture**.**
A. adeninivorans strains G1212/YIC102, G1212/YIC102ACDO1-6H, G1235 [*Δacdo1*] were cultivated on HMM-$NaNO_3$ with 0.75 % glucose **(A)**, 0.25% protocatechuic acid **(B**) and 0.25 % protocatechuic acid + 0.5 % glucose **(C).** During the cultivation substrate, protocatechuic acid, was transformed in different products what cased in visible culture colour changes. Photos were made for every 24 h of cultivation.

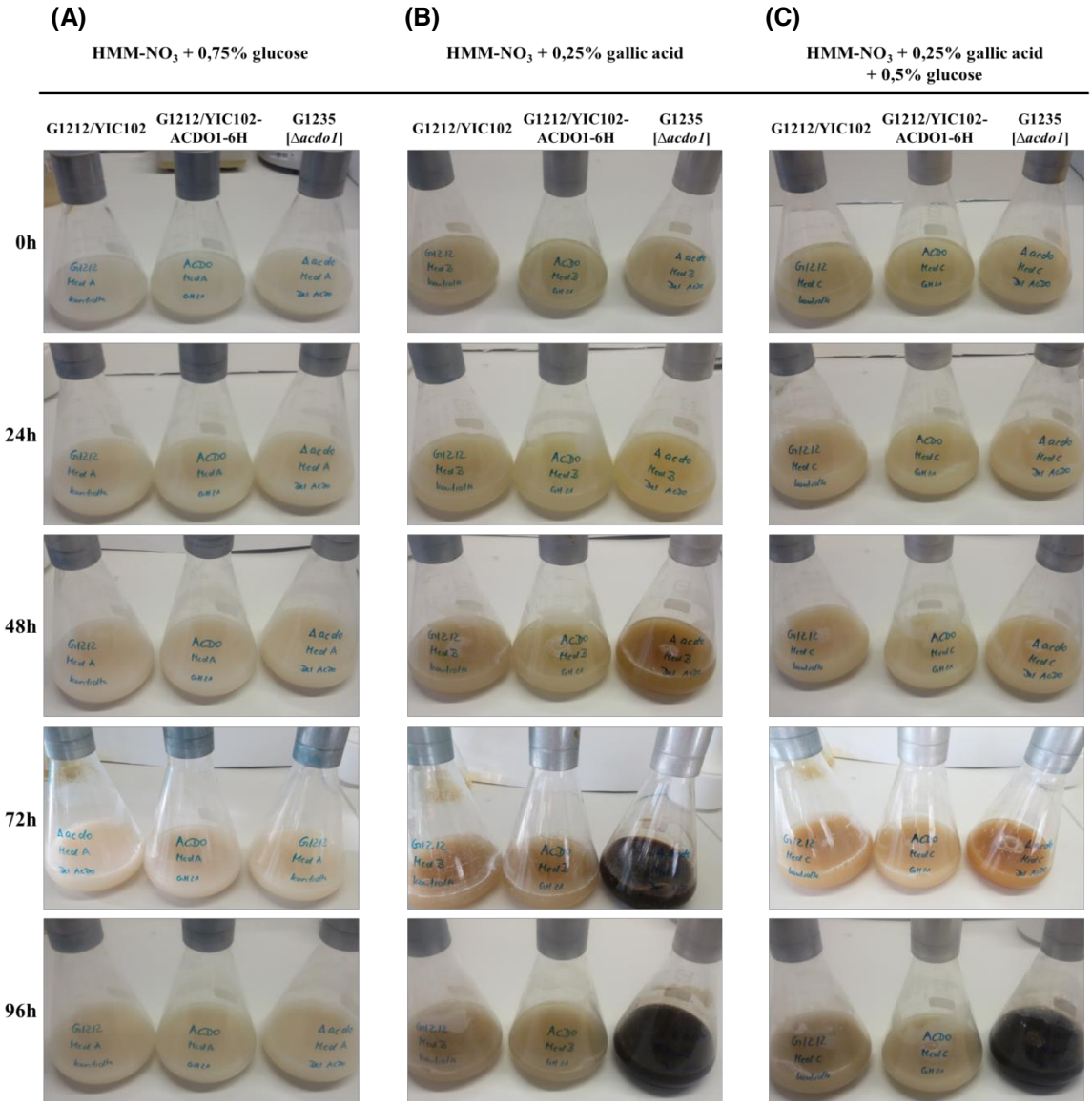

Figure 75 Substrate – product conversion during cultivation of *A. adeninivorans* on gallic acid in shaking flask culture**.**

A. adeninivorans strains G1212/YIC102, G1212/YIC102ACDO1-6H, G1235 [*Δacdo1*] were cultivated on HMM-$NaNO_3$ with 0.75 % glucose **(A)**, 0.25 % gallic acid **(B**) and 0.25 % gallic acid + 0.5 % glucose **(C).** During the cultivation substrate, gallic acid, was transformed in different products what cased in visible culture colour changes. Photos were made for every 24 h of cultivation.

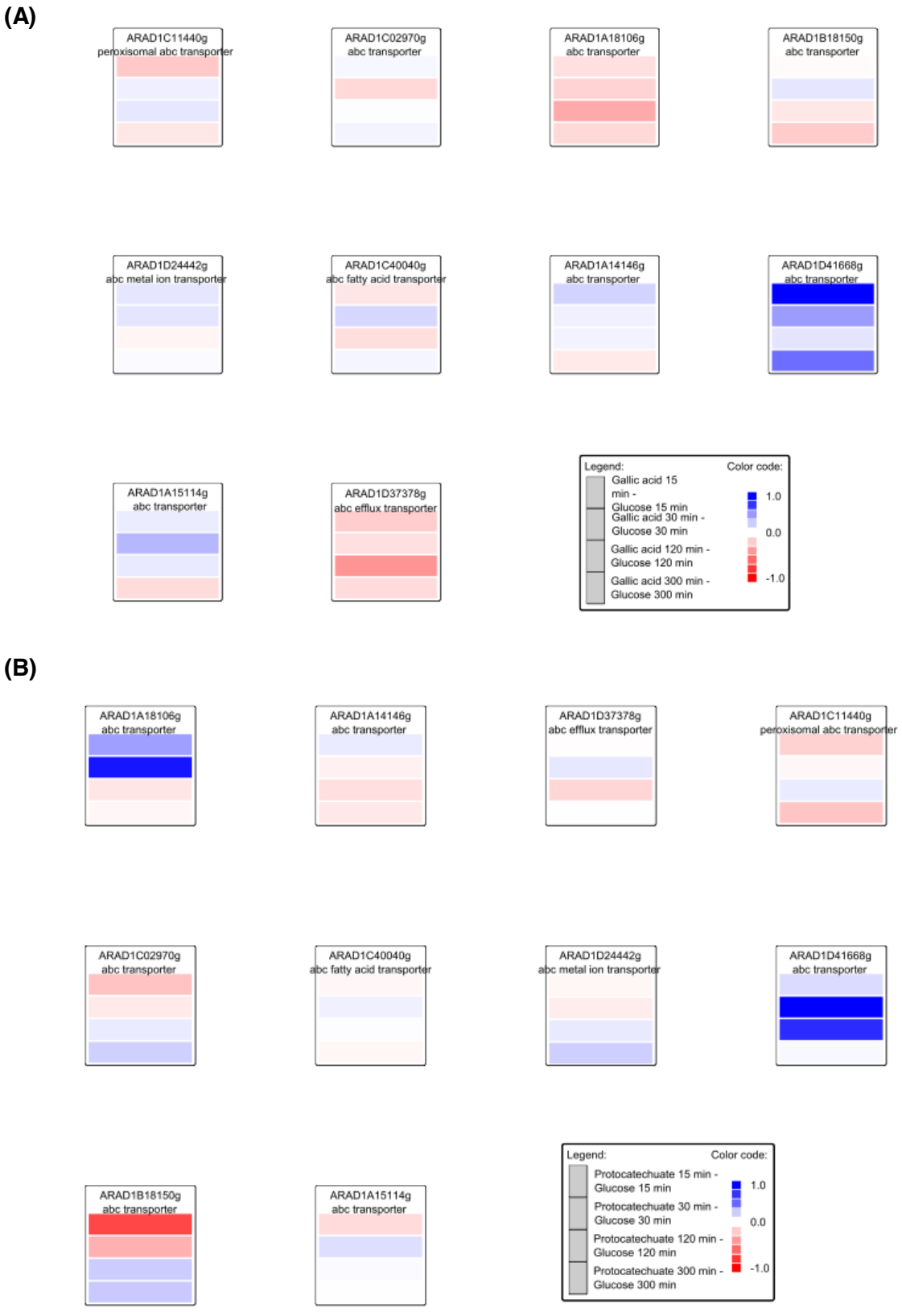

Figure 76 Expression analysis of ABC transporters.
The colours represent upregulation (blue) and downregulation (red) of genes in *A. adeninivorans* LS3 shifted to a medium containing 0.5% gallic acid and 1 % glucose **(A)** and 0.5 % protocatechuic acid and 1 % glucose **(B)** as the carbon sources compared to cells grown with 1 % glucose [produced using VANTED – (Junker *et al.*, 2012, Rohn *et al.*, 2012)].

(A)

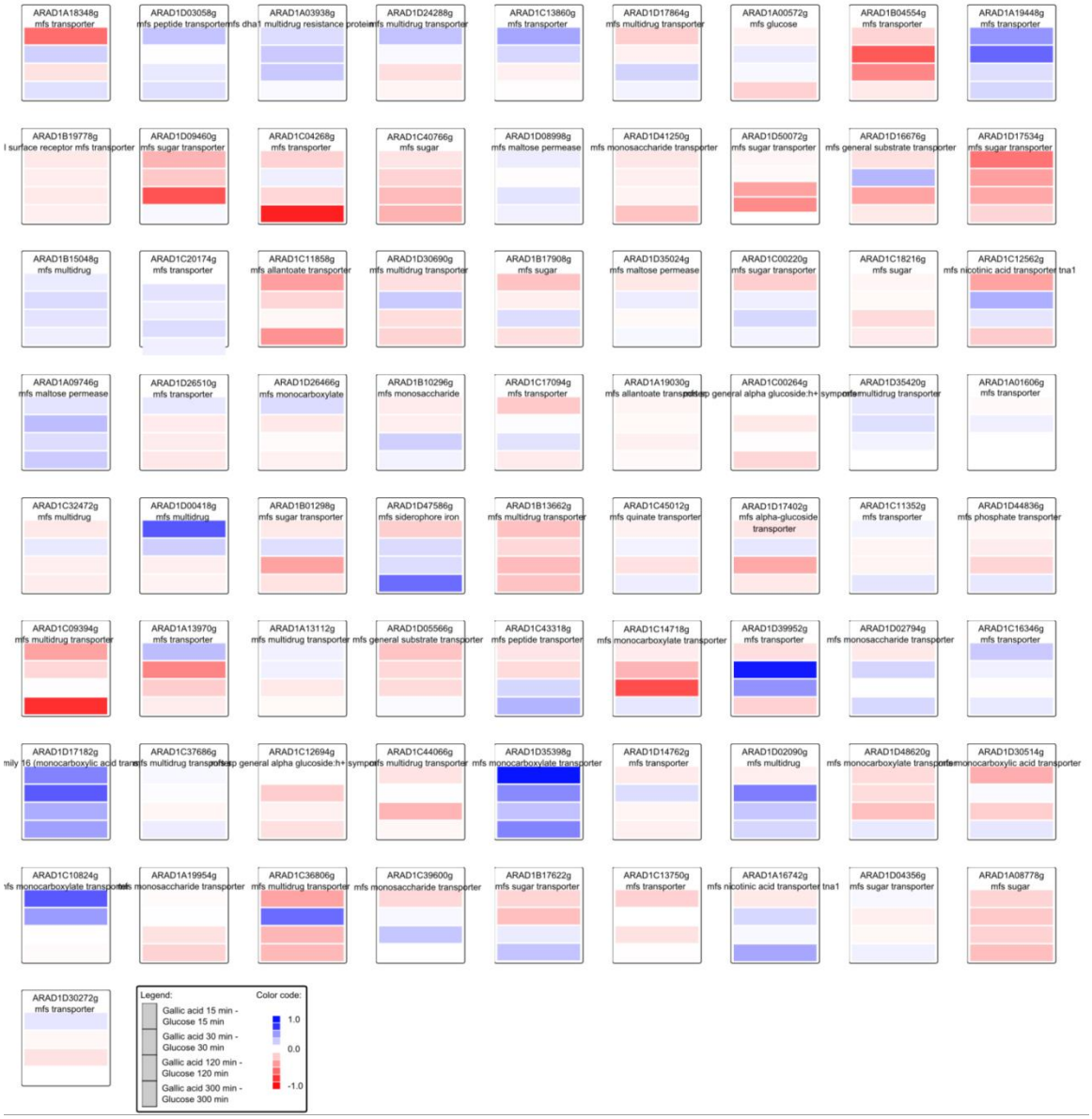
ARAD1A18348g mfs transporter
ARAD1D03058g mfs peptide transporter
ARAD1A03938g mfs dha1 multidrug resistance protein
ARAD1D24288g mfs multidrug transporter
ARAD1C13860g mfs transporter
ARAD1D17864g mfs multidrug transporter
ARAD1A00572g mfs glucose
ARAD1B04554g mfs transporter
ARAD1A19448g mfs transporter
ARAD1B19778g l surface receptor mfs transporter
ARAD1D09460g mfs sugar transporter
ARAD1C04268g mfs transporter
ARAD1C40766g mfs sugar
ARAD1D08998g mfs maltose permease
ARAD1D41250g mfs monosaccharide transporter
ARAD1D50072g mfs sugar transporter
ARAD1D16676g mfs general substrate transporter
ARAD1D17534g mfs sugar transporter
ARAD1B15048g mfs multidrug
ARAD1C20174g mfs transporter
ARAD1C11858g mfs allantoate transporter
ARAD1D30690g mfs multidrug transporter
ARAD1B17908g mfs sugar
ARAD1D35024g mfs maltose permease
ARAD1C00220g mfs sugar transporter
ARAD1C18216g mfs sugar
ARAD1C12562g mfs nicotinic acid transporter tna1
ARAD1A09746g mfs maltose permease
ARAD1D26510g mfs transporter
ARAD1D26466g mfs monocarboxylate
ARAD1B10296g mfs monosaccharide
ARAD1C17094g mfs transporter
ARAD1A19030g mfs allantoate transporter
ARAD1C00264g mfs general alpha glucoside:h+ symporter
ARAD1D35420g mfs multidrug transporter
ARAD1A01606g mfs transporter
ARAD1C32472g mfs multidrug
ARAD1D00418g mfs multidrug
ARAD1B01298g mfs sugar transporter
ARAD1D47586g mfs siderophore iron
ARAD1B13662g mfs multidrug transporter
ARAD1C45012g mfs quinate transporter
ARAD1D17402g mfs alpha-glucoside transporter
ARAD1C11352g mfs transporter
ARAD1D44836g mfs phosphate transporter
ARAD1C09394g mfs multidrug transporter
ARAD1A13970g mfs transporter
ARAD1A13112g mfs multidrug transporter
ARAD1D05566g mfs general substrate transporter
ARAD1C43318g mfs peptide transporter
ARAD1C14718g mfs monocarboxylate transporter
ARAD1D39952g mfs transporter
ARAD1D02794g mfs monosaccharide transporter
ARAD1C16346g mfs transporter
ARAD1D17182g mily 16 (monocarboxylic acid trans
ARAD1C37686g mfs multidrug transporter
ARAD1C12694g mfs general alpha glucoside:h+ symporter
ARAD1C44066g mfs multidrug transporter
ARAD1D35398g mfs monocarboxylate transporter
ARAD1D14762g mfs transporter
ARAD1D02090g mfs multidrug
ARAD1D48620g mfs monocarboxylate transporter
ARAD1D30514g monocarboxylic acid transporter
ARAD1C10824g fs monocarboxylate transporter
ARAD1A19954g mfs monosaccharide transporter
ARAD1C36806g mfs multidrug transporter
ARAD1C39600g mfs monosaccharide transporter
ARAD1B17622g mfs sugar transporter
ARAD1C13750g mfs transporter
ARAD1A16742g mfs nicotinic acid transporter tna1
ARAD1D04356g mfs sugar transporter
ARAD1A08778g mfs sugar
ARAD1D30272g mfs transporter
Legend:
Gallic acid 15 min - Glucose 15 min
Gallic acid 30 min - Glucose 30 min
Gallic acid 120 min - Glucose 120 min
Gallic acid 300 min - Glucose 300 min
Color code:
1.0
0.0
-1.0

(B)

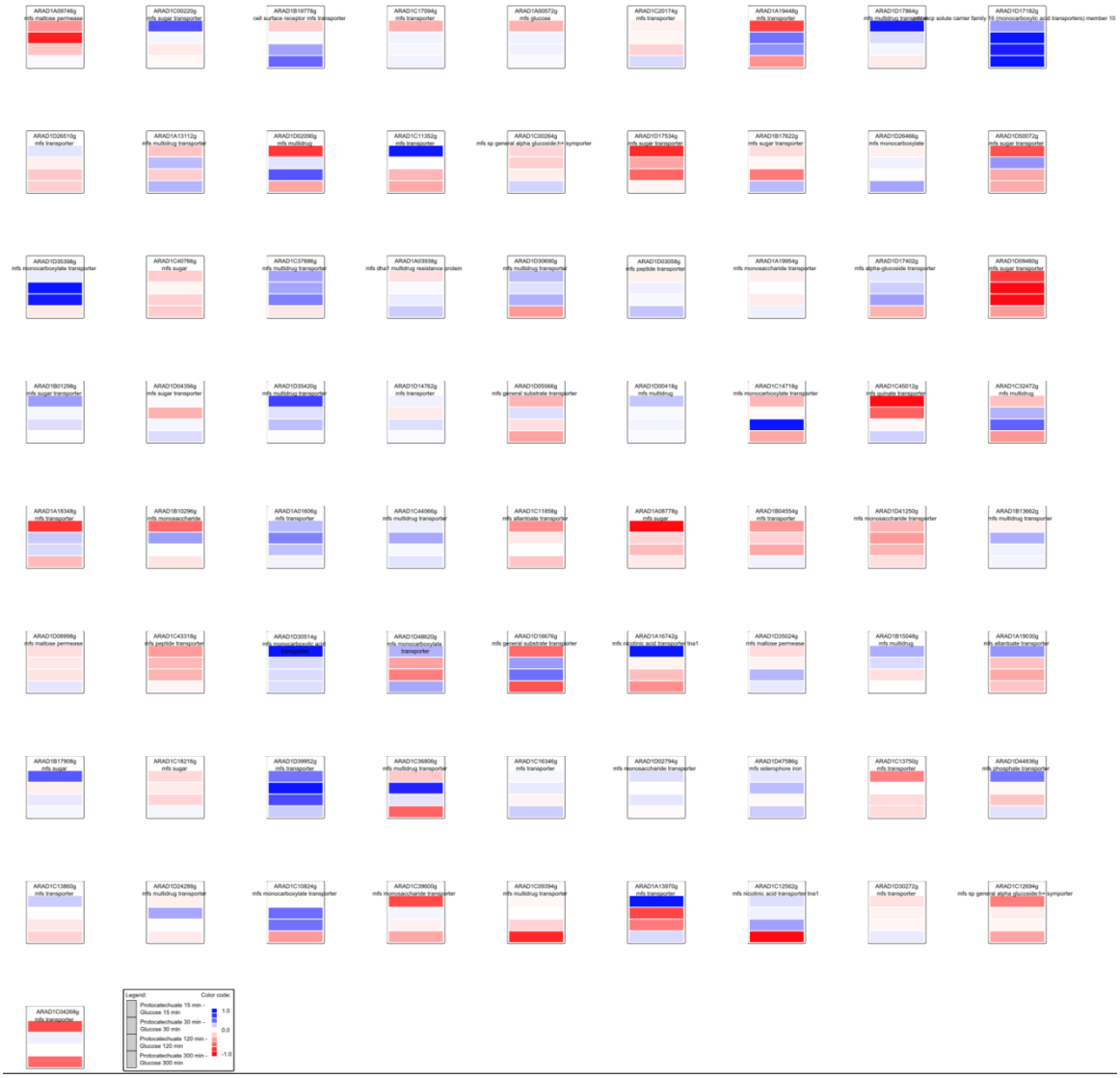

Figure 77 Expression analysis of MFS transporters.
The colours represent upregulation (blue) and downregulation (red) of genes in *A. adeninivorans* LS3 shifted to a medium containing 0.5 % gallic acid and 1 % glucose **(A)** and 0.5 % protocatechuic acid and 1 % glucose **(B)** as the carbon sources compared to cells grown with 1 % glucose [produced using VANTED – (Junker *et al.*, 2012, Rohn *et al.*, 2012)].

9 Declaration of originality

Hiermit erkläre ich, dass diese Arbeit bisher von mir weder an der Mathematisch-Naturwissenschaftlichen Fakultät der Universität Greifswald noch einer anderen wissenschaftlichen Einrichtung zum Zwecke der Promotion eingereicht wurde.

Ferner erkläre ich, dass ich diese Arbeit selbständig verfasst und keine anderen als die darin angegebenen Hilfsmittel und Hilfen benutzt und keine Textabschnitte eines Dritten ohne Kennzeichnung übernommen habe.

.....

Anna Karolina Meier